ACS SYMPOSIUM SERIES 1098

Recent Advances in the Analysis of Food and Flavors

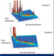

EDITED BY
Stephen Toth and Cynthia Mussinan

Downloaded by 89.163.35.42 on May 29, 2012 | http://pubs.acs.org
Publication Date (Web): May 29, 2012 | doi: 10.1021/bk-2012-1098.fw001

Recent Advances in the Analysis of Food and Flavors

Downloaded by 89.163.35.42 on May 29, 2012 | http://pubs.acs.org
Publication Date (Web): May 29, 2012 | doi: 10.1021/bk-2012-1098.fw001

Downloaded by 89.163.35.42 on May 29, 2012 | http://pubs.acs.org
Publication Date (Web): May 29, 2012 | doi: 10.1021/bk-2012-1098.fw001

ACS SYMPOSIUM SERIES **1098**

Recent Advances in the Analysis of Food and Flavors

Stephen Toth, Editor
International Flavors and Fragrances
Union Beach, New Jersey

Cynthia Mussinan, Editor
International Flavors and Fragrances
Union Beach, New Jersey

Sponsored by the
ACS Division of Agricultural and Food Chemistry, Inc.

American Chemical Society, Washington, DC

Distributed in print by Oxford University Press, Inc.

Downloaded by 89.163.35.42 on May 29, 2012 | http://pubs.acs.org
Publication Date (Web): May 29, 2012 | doi: 10.1021/bk-2012-1098.fw001

Library of Congress Cataloging-in-Publication Data

Recent advances in the analysis of food and flavors / Stephen Toth, Cynthia Mussinan, editor[s] ; sponsored by the ACS Division of Agricultural and Food Chemistry, Inc.
p. cm. -- (ACS symposium series ; 1098)
Includes bibliographical references and index.
ISBN 978-0-8412-2759-0 (alk. paper)
1. Flavor--Congresses. 2. Food--Analysis--Congresses. I. Toth, Stephen. II. Mussinan, Cynthia J., 1946- III. American Chemical Society. Division of Agricultural and Food Chemistry.
TP372.5.R43 2012
664′.06--dc23
2012014008

The paper used in this publication meets the minimum requirements of American National Standard for Information Sciences—Permanence of Paper for Printed Library Materials, ANSI Z39.48n1984.

Copyright © 2012 American Chemical Society

Distributed in print by Oxford University Press, Inc.

All Rights Reserved. Reprographic copying beyond that permitted by Sections 107 or 108 of the U.S. Copyright Act is allowed for internal use only, provided that a per-chapter fee of $40.25 plus $0.75 per page is paid to the Copyright Clearance Center, Inc., 222 Rosewood Drive, Danvers, MA 01923, USA. Republication or reproduction for sale of pages in this book is permitted only under license from ACS. Direct these and other permission requests to ACS Copyright Office, Publications Division, 1155 16th Street, N.W., Washington, DC 20036.

The citation of trade names and/or names of manufacturers in this publication is not to be construed as an endorsement or as approval by ACS of the commercial products or services referenced herein; nor should the mere reference herein to any drawing, specification, chemical process, or other data be regarded as a license or as a conveyance of any right or permission to the holder, reader, or any other person or corporation, to manufacture, reproduce, use, or sell any patented invention or copyrighted work that may in any way be related thereto. Registered names, trademarks, etc., used in this publication, even without specific indication thereof, are not to be considered unprotected by law.

PRINTED IN THE UNITED STATES OF AMERICA

Downloaded by 89.163.35.42 on May 29, 2012 | http://pubs.acs.org
Publication Date (Web): May 29, 2012 | doi: 10.1021/bk-2012-1098.fw001

Foreword

The ACS Symposium Series was first published in 1974 to provide a mechanism for publishing symposia quickly in book form. The purpose of the series is to publish timely, comprehensive books developed from the ACS sponsored symposia based on current scientific research. Occasionally, books are developed from symposia sponsored by other organizations when the topic is of keen interest to the chemistry audience.

Before agreeing to publish a book, the proposed table of contents is reviewed for appropriate and comprehensive coverage and for interest to the audience. Some papers may be excluded to better focus the book; others may be added to provide comprehensiveness. When appropriate, overview or introductory chapters are added. Drafts of chapters are peer-reviewed prior to final acceptance or rejection, and manuscripts are prepared in camera-ready format.

As a rule, only original research papers and original review papers are included in the volumes. Verbatim reproductions of previous published papers are not accepted.

ACS Books Department

Downloaded by 89.163.35.42 on May 29, 2012 | http://pubs.acs.org
Publication Date (Web): May 29, 2012 | doi: 10.1021/bk-2012-1098.pr001

Preface

The evolving landscape of analytical instrumentation has produced a plethora of extremely sensitive and selective methods for the analysis of trace components. Typically, the key character donating components of a food flavor are present in only trace levels. As instruments become more sensitive, detection limits are driven down, permitting the identification of new important flavor compounds. Armed with these new instruments, scientists seek to understand the links between what we eat and our health, and new demands are made for compliance with legal and labeling requirements.

This book is based on presentations made in the symposium "Recent Advances in the Analysis of Foods and Flavors" held at the Denver ACS meeting in August 2011. The symposium was sponsored by the Agricultural and Food Chemistry Division.

The 14 chapters in this book cover a variety of currently relevant topics, which include metabolomics, trace level aroma active compound identification, and the analysis of furocoumarins. The main objective of this book is to illustrate how new, highly sophisticated instrumentation can be used to address the issues of most interest to today's food and flavor chemists.

The editors would like to thank all of the authors for the timely submission of their manuscripts and International Flavors & Fragrances, Inc. for their financial support of this symposium.

Cynthia J. Mussinan
International Flavors & Fragrances, Inc.
1515 Highway 36
Union Beach, NJ 07735

Stephen Toth
International Flavors & Fragrances, Inc.
1515 Highway 36
Union Beach, NJ 07735

In Recent Advances in the Analysis of Food and Flavors; Toth, S., et al.;
ACS Symposium Series; American Chemical Society: Washington, DC, 2012.

Downloaded by PENNSYLVANIA STATE UNIV on May 30, 2012 | http://pubs.acs.org
Publication Date (Web): May 29, 2012 | doi: 10.1021/bk-2012-1098.ot001

Editors' Biographies

Stephen Toth

Stephen Toth is a Research Investigator in the Analytical and Sensory Measurement Department at International Flavors and Fragrances. He has spent the majority of his career at IFF working in fragrance delivery, chromatography, and ultimately in mass spectrometry. He is active in the Agricultural and Food Chemistry Division of the American Chemical Society and currently serves as treasurer of the division. He is also active in the North Jersey local section of the ACS, where he has served as chair of the Chromatography Discussion Group. He holds a B.S. and M.S. in chemistry from Seton Hall University and a Ph.D. in food science from Rutgers University.

Cynthia Mussinan

Cynthia Mussinan is currently Director of Analytical and Sensory Measurement and VP R&D at International Flavors and Fragrances. She has spent her whole career at IFF, working first in flavor research and then natural products before her current position. She is active in the Agricultural and Food Chemistry Division of the American Chemical Society, having served as treasurer for more than thirty years, and is a past president of the American Laboratory Manager's Association. In 2011 she was named a Fellow of the American Chemical Society. She holds a B.A. in biology from Georgian Court University and an M.S. in analytical chemistry from Rutgers.

Downloaded by 89.163.35.42 on May 29, 2012 | http://pubs.acs.org
Publication Date (Web): May 29, 2012 | doi: 10.1021/bk-2012-1098.ch001

Chapter 1

Metabolomics and the Quest for Understanding Quality in Flavor Chemistry and Wine Research

M. J. Herderich,* T. E. Siebert, M. Parker, Y. Hayasaka, C. Curtin, and M. Mercurio

The Australian Wine Research Institute, P.O. Box 197,
Glen Osmond, SA 5064, Australia
***E-mail: markus.herderich@awri.com.au**

With a focus on sesquiterpenes, phenolic glycosides and secondary metabolites from yeast, examples are presented from recent targeted and non-targeted metabolomics studies into wine quality, flavor chemistry, and from experiments requiring efficient yeast strain phenotyping. In this context, challenges, success factors and future development needs for metabolomic profiling and quality marker discovery are discussed.

Introduction

The first comprehensive description of metabolomics principles dates back to the 1960s (*1*), and in wine science metabolomics approaches have been used since the early 1970s, initially for studies aiming to profile, identify and quantify grape and wine aroma compounds (*2*). This is not surprising given that wine aroma and quality result from distinctive combinations of volatile secondary metabolites.

Since metabolomics has been recognized as a specialized scientific discipline in its own right more than ten years ago (*3*, *4*), significant advancements in commercially available analytical instrumentation have been made. Reliable, fast and multidimensional separation techniques, together with tandem- and high resolution-mass spectrometry have become widely available and are commonly used for the identification and quantification of volatile and non-volatile trace metabolites. Novel tools for data mining and annotation are allowing us to fully realize the value of complex and vast data sets obtained from unique biological samples through comprehensive, efficient and sophisticated analytical

In Recent Advances in the Analysis of Food and Flavors; Toth, S., et al.;
ACS Symposium Series; American Chemical Society: Washington, DC, 2012.

strategies. Multivariate data analysis, data visualization tools and specialised metabolite databases are being further developed, thus enabling efficient chemical phenotyping and novel insights into biological networks (*5*, *6*).

Materials and Methods

Experimental details about grape samples, sensory evaluation of ‘peppery’ aromas in grape homogenates, GC-MS analysis of sesquiterpenes and the non-targeted GC-MS metabolomics strategy that led to the identification of the Shiraz grape sesquiterpene, α-ylangene, as marker for ‘pepper’ aroma have been described by Parker and co-workers (*7*). The GC-MS-O experiments and sensory studies to identify rotundone as an important impact compound with a strong ‘spicy’, ‘pepper’ aroma have been summarised in (*8*), and the analytical method used to quantify rotundone has been described in (*9*).

The glycosides of the volatile phenols were identified and analysed by high performance liquid chromatography-tandem mass spectrometry (HPLC-MS/MS) (*10*, *11*) and the contribution of several volatile phenols and their glycoconjugates to smoke related sensory properties of red wine was established by sensory analysis (*12*).

The breeding strategy to generate *Saccharomyces* interspecific hybrids that enhance flavor diversity in wine was based on sporulation and subsequent mass mating of yeasts strains AWRI 1116, 1539 and 1640 (*13*). Secondary fermentation metabolites in wine made from the parent strains were quantified by targeted profiling of higher alcohols, acetate- and ethyl-esters by GC-MS and a stable isotope dilution assay (*14*). High-throughput fingerprinting of wine volatiles by headspace MS analysis without chromatographic separation was achieved injecting 2.5 mL of headspace into a PTV inlet (Gerstel CIS 4) fitted with a Tenax TA inlet liner cooled to 15 °C using solvent vent mode. Following capture of analytes on the Tenax liner the injector was heated to 330 °C at 12 °C s^{-1} and positive ion electron impact spectra were recorded in scan mode with a mass range of 50 – 400 and 4 scans s^{-1} (*13*).

Downloaded by 89.163.35.42 on May 29, 2012 | http://pubs.acs.org
Publication Date (Web): May 29, 2012 | doi: 10.1021/bk-2012-1098.ch001

Results and Discussion

Typical metabolomics experiments are based on correlation analysis of complex data sets from often unique biological samples. For realising the value of the chemical metabolite analysis, as well as for maximising the knowledge generated, it is critical to capture all relevant meta data and to objectively define and robustly quantify the underlying phenotype(s). When using metabolomics approaches to identify important compositional drivers of quality in food products like grapes or wine, key is to first establish a comprehensive sample set that covers a range of relevant sensory properties, and/or well-defined non-sensory quality characteristics and other relevant traits. In this context, product-, production- or market-related traits are suitable as proxy for measuring grape and wine quality. Common quality phenotypes in grape or wine production can be objectively defined through presence and intensity of positive aromas (for example key grape aroma compounds or desirable fermentation metabolites from yeast), or absence of negatives (such as moulds, degree of sunburn or millerandage in grapes; off flavors or unbalanced ethanol concentration in wine); alternatively quality concepts may be based on production and process related traits like achieving homogenous grape maturity or reliable fermentation kinetics; finally quality definitions can be derived also from consumer preferences or market demands.

In the following examples will be given from recent experiments at The Australian Wine Research Institute where we used non-targeted metabolomics approaches for the discovery of key aroma compounds and quality markers in Shiraz grapes (*7*, *8*); established the profiles of key metabolites from xenobiotic phenols to improve diagnostics techniques for assessing smoke exposure of grapes (*10*, *11*, *15*); and explored rapid GC-MS analysis of fermentation volatiles for metabolic phenotyping and rapid screening in yeast strain development (*13*).

Downloaded by 89.163.35.42 on May 29, 2012 | http://pubs.acs.org
Publication Date (Web): May 29, 2012 | doi: 10.1021/bk-2012-1098.ch001

Biomarker Discovery through Nontargeted Metabolomics of Volatile Trace Metabolites in Shiraz Grapes

Shiraz (Syrah in Europe), is Australia's most widely planted and versatile red grapevine variety. Broadly, Australian Shiraz styles include elegant, peppery cool-climate wines; more intensely flavored, spicy and sometimes minty styles; sweet chocolaty, muscular and ripe-fruited wines; and leathery and rich wines. Some Australian Shiraz wines have a distinctive 'black pepper' aroma and flavor and such spicy, 'peppery' aromas are regarded as positive sensory attributes, especially when in balance with ripe, fruity berry aromas. Despite the importance of Shiraz to the Australian wine industry, little was known until recently about the aroma compounds that are the key contributors to the perceived aroma and flavor of premium quality Shiraz wine. Furthermore, 'peppery' aromas are highly variable between vineyards and also vintages, hence our interest in characterising the underlying factors that contribute to the desirable 'peppery' notes. As no aroma compound(s) responsible for 'peppery' aromas in grapes, wine, or indeed 'pepper' from *Piper nigrum* was known at the time we initiated our research, no objective analytical method to assess 'pepper' grape aromas was available. Yet, the 'black pepper' flavor could be perceived in individual berries and deseeded Shiraz grape berry homogenates by some individuals (*7*).

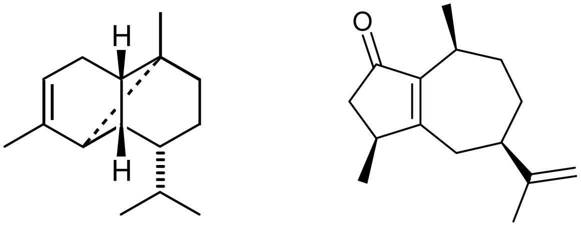

Figure 1. α-Ylangene, a sesquiterpene biomarker for pepper aroma in grapes, and rotundone, the key pepper aroma compound in grape and wine.

In Recent Advances in the Analysis of Food and Flavors; Toth, S., et al.;
ACS Symposium Series; American Chemical Society: Washington, DC, 2012.

To prepare for the metabolomics experiments, samples of potentially ‘spicy’/‘peppery’ grapes were obtained from a number of vineyards in South Australia and Victoria over two vintages and important sensory attributes of the grapes, including the aroma descriptor ‘pepper’, were rated by a sensory panel. This quantitative descriptive analysis revealed a strong correlation between the intensity of ‘pepper’ aroma and the intensity of ‘pepper’ flavor perceived on the palate, and indicated that we could concentrate on profiling volatile grape metabolites. Subsequently, grape homogenates were analyzed by static headspace GC-MS using a cool inlet system, to achieve enrichment of trace volatile aroma compounds for improved limits of detection, and to avoid undesirable discrimination and matrix effects. GC-MS analysis yielded over 13000 individual mass spectra per grape sample. Prior to multivariate data analysis the data were preprocessed, summed to obtain a single mass spectrum per sample, or binned. To explain the intensity of the rating of the ‘pepper’ character, principal component analysis and partial least-squares regression were then used to develop multivariate models based on mass spectra and aroma descriptors. Additional optimization of the methodology enabled selection of a single region of the GC-MS chromatogram that allowed prediction of ‘pepper’ aroma intensity with a good correlation coefficient better than 0.98. This led to the identification of α-ylangene, a tricyclic sesquiterpene (Figure 1), which was corroborated through co-injection with an authentic reference compound. Although not a significant aroma compound by itself, α-ylangene was a very good marker for the ‘pepper’ aroma in grapes and wine, and its concentration showed similar discrimination between ‘peppery’ vineyards and vintages as that obtained using sensory data (*7*).

Downloaded by 89.163.35.42 on May 29, 2012 | http://pubs.acs.org
Publication Date (Web): May 29, 2012 | doi: 10.1021/bk-2012-1098.ch001

Notably, multivariate analysis of data from metabolomics experiments typically results in the identification of key features and metabolites based on correlation with other metadata, but does not establish cause-effect relationships. In this example, we were able to identify a single sesquiterpene marker, α-ylangene, at trace concentrations of 1 to 15 μg/kg through an non-targeted GC-MS experiment and in presence of a range of other sesquiterpenes. At the same time we initially missed out on detecting any key peppery volatiles. The subsequent identification of rotundone, the ‘peppery’ aroma impact compound (Figure 1), required traditional GC-MS-O experiments, and succeeded only after sensory guided elaborate optimisation of sample preparation and enrichment (*8*). This may serve as example that metabolomics strategies complement, but do not substitute for, established approaches to identify bioactives such as impact aroma compounds that may be present and active at very low concentrations.

Targeted Metabolic Profiling and Identification of Markers for Smoke Exposure in Grapes

In many grape producing countries, forest- and wildfire incidents in the vicinity of grapegrowing regions have significantly increased in the last decade and - in-line with climate change forecasts - we are most likely to experience even more smoke events in the future. This is a concern as vineyards cannot avoid exposure to smoke drift, and wine made from smoke affected grapes is difficult, if not impossible, to market because it is often characterised by objectionable ‘smoky’, ‘burnt’, ‘ash’, and ‘ashtray’ aromas, having ‘an excessively drying’ back-palate and a retronasal ‘ash’ character. Some viticultural and winemaking practices might help to limit the presence of smoke-derived compounds and prove successful in reducing smoke taint in wine in some cases. However, the options to minimise or avoid quality loss from smoke taint are limited. Hence we have been concentrating on the development of diagnostic assays, using metabolomics approaches, to reliably identify smoke exposure in grapes after a bushfire event. The aim was to enable evidence-based critical decisions concerning harvest, purchase of grapes or bulk wine, and choice of winemaking practices with confidence and as early as possible after a smoke event (*15*).

Volatile phenols, guaiacol and 4-methylguaiacol, are commonly found in smoke from forest fires and, in the past, have been successfully used as first pass markers for detecting smoke exposure of grapes (*16*, *17*). However, their presence cannot always explain the smoky sensory attributes observed in wines made from smoke-exposed grapes, with levels of these compounds often at or below levels found in oak-barrel aged wines (*18*, *19*). Also, guaiacol and 4-methylguaiacol can be found in some grape varieties as natural compounds, and the concentrations of these phenols have been reported to increase during fermentation and after bottling. Notably, we observed that a substantial number of grape samples submitted for analysis after the 2009 bushfires had guaiacol concentrations below the detection limit. These grapes came from clearly smoke-affected regions and this observation pointed towards a substantial risk for obtaining false-negative results from GC-MS analysis of free guaiacol. Taken together, the diagnostic value of free guaiacol and 4-methylguaiacol at low concentrations is limited and the interpretation of wine data is complicated. Clearly, better markers to assess the extent of smoke exposure on grapes and wine were needed.

In some instances, winemakers had observed that the smoke-related sensory characters increased after fermentation and continued intensifying in a wine over time, even after bottling. This anecdotal observation pointed towards formation of hydrolysable grape metabolites of smoke compounds and we confirmed the presence of guaiacol glucoside as a non-volatile metabolite in grapes exposed to smoke from bushfires and model smoke experiments (*20*). Next, we studied the formation of glycosidic metabolites in detail using a stable isotope tracer technique, directly applying an equimolar mixture of d_0- and d_3-labelled guaiacol solution to grape berries and leaves (*10*). Through this targeted metabolite profiling experiment, characteristic isotope patterns were observed in a number of mass spectra that allowed the identification of seven different glycoconjugates of guaiacol in grape berries and leaves. Tandem mass spectrometry helped to tentatively identify these grape metabolites as monoglucoside, gentiobioside, a group of four isomeric glucosylpentosides, and rutinoside of guaiacol. The study also indicated that minimal translocation of guaiacol glycosides occurred between grapevine leaves and berries (at least in the potted Cabernet Sauvignon vines used for the model experiments) and that the glycosides were present as low-level natural compounds in control leaves and berries. HPLC-MS/MS analysis confirmed the presence of the guaiacol glycosides in significantly elevated amounts in leaves and berries following exposure of grapevines to smoke derived from actual bushfires.

Downloaded by 89.163.35.42 on May 29, 2012 | http://pubs.acs.org
Publication Date (Web): May 29, 2012 | doi: 10.1021/bk-2012-1098.ch001

Further metabolite profiling by HPLC-MS/MS confirmed the presence of a broad range of glycosides of other volatile phenols from smoke, including the glycosides of methylguaiacol, syringol, methylsyringol, *o*-, *p*- and *m*-cresol, and phenol (*11*). Together, these glycosidic metabolites represent a large pool of smoke-related flavor precursors that may release significant concentrations of free aroma compounds during the winemaking and ageing, and tasting of wine. Indeed, we have recently confirmed that β-D-glucosides of guaiacol and *m*-cresol in model wine can give rise to a *smoky/ashy* flavor in-mouth, through release of the respective free volatile phenol (*12*). In summary, targeted metabolite profiling has provided us with the essential knowledge that a range of xenobiotic phenols can be very effectively metabolised into numerous non-volatile glycosides by vines and grapes; this led to major improvements and critical evaluation of the diagnostic assays for detection of smoke exposure in grapes (*21*, *22*). In addition, mass spectra of compounds identified from the metabolic profiling experiments directed the chemical synthesis of key reference glycosides and facilitated sensory studies that demonstrated the generation of flavor from non-volatile glycoconjugates in-mouth, an observation that has potentially important implications for many desirable flavor attributes of wine (*12*).

Downloaded by 89.163.35.42 on May 29, 2012 | http://pubs.acs.org
Publication Date (Web): May 29, 2012 | doi: 10.1021/bk-2012-1098.ch001

High-Throughput GC-MS Analysis of Fermentation Volatiles for Metabolic Phenotyping and Rapid Screening in Yeast Strain Development

Improvement of wine yeast properties requires not only enhancing fermentation performance, but also optimizing the production of yeast metabolites that contribute to wine aroma. We recently demonstrated a non-GM approach to develop novel wine yeast strains with improved aroma traits, based on generation of interspecies hybrids within the *Saccharomyces* sensu stricto group (*23*). As the next step, we aimed to demonstrate that existing *Saccharomyces* interspecies hybrids (AWRI 1539 or AWRI 1116), which are known to produce relatively high concentrations of positive fermentation metabolites, can be used in breeding programs together with established *S. cerevisiae* mutants (such as AWRI 1640) that produce little H_2S (*24*).

A total of 96 potential hybrid strains were obtained after mass-mating of wine yeast strains AWRI 1640 with AWRI 1539 or AWRI 1116; the hybrids were then screened for H_2S production on agar plates and 44 colonies were chosen for further molecular characterization. This lead to the selection of five novel confirmed hybrids for further fermentation trials. Targeted quantitative GC-MS analysis of key fermentation metabolites in wine made from the three parent strains confirmed that the yeast strains could be differentiated based on their metabolite profile, with both AWRI 1116 and 1539 producing increased levels of acetate esters - excluding ethyl acetate - and higher alcohols than AWRI 1640. In the case of AWRI 1539, this strain also produced significantly higher levels of 2-phenylethyl acetate than AWRI 1640 (*13*).

To efficiently characterize the fermentation related secondary metabolites in a total of 48 wine samples from fermentations with the three parental strains and the five novel hybrids, metabolite fingerprints were obtained by high-throughput analysis of wine volatiles using direct headspace MS analysis without chromatographic separation. Thermodesorption of volatile metabolites directly from a Tenax liner via a deactivated capillary transfer into the mass spectrometer allowed to reduce the run time to a few minutes and improved through-put approximately by a factor of ten. Principle component analysis (PCA, Figure 2) of the binned and summed mass spectra gave similar metabolite profiles for wine made with parents AWRI 1116 and AWRI 1539, while AWRI 1640 was clearly separated, as had been seen in the data from the quantitative GC-MS analysis. Wines made with each of the novel hybrids clustered intermediate to their respective parental strains. Interestingly, the hybrids between AWRI 1116 and AWRI 1640 exhibited a volatile metabolite profile that was closer to that of the AWRI 1640 parental strain, while the AWRI 1539 and AWRI 1640 hybrids consistently clustered more closely to the AWRI 1539 parental strain (*13*). It will be interesting to observe whether these differences in fermentation metabolites are reflected in the sensory analysis from larger scale fermentations that are planned for the upcoming vintage.

Downloaded by 89.163.35.42 on May 29, 2012 | http://pubs.acs.org
Publication Date (Web): May 29, 2012 | doi: 10.1021/bk-2012-1098.ch001

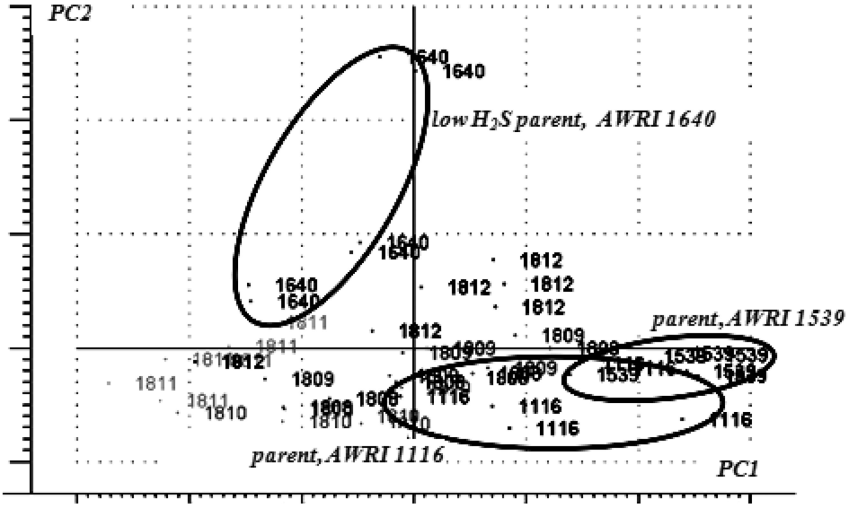

Figure 2. Profiling of volatile yeast metabolites using direct headspace-thermodesorption mass spectrometry. Principle component analysis of wine produced by replicated fermentations with parent yeast strains AWRI 1116, 1539, 1640, and novel hybrids 1808, 1809, 1810, 1811, 1812. PC1 explains 73% of variation in the dataset, and PC2 15%.

Based on the mass-mating strategy, the simplicity of the plate method used for screening of H_2S production, and the use of complementary phenotypic markers for the selection of hybrids we developed novel hybrid wine yeast strains that express the desired metabolite profiles and have reliable fermentation characteristics. As part of this strategy the metabolite fingerprinting approach confirmed that the selected hybrids put the desired ’mixed’ genotype to work and were able to produce wine with the desired phenotype, an enhanced concentration of positive fermentation aromas. Encouraged by this successful proof-of-concept study, we are now employing metabolite fingerprinting to screen hundred’s of wine samples from 30 mL ferments at early stages of strain development to select candidate hybrid strains for upscaling, sensory evaluation and potential commercialization.

Conclusions

Metabolomics approaches offer effective strategies to gain novel insights into what compounds shape the sensory characteristics of wine and define wine quality attributes. Combining comprehensive chemical analysis with sophisticated data mining tools enables us to establish new evidence-based quality measures for grape and wine production; this also provides for a much greater understanding of how variables, such as winemaking practices, environmental conditions, or genetic variation of vines and yeast, may define wine sensory and quality. In the examples above, we have demonstrated the discovery of new biomarkers and bioactives responsible for quality attributes of wine through non-targeted and unbiased analysis of trace grape metabolites that were present at low ppb to ppm concentrations. As long as potentially confounding factors are understood and false positive features are effectively discarded, sensitivity and selectivity of established metabolite profiling approaches and multivariate data analysis techniques are already adequate to successfully identify many trace compounds that are important to wine aroma, flavor and quality. Obviously, application of comprehensive non-targeted analytical methods to achieve maximum coverage will come at the expense of sensitivity, at least for some compounds. This may be a disadvantage for some metabolomics approaches aiming to discover potent aroma compounds; a good understanding of coverage and balancing this with required sensitivity is key for successful metabolomics applications in flavor chemistry. At the same time comprehensive analysis at ultra high sensitivity and/or resolution comes with its own challenges, i.e. enhanced risks for overfitting data, for identifying statistical correlations that are not based on cause-effect relationships, and for getting side-tracked in ubiquitous chemical noise and through false-positive features. In our own work, it has been proven advantageous to minimize the identification of false-positives, i.e. to accept initially a smaller ‘hit rate’ that informs subsequent isolation, synthesis, large scale fermentation, or reconstitution and sensory experiments. Clearly, a need for further, more comprehensive and sensitive experiments can always be re-tested once the first obvious key factors have been established through metabolomics approaches.

To further unravel the secrets behind wine quality and flavor through metabolomics approaches, a number of areas require special attention in future research. In particular, the quality traits described in this paper – presence of peppery aromas, and absence of smoke related taints – are phenotypes that can be linked to a single compound, or a small group of structurally related compounds. However, in many cases wine flavor, quality or style result from combinations and interactions of dozens if not hundreds of individual compounds, volatiles

Downloaded by 89.163.35.42 on May 29, 2012 | http://pubs.acs.org
Publication Date (Web): May 29, 2012 | doi: 10.1021/bk-2012-1098.ch001

Downloaded by 89.163.35.42 on May 29, 2012 | http://pubs.acs.org
Publication Date (Web): May 29, 2012 | doi: 10.1021/bk-2012-1098.ch001

and non-volatiles. Consequently, more work is required to refine experimental designs and biostatistical tools to allow identification of additive, synergistic or inhibitory effects between multiple metabolites that contribute to wine flavor and quality. Characterising multi-trait phenotypes, such as wine flavor, typically requires the simultaneous quantification of a huge number of known metabolites through stable isotope dilution analysis using GC-MS or HPLC-MS, which is a highly accurate and precise approach, but also very time consuming and costly to develop, validate, maintain and apply. Where metabolic 'fingerprinting' is required to pre-screen or categorize hundreds of samples, rapid and inexpensive methods based on mass spectrometry (on its own or in combination with NMR, electron or vibrational spectroscopy) can be used for metabolic phenotyping of fermentation volatiles, for yeast strain selection or for de-replication of larger sample sets prior to sensory characterisation. For example, the potential of soft ionization techniques in combination with direct infusion high resolution mass spectrometry has yet to be fully explored.

Secondly, improved strategies are required to obtain unbiased and accurate quantitative data from comprehensive analysis of structurally diverse metabolites, especially from sample sets such as grapes, ferments or wine that typically feature significant variability in matrix composition. Comparing relative differences between samples with specific sensory and quality phenotypes has been useful to identify key metabolites and flavor compounds. However, reliability of quantitative analytical data is a prerequisite for correct interpretation (*25*), not only for studies aiming to identify additive or synergistic interactions of flavor compounds, but also for other applications such as flux analysis and metabolic engineering, or the development of systems biology models of metabolism (*26*).

To take full advantage of metabolomics approaches in wine research, as well as in flavor chemistry, it remains important to base metabolomics experiments on a deep understanding of natural products chemistry, biochemistry, and grape growing and winemaking. Another key to successful metabolomics is a comprehensive sample set: i.e. grape or wine samples that are typical examples of the phenotype under study; include sufficiently robust biological replicates and controls; and come with a good understanding of relevant metadata and potentially confounding factors. It is only through combining appropriate sampling strategies with state-of-the-art instrumentation and sophisticated biostatistical tools that we are unlocking the full potential of metabolomics, and may achieve conclusive answers and novel insights from metabolomics experiments.

Acknowledgments

We thank all AWRI colleagues, past and present, who contributed to this research and co-authored the publications listed under references. We are grateful for support and valuable contributions by Cory Black, Kevin Pardon, Katryna van Leeuwen, Mark Solomon, and acknowledge AWRI's sensory panellists as well as Brooke Travis, Belinda Bramley and Jennifer O'Mahony for their assistance with the sensory studies. We very much appreciate the ongoing support and interest by many Australian wine companies. This work was funded by Australia's grapegrowers and winemakers through their investment body, the Grape and Wine Research and Development Corporation (GWRDC), with matching funds from the Australian Government; we also acknowledge the financial support provided by Bioplatforms Australia (BPA) for establishing AWRI's Metabolomics facility. The Australian Wine Research Institute (AWRI) is a member of the Wine Innovation Cluster located on the Waite Campus in Adelaide, Australia.

References

1. Dalgliesh, C. E.; Horning, E. C.; Horning, M. G.; Know, K. L.; Yarger, K. *Biochem. J.* **1966**, *101*, 792–810.
2. Schreier, P.; Drawert, F.; Junker, A. *J. Agric. Food Chem.* **1976**, *24*, 331–336.
3. Oliver, S. G.; Winson, M. K.; Kell, D. B.; Baganz, F. *Trends Biotechnol.* **1998**, *16*, 373–378.
4. Trethewey, R. N.; Krotzky, A. J.; Willmitzer, L. *Curr. Opin. Biotechnol.* **1999**, *2*, 83–85.
5. Xia, J.; Wishart, D. S. *Nat. Protoc.* **2011**, *6*, 743–760.
6. Baumgartner, C.; Osl, M.; Netzer, M.; Baumgartner, D. *J. Clin. Bioinf.* **2011**, *1*, 2.
7. Parker, M.; Pollnitz, A. P.; Cozzolino, D.; Francis, I. L.; Herderich, M. J. *J. Agric. Food Chem.* **2007**, *55*, 5948–5955.
8. Wood, C.; Siebert, T. E.; Parker, M.; Capone, D. L.; Elsey, G. M.; Pollnitz, A. P.; Eggers, M.; Meier, M.; Vossing, T.; Widder, S.; Krammer, G.; Sefton, M. A.; Herderich, M. J. *J. Agric. Food Chem.* **2008**, *56*, 3738–3744.
9. Siebert, T. E.; Wood, C.; Elsey, G. M.; Pollnitz, A. P. *J. Agric. Food Chem.* **2008**, *56*, 3745–3748.
10. Hayasaka, Y.; Baldock, G. A.; Pardon, K. H.; Jeffery, D. W.; Herderich, M. J. *J. Agric. Food Chem.* **2010**, *58*, 2076–2081.
11. Hayasaka, Y.; Baldock, G. A.; Parker, M.; Pardon, K. H.; Black, C. A.; Herderich, M. J.; Jeffery, D. W. *J. Agric. Food Chem.* **2010**, *58*, 10989–10998.
12. Parker, M.; Osidacz, P.; Baldock, G. A.; Hayasaka, Y.; Black, C. A.; Pardon, K. H.; Jeffery, D. W.; Geue, J. P.; Herderich, M. J.; Francis, I. L. *J. Agric. Food Chem.* **2011**, submitted for publication.
13. Bizaj, E.; Cordente, A. G.; Bellon, J. R.; Raspor, P.; Curtin, C. D.; Pretorius, I. S. *FEMS Yeast Res.* **2012**, submitted for publication.
14. Siebert, T. E.; Smyth, H. E.; Capone, D. L.; Neuwöhner, C.; Pardon, K. H.; Skouroumounis, G. K.; Herderich, M. J.; Sefton, M. A.; Pollnitz, A. P. *Anal. Bioanal. Chem.* **2005**, *381*, 937–947.
15. Hayasaka, Y.; Baldock, G.; Parker, M.; Herderich, M.; Pretorius, I. *Wine Vitic. J.* **2011**, *26* (5), 26–31.
16. Kennison, K. R.; Gibberd, M. R.; Pollnitz, A. P.; Wilkinson, K. L. *J. Agric. Food Chem.* **2008**, *56*, 7379–7383.
17. Kennison, K. R.; Wilkinson, K. L.; Williams, H. G.; Smith, J. H.; Gibberd, M. R. *J. Agric. Food Chem.* **2007**, *55*, 10897–10901.

Downloaded by 89.163.35.42 on May 29, 2012 | http://pubs.acs.org
Publication Date (Web): May 29, 2012 | doi: 10.1021/bk-2012-1098.ch001

18. Prida, A.; Chatonnet, P. *Am. J. Enol. Vitic.* **2010**, *61*, 408–413.
19. Spillman, P. J.; Sefton, M. A.; Gawel, R. *Aust. J. Grape Wine Res.* **2004**, *10*, 216–226.
20. Hayasaka, Y.; Dungey, K. A.; Baldock, G. A.; Kennison, K. R.; Wilkinson, K. L. *Anal. Chim. Acta* **2010**, *660*, 143–148.
21. Dungey, K. A.; Hayasaka, Y.; Wilkinson, K. L. *Food Chem.* **2011**, *126*, 801–806.
22. Wilkinson, K. L.; Ristic, R.; Pinchbeck, K. A.; Fudge, A. L.; Singh, D. P.; Pitt, K. M.; Downey, M. O.; Baldock, G. A.; Hayasaka, Y.; Parker, M.; Herderich, M. J. *Aust. J. Grape Wine Res.* **2011**, *17*, 22–28.
23. Bellon, J. R.; Eglinton, J. M.; Siebert, T.; Pollnitz, A. P.; Rose, L.; De Barros Lopes, M.; Chambers, P. J. *Appl. Microbiol. Biotechnol.* **2011**, *91*, 603–612.
24. Cordente, A. G; Heinrich, A.; Pretorius, I. S.; Swiegers, J. H. *FEMS Yeast Res.* **2009**, *9*, 446–459.
25. Koek, M. M.; Jellema, R. H.; van der Greef, J.; Tas, A. C.; Hankemeier, T. *Metabolomics* **2011**, *7*, 307–328.
26. Szappanos, B.; Kovács, K.; Szamecz, B.; Honti, F.; Costanzo, M.; Baryshnikova, A.; Gelius-Dietrich, G.; Lercher, M. J.; Jelasity, M.; Myers, C. L.; Andrews, B. J.; Boone, C.; Oliver, S. G.; Pál, C.; Papp, B. *Nat. Genet.* **2011**, *43*, 656–662.

Downloaded by 89.163.35.42 on May 29, 2012 | http://pubs.acs.org
Publication Date (Web): May 29, 2012 | doi: 10.1021/bk-2012-1098.ch001

Chapter 2

Identification of Urinary and Salivary Biomarkers for Coffee Consumption

Roman Lang,* Anika Wahl, Timo Stark, and Thomas Hofmann

Chair of Food Chemistry and Molecular Sensory Science, Technical University of Munich, Lise-Meitner-Str 34, 85354 Freising, Germany
***E-mail: roman.lang@tum.de**

Downloaded by STANFORD UNIV GREEN LIBR on May 30, 2012 | http://pubs.acs.org
Publication Date (Web): May 29, 2012 | doi: 10.1021/bk-2012-1098.ch002

To evaluate putatively beneficial effects of coffee on human health, intervention studies are conducted. To correlate possible short term effects of consumption, the subjects need to run through washout periods prior to the coffee intervention to serve as their own control. The coffee constituents trigonelline and *N*-methylpyridinium (NMP) were identified as compounds contributing most to the dissimilarities between the urine of coffee drinkers and non-coffee drinkers. Application of a developed stable isotope dilution assay in a coffee intervention study revealed significantly higher values of trigonelline and NMP (normalized to creatinine) in coffee drinker urine for up to 48 h and 72 h, respectively, when compared to non-coffee drinkers, proposing these two compounds as indicators for coffee consumption. Further investigations demonstrated, that trigonelline and NMP can be detected in human salivary fluid for ~16 h. According to acquired food data, roast coffee appears to be the predominating source for trigonelline and NMP in human diet.

Introduction

Food is meant to taste good and provide sufficient energy and nutrients to the body to meet the metabolic requirements. However, nutrition has a fundamental impact on human health and plays an important role in the development of chronic diseases.

In Recent Advances in the Analysis of Food and Flavors; Toth, S., et al.;
ACS Symposium Series; American Chemical Society: Washington, DC, 2012.

Downloaded by STANFORD UNIV GREEN LIBR on May 30, 2012 | http://pubs.acs.org
Publication Date (Web): May 29, 2012 | doi: 10.1021/bk-2012-1098.ch002

Evidence was found for an association of a diet rich in foods with high glycemic load and the development of coronary heart disease and diabetes type 2. Epidemiologic studies suggest "healthy" nutritional patterns rich in fruit, vegetables, fish and whole grain cereals are linked to lower rates of coronary heart disease, cancers and diabetes (*1–5*). The fact, that the instant impact of the diet may be small or even negligible, while the consumption over a life span may significantly affect health (*6*), severely complicates the investigations of the underlying mechanisms involved.

In contrast to controlled studies with rigid dietary recommendations, data on nutritional habits in "free-living populations" are recorded by questionnaires. These, however, are prone to bias since they rely on the study participant recalling the consumed diet in rather great detail. Suitable markers could help objectify these data with respect to accuracy (*7*). The compounds in Figure 1 give an overview on some of the few food biomarkers developed and validated as objective measures to assess dietary intake.

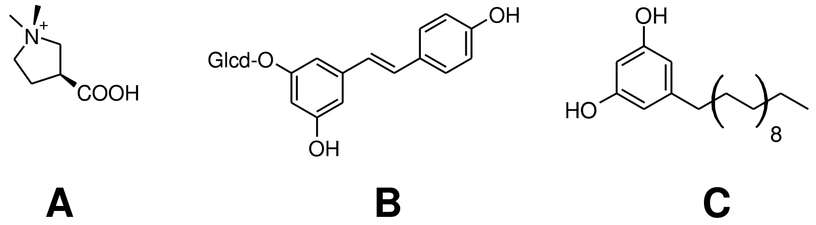

Figure 1. Structures of proposed biomarkers indicating consumption of citrus fruit (A: proline betaine), wine (B: metabolites of resveratrol, e.g. resveratrol-3-O-glucuronide) and whole-grain rye (C: alkylresorcinols, e.g. 1,3-dihydroxy-5-nonadecylbenzene).

Determination of urinary proline betaine has been proposed as a quantitative marker for consumption of citrus fruit (*7*). Alkylresorcinols, which are present nearly exclusively in the outer parts of wheat and rye grains have been investigated as markers for consumption of whole grain cereals (*8*, *9*). Metabolites of the stilbenoid resveratrol, present in e.g. berries and grapes, were found to be suitable biomarkers for wine consumption (*10*).

A luxury much appreciated and habitually consumed by millions of people is roast coffee. Valued particularly for its stimulating effect and its pleasant flavor, moderate consumption of the brew is discussed in the context of putative beneficial side effects on human health, e.g. lowering the risk to develop diabetes type 2 or Alzheimer‘s disease (*11–13*). The underlying mechanisms, however, are unclear. In order to examine both short and long term effects of roast coffee on health by means of intervention studies, the intake of coffee needs to be recorded. A valid quantitative biomarker for coffee consumption could help to objectify and to add accuracy to the data from dietary questionnaires. Some compounds have

Downloaded by STANFORD UNIV GREEN LIBR on May 30, 2012 | http://pubs.acs.org
Publication Date (Web): May 29, 2012 | doi: 10.1021/bk-2012-1098.ch002

been proposed for this purpose in the past, e.g. feruloylglycine, which is a major urinary metabolite of chlorogenic acids (*14*). However, chlorogenic acids are widely distributed in plants and therefore are not specific for coffee (*15*).

The aim of the studies was to identify coffee specific compounds in human urine suitable to trace coffee consumption, develop a high throughput quantitation method and evaluate the feasibility of the markers in a pilot scale human intervention study.

Experimental Section

Chemicals were obtained from Sigma-Aldrich (Steinheim, Germany). d_3-creatinine was obtained from CDN (Dr. Ehrenstorfer, Augsburg, Germany). *N*-methylpyridinium iodide, d_3-*N*-methylpyridinium iodide and d_3-trigonelline hydroiodide were synthesized (*16*).

The holistic screening of samples of coffee drinker urine and non-coffee drinker urine by HILIC-UPLC-Time-of-Flight-mass spectrometry, principal component analysis, validation of a stable isotope dilution assay (SIDA) for LC-MS/MS quantitation of *N*-methylpyridinium, trigonelline and creatinine in human urine, as well as the design of the human intervention study are published elsewhere (*17*).

Quantitation of *N*-Methylpyridinium and Trigonelline in Human Urine

For quantitation of *N*-methylpyridinum, trigonelline and creatinine, the urine sample (10 µL) was diluted with the internal standards (d_3-NMP 1 µM, d_3-trigonelline 1 µM and d_3-creatinine 10 µM in acetonitrile/water 9/1, 1 mL), centrifuged (12,500 rpm, 5 min) and the supernatant injected into the LC-MS/MS system (1 µL).

Quantitation of *N*-Methylpyridinium and Trigonelline in Human Saliva

For quantitation of *N*-methylpyridinium (NMP) and trigonelline in human saliva, calibration standards were prepared by mixing aliquots of blank saliva (900 µL) with aqueous dilutions of NMP and trigonelline (0.200-500 µM, 100 µL) yielding saliva samples containing NMP and trigonelline in concentrations of 0.02-50 µM. To evaluate precision and accuracy, quality control samples were prepared by spiking blank saliva (900 µL) with solutions of NMP and trigonelline (100 µL) yielding samples with low (0.31 µM in saliva) and high (2.5 µM in saliva) addition levels. The lower limit of quantification (LLOQ) was defined as the lowest calibration standard with precision <15% relative standard deviation (RSD) and accuracy >80 %. The calibration standards, quality control samples and authentic saliva samples (200 µL) were mixed with the internal standard solution (d_3-NMP and d_3-trigonelline, 1 µM, 200 µL) and acetonitrile (600 µL) and vortexed briefly. The samples were centrifuged (12,500 rpm, 5 min) and the clear supernatant analysed by LC-MS/MS (*17*).

Saliva samples were obtained from coffee drinkers (n=2) before and directly after coffee ingestion, as well as after extensive mouth rinsing with citric acid (0.5% in drinking water) and drinking water. Within the first 30 min, saliva samples were collected at 5 min intervals, and finally after 40, 50, 60, 90 and 120 min. Saliva samples were processed and analysed in triplicate (n=3).

Analysis of Trigonelline and NMP in Coffee Powder and Food Products

The sample (200 mg) was mixed with aqueous ethanol (50/50, v/v, 5 mL) and heated in a closed reaction vessel (1 h, 100 °C). After cooling, the suspension was decanted into a 25 mL volumetric flask, filled with water and mixed. An aliquot (100 µL) was added to the internal standard solution (d_3-trigonelline 1 mM and d_3-NMP 0.25 mM, 100 µL) and incubated with light shaking (5 min). An aliquot of the mixture (100 µL) was applied on a 96 well plate SPE (100 mg, RP18) preconditioned with acetonitrile and water (200 µL each). The sample was sucked through the material and washed with water (2×100 µL). The combined filtrates were diluted with acetonitrile (1+9, v+v) and injected into the HPLC-MS/MS system (2 µL). Each sample was extracted, processed and analysed in duplicate (n=2).

Results and Discussion

Identification of Coffee Specific Compounds in Human Urine

In order to locate coffee specific compounds in human urine, a holistic screening of individual as well as pooled urine samples of habitual coffee drinkers (n=9) and non-coffee drinkers (n=9) was performed by means of HILIC-UPLC-Time-of-Flight mass spectrometry. Each sample was injected in quadruplicate and from the exact mass-retention time data, a principal component analysis revealed a distinct differentiation of coffee drinker- and non-coffee drinker urine (*17*). Comparison of the pooled samples and visualization of the differences in an S-Plot forwarded three ions (see Figure 2) contributing most to the dissimilarities of the two samples. Calculation of the sum formulae based on the exact masses proposed $C_7H_8NO_2$, $C_7H_9N_2O$ and C_6H_8N, fitting well to the compounds trigonelline (A), N-methylnicotinamide (B) and *N*-methylpyridinium (C).

The identity of these compounds was verified by comparison of the retention times and the exact masses of reference compounds and authentic coffee-drinker urine samples as given in Figure 3.

Trigonelline is a phytohormone widely distributed in plants and therefore present in many foods like tomatoes, barley corn and particularly legumes (*18*). In green coffee, it is the second most abundant alkaloid beside caffeine and accounts for roughly 0.3% to 1% dry weight basis (*19*). It is known that trigonelline degrades to volatile pyridines and pyrroles, nicotinic acid, *N*-methylpyridinium and other compounds during coffee roasting (*20*). Pyrolysis experiments with various salts of trigonelline demonstrated, that *N*-methylpyridinium becomes a major reaction product when temperatures at 245°C were applied (*21*). In

Downloaded by STANFORD UNIV GREEN LIBR on May 30, 2012 | http://pubs.acs.org
Publication Date (Web): May 29, 2012 | doi: 10.1021/bk-2012-1098.ch002

Downloaded by STANFORD UNIV GREEN LIBR on May 30, 2012 | http://pubs.acs.org
Publication Date (Web): May 29, 2012 | doi: 10.1021/bk-2012-1098.ch002

contrast to trigonelline and *N*-methylpyridinium, *N*-methylnicotinamide is one of the major metabolites of niacin, a compound present in many different foods. We excluded *N*-methylnicotinamide as it was not a coffee specific substance, and focused on trigonelline and NMP as potential markers for coffee consumption.

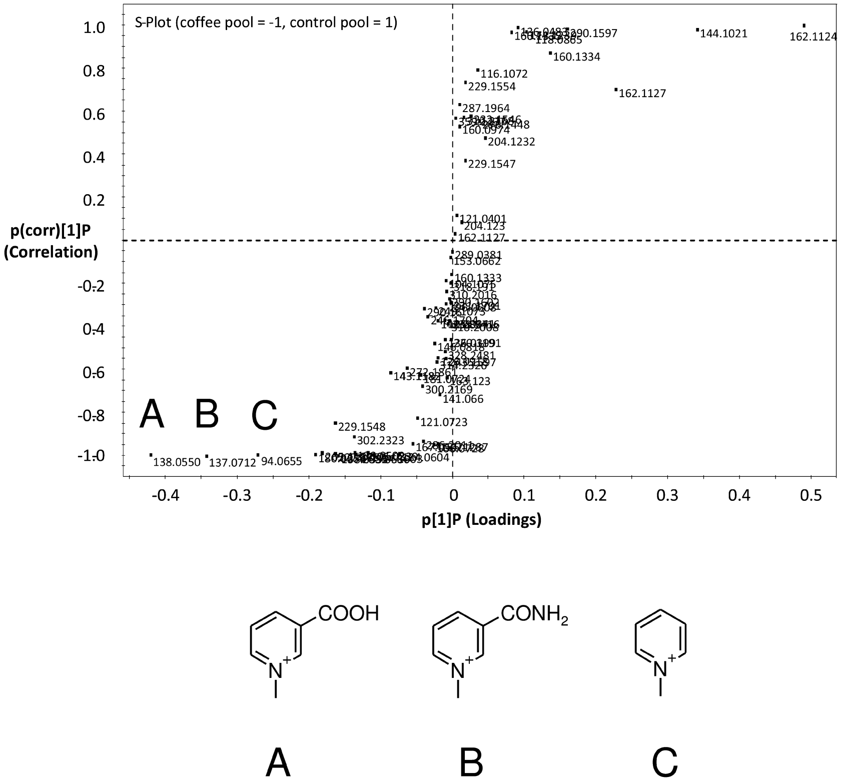

Figure 2. Visualization of ions (m/z) contributing most to the dissimilarities between pooled samples of coffee drinker urine and non-coffee drinker urine by means of an S-Plot (Markerlynx™). The compounds at the bottom left area are the most specific markers for coffee drinker's urine: A) trigonelline, B) N-methynicotinamide, C) N-methylpyridinium. Original data from (17).

Method Development for Quantitation of the Coffee Specific Compounds in Urine

The quantitative analysis of trigonelline and *N*-methylpyridinium (NMP) in urine specimens was planned to be a high throughput stable isotope dilution analysis involving a minimum of sample preparation.

Downloaded by STANFORD UNIV GREEN LIBR on May 30, 2012 | http://pubs.acs.org
Publication Date (Web): May 29, 2012 | doi: 10.1021/bk-2012-1098.ch002

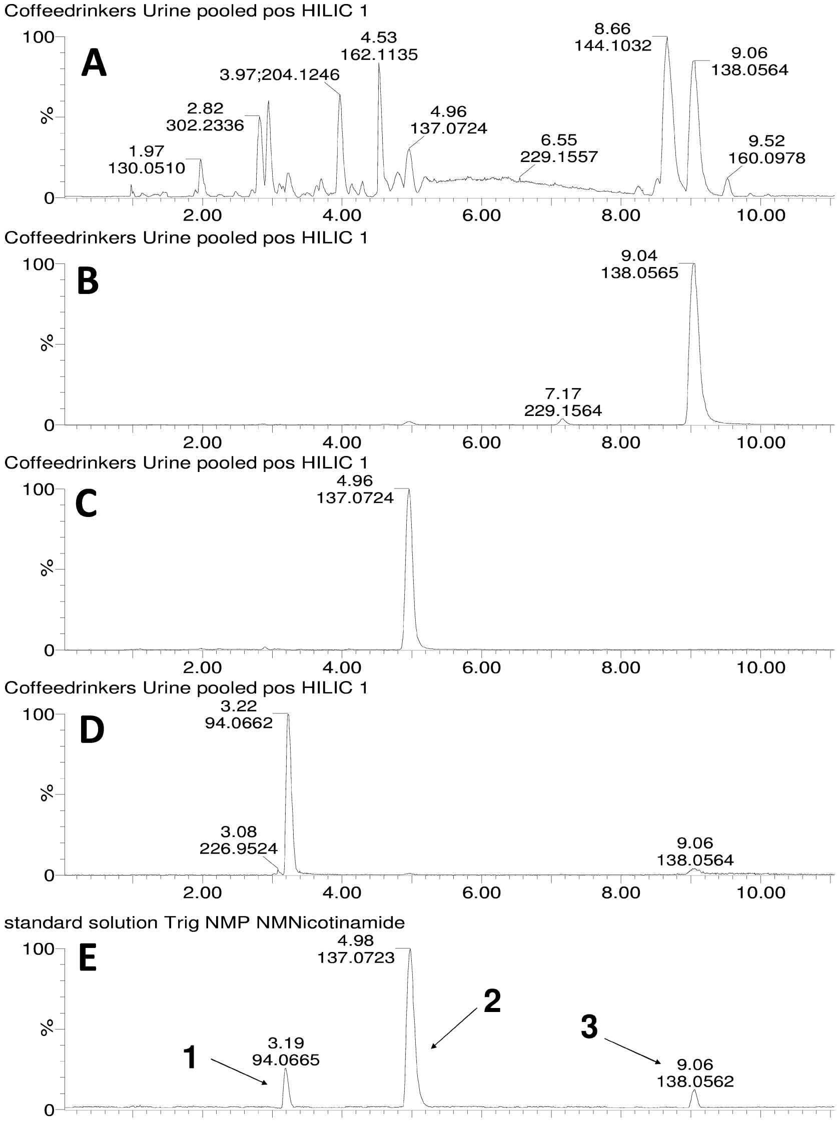

Figure 3. Base peak Ion chromatograms (ESI$^+$, m/z 50-600) of pooled coffee drinker urine (A), the extracted ion chromatograms of the most important markers m/z 138.0565 (B), 137.0724 (C), 94.0662 (D), and the Base Peak Ion chromatogram of a standard solution containing the reference compounds N-methylpyridinium (1), N-methylnicotinamide (2) and trigonelline (3) (E).

The composition of the eluent was a mixture of aqueous acetonitrile containing formic acid and ammonium acetate, allowing baseline separation of creatinine, trigonelline and NMP under isocratic conditions. The mass spectrometer was operated in positive electrospray mode. Compound specific mass transitions were optimized for selective quantitation in MS/MS. Calibration standards of mixtures of analytes and deuterated internal standards were prepared in artificial urine since no urine matrix void of NMP, trigonelline and creatinine could be obtained. The area ratios of analyte and internal standard were plotted versus the concentration ratios, and linear regressions were calculated with 1/x weighing. In the final protocol, a small aliquot of sample was diluted in a solution of the labeled internal standards in acetonitrile. Occasionally occurring precipitates were removed by centrifugation, and the resulting solution could be directly injected into the LC-MS/MS system. Creatinine, trigonelline and NMP could be quantified in urine with a precision <5% RSD and accuracy 90.7 – 103.0% (*17*).

Downloaded by STANFORD UNIV GREEN LIBR on May 30, 2012 | http://pubs.acs.org
Publication Date (Web): May 29, 2012 | doi: 10.1021/bk-2012-1098.ch002

Urinary Trigonelline and NMP as Measures for Compliance

In order to assess the value of trigonelline and *N*-methylpyridinium concentrations in human urine as a measure to monitor the compliance in the washout-period of a coffee intervention study, a pilot-scale study was conducted. The morning urines of the participants (4 males, 5 females) before (0 h) and 8, 24, 48, 72 and 240 h after ingestion of a single bolus dose of roast coffee brew were analyzed as well as the morning urines of non-coffee drinkers (4 males, 5 females). The data of trigonelline and *N*-methylpyridinium, normalized to individual creatinine concentrations, are depicted in Figure 4 (*17*).

The data of coffee drinker- and non-coffee drinker samples were compared by means of a two tailed t-test revealing significantly elevated trigonelline/creatinine and NMP/creatinine values for up to 48 h (p=0.0011) and 72 h (p=0.0021), respectively. These results led to the conclusion, that recent consumption of roast coffee brew can be detected for up to 72 h by quantifying urinary NMP.

While we already reported pharmacokinetic data on the bioappearance of trigonelline and N-methylpyridnium in human plasma after coffee consumption (*16*), the high throughput stable isotope dilution assay for quantitation of creatinine, trigonelline and N-methylpyridinum in urine was developed as a non-invasive tool for compliance control in washout periods of future coffee intervention studies.

Downloaded by STANFORD UNIV GREEN LIBR on May 30, 2012 | http://pubs.acs.org
Publication Date (Web): May 29, 2012 | doi: 10.1021/bk-2012-1098.ch002

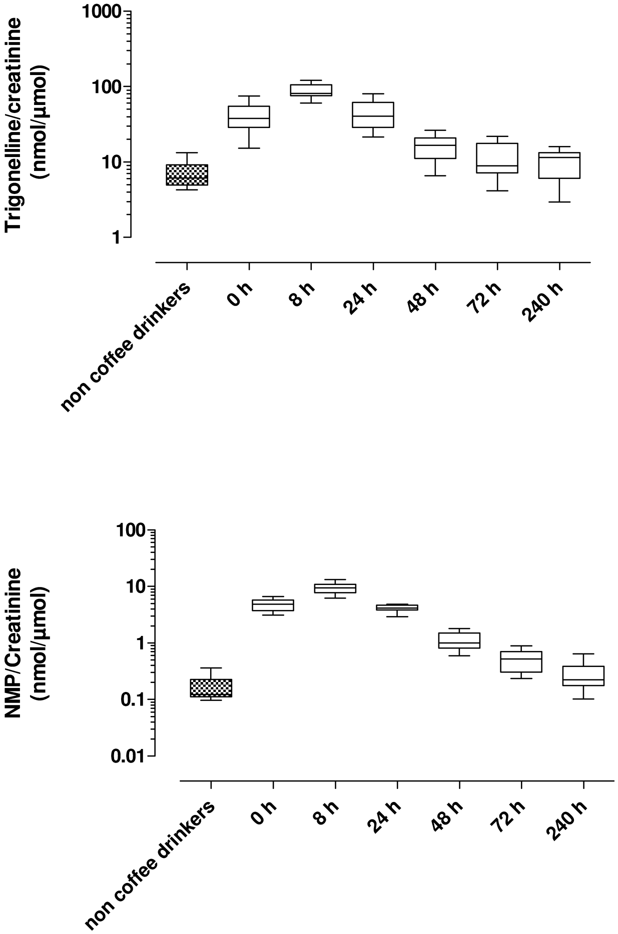

Figure 4. Box-Whisker plots (Median, 25 and 75 % quantiles, observed range) of N-methylpyridinium (bottom) and trigonelline (top) in the urine of non-coffee drinkers, and in the urine of habitual coffee drinkers before (0h) and 8, 24, 48, 72 and 240 hours after a single dose of roast coffee brew. Concentrations are normalized to individual creatinine and given as nmol analyte per µmol of creatinine.

Trigonelline and NMP in Salivary Fluid

Besides urine, we considered saliva as an alternative, non-invasive type of conveniently obtainable sample. In initial experiments, we analyzed human saliva to which the isotopically labeled internal standards d_3-NMP and d_3-trigonelline were added followed by precipitation of proteins with cold acetonitrile. Surprisingly, trigonelline and NMP could be quantified in saliva 2 and even 16 h after coffee ingestion, while these compounds were not detectable in non-coffee drinker saliva (cf. Figure 5).

Downloaded by STANFORD UNIV GREEN LIBR on May 30, 2012 | http://pubs.acs.org
Publication Date (Web): May 29, 2012 | doi: 10.1021/bk-2012-1098.ch002

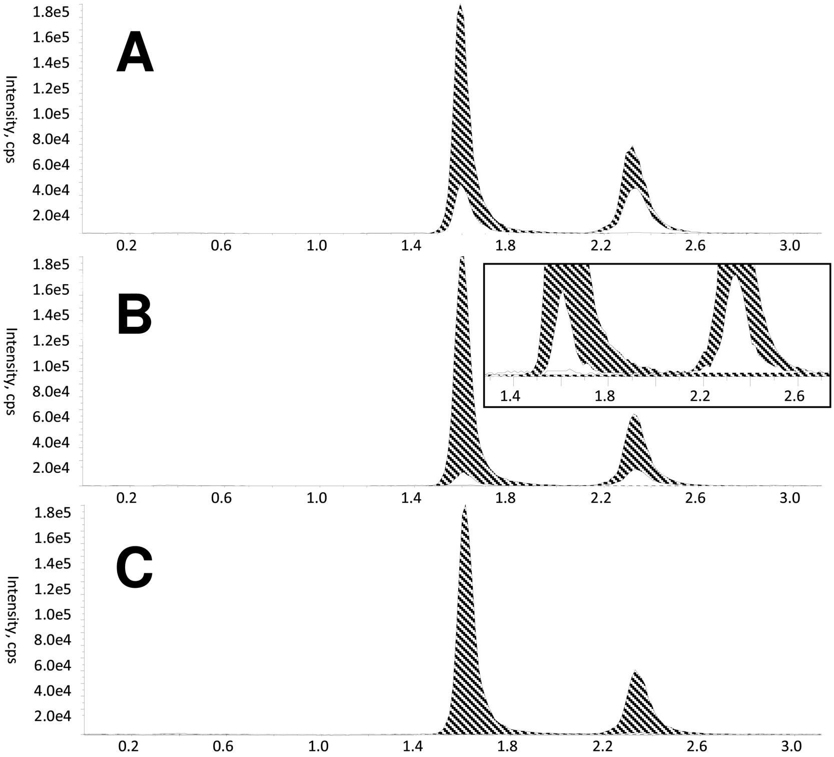

Figure 5. LC-MS/MS chromatograms of N-methylpyridinium (first eluting compound) and trigonelline (second eluting compound) in human saliva. The internal standards d_3-NMP (m/z 97>79) and d_3-trigonelline (m/z 141>97) are shaded, the analytes NMP (m/z 94>79) and trigonelline (m/z 138>94) are given in white. A) 120 min after coffee ingestion, B) 16 h after coffee ingestion (with enlargement 1.4 to 2.6 min), C) saliva of a non-coffee drinker.

To investigate the value of oral fluid as an alternative to urine for control of coffee ingestion, we validated the quantitation method for saliva matrix. Calibration of the standards and references was done in saliva with no detectable amounts of NMP and only small concentrations of trigonelline (56 pmol/mL) leading to an offset of the calibration (cf. Table 1). The precision and accuracy of the standards based on the back calculated data were <15% RSD precision and 94-103% accuracy. Spiked saliva samples showed precision <6% RSD and accuracy between 99 and 102% (cf Table 1 and 2).

In a small scale study, saliva samples were collected from the participating volunteers (coffee drinkers) in the morning before and directly after one cup (125 mL) of roast coffee brew, after extensive mouth rinsing with aqueous citric acid and water, and then in intervals of 5 min and 10 min. The volunteers had to abstain from further coffee consumption throughout the day. The last sample was collected on the following morning, ~20 h after coffee ingestion.

Table 1. Properties of calibration curves prepared in salivary fluid

	Linear range (µM)	*Linear regression*[2]	*RSD (%)*[1]	*Accuracy*[1]	*LLOQ (µM)*
NMP	0.04 – 50	y = 0.829x + 0.002	1 – 14%	94 – 103%	0.04
Trigonelline	0.31 – 50	y = 1.170x + 0.127	1 – 13%	98 – 102%	0.31

[1] Precision and accuracy of back calculated standards. Weighing factor was 1/x, R^2 was >0.99. [2] y=Area A/IS, x= concentration A/IS.

Table 2. Accuracy and precision of the quantification of trigonelline and NMP in salivary fluid

	Addition (µM)	*Addition found (±RSD%, µM)*[1]	*Accuracy (%)*[1]
NMP	0.31	0.31(±2.6)	100
	2.50	2.48(±2.8)	99.4
Trigonelline	0.31	0.31(±5.2)	102
	2.50	2.54(±4.7)	102

[1] Data are calculated from n=3.

The concentration-time profiles obtained for trigonelline and NMP (Figure 6) were similarly shaped, however, trigonelline was more abundant by a factor of roughly 10 in each sample. From the basal levels (A in Figure 6), there was a steep incline to maximum concentrations directly after coffee (B). Concentrations drastically dropped after rinsing with citric acid and water (C, D), and further sampling showed that trigonelline and NMP concentrations decreased within the following 2 h reaching a plateau. After 20 h, NMP and trigonelline were still detectable but the concentrations measured were below the LLOQ in case of NMP and in the dimension of the LLOQ in the case of trigonelline (0.51±0.10 µM).

These initial experiments revealed that oral fluid might serve as a type of sample suitable for analysis in the context of compliance control in coffee intervention studies. However, while the process of sampling could be considered non-invasive and more convenient than the collection of human urine, the relatively short-lived detectability of trigonelline and NMP in saliva would necessitate daily sampling to consistently monitor the adherence to coffee abstinence.

Downloaded by STANFORD UNIV GREEN LIBR on May 30, 2012 | http://pubs.acs.org
Publication Date (Web): May 29, 2012 | doi: 10.1021/bk-2012-1098.ch002

Downloaded by STANFORD UNIV GREEN LIBR on May 30, 2012 | http://pubs.acs.org
Publication Date (Web): May 29, 2012 | doi: 10.1021/bk-2012-1098.ch002

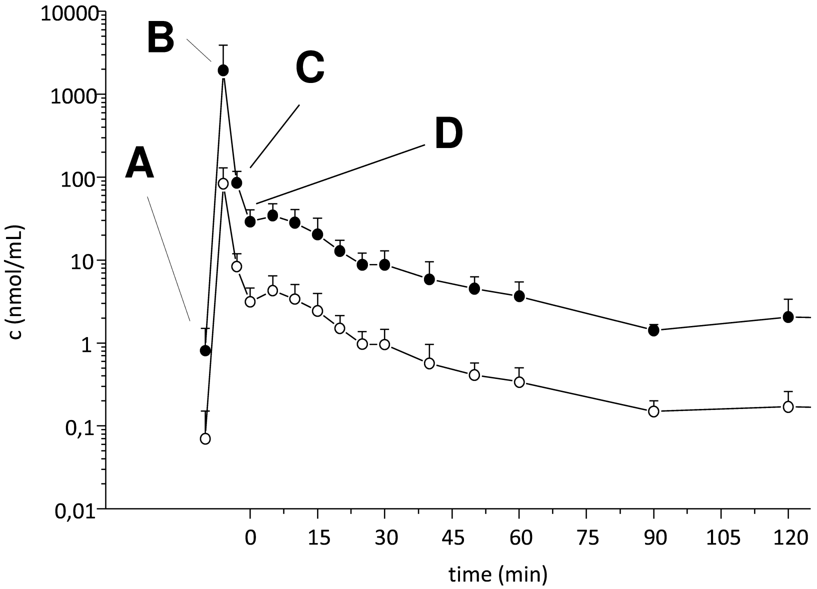

Figure 6. Concentrations of N-methylpyridinium (circles) and trigonelline (dots) in human saliva after coffee ingestion. A) before coffee ingestion, B) after coffee ingestion, C) after rinsing with aqueous citric acid (0.5%), D) after further rinsing with water. Every point is the mean+SD of saliva from two individuals, each analyzed in triplicate.

Dietary Sources for Trigonelline and NMP

While both the holistic screening of urine specimens by UPLC-ToF MS as well as analysis of urine and saliva samples from coffee intervention studies by HPLC-MS/MS demonstrated roast coffee consumption as the predominant source for the substantial levels of trigonelline and NMP in coffee drinkers, we found traces even in non-coffee drinker urine and saliva (cf. figures 4 and 6). While small amounts of trigonelline can originate from niacin metabolism (*18*), we analyzed several legumes, leaves and seeds as well as buckwheat and curry powder to get an insight into dietary sources of the two compounds beside roast coffee (Table 3).

In accordance with literature data (*18*), trigonelline was present in all legumes analyzed with quantities between 68 and 258 ppm. Fenugreek contained 430 – 608 ppm while in tobacco, sesame, buckwheat and flax only traces were detected. Roast coffee was found to be the richest source for trigonelline with a concentration of 5,313 µg/g exceeding that of the legumes by a factor of roughly 20. Surprisingly, only minor amounts of trigonelline were found in curry powder, although fenugreek is a basic ingredient of this mixture of spices (Table 3). *N*-methylpyridinium was detected exclusively in roast coffee and to a minor extent in fenugreek seeds submitted to roasting. Not even trace amounts were detected in the other samples.

Downloaded by STANFORD UNIV GREEN LIBR on May 30, 2012 | http://pubs.acs.org
Publication Date (Web): May 29, 2012 | doi: 10.1021/bk-2012-1098.ch002

Table 3. Dietary sources for trigonelline and NMP

		Trigonelline[1] *(ppm)*	*NMP*[1] *(ppm)*
Legumes	White beans	258 (±5.4%)	n.d.
	Green peas	128 (±3.1%)	n.d.
	Kidney beans	252 (±1.2%)	n.d.
	Red lentils	91 (±2.1%)	n.d.
	Plate lentils	68 (±1.5%)	n.d.
Leaves	Tobacco (burley)	15 (±6.7%)	n.d.
	Tobacco (oriental)	36 (±11%)	n.d.
Seeds	Sesame	2 (±25%)	n.d.
	Flax seed	10 (±10%)	n.d.
	Fenugreek (fresh)	430 (±2.3%)	n.d.
	Fenugreek (roasted)	608 (±0.9%)	78 (±5.1%)
	Coffee (roasted, Brazil)[2]	5,313 (±7.2%)[2]	855 (±6.5%)[2]
Miscellaneous	Buckwheat	11 (±27%)	n.d.
	Curry powder	22 (±4.5%)	n.d.

[1] Data are means (±RSD) of duplicate extractions (n=2); ppm: µg/g; data are based on fresh weight. [2] concentration in roast coffee was calculated on the basis of the concentration of the hot water extract (coffee brew, n=8) using the standard recipe (48 g, 800 mL brew) and the extraction yield of 90% for NMP and 100% for trigonelline. Original data on the concentrations in the brew are from (*16*)

While Table 3 gives only a brief survey on some foods, the data suggests that consumption of trigonelline rich foods like legumes can add to the small amounts formed from niacin metabolism, thus explaining the observed basal concentrations of trigonelline in urine and saliva. Considering NMP found in the food samples, roast coffee was by far the dominating source.

Conclusions

The coffee compounds trigonelline and *N*-methylpyridinium were identified as dietary biomarkers for coffee consumption. Quantitative studies revealed that a single cup of coffee can be detected by analysis of *N*-methylpyridinium in salivary fluid and urine samples for up to 16 h and 72 h, respectively, proposing this method as a tool to monitor adherence to dietary restrictions in coffee intervention studies.

References

1. Mente, A.; de Koning, L.; Shannon, H. S.; Anand, S. S. *Arch. Intern Med.* **2009**, *169*, 659–669.
2. Hu, F. B.; Manson, J. E.; Stampfer, M. J.; Colditz, G.; Liu, S.; Solomon, C.; Willett, W. C. *N. Engl. J. Med.* **2001**, *345*, 790–797.
3. Greenberg, J. A.; Boozer, C. N.; Geliebter, A. *Am. J. Clin. Nutr.* **2006**, *84*, 682–693.
4. Riboli, E.; Norat, T. *Am. J. Clin. Nutr.* **2003**, *78* (suppl.), 559S–569S.
5. Venn, B. J.; Mann, J. I. *Eur. J. Clin. Nutr.* **2004**, *58*, 1443–61.
6. Weber, P. *Br. J. Nutr.* **2001**, *86* (suppl. 1), S93–S95.
7. Heinzmann, S. S.; Brown, I. J.; Chan, Q.; Bictash, M.; Dumas, M.-E.; Kochhar, S.; Stamler, J.; Holmes, E.; Elliott, P.; Nicholson, J. K. *Am. J. Clin. Nutr.* **2010**, *92*, 436–443.
8. Landberg, R.; Kamal-Eldin, A.; Andersson, A.; Vessby, B.; Åman, P. *Am. J. Clin. Nutr.* **2008**, *87*, 832–838.
9. Landberg, R.; Åman, P.; Friberg, E. F.; Vessby, B.; Adlercreutz, H.; Kamal-Eldin, A. *Am. J. Clin. Nutr.* **2009**, *89*, 290–296.
10. Zamora-Ros, P.; Urpí-Sardà, M.; Lamuela-Raventós, R. M.; Estruch, A.; Vásquez-Agell, M.; Serrano-Martínez; Jaeger, W.; Lacueva-Andres, C. *Clin. Chem.* **2006**, *52*, 1373–1380.
11. van Dam, R. M.; Hu, F. B. *J. Am. Med. Assoc.* **2005**, *294*, 97–104.
12. Lindsay, J.; Laurin, D.; Verreault, R.; Helliwell, B.; Hill, G. B.; McDowell, I. *Am. J. Epidemiol.* **2002**, *56*, 445–453.
13. Cao, C.; Wang, L.; Lin, X.; Mamcarz, M.; Zhang, C.; Bai, G.; Nong, J.; Sussman, S.; Arendash, G. J. *Alzheimer Dis.* DOI 10.3233/JAD-2011-110110.
14. Stalmach, A.; Mullen, W.; Barron, D.; Uchida, K.; Yokota, T.; Cavin, C.; Steiling, H.; Williamson, G.; Crozier, A. *Drug Metab. Dispos.* **2009**, *37*, 1749–1758.
15. Clifford, M. N. *J. Sci. Food Agric.* **1999**, *79*, 362–372.
16. Lang, R.; Wahl, A.; Skurk, T.; Yagar, E. F.; Schmiech, L.; Eggers, R.; Hauner, H.; Hofmann, T. *Anal.Chem.* **2010**, *82*, 1486–1497.
17. Lang, R.; Wahl, A.; Stark, T.; Hofmann, T. *Mol. Nutr. Food Res.* **2011**, DOI:10.1002/mnfr.201000656.
18. http://ntp.niehs.nih.gov/ntp/htdocs/Cherm_Background/ExSumPdf/Trigonelline.pdf accessed via the internet on 14/12/2010.
19. Stennert, A.; Maier, H. G. *Z. Lebensm. Unters. Forsch.* **1993**, *196*, 430–434.
20. Viani, R.; Horman, I. *J. Food Sci.* **1974**, *39*, 1216–1217.
21. Stadler, R. H.; Varga, N.; Hau, J.; Arce Vera, F.; Welti, D. *J. Agric Food Chem.* **2002**, *50*, 1192–1199.

Downloaded by STANFORD UNIV GREEN LIBR on May 30, 2012 | http://pubs.acs.org
Publication Date (Web): May 29, 2012 | doi: 10.1021/bk-2012-1098.ch002

Downloaded by UNIV OF GUELPH LIBRARY on May 29, 2012 | http://pubs.acs.org
Publication Date (Web): May 29, 2012 | doi: 10.1021/bk-2012-1098.ch003

Chapter 3

Analytical and Sensory Characterization of Chiral 4-Mercapto-2-alkanones, 4-Acetylthio-2-alkanones, and the Corresponding Alcohols

M. Wakabayashi,[2,3] H. Wakabayashi,[4] S. Nörenberg,[1] B. Reichardt,[1] K. Kubota,[3] and K.-H. Engel*,[1]

[1]Technische Universität München, Lehrstuhl für Allgemeine Lebensmitteltechnologie, Maximus-von-Imhof-Forum 2, D-85350 Freising-Weihenstephan, Germany
[2]Department of Nutrition and Dietetics, Kamakura Women's University, 6-1-3 Ofuna, Kamakura-shi, Kanagawa 247-8512, Japan
[3]Department of Food and Nutritional Sciences, Graduate School of Humanities and Sciences, Ochanomizu University, 2-1-1 Otsuka, Bunkyo-ku, Tokyo 112-8610, Japan
[4]Institute of Environmental Science for Human Life, Ochanomizu University, 2-1-1 Otsuka, Bunkyo-ku, Tokyo 112-8610, Japan
***E-mail: k.h.engel@wzw.tum.de**

Polyfunctional thiols are known to play important roles as aroma compounds owing to their pronounced odor qualities and their low odor thresholds; β-mercaptocarbonyls as well as β-mercaptoalcohols are prominent examples. This chapter describes (i) the enantioseparation of a homologous series of 4-mercapto-2-alkanones and 4-acetylthio-2-alkanones, (ii) the determination of the absolute configurations using a combination of the ^{1}H-NMR anisotropy method and lipase-catalyzed kinetic resolution, (iii) the assessment of the sensory properties of enantiomers by GC/O using a chiral stationary phase, and (iv) the synthesis and the establishment of chromatographic and sensory data on 4-mercapto-2-alkanols and 4-acetylthio-2-alkanols.

In Recent Advances in the Analysis of Food and Flavors; Toth, S., et al.;
ACS Symposium Series; American Chemical Society: Washington, DC, 2012.

Downloaded by UNIV OF GUELPH LIBRARY on May 29, 2012 | http://pubs.acs.org
Publication Date (Web): May 29, 2012 | doi: 10.1021/bk-2012-1098.ch003

Introduction

Sulfur-containing volatiles play important roles as aroma compounds in foods (*1–4*). In particular, polyfunctional thiols exhibit pronounced odor properties and low odor thresholds (*5*). Many aroma compounds with tropical, fruity and vegetable odor properties are characterized by a common structure based on a 1,3-oxygen-sulfur functionality; therefore, this structural feature has been termed “tropical olfactophore” (*6*). Passion fruits, for example, contain 3-mercaptohexanol, 3-methylthiohexanol, the corresponding esters and 2-methyl-4-propyl-1,3-oxathianes as volatiles fulfilling these structural requirements (*7*, *8*). Absolute configurations of these substances have been determined (*9*), lipase-catalyzed approaches to obtain the enantiomers via kinetic resolution have been reported (*10*), and the sensory properties of the enantiomers have been described (*11–13*).

In addition to primary 3-mercaptoalcohols, the corresponding ß-mercaptocarbonyls and ß-mercaptoalcohols have been shown to be of sensorial relevance. Selected representatives, such as 4-mercapto-2-pentanone and 4-mercapto-2-nonanone as well as the corresponding alcohols have been prepared via combinatorial synthesis and their odor properties have been determined by gas chromatography/olfactometry (GC/O) (*14*). 4-Mercapto-2-heptanone, 4-mercapto-2-heptanol and 4-mercapto-2-nonanol have been identified in cooked bell pepper and their sensory properties have been assessed in NaCl and sugar solutions (*15*). 4-Mercapto-2-pentanone and 4-mercapto-2-pentanol have been tentatively identified in aged Cheddar cheese (*16*).

Potential differences in odor properties between the enantiomers of 4-mercapto-2-alkanones have not yet been investigated. For 4-mercapto-2-alkanols sensory data were only available for selected diastereoisomers (*14*) or mixtures of diastereoisomers (*15*). Therefore, the objectives of this study were (i) to synthesize a homologous series of 4-mercapto-2-alkanones (ii) to separate their enantiomers via capillary gas chromatography using a chiral stationary phase, and (iii) to assess the sensory properties of the enantiomers by GC/O. Considering the suggestion that the 1,3-oxygen-sulfur functionality required for the “olfactophore” may be extended to the acetylthio-derivatives (*17*), the sensory properties of the structurally related 4-acetylthio-2-alkanones were also investigated. In addition, a first set of chromatographic and sensory data for a homologous series of 4-mercapto-2-alkanols and 4-acetylthio-2-alkanols should be elaborated.

Experimental Section

Synthesis of 4-Mercapto-2-alkanones and 4-Acetylthio-2-alkanones

4-Mercapto-2-alkanones and 4-acetylthio-2-alkanones were synthesized by Michael-type addition of hydrogen sulfide (2.5 equiv.) and thioacetic acid (1.5 equiv.), respectively, to 3-alken-2-ones (1.0 equiv.). Experimental details, chromatographic, mass spectrometric and NMR data have been previously reported (*18*).

Synthesis of 4-Mercapto-2-alkanols and 4-Acetylthio-2-alkanols

4-Mercapto-2-alkanols were synthesized by reduction of the corresponding 4-acetylthio-2-alkanones (1.0 equiv.) using lithium aluminium hydride (4.5 equiv.) in THF (*15*). *4-Mercapto-2-pentanol.* Yield: 105%, purity: 87% by GC (ratio of diastereoisomers, 39:61), linear retention index (LRI) (DB-Wax): 1573, 1599, (DB-1): 915, 927, GC-MS (*m/z*, rel.%) (both isomers show the same fragmentation): 45 (100), 86 (44), 61 (38), 71 (37), 43 (32), 41 (30), 60 (27), 69 (23), 42 (20), 59 (13), 120 (M^+, 6). *4-Mercapto-2-heptanol.* Yield: 101%, purity: 94% by GC (ratio of diastereoisomers, 39:61), LRI (DB-Wax): 1751, 1768, (DB-1): 1112, 1118, GC-MS (*m/z*, rel.%): 45 (100), 55 (98), 71 (76), 43 (46), 114 (43), 41 (32), 87 (28), 97 (26), 61 (23), 58 (20), 148 (M^+, 6). *4-Mercapto-2-octanol.* Yield: 84%; purity: 92% by GC (ratio of diastereoisomers, 41:59), LRI (DB-Wax): 1847, 1862, (DB-1): 1209, 1218, GC-MS (*m/z*, rel.%): 45 (100), 69 (87), 71 (87), 55 (54), 43 (54), 41 (52), 128 (48), 60 (28), 74 (27), 102 (26), 162 (M^+, 5). *4-Mercapto-2-nonanol.* Yield: 97%, purity: 96% by GC (ratio of diastereoisomers, 41:59), LRI (DB-Wax): 1946, 1961, (DB-1): 1311, 1319, GC-MS (*m/z*, rel.%): 45 (100), 71 (92), 55 (82), 69 (63), 41 (51), 43 (50), 142 (46), 83 (34), 58 (31), 57 (28), 176 (M^+, 4). *4-Mercapto-2-decanol.* Yield: 94%, purity: 95% by GC (ratio of diastereoisomers, 40:60), LRI (DB-Wax): 2058, 2073, (DB-1): 1414, 1421, GC-MS (*m/z*, rel.%): 71 (100), 55 (98), 45 (93),43 (67), 41 (58), 69 (57), 156 (42), 83 (39), 58 (35), 102 (33), 190 (M^+, 4).

4-Acetylthio-2-alkanols were synthesized by reduction of 4-acetylthio-2-alkanones (1.0 equiv.) using sodium borohydride (2.0 equiv.) dissolved in a mixture of methanol and potassium phosphate buffer (50 mM, pH 7.4), (1:4, v/v), (*19*). *4-Acetylthio-2-pentanol.* Yield: 110%, purity: 91% by GC (ratio of diastereoisomers, 48:52), LRI (DB-Wax): 1820, 1919, (DB-1): 1133, 1160, GC-MS (*m/z*, rel.%) (both isomers shows same fragmentation): 43 (100), 45 (35), 102 (22), 71 (22), 69 (21), 119 (20), 60 (19), 162 (M^+, 0.10). *4-Acetylthio-2-heptanol.* Yield: 129%, purity: 69% by GC (ratio of diastereoisomers, 62:38), LRI (DB-Wax): 1939, 2038, (DB-1): 1302, 1323, GC-MS (*m/z*, rel.%): 43 (100), 55 (41), 45 (32), 71 (23), 147 (18), 87 (16), 97 (16), 130 (15), 190 (M^+, 0.19).

4-Acetylthio-2-octanol. Yield: 108%, purity: 84% by GC (ratio of diastereoisomers, 56:44), LRI (DB-Wax): 2042, 2133, (DB-1): 1398, 1416, GC-MS (*m/z*, rel.%): 43 (100), 69 (44), 45 (33), 71 (25), 55 (23), 102 (23), 161 (21), 41 (20), 204 (M^+, 0.19). *4-Acetylthio-2-nonanol.* Yield: 60%, purity: 69% by GC (ratio of diastereoisomers, 62:38), LRI (DB-Wax): 2137, 2222, (DB-1): 1495, 1511, GC-MS (*m/z*, rel.%): 43 (100), 55 (36), 69 (34), 45 (33), 71 (26), 83 (24), 41 (21), 175 (21), 218 (M^+, 0.13).

4-Acetylthio-2-decanol. Yield: 63%, purity: 54% by GC (ratio of diastereoisomers, 76:24), LRI (DB-Wax): 2240, 2320, (DB-1): 1532, 1610, GC-MS (*m/z*, rel.%): 43 (100), 55 (39), 45 (30), 69 (29), 71 (27), 83 (24), 41 (23), 102 (22), 232 (M^+, 0.13).

Downloaded by UNIV OF GUELPH LIBRARY on May 29, 2012 | http://pubs.acs.org
Publication Date (Web): May 29, 2012 | doi: 10.1021/bk-2012-1098.ch003

Enzyme-Catalyzed Hydrolysis of 4-Acetylthio-2-alkanones

The acetylthioester substrates (chain lengths C6 to C10; 50 µmol) were treated with porcine pancreas lipase (PPL) (10 mg) in potassium phosphate buffer (500 µL, 50 mM, pH 7.4). For 4-acetylthio-2-pentanone immobilized CAL-B (10 mg) was employed as biocatalyst. After 1 h, the reaction mixture was extracted twice with 700 •L of dichloromethane. After drying over sodium sulfate, the obtained organic phase was subjected to GC analysis (*18*).

Synthesis and HPLC-Separation of (S)-MαNP-thioesters of 4-Mercapto-2-alkanones

The obtained 4-mercapto-2-alkanones were esterfied with (*S*)-2-methoxy-2-(1-naphthyl)propionic acid ((*S*)-M•NP), as previously reported (*18*). Purified (*S*)-M•NP thioesters of 4-mercapto-2-alkanones were obtained by repetitive HPLC fractionations from crude products.

Capillary Gas Chromatography (GC-FID)

System I

Separations of the diastereoisomeric mixtures of 4-mercapto- and 4-acetylthio-2-alkanols were performed on an HP5890 A gas chromatograph: split/splitless injector (215 °C, split ratio 7:1), FID (350 °C), DB-Wax column (30 m x 0.25 mm (i.d.), 0.5 µm film thickness; J&W Scientific), oven temperature: 40 °C (5 min hold) to 240 °C (30 min hold) at 4 °C/min, carrier gas: hydrogen at a constant pressure of 135 kPa.

System II

Separation of the stereoisomers of 4-mercapto-2-alkanols was performed on a Carlo Erba Mega 5160 series gas chromatograph: split/splitless injector (200 °C, split ratio 10:1), FID (200 °C), 50% heptakis(2,3-di-*O*-acetyl-6-*O*-*tert*-butyl dimethylsilyl)-•-cyclodextrin (30 m x 0.25 mm (i.d.), 0.25 µm film thickness, in OV1701-vi), oven temperature: 85 °C (0 min hold) to 110 °C (50 min hold) at 0.5 °C/min and from 110 to 180 °C (5 min hold) at 2 °C/min, carrier gas: hydrogen at a constant pressure of 75 kPa.

System III

Separation of the stereoisomers of 4-acetylthio-2-alkanols was performed on an HP5890 A gas chromatograph: split/splitless injector (200 °C, split ratio 5:1), FID (350 °C), 25% heptakis(2,3-di-*O*-methyl-6-*O*-*tert*-butyl dimethylsilyl)-•-cyclodextrin (30 m x 0.32 mm i.d.; 0.25 µm film thickness, in

Downloaded by UNIV OF GUELPH LIBRARY on May 29, 2012 | http://pubs.acs.org
Publication Date (Web): May 29, 2012 | doi: 10.1021/bk-2012-1098.ch003

SE54), oven temperature: 75 °C at 2 °C/min to 180 °C (10 min hold), carrier gas: hydrogen at a constant pressure of 176 kPa.

Gas Chromatography-Olfactometry (GC/O)

The odor descriptions of the diastereoisomers of 4-mercapto-2-alkanols and 4-acetylthio-2-alkanols were determined by injecting about 800 ng of each compound onto a HP5890 A Series II (Hewlett-Packard INC) equipped with on-column injector and FID (260 °C). The column used was a DB-Wax (30 m x 0.25 mm i.d.; 0.25 µm film thickness; J&W Scientific). The effluent of the column was split 1:1 via a press-fit Y-piece and short pieces of deactivated fused silica capillaries to a heated sniffing port (200 °C) and detector. The oven temperature was programmed from 40 °C (5 min hold) to 240 °C (30 min hold) at 4 °C/min. Carrier gas used was hydrogen at a constant pressure of 70 kPa.

The odor descriptions of the enantiomers of 4-mercapto-2-alkanones and 4-acetylthio-2-alkanones were determined by using CycloSil-B (30 m x 0.25 mm i.d.; film thickness 0.25 µm; Agilent Technologies INC). Flavor dilution factors (FD) of the 4-mercapto-2-alkanones and the 4-acetylthio-2-alkanones were determined by aroma extract dilution analysis (AEDA). After stepwise dilutions, aliquots were analyzed by GC/O. Odor thresholds were calculated using (E)-2-decenal as internal standard (*20*).

Gas Chromatography-Mass Spectrometry (GC-MS)

MS data of 4-mercapto-2-alkanones and 4-acetylthio-2-alkanones have been previously reported (*18*). MS data of 4-mercapto-2-alkanols and the corresponding acetates were obtained on a GC 8000^{TOP} with a Voyager GC-MS (Thermo Fischer Scientific) equipped with a split/splitless injector (220 °C, split ratio 50:1). The installed column was a 30 m x 0.25 mm (i.d.) fused silica capillary column coated with DB-Wax (0.5 µm film thickness; J&W Scientific). The oven temperature was programmed from 40 °C (5 min hold) to 240 °C (25 min hold) at 4 °C/min. Carrier gas used was hydrogen at a constant pressure of 75 kPa. The mass spectrometer was operated on scan mode at 25 - 445 amu and the ionization energy was set at 70 eV. The source temperature was 200 °C and the interface temperature was 240 °C. Data acquisition was done via Xcalibur (version 1.4; Thermo Scientific).

High-Performance Liquid Chromatography (HPLC)

(*S*)-MαNP thioesters of 4-mercapto-2-alkanones were analyzed by HPLC (LC-2000 Plus, JASCO, Japan) using an Inertsil Prep-Sil column (6.0 mm i.d. x 250 mm; particle size 10 µm, GL Sciences, Japan) with an Inertsil Sil guard column (column size 4.0 mm i.d. x 50 mm, GL Sciences, Japan); UV detection was employed (λ=254 nm). An isocratic mode with 8% ethyl acetate in *n*-hexane and a flow rate of 1.5 mL/min was used.

Downloaded by UNIV OF GUELPH LIBRARY on May 29, 2012 | http://pubs.acs.org
Publication Date (Web): May 29, 2012 | doi: 10.1021/bk-2012-1098.ch003

Downloaded by UNIV OF GUELPH LIBRARY on May 29, 2012 | http://pubs.acs.org
Publication Date (Web): May 29, 2012 | doi: 10.1021/bk-2012-1098.ch003

Results and Discussion

GC Separation of the Enantiomers of 4-Mercapto-2-alkanones and the Corresponding 4-Acetylthio-2-alkanones

4-Mercapto-2-alkanones and 4-acetylthio-2-alkanones were synthesized by addition of hydrogensulfide anion and thioacetic acid, respectively, to the corresponding 3-alken-2-ones (*18*). The enantiomers could be separated using a chiral stationary phase (Figure 1).

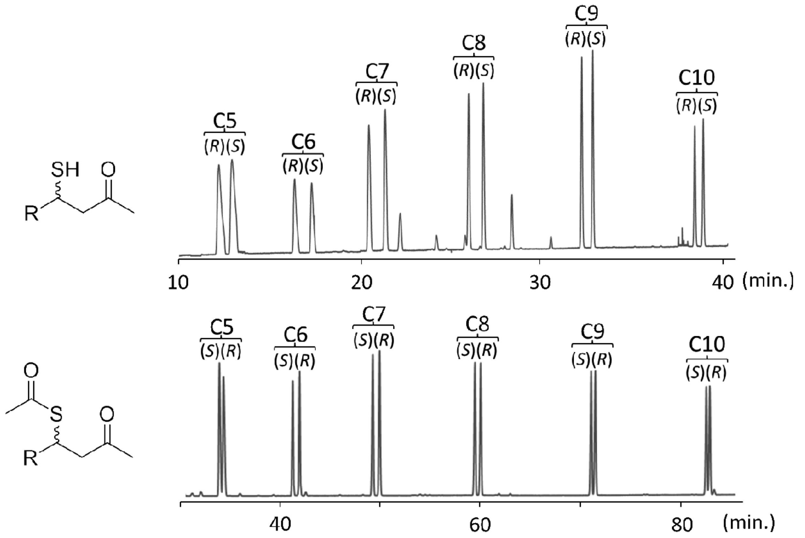

Figure 1. Capillary gas chromatographic separation of the enantiomers of 4-mercapto-2-alkanones and 4-acetylthio-2-alkanones using heptakis(2,3-di-O-methyl-6-O-tert-butyl dimethylsilyl)-•-cyclodextrin as stationary phase. For conditions see (18).

Determination of the Absolute Configurations Using a Combination of the ^{1}H-NMR Anisotropy Method and Lipase-Catalyzed Kinetic Resolution

The 4-mercapto-2-alkanones were derivatized with (*S*)-2-methoxy-2-(1-naphthyl) propionic acid (M•NP). The absolute configurations of the obtained diastereoisomeric thioesters were determined on the basis of ^{1}H-NMR anisotropy effects (*21*, *22*). The naphthyl group of M•NP causes larger chemical shifts than the traditionally used Mosher´s reagent; in addition, the diastereoisomeric derivatives are well separated via normal-phase HPLC. The assignment of the configurations was based on the sector rule established for M•NP-esters of secondary alcohols (*22*). When (*S*)- M•NP acid is used for enantioresolution, the absolute configuration is based on Δ• = • (second LC peak) - • (first LC peak). As shown in Figure 2 for the diastereoisomeric (*S*)-M•NP-thioesters of 4-mercapto-2-heptanone as example, the Δ• value for the H-1 proton is 0.06 and that for the H-7 proton is -0.03. When the M•NP ester group and the methine proton are fixed in the down/front and down/rear sides, respectively, protons with a positive Δ• value are placed on the right side and those with a negative value on the left side. Therefore, the H-1 proton should be on the right side and the H-7 proton on the left side, corresponding to (*S*)-configuration of the first eluted LC-peak.

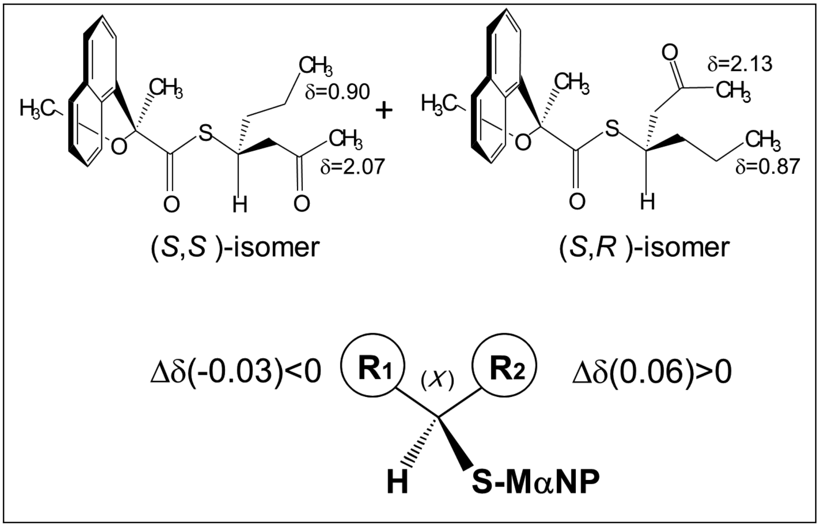

Figure 2. Structures of synthesized diastereomeric (S)-MαNP-thioesters of 4-mercapto-2-heptanone with ^{1}H-chemical shifts calculated by the sector rule according to (22).

Normally, the diastereoisomeric MαNP-derivatives obtained after HPLC fractionation are hydrolytically cleaved under alkaline conditions to obtain the respective enantiomers. For 4-mercapto-2-alkanones this approach was not applicable, because of the occurrence of retro-Michael-type addition at the β-carbonyl position. Considering the previously shown stereoselectivity of the hydrolysis of *sec*-acetylthioesters (*19*), an enzyme-mediated approach was chosen. The synthesized 4-acetylthio-2-alkanones were subjected to a kinetic resolution using lipases to obtain enantiomerically enriched thiols via enzyme-catalyzed hydrolysis of the thioester bond. As example, the enantiomeric ratios determined after 1 h from the porcine pancreas lipase-catalyzed kinetic resolution of 4-acetylthio-2-heptanone are shown in Figure 3.

Downloaded by UNIV OF GUELPH LIBRARY on May 29, 2012 | http://pubs.acs.org
Publication Date (Web): May 29, 2012 | doi: 10.1021/bk-2012-1098.ch003

Downloaded by UNIV OF GUELPH LIBRARY on May 29, 2012 | http://pubs.acs.org
Publication Date (Web): May 29, 2012 | doi: 10.1021/bk-2012-1098.ch003

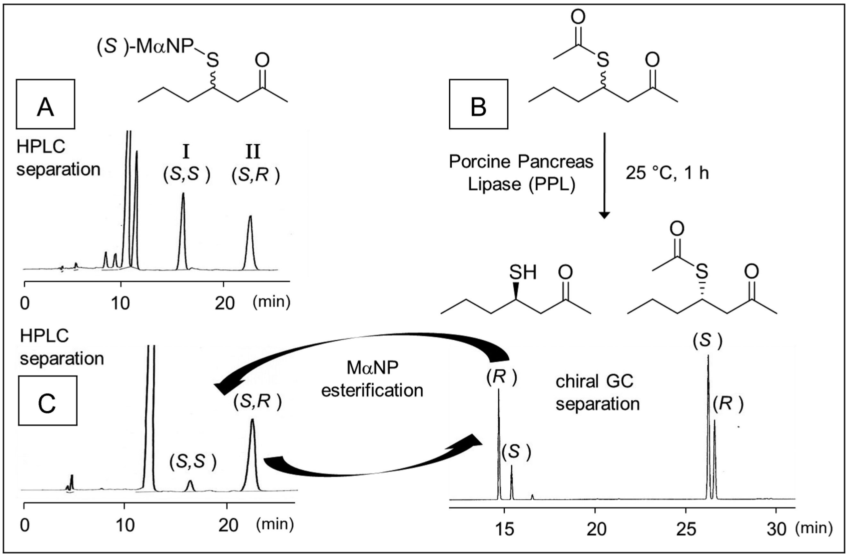

Figure 3. Approch employed to assign the GC-elution order of enantiomers, shown for 4-mercapto-2-heptanone and 4-acetylthio-2-heptanone as examples. A: HPLC-separation of diastereoisomeric (S)-MαNP-thioesters of racemic 4-mercapto-2-heptanol on a normal phase. For conditions see Experimental. B: GC-separations of the enantiomers of 4-mercapto- and 4-acetylthio-2-heptanone obtained by lipase-catalyzed kinetic resolution using heptakis(2,3-di-O-methyl-6-O-tert-butyl dimethylsilyl)-β-cyclodextrin. For conditions see (18). C: HPLC-separation of diastereoisomeric (S)-MαNP-thioesters of enantiomerically enriched 4-mercapto-2-heptanone obtained by lipase-catalyzed kinetic resolution.

The enantiomerically enriched product (4-mercapto-2-heptanone) was derivatized with MαNP; the diasteroisomeric ratio determined for the obtained thioester derivative by HPLC (peak I: 27.9%, peak II: 72.1%) corresponds to the enantiomeric ratio determined for the thiol by GC (peak I: 76.4%, peak II: 23.6%). As the order of elution of the HPLC-separated diastereoisomeric (*S*)-MαNP thioesters has been assigned as (*S*,*S*) before (*S*,*R*), the order of elution of the 4-mercapto-2-heptanone enantiomers on the chiral GC stationary phase is (*R*) before (*S*), and that of the corresponding acetylthioester (*S*) before (*R*).

Downloaded by UNIV OF GUELPH LIBRARY on May 29, 2012 | http://pubs.acs.org
Publication Date (Web): May 29, 2012 | doi: 10.1021/bk-2012-1098.ch003

Assessment of the Sensory Properties of the 4-Mercapto-2-alkanone and 4-Acetylthio-2-alkanone Enantiomers by GC/O

The odor thresholds of the enantiomers of 4-mercapto-2-alkanones and 4-acetylthio-2-alkanones were determined by GC/O (*20*). As shown in Figure 4, both homologous series exhibited minima of the odor thresholds at chain length C8 (4-mercapto-2-alkanones) and C7 (4-acetylthio-2-alkanones), respectively. Similar minima in the odor thresholds have recently been reported for thiols (*23*). For both compound classes, the C6-representatives showed significant differences in the odor thresholds of the enantiomers. (*S*)-3-acetylthio-2-hexanone was approximately 5 times more potent than the (*R*)-enantiomer. For 3-mercapto-2-hexanone this difference was even more pronounced; the threshold of the (*S*)-enantiomer was approximately 150 times lower than that of the (*R*)-enantiomer. These differences were consistently perceived by two trained panelists.

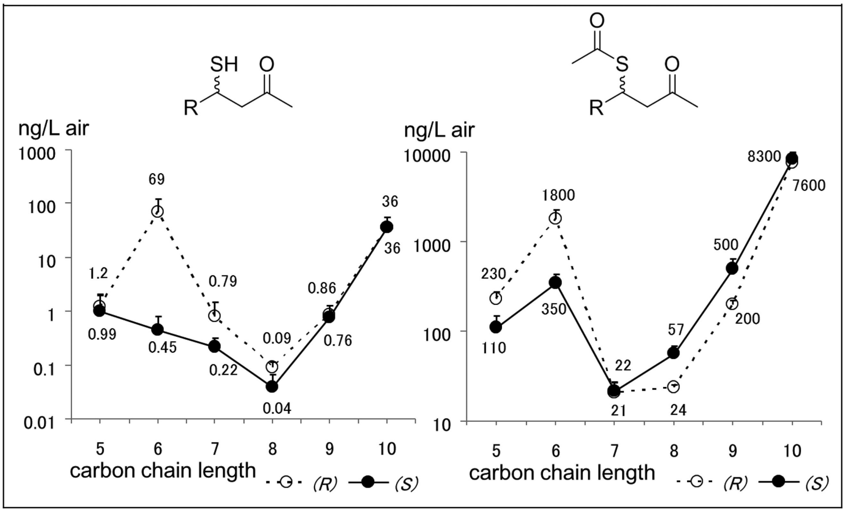

Figure 4. Odor thresholds of the enantiomers of 4-mercapto-2-alkanone and 4-acetylthio-2-alkanone homologs determined by GC/O.

Downloaded by UNIV OF GUELPH LIBRARY on May 29, 2012 | http://pubs.acs.org
Publication Date (Web): May 29, 2012 | doi: 10.1021/bk-2012-1098.ch003

Generally, the odor thresholds determined for the 3-mercapto-compounds were significantly lower than those of the corresponding 3-acetylthio-compounds.

GC/O was also employed to describe the odor properties of the enantiomers. The olfactometric evaluation of long-lasting odors such as sulfur compounds may be hampered by insufficient resolutions. Accordingly, approaches such as multi-dimensional gas chromatography combined with a double-cool-strand interface have been developed (*24*). In the present study, the odor properties were assessed at concentrations corresponding to one dilution step above the thresholds. These amounts resulted in sufficient separations and revealed more fruity-pleasant (grapefruit, blackcurrant) notes for the (*S*)-enantiomers and more unpleasant (catty, sulfury) descriptions for the (*R*)-enantiomers.

Chromatographic and Sensory Data on 4-Mercapto-2-alkanols and 4-Acetylthio-2-alkanols

4-Mercapto-2-alkanols and 4-acetylthio-2-alkanols were obtained from the corresponding 4-acetylthio-2-alkanones by reduction with $LiAlH_4$ and $NaBH_4$, respectively. The separations of the diastereoisomers on a DB-Wax column are shown in Figures 5 and 6.

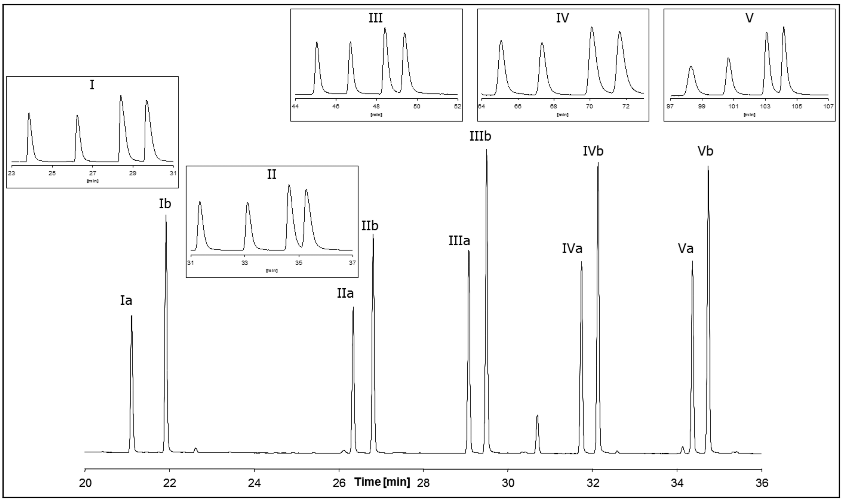

Figure 5. Capillary gas chromatographic separation of the diastereoisomers (main chromatogram; GC-system I) and of the stereoisomers (chromatograms shown in boxes; GC-system II) of 4-mercapto-2-alkanols; I: 4-mercapto-2-pentanol, II: 4-mercapto-2-heptanol, III: 4-mercapto-2-octanol, IV: 4-mercapto-2-nonanol, V: 4-mercapto-2-decanol. For conditions see Experimental Section.

Using heptakis(2,3-di-*O*-acetyl-6-*O*-*tert*-butyl dimethylsilyl)-•-cyclodextrin and heptakis(2,3-di-*O*-metyl-6-*O*-*tert*-butyl dimethylsilyl)-•-cyclodextrin as chiral stationary phases, separations of the four stereoisomers could be achieved for each of the homologs (Figure 5 and 6).

The odor properties of the diastereoisomers were determined by GC/O. As shown in Table I, the first eluted diastereoisomers of 4-mercapto-2-alkanols exhibited mainly green, fruity, flowery odors, whereas the second diastereoisomers showed more meaty, roasty, sweaty, onion-type notes. For the 4-acetylthio-2-alkanols these patterns of odor descriptions were opposite: sweaty, savory, onion-type odors for the first eluted diasteroisomers and green, tropical, fruity notes for the second diastereoisomers.

Downloaded by UNIV OF GUELPH LIBRARY on May 29, 2012 | http://pubs.acs.org
Publication Date (Web): May 29, 2012 | doi: 10.1021/bk-2012-1098.ch003

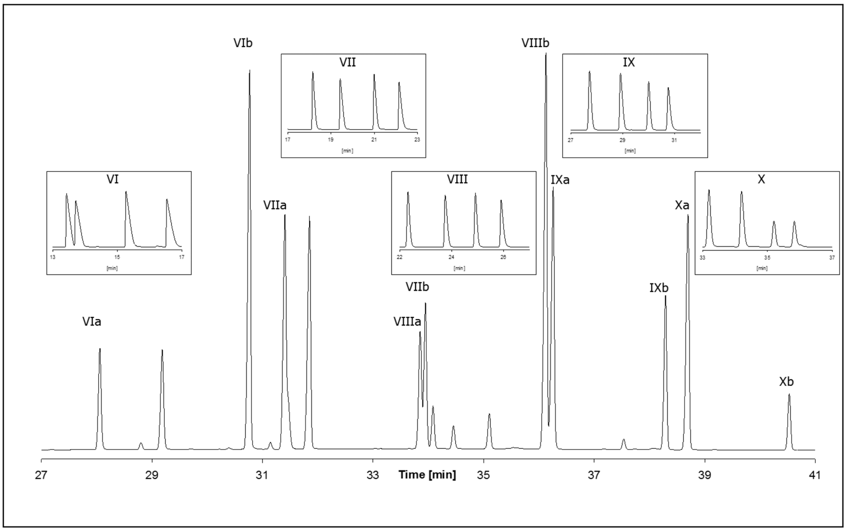

Figure 6. Capillary gas chromatographic separation of the diastereoisomers (main chromatogram; GC-system I) and stereoisomers (chromatograms shown in boxes; GC-system III) of 4-acetylthio-2-alkanols; VI: 4-acetylthio-2-pentanol, VII: 4-acetylthio-2-heptanol, VIII: 4-acetylthio-2-octanol, IX: 4-acetylthio-2-nonanol, X: 4-acetylthio-2-decanol. For conditions see Experimental Section.

Downloaded by UNIV OF GUELPH LIBRARY on May 29, 2012 | http://pubs.acs.org
Publication Date (Web): May 29, 2012 | doi: 10.1021/bk-2012-1098.ch003

Table I. Odor properties of the diastereoisomers of 4-mercapto-2-alkanols and 4-acetylthio-2-alkanols determined by GC/O

	no.	chain length	odor description[a]	
			diastereomer a	diastereomer b
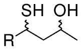	I	C_5	sulfury, green, sweet, onion	savory, meaty, roasty, onion
	II	C_7	sweet, fruity, sulfury	dill, sauerkraut, sweaty
	III	C_8	sweet, flowery, green, sulfury	sweet, onion
	IV	C_9	sweaty, onion	sweet, green, sulfury
	V	C_{10}	sweet, flowery, green, refreshing	sour, sulfury
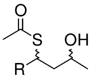	VI	C_5	sweaty, savory, onion	cooked giblets, iron, savory
	VII	C_7	sweaty, onion, sulfury, sweet	fresh, green tea, sweet, tropical
	VIII	C_8	sweaty, sweet, onion, garlic	green, sweet
	IX	C_9	sulfury, savory	sweet, fresh, fruity
	X	C_{10}	sweet, dried orange	savory, roasty

[a] 400 ng at the sniffing port

In conclusion, the combination of (i) NMR analysis of diastereoisomeric MαNP thioesters, (ii) the GC-separation of enantiomers, and (iii) the use of lipases for kinetic resolutions proved to be a useful approach to determine the absolute configurations of 4-mercapto-2-alkanones and the corresponding 4-acetylthio-2-alkanones. Assessments of the enantiomers by GC/O revealed a strong impact of the configuration at position 3 of the 1,3-oxygen-sulfur functionality on odor properties and for some homologs on odor thresholds of these substance classes. The sensory evaluations and the assignments of the absolute configurations of the four stereoisomers of 4-mercapto-2-alkanols and 4-acetylthio-2-alkanols separated on the chiral stationary phases are in progress.

References

1. Boelens, M. H.; van Gemert, L. J. *Perfum. Flavor.* **1993**, *18*, 29–39.
2. Mussinan, C. J.; Keelan, M. E. In *Sulfur Compounds in Foods*; Mussinan, C. J., Keelan, M. E., Eds.; ACS Symposium Series 564; American Chemical Society: Washington, DC, 1994; pp 1−6.
3. Blank, I. In *Heteroatomic Aroma Compounds*; Reineccius, G. A., Ed.; ACS Symposium Series 826; American Chemical Society: Washington, DC, 2002; pp 25−53.
4. Vermeulen, C.; Gijs, L.; Collin, S. *Food Rev. Int.* **2005**, *21*, 69–137.
5. Vermeulen, C.; Pellaud, J.; Gijs, L.; Collin, S. *J. Agric. Food Chem.* **2001**, *49*, 5445–5449.

6. Rowe, D. J. In *Advances in Flavours and Fragrances-From the Sensation to the Synthesis*; Swift, K. A. D., Ed.; The Royal Society of Chemistry: Cambridge, U.K., 2002; pp 202−226.
7. Winter, M.; Furrer, A.; Willhalm, B.; Thommen, W. *Helv. Chim. Acta.* **1976**, *59*, 1613–1620.
8. Engel, K.-H.; Tressl, R. *J. Agric. Food Chem.* **1991**, *39*, 2249–2252.
9. Heusinger, G.; Mosandl, A. *Tetrahedron Lett.* **1984**, *25*, 507–510.
10. Wakabayashi, H.; Wakabayashi, M.; Eisenreich, W.; Engel, K.-H. *J. Agric. Food Chem.* **2004**, *52*, 110–116.
11. Singer, G.; Heusinger, G.; Fröhlich, O.; Schreier, P.; Mosandl, A. *J. Agric. Food Chem.* **1986**, *34*, 1029–1033.
12. Werkhoff, P.; Guntert, M.; Krammer, G.; Sommer, H.; Kaulen, J. *J. Agric. Food Chem.* **1998**, *46*, 1076–1093.
13. Steinhaus, M.; Sinuco, D.; Polster, J.; Osorio, C.; Schieberle, P. *J. Agric. Food Chem.* **2008**, *56*, 4120–4127.
14. Vermeulen, C.; Guyot-Declerck, C.; Collin, S. *J. Agric. Food Chem.* **2003**, *51*, 3623–3628.
15. Naef, R.; Velluz, A.; Jaquier, A. *J. Agric. Food Chem.* **2008**, *56*, 517–527.
16. Kleinhenz, J. K.; Kuo, C. J.; Harper, W. J. *Milchwissenschaft* **2006**, *61*, 300–304.
17. Robert, F.; Héritier, J.; Quiquerez, J.; Simian, H.; Blank, I. *J. Agric. Food Chem.* **2004**, *52*, 3525–3529.
18. Wakabayashi, M.; Wakabayashi, H.; Eisenreich, W.; Morimitsu, Y.; Kubota, K.; Engel, K.-H. *Eur. Food Res. Technol.* **2011**, *232*, 753–760.
19. Wakabayashi, H.; Wakabayashi, M.; Eisenreich, W.; Engel, K.-H. *J. Agric. Food Chem.* **2003**, *51*, 4349–4355.
20. Ullrich, G.; Grosch, W. *Z. Lebensm.-Unters. Forsch.* **1987**, *184*, 277–282.
21. Harada, N.; Watanabe, M.; Kuwahara, S.; Sugio, A.; Kasai, Y.; Ichikawa, A. *Tetrahedron: Asymmetry* **2000**, *11*, 1249–1253.
22. Taji, H.; Kasai, Y.; Sugio, A.; Kuwahara, S.; Watanabe, M.; Harada, N.; Ichikawa, A. *Chirality* **2002**, *14*, 81–84.
23. Polster, J.; Schieberle, P. In *Advances and Challenges in Flavor Chemistry and Biology*; Hofmann, T., Meyerhof, W., Schieberle, P., Eds.; Proceedings of the 9th Wartburg Aroma Symposium: Eisenach, Germany, 2010; pp 69−74.
24. Begnaud, F.; Starkenmann, C.; Van de Waal, M.; Chaintreau, A. *Chem. Biodiv.* **2006**, *3*, 150–160.

Downloaded by UNIV OF GUELPH LIBRARY on May 29, 2012 | http://pubs.acs.org
Publication Date (Web): May 29, 2012 | doi: 10.1021/bk-2012-1098.ch003

Downloaded by PENNSYLVANIA STATE UNIV on May 30, 2012 | http://pubs.acs.org
Publication Date (Web): May 29, 2012 | doi: 10.1021/bk-2012-1098.ch004

Chapter 4

Confirmation of Trace Level Aroma-Impact Compounds in Cantaloupe (*Cucumis melo* L. var. *cantalupensis* Naudin) by GC-MS/MS Analysis

J. Lin[*] and Y. Wang

**Firmenich Inc., North America R&D, P.O. Box 5880,
Princeton, NJ 08543, U.S.A.
[*]E-mail: Jianming.lin@firmenich.com**

A room temperature sample preparation method combining solid phase extraction (SPE) and gel permeation chromatography (GPC) was used to obtain an authentic aroma extract of fresh cantaloupe purchased from a local farm. More than thirty aroma-impact compounds of the cantaloupe were determined by GC-O analysis. No EI mass spectra were obtained for the unequivocal identification of ten trace level aroma-impact compounds. To demonstrate the usefulness of GC-MS/MS analysis in the identification of trace level aroma-impact compounds, selected reaction monitoring (SRM) GC-MS/MS methods were developed for simultaneous analysis of six C9 compounds by choosing GC columns and MS ionization modes, optimization of the CI source temperature and pressure, and collision energy, and selection of product ions. The application of SRM GC-MS/MS analysis led to the confirmation of 6Z-nonenal, 2E-nonenal and 2E,6Z-nonadienal and the unambiguous identification of 3Z-nonenyl acetate and 3Z,6Z-nonadienyl acetate in cantaloupe. The presence of 3Z,6Z-nonadienal in cantaloupe was not confirmed by our GC-MS/MS analysis.

In Recent Advances in the Analysis of Food and Flavors; Toth, S., et al.;
ACS Symposium Series; American Chemical Society: Washington, DC, 2012.

Introduction

The inherent sensitivity and selectivity of gas chromatography-tandem mass spectrometry (GC-MS/MS) make it a powerful tool for challenging food product analysis. The main application of GC-MS/MS is for quantification of trace level analytes in complex matrices, such as mycotoxins and contaminants in foods (*1*, *2*), and pesticide residues in agricultural products (*3*, *4*). GC-MS/MS has also been used in qualitative targeted compounds analysis. The presence of khusimone (*5*) and, khusimene and acoradiene (*6*) in vetiver oil were confirmed in very sensitive and selective ways using combined GC-MS/MS analysis, i.e. daughter ion scan with neutral loss scan and, parent ion scan with neutral loss scan, respectively. Recently, 2E,6Z-nonadienyl acetate was identified for the first time in melon using a sensitive and selective selected ion monitoring GC-MS/MS method (*7*).

In the aroma extract dilution analysis of muskmelon, 46 aroma impact compounds were detected (*8*). Only 15 of them were identified on the basis of mass spectra, retention indices and odor descriptors. The others remained unknown, most likely because these odorants occurred at trace levels and couldn't be identified by GC-MS. Identification of these unknown odorants can be achieved by proposing molecules based on aroma characteristics, retention index, as well as other clues. GC-MS/MS methods can then be used to confirm or disapprove the initial structural proposals.

In this work, GC-O analysis was conducted on an aroma extract of cantaloupe to determine aroma impact compounds. Sensitive GC-MS/MS methods were then developed to confirm the presence of several trace level C9 aroma-impact compounds in cantaloupe. Our goal was to use this as an example to demonstrate the value of sensitive and selective GC-MS/MS analyses in the identication of trace level aroma impact compounds.

Experimental Section

Plant Materials

Fresh ripe cantaloupes (*Cucumis melo* L. var. *cantalupensis* Naudin) were purchased from a local farm near Princeton, NJ. The mesocarp tissues of a 2.7 kg cantaloupe were cut into 1 inch cubes and immediately comminuted to puree with a Waring Juice Extractor. The puree was then centrifuged at 15°C at a speed of 8000 rpm for 10 min. About 1 L of the supernatant was obtained and used for aroma extraction by SPE described below.

No effort was made to inactivate enzymes in order to be consistent with how melon is commonly eaten. The mesocarp tissues of the other melons were also cut into 1 inch cubes and then stored under vacumn at -15 °C until use.

Downloaded by PENNSYLVANIA STATE UNIV on May 30, 2012 | http://pubs.acs.org
Publication Date (Web): May 29, 2012 | doi: 10.1021/bk-2012-1098.ch004

Downloaded by PENNSYLVANIA STATE UNIV on May 30, 2012 | http://pubs.acs.org
Publication Date (Web): May 29, 2012 | doi: 10.1021/bk-2012-1098.ch004

Preparation of Cantaloupe Aroma Extract

Solid Phase Extraction (SPE)

Three Oasis® HLB cartridge (20cc/1g, 60 µm) (Waters, Milford, MA) were all conditioned sequentially with 10 mL dichloromethane, 20 mL methanol and 30 mL 18 MΩ water. The juice supernatant (1 L total, 500 mL each) was passed through two conditioned cartridges at a flow rate of approximately 8 mL/min. The sample load was collected and combined and passed through the third cartridge. Each cartridge was washed with 60 mL of water then eluted with 17 mL dichloromethane/methanol (9/1, v/v). The eluates from the three cartridges were combined and dried with anhydrous magnesium sulfate and then filtered. The filtrate was concentrated to a final volume of about 12 mL with a gentle stream of nitrogen and then evaluated organoleptically on a perfume blotter. Ten mL of the extract was further concentrated to about 2.5 mL with a gentle stream of nitrogen and some precipitation was observed during this process.

Gel Permeation Chromatography (GPC)

This was performed on a GPC system modified from a Biotage SP1™ Purification System, which was equipped with a pump, a UV detector and an automatic fraction collector. A manual sample injector (model 7725, with a 5mL sample loop, Rheodyne) was connected to the system between the exit of the pump and the head of column for sample introduction. One three-way valve (Omnifrit, purchased from VWR) was connected to the end of the column for ease of operation. With such a valve, the column flow can be switched to the fraction collector, waste, or simply stopped.

The column (25 mm i.d. x 500 mm l., with 25 µm PTFE frits., Omnifrit) was packed with 50 g of Biobeads® S-X3 using 150 mL of DCM according to the directions provided by Bio-RAD. The bed length of the column was 400 mm. Sample (2.5 mL) obtained from SPE was manually injected. DCM was used as the mobile phase. The flow rate was 5 mL/min. The eluent was collected into 6 mL fractions and the fractions were evaluated with perfume blotters. Fractions 15 to 24 were found to have aroma and therefore combined and concentrated to a final volume of 0.5 mL. This aroma extract was then analyzed by GC-O/MS and GC-MS/MS.

Downloaded by PENNSYLVANIA STATE UNIV on May 30, 2012 | http://pubs.acs.org
Publication Date (Web): May 29, 2012 | doi: 10.1021/bk-2012-1098.ch004

GC-O/MS Analysis

This was performed on a custom-designed Multidimensional AromaTrax™ GC-O System (Microanalytics, TX). It integrates an Agilent 6890 based dual column multidimensional gas chromatograph (MDGC) with an Agilent model 5973N mass spectrometer and an olfactory port with humidifier. The MDGC is installed with dual columns, including Rxi-1MS column (30m x 0.53 mm i.d. x 0.5 µm, Restek) as the first column and DB-Wax (30 m x 0.53 mm i.d. x 0.5 µm, J&W) as the second column. Samples (1 µL) for GC-O analysis were directly introduced to the second column via splitless injection. The eluent of the second column was split between the MS and the olfactory detectors at a ratio of about 1/5 via an open split interface. Six GC-O runs with three experienced panelists were used to determine aroma-impact compounds.

GC-MS/MS Analysis

GC-MS/MS experiments were performed on a Varian 3800 GC coupled to a Varian 300 MS. The system was equipped with a CombiPal autosampler, two split/splitless injectors, a DB-WaxETR column (30m x 0.25 mm id x 0.25 µm, J&W) on the front injector and a DB-17MS column (20m x 0.18 mm id x 0.18 µm, J&W) installed on the back injector. The ends of both columns combine and transfer to the MS via a zero-dead-volume T-union (Valco) and a restrictor (~0.3 m x 0.11mm i.d.).

Synthesis of Standards

Standard compounds were needed to develop GC-MS/MS methods. 3Z,6Z-Nonadienyl acetate, 3Z-nonenyl acetate and 3Z,6Z-nonadienal were not available commercially or in house. They were prepared according to the synthesis schemes shown in Figure 1. The targets obtained were characterized by NMR.

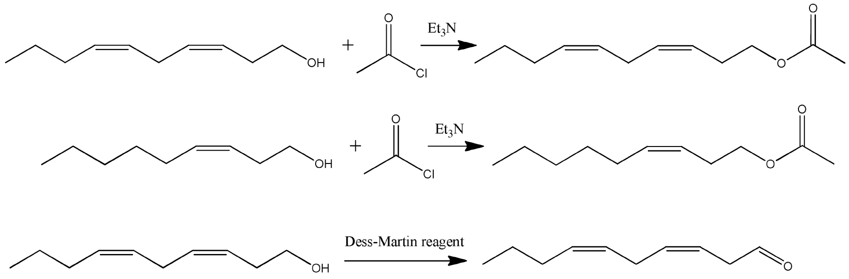

Figure 1. Synthesis schemes for the standard compounds.

Downloaded by PENNSYLVANIA STATE UNIV on May 30, 2012 | http://pubs.acs.org
Publication Date (Web): May 29, 2012 | doi: 10.1021/bk-2012-1098.ch004

Results and Discussion

Isolation of Volatile Compounds

Initially, we planned to isolate the volatile compounds of cantaloupe via hydrodistillation under vacuum, followed by solid phase extraction (SPE). The aroma of the hydrodistillate obtained was described as cooked, meaty, sulfury, slightly melon, although the same method applied to honeydew melon resulted in an aroma extract resembling that of the original fruit (*7*). A room temperature volatile isolation method combining SPE and gel permeation chromatography (GPC) cleanup was then devised and applied, giving rise to a very authentic cantaloupe aroma extract. GPC was effective in removing co-extracted carotenoids, waxes and other lipophilic components because their molecular sizes are larger than those of aroma molecules. The main advantage of this volatile isolation method is the absence of thermal stress. Additionally, it is quick and easy to perform.

Aroma-Impact Compounds

Based on GC-O analysis, 33 odorants were determined to be aroma-impact compounds of the cantaloupe sample (Table 1). The aromagram plotting these 33 compounds versus their total GC-O intensity is inversely overlaid with the GC-MS chromatogram of the cantaloupe aroma extract in Figure 2. The six most intense aroma-impact compounds were 3Z-hexenyl acetate (**11**, fruity), 3Z-hexen-1-ol (**13**, green), ethyl 2-(methylthio)acetate (**16**, potato, fruity), 6E-nonen-1-ol (**24**, melon, sweet), 3Z,6Z-nonadien-1-ol (**27**, fresh, melon) and phenethanol (**29**, sweet). The odor characteristics of these compounds were in good agreement with the overall cantaloupe aroma impression described as melon, fresh, fruity and sweet.

Sixteen out of the 33 aroma-impact compounds were lipid degradation products, including saturated and unsaturated fatty alcohols, aldehdyes and ketones. The alcohols had higher odor thresholds therefore, they must be present at higher concentrations to contribute to the overall aroma. Their mass spectra were acquired for their identification. However, unsaturated aldehydes and ketones are often very potent odorants. It is extremely difficult to obtain their EI spectra to confirm their identities. As shown in Table 1, 3Z-hexenal (**8**), 1,5Z-octadien-3-one (**12**), 6Z-nonenal (**15**), 2Z-nonenal (**18**), 2E-nonenal (**19**), 2E,6E-nonadienal (**20**), 2E,6Z-nonadienal (**21**)and trans-4,5-epoxy-2E-decenal (**31**) were identified based on aroma characteristics and retention indices on two columns of different polarity. This is commonly realized via an experienced GC-O panelist's recognizing the characteristic odor at the GC sniff port, followed by further confirmation by RIs on two different columns. In some cases, due to overlapping with another odorant, a panelist might not be able to recognize the odor characteristics on another column, and therefore it may not be possible to confirm the identification by this means. On the other hand, library and literature data on retention indices and aroma descriptors can be a good starting point to propose candidate molecules for the identification of trace aroma-impact compounds. Other evidence, such as quantitative structure-retention relationship and the presence of other homologues, isomers, precursors or degradation products, can be used to propose structures for trace level unknown aroma-impact compounds. Inexperience in recognizing odor characteristics may lead to the inability to identify trace aroma-impact compounds or misidentification.

Therefore, sensitive and selective methods that do not depend on olfactive acumen and experience can be very useful to confirm the structure proposals of trace level aroma-impact compounds.

Table 1. Aroma-impact compounds identified in the cantaloupe aroma extract

No.	*ID*	*RI* (GC-O)*	*RI (inj/ lit.)*	*Descriptors*	*Total Int.*	*ID criteria*
1	propyl acetate	985	986	solventy, estery, pineapple, fruity	174	RI, MS, O
2	methyl butyrate	995	995	butric, cheesy, sharp	159	RI, MS, O
3	ethyl acrylate	999	1000	pungent, plastic, fruity, slightly tropical	241	RI, MS, O
4	ethyl butyrate	1047	1046	cheesy, estery, pineapple, fruity	168	RI, MS, O
5	methyl thioacetate	1055	1054	sulfury, mango, sulfury-pineapple, tropical fruit	231	RI, MS, O
6	ethyl 2-methylbutyrate	1061	1060	slightly fruity, green, apple, sweet, honey	191	RI, MS, O
7	hexanal	1085	1092	green, leafy	150	RI, MS, O
8	3Z-hexenal	1144	1148	green, leafy, hexanol, melon, aldehydic	169	RI, RI, O
9	eucalyptol	1209	1202	camphoraceous, menthol	179	RI, MS, O
10	2-methyl-1-butanol	1212	1212	chocolate, green, musty, cheesey	180	RI, MS, O
11	3Z-hexenyl acetate	1321	1320	fruity, olive, creamy, green apple, pea	386	RI, MS, O
12	1,5Z-octadien-3-one	1375	1380	geranium, vegetative, metallic, bloody	167	RI, RI, O

Continued on next page.

Downloaded by PENNSYLVANIA STATE UNIV on May 30, 2012 | http://pubs.acs.org
Publication Date (Web): May 29, 2012 | doi: 10.1021/bk-2012-1098.ch004

Table 1. (Continued). Aroma-impact compounds identified in the cantaloupe aroma extract

No.	*ID*	*RI* (GC-O)*	*RI (inj/ lit.)*	*Descriptors*	*Total Int.*	*ID criteria*
13	3Z-hexen-1-ol	1390	1396	fruity, herbaceous, leafy, green, aldehyde	331	RI, MS, O
14	unknown	1433	NA	sulfury, earthy, musty, cardboard, dirty	262	NA
15	6Z-nonenal	1444	1442	creamy, sweet, watermelon, dairy, lactonic	280	RI, RI, O
16	ethyl 2-(methylthio)acetate	1451	1452	potato, fruity, green, vegetative, tomato, aldehyde	445	RI, MS, O
17	1,5Z-octadien-3-ol	1492	1497	mushroom, bloody, metallic, green	219	RI, RI, O
18	2Z-nonenal	1506	1509	geranium, aldehyde, fruity, floral	159	RI, RI, O
19	2E-nonenal	1536	1538	soapy, chalky, waxy, cardboard	255	RI, RI, O
20	2E,6E-nonadienal	1566	1566	geranium, aldehyde, gamma lactone, candy, metalic	216	RI, RI, O
21	2E,6Z-nonadienal	1583	1578	fresh cucumber, green pepper, green, rindy	246	RI, RI, O
22	3-(methylthio)propyl acetate	1629	1618	potato, mushroom, metallic, soysauce, meaty, fried	252	RI, MS, O
23	1-nonanol	1668	1666	fruity, geranium, green, soapy	189	RI, MS, O
24	6E-nonen-1-ol	1712	1713	sweet, melon, creamy, candy, lactonic, dairy	330	RI, MS, O
25	methionol	1719	1722	vegetative, green pepper, rubbery	185	RI, MS, O

Continued on next page.

Downloaded by PENNSYLVANIA STATE UNIV on May 30, 2012 | http://pubs.acs.org
Publication Date (Web): May 29, 2012 | doi: 10.1021/bk-2012-1098.ch004

Downloaded by PENNSYLVANIA STATE UNIV on May 30, 2012 | http://pubs.acs.org
Publication Date (Web): May 29, 2012 | doi: 10.1021/bk-2012-1098.ch004

Table 1. (Continued). Aroma-impact compounds identified in the cantaloupe aroma extract

No.	*ID*	*RI* (GC-O)*	*RI (inj/lit.)*	*Descriptors*	*Total Int.*	*ID criteria*
26	6Z-nonen-1-ol	1720	1721	fresh, seaweed, green, cucumber, fatty, melon	219	RI, MS, O
27	3Z,6Z-nonadien-1-ol	1756	1758	fresh, melon, aldehydic, cucumber, green	382	RI, MS, O
28	2E,6Z-nonadien-1-ol	1773	1770	fresh, cucumber, melon, aldehyde, green, candy	213	RI, MS, O
29	phenethanol	1906	1916	sweet, hay, cinnamon, creamy, lactone, musky	334	RI, MS, O
30	beta-ionone	1936	1937	paprika, oakmoss, algae like, green,metallic, sweet	214	RI, MS, O
31	*trans*-4,5-epoxy-2E-decenal	2002	2000	green,metallic, rusty, fruity, sweet, hay, weak	253	RI, RI, O
32	Furaneol®**	2038	2039	caramel, maltol, hay-like, sweet	249	RI, RI, O
33	unknown	2077	NA	sweet, spicy, dried fruit, woody, cinnamon	174	NA

* RI on a DB-Wax column; ** Registered trademark of Firmenich SA, Switzerland

GC-MS/MS Analysis of C9 Aroma-Impact Compounds

Ten C9 compounds have been revealed by GC-O analysis to be important aroma contributors of cantaloupe as shown in Table 1, but five of them (**15**, **18**, **19**, **20** and **21**) occurred in the extract at trace levels. It was not possible to confirm their identification by MS. In addition, 3Z-nonenyl acetate had been identified and 3Z,6Z-nonadienyl acetate tentatively identified in cantaloupe by Kourkoutas et al. (*9*). 3Z,6Z-Nonadienal is a degradation product of linolenic acid and was thought to be the precursor of 3Z,6Z-nonadien-3-ol and 2E, 6Z-nonadienal (*10*). These three compounds were not detected in our cantaloupe aroma extract by GC-MS analysis. The structures of the eight C9 compounds are shown in Figure 3. Next, the development of GC-MS/MS method for the detection of these C9 compounds in cantaloupe will be presented.

Downloaded by PENNSYLVANIA STATE UNIV on May 30, 2012 | http://pubs.acs.org
Publication Date (Web): May 29, 2012 | doi: 10.1021/bk-2012-1098.ch004

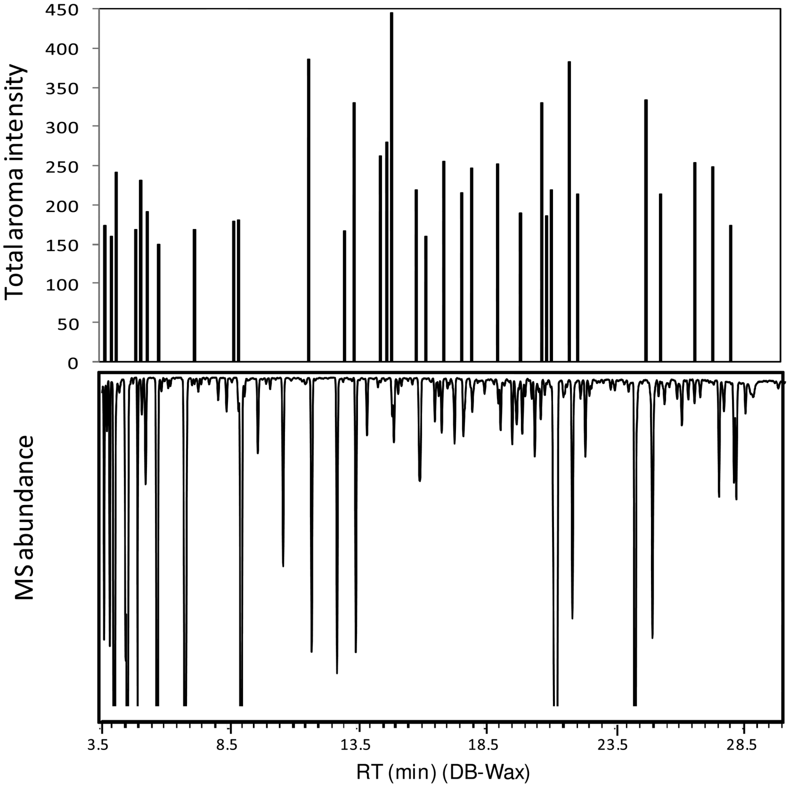

Figure 2. Aromagram of the cantaloupe extract as compared to its GC-MS chromatogram.

Optimization of GC and MS/MS Conditions

Stock solutions containing six target compounds (**15**, **19**, **21**, **34**, **35** and **36**) were prepared and used to optimize GC-MS/MS conditions in terms of resolution, ionization modes, CI source temperature and pressure, collision energy and transition ions. All the six compounds were well resolved from each other on a DB-WaxETR column. However, severe peak broadening of 3Z,6Z-nonadienal was observed, most likely due to its isomerization to 2E,6Z-nonadienal on the polar stationary phase. Fortunately, 3Z,6Z-nonadienal eluted as a sharp peak on a Rxi-1ms column. However, 3Z,6Z-nonadienyl acetate and 3Z-nonenyl acetate were not resolved on this column. A DB-17MS column was found to provide excellent peak shapes and satisfactory resolution of all the compounds although 6Z-nonenal and 3Z,6Z-nonadienal were not baseline resolved.

Downloaded by PENNSYLVANIA STATE UNIV on May 30, 2012 | http://pubs.acs.org
Publication Date (Web): May 29, 2012 | doi: 10.1021/bk-2012-1098.ch004

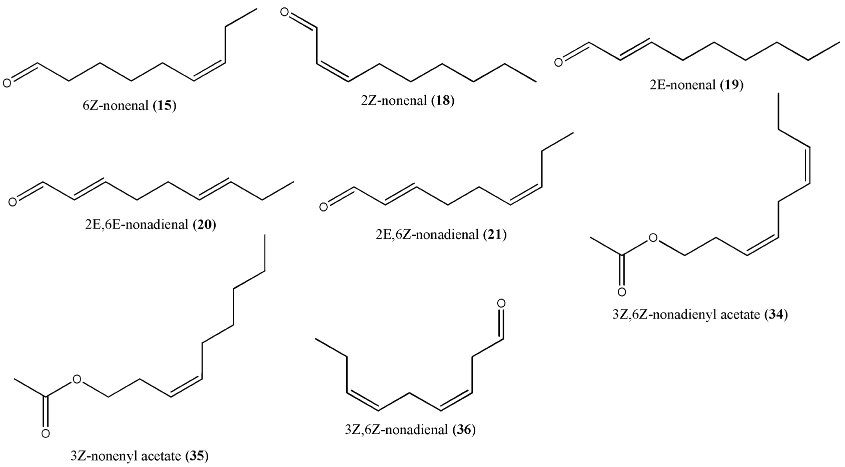
6Z-nonenal (**15**)
2Z-nonenal (**18**)
2E-nonenal (**19**)
2E,6E-nonadienal (**20**)
2E,6Z-nonadienal (**21**)
3Z,6Z-nonadienyl acetate (**34**)
3Z-nonenyl acetate (**35**)
3Z,6Z-nonadienal (**36**)
O

Figure 3. Chemical strucrures of C9 aroma compounds found or suspected in cantaloupe.

The mass spectra, i.e. EI-MS, PCI (CH_4)-MS, NCI (CH_4)-MS, PCI (NH_3)-MS and NCI (NH_3)-MS, of the standard compounds were examined to select the best ionization mode. The principle of this selection process is to choose an ionization mode that gives strong molecular ions and the lowest detection limits for the benefit of sensitivity and selectivity. The EI spectra did not have the expected molecular ions and there were no other good candidate precursor ions for MS/MS experiments. No intense molecular ions were observed in the PCI (CH_4) spectra due to further fragamentation into small ions. The sensitivity of PCI with CH_4 as the reagent gas was found to be best at a source temperature of 180 °C and a source pressure of 8 torr. No good NCI (CH_4) spectra of the standard compounds were obtained. When using NH_3 as the reagent gas, intense molecular ions of all the standard compounds appeared in their spectra in both positive and negative modes. The sensitivity of PCI and NCI with NH_3 as reagent gas was optimized at a source temperature of 150 °C and a source pressure of 6 torr. NCI was found to be much more sensitive than PCI for all the standard compounds. Therefore, NCI (NH_3) was selected as the best ionization mode for this study.

Product ion spectra of the standard compounds' molecular ions $[M-1]^-$ were acquired at various collision energy (CE) levels (4, 8, 12 and 16 eV) and investigated. This led to the selection of two product ions of each compound for selected reaction monitoring (Table 2). The principle that guided this selection process was to choose the product ions giving the best sensitivity and specificity. For the benefit of sensitivity, product ions should be strong in intensity and have large intensity increases when the intensities of the precursor ions were reduced by varying the CE level. In general, product ions with higher m/z values have better specificity. Due to the nature of these compounds, the selected product ions are not of high specificity. If an interference is encountered in a sample analysis, it might be overcome by choosing a different product ion. As an example, the product ion spectrum of ion m/z 137 at 12.0 eV for 2E,6Z-nonadienal is shown in Figure 4. An intense peak at m/z 69, which could be attributed to the neutral loss of 1,3-pentadiene, was observed and selected as one product ion. Ion m/z 119, likely produced by a neutral loss of water from ion m/z 137, was chosen as the second product ion.

Downloaded by PENNSYLVANIA STATE UNIV on May 30, 2012 | http://pubs.acs.org
Publication Date (Web): May 29, 2012 | doi: 10.1021/bk-2012-1098.ch004

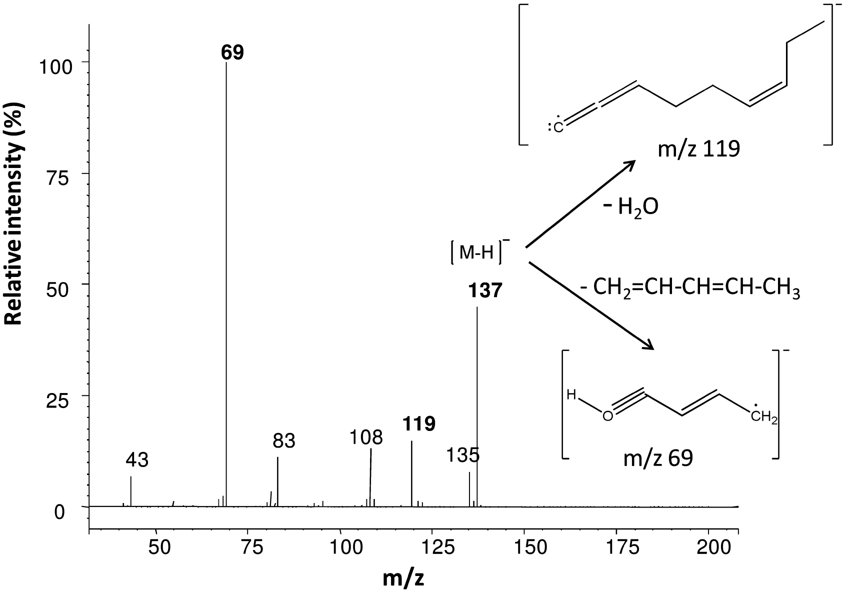

Figure 4. Product ion spectrum of ion m/z 137 of 2E,6Z-nonadienal at a collision energy of 12.0 eV, with structural explanation for transitions m/z 137→69 and m/z 137→119.

Once the transitions to be monitored had been selected for each compound, the CE was further optimized to obtain the most intense signals for both transitions. In practice, this was conducted by varying the CE by large increments (4 eV), followed by fine-tuning of the CE (1 eV increments). Comparing the relative intensities of the two transitions of each compound at different CEs, it was straight forward to find the the best CE for each transition as shown in Table 3. When the best CEs for the two transitions were different, we decided to sacrifice the intensity of the more intense transitions and optimize the CE to favor the weaker transitions. Taking compound 2E-nonenal as an example, according to the data shown in Table 3, 8 eV and 12 eV were the best CEs for transitions m/z 139→69 and m/z 139→82 respectively. The CE was optimized at 12 eV to favor the weaker transition m/z 139→82. After fine-tuning the CE, the optimum CEs were obtained as listed in Table 2.

Downloaded by PENNSYLVANIA STATE UNIV on May 30, 2012 | http://pubs.acs.org
Publication Date (Web): May 29, 2012 | doi: 10.1021/bk-2012-1098.ch004

Table 2. The SRMs and the optimum collision energy (CE) of the standard compounds

Compound Name	*MW*	*Precursor ion (m/z)*	*Product ion (m/z)*	*Collision Energy (eV)*
6Z-nonenal	140	139	57	12
			83	
2E-nonenal	140	139	69	12
			82	
2E,6Z-nonadienal	138	137	69	8
			119	
3Z-nonenyl acetate	184	183	153	8
			41	
3Z,6Z-nonadienyl-acetate	182	181	59	8
			151	
3Z,6Z-nonadienal	138	137	69	8
			119	

Identification of C9 Aroma Compounds in Cantaloupe by GC-MS/MS Analysis

With the optimized GC and MS/MS conditions, two GC-MS/MS methods, one using the DB-WaxETD column and the other using the DB-17MS column, were set up and applied to identify or confirm the targeted C9 compounds in cantaloupe. Three samples, cantaloupe aroma extract, the aroma extract spiked with standards and a solution of standard compounds, were prepared and analyzed using both methods. The samples were analyzed in the above order with a blank sample before and after each sample. The relative intensities of any two SRMs of a given compound under particular conditions is specific to the compound. Therefore it is considered as one Identification Point (IP) (*11*). The accepted deviation in relative intensity depends on the scale of the relative intensity . The relative intensities of the two SRMs of each compound were calculated and compared among the three samples. The results are summarized in Table 4 along with the retention times and the accepted deviation in relative intensity.

As shown in Table 4, the relative intensities of the two SRMs for each compound were extremely consistent among the three samples, with the exception of 2E-nonenal on the DB-WaxETR column. These consistencies in relative intensity (1 IP), one precusor ion (1 IP) and two product ions (2 IPs) added to a total of 4 IPs for the positive identification of the compounds. Therefore, the GC-MS/MS analysis with the DB-WaxETR column led to the confirmation of trace level aroma-impact compounds 6Z-nonenal and 2E,6Z-nonadienal in cantaloupe. Furthermore, 3Z-nonenyl acetate and 3Z,6Z-nonadienyl acetate were unambiguously identified in cantaloupe in this analysis. The presence of 2E-nonenal in cantaloupe was confirmed only by the GC-MS/MS analysis with the DB-17MS column because an interference was encountered in the analysis with the DB-WaxETR column. Finally, this analysis did not lead to the identification of 3Z,6Z-nonadienal in cantaloupe.

Downloaded by PENNSYLVANIA STATE UNIV on May 30, 2012 | http://pubs.acs.org
Publication Date (Web): May 29, 2012 | doi: 10.1021/bk-2012-1098.ch004

Table 3. Effect of collision energy (CE) on signal intensities of each SRM

Compound Name	*Transitions*	*Relative signal intensity*			
CE=4 eV	*CE=8 eV*	*CE=12 eV*	*CE=16 eV*		
6Z-nonenal	139→57	10	32	**40**	35
	139→83	60	170	**75**	30
2E-nonenal	139→69	100	250	**190**	100
	139→82	5	60	**120**	75
2E,6Z-nonadienal	137→69	90	**400**	310	190
	137→119	60	**125**	60	5
3Z-nonenyl acetate	183→153	1.0	**1.0**	0.5	0.35
	183→41	0.45	**1.15**	0.75	0.25
3Z,6Z-nonadienyl-acetate	181→59	2.7	**2.7**	2.3	1.5
	181→151	75	**190**	180	60
3Z,6Z-nonadienal	137→69	0.25	**1.4**	1.6	1.1
	137→119	1.65	**2.5**	0.8	0.3

GC-MS/MS chromatograms of SRMs m/z 181→59 and m/z 181→151 in the standard 3Z,6Z-nonadienyl acetate solution, cantaloupe aroma extract and the aroma extract spiked with the standards were compared and shown in Figure 5 as an example. This figure shows the excellent selectivity of the method because no other surrounding interfering peaks obscured the identification of the compound. The high signal-to-noise ratios of the peaks were due to the sensitive and selective nature of GC-MS/MS method. This in turn allowed accurate determination of the peak areas and increased the reliability of the calculated relative intensities which contributed to the consistency of the relative intensities shown in Table 4.

Downloaded by PENNSYLVANIA STATE UNIV on May 30, 2012 | http://pubs.acs.org
Publication Date (Web): May 29, 2012 | doi: 10.1021/bk-2012-1098.ch004

Table 4. Retention times and relative intensities of the SRMs of each compound, compared to the cantaloupe aroma extract and the spiked extract

Compound	*Sample*	*Standard compounds*	*Aroma extract*	*spiked aroma extract*	*Accepted deviation**
Analyzed on the DB-WaxETR column					
6Z-nonenal	*RT (min)*	15.34	15.33	15.36	—
	Rel. Int.(%)	18	17	17	5
2E-nonenal	*RT (min)*	17.40	17.40	17.41	—
	Rel. Int.(%)	74	37	48	15
2E,6Z-nonadienal	*RT (min)*	18.58	18.59	18.60	—
	Rel. Int.(%)	34	33	37	9
3Z-nonenyl acetate	*RT (min)*	19.09	19.01	19.13	—
	Rel. Int.(%)	68	70	71	14
3Z,6Z-nonadienyl acetate	*RT (min)*	20.45	20.47	20.51	—
	Rel. Int.(%)	3	3	3	2
Analyzed on the DB-17MS column					
6Z-nonenal	*RT (min)*	11.52	11.61	11.63	—
	Rel. Int.(%)	12	12	13	4
2E-nonenal	*RT (min)*	12.98	13.05	13.03	—
	Rel. Int.(%)	74	68	83	15
2E,6Z-nonadienal	*RT (min)*	13.34	13.41	13.38	—
	Rel. Int.(%)	41	41	45	10
3Z-nonenyl acetate	*RT (min)*	15.98	16.14	16.14	—
	Rel. Int.(%)	76	71	76	15
3Z,6Z-nonadienyl acetate	*RT (min)*	16.50	16.67	16.67	—
	Rel. int.(%)	3	3	4	2
3Z,6Z-nonadienal	*RT (min)*	11.60	nd	11.65	—
	Rel. Int.(%)	13	nd	18	4

[*] Based on the Identification Points (IPs) recommended in the European directive (*11*).

Downloaded by PENNSYLVANIA STATE UNIV on May 30, 2012 | http://pubs.acs.org
Publication Date (Web): May 29, 2012 | doi: 10.1021/bk-2012-1098.ch004

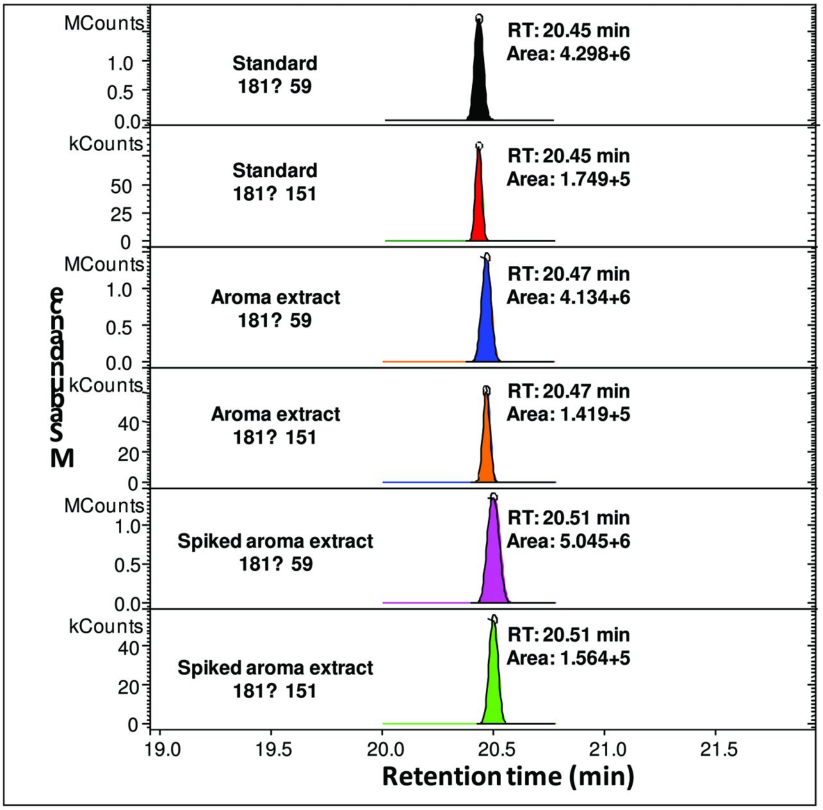

Figure 5. SRM (m/z 181→59 and m/z 181→151) signals of 3Z,6Z-nonadienyl acetate in standard solution, cantaloupe aroma extract and the aroma extract spiked with the standard.

Conclusions

Confirmation of trace level aroma-impact compounds in complex aroma extracts can be achieved by a combination of GC-MS/MS analyses. The application of sensitive and selective GC-MS/MS methods to cantaloupe aroma extract led to the confirmation of 6Z-nonenal, 2E-nonenal and 2E,6Z-nonadienal in cantaloupe and the unambiguous identification of 3Z-nonenyl acetate and 3Z,6Z-nonadienyl acetate in cantaloupe. The presence of 3Z,6Z-nonadienal in cantaloupe was not confirmed by our GC-MS/MS analysis. It would be interesting to explore the deployment of other sensitive and selective GC-MS/MS methods in various flavor related studies.

Acknowledgments

We would like to thank botanist Dr. Yong Ming Yuan for his assistance in the classification of melon, and flavorists Jung-A Kim and Fred Triolo, Jr. for their valuable help in GC-sniffing..

References

1. Melchert, H.-U.; Pabel, E. *J. Chromatogr. A* **2004**, *1056* (1-2), 195–199.
2. Abdulkadar, A. H. W.; Kunhi, A. A. M.; Jassim, A.-J.; Abdulla, A.-A. *Food Addit. Contam.* **2003**, *20* (12), 1164–1169.
3. Lehotay, S. J. *J. AOAC Int.* **2000**, *83* (3), 680–697.
4. Cervera, M. I.; Medina, C.; Portoles, T.; Pitarch, E.; Beltran, J.; Serrahima, E.; Pineda, L.; Munoz, G.; Centrich, F.; Hernandez, F. *Anal. Bioanal Chem.* **2010**, *397* (7), 2873–2891.
5. Cazaussus, A.; Pes, R.; Sellier, N.; Tabet, J. C. *Chromatographia* **1988**, *25* (10), 865–869.
6. Sellier, N.; Cazaussus, A. *J. Chromatogr.* **1991**, *557*, 451–458.
7. Perry, P. L.; Wang, Y.; Lin, J. *Flavour Fragrance J.* **2009**, *24*, 341–347.
8. Hayata, Y.; Sakamoto, T.; Maneerat, C.; Li, X.; Kozuka, H.; Sakamoto, K. *J. Agric. Food. Chem.* **2003**, *51*, 3415–3418.
9. Kourkoutas, D.; Elmore, J. S.; Mottram, D. S. *Food Chem.* **2006**, *97*, 95–102.
10. Hatanaka, A.; Kajiwara, T.; Harada, T. *Phytochemistry* **1975**, *14* (12), 2589–2592.
11. Commission decision of 12 August 2002 implementing Council Directive 96/23/EC concerning the performance of analytical methods and the interpretation of results. *Off. J. Eur. Communities* **2002**, *L221* (2002/657/EC), 8–36.

Downloaded by PENNSYLVANIA STATE UNIV on May 30, 2012 | http://pubs.acs.org
Publication Date (Web): May 29, 2012 | doi: 10.1021/bk-2012-1098.ch004

Chapter 5

Improved Synthesis of Deuterium-Labeled Alkyl Pyrazines for Use in Stable Isotope Dilution Analysis

Mingchih Fang and Keith R. Cadwallader*

Department of Food Science and Human Nutrition, University of Illinois,
1302 W. Pennsylvania Ave., Urbana, IL 61801, U.S.A.
***E-mail: cadwlldr@illinois.edu**

Downloaded by OHIO STATE UNIV LIBRARIES on May 29, 2012 | http://pubs.acs.org
Publication Date (Web): May 29, 2012 | doi: 10.1021/bk-2012-1098.ch005

Quantitative analysis by GC-MS coupled with the use of stable isotopes as internal standards, so called stable isotope dilution analysis (SIDA), is an extremely accurate and precise way to quantify potent odorants in foods. Despite its many advantages, SIDA is not widely used due to the high cost associated with the purchase and/or synthesis of the isotopically labeled standards. This chapter describes an improved approach for the synthesis of stable deuterium labeled alkylpyrazines. Three deuterium labeled alkylpyrazines, namely [$^2H_5$]-2-ethyl-3,5-dimethylpyrazine, [$^2H_5$]-2-ethyl-3,6-dimethylpyrazine and 2,3-diethyl-5-[$^2H_3$]-methylpyrazine, whose unlabeled counterparts are previously reported to be important character-impact odorants in roasted peanut products, were synthesized by nucleophilic addition of a deuterated alkyl Grignard reagent to a chloroalkylpyrazine. The application of SIDA to quantify the above mentioned alkylpyrazines in four commercial peanut butters demonstrated the ease of use and the excellent precision and accuracy of the method.

In Recent Advances in the Analysis of Food and Flavors; Toth, S., et al.;
ACS Symposium Series; American Chemical Society: Washington, DC, 2012.

Downloaded by OHIO STATE UNIV LIBRARIES on May 29, 2012 | http://pubs.acs.org
Publication Date (Web): May 29, 2012 | doi: 10.1021/bk-2012-1098.ch005

Introduction

Stable isotope dilution analysis (SIDA) is a state-of-the-art method for quantitative analysis, enabling both high precision and accuracy. The first published use of SIDA on a food material was in 1966, in which D-glucose containing seven deuterium atoms was used as an isotope tracer for the determination of glucose (*1*). SIDA, in which a stable isotope labeled (typically deuterium or carbon-13 is used for labeling) analogue of an unlabeled analyte is used as the internal standard during quantitative analysis. The stable isotope could be considered as the ultimate internal standard because of its great similarity in both physical and chemical properties to its unlabeled counterpart, the target analyte. After spiking and equilibration of a known amount of the stable isotope in the sample, the ratio of labeled and unlabeled compounds is maintained throughout extraction, workup and analysis steps (figure 1). Consequently, the two isotopologues, which differ in mass, are detected and differentiated by a mass spectrometer (MS) and the mass ion ratio of the two is used to determine the abundance of the target analyte in the initial sample.

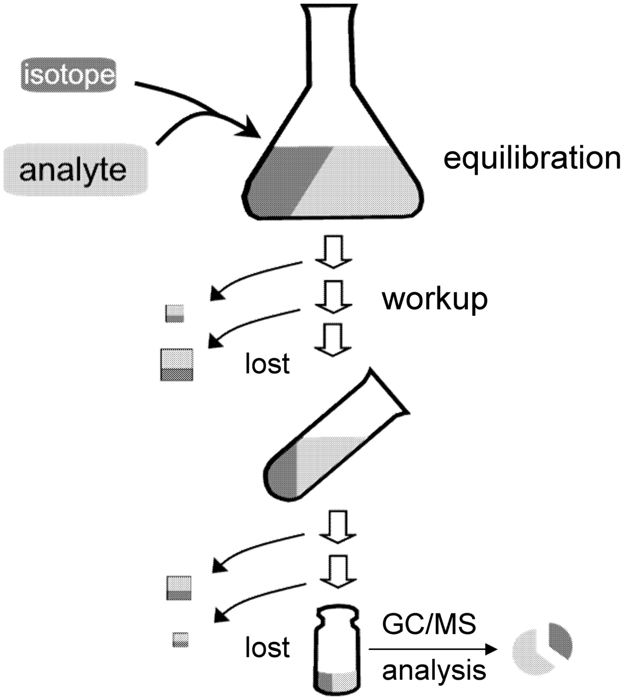

Figure 1. Concept of SIDA, where the isotopologue ratio remains stable throughout extraction and analysis.

SIDA has been applied for detection and quantitation of food contaminants by U.S. Food and Drug Administration (FDA) (*2*), and utilized in the investigation of food flavor (*3*), environmental hazards and pesticide residues (*4*). Despite its many advantages, SIDA is not widely used today due to the high cost associated with the purchase and/or synthesis of the isotope labeled standards. For example, the syntheses of deuterium labeled pyrazines have been challenging because of low yields and low purities based on previous literature. This chapter describes an improved method for the synthesis of deuterium labeled alkypyrazines to be used as internal standards for quantitative analysis (i.e. SIDA) of selected important alkylpyrazines in commercial peanut butters.

Downloaded by OHIO STATE UNIV LIBRARIES on May 29, 2012 | http://pubs.acs.org
Publication Date (Web): May 29, 2012 | doi: 10.1021/bk-2012-1098.ch005

Pyrazines - Formation and Occurrence in Foods

Pyrazines belong to a class of heterocyclic nitrogen-containing compounds which contain four carbon and two nitrogen atoms in a ring skeleton (figure 2). Various combinations of side groups on positions 2, 3, 5 or 6 provide for a variety of substituted pyrazines having various odor characteristics (e.g., nutty, earthy and roasty) and different odor detection thresholds (*5*).

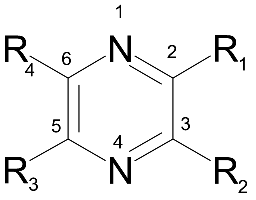

Figure 2. Pyrazine ($R_{1\sim4}$ = hydrogen, alkyl group, alkoxy group, alkanone group, etc.).

The earliest reports of pyrazines in food consist of patent documents from 1926 and 1928 which described methods for the preparation of natural coffee essential oil (*6*) and artificial coffee oil in which pyrazines were added (*7*). Alkyl pyrazines can be formed from amino acids and reducing sugars via the Maillard reaction and Strecker degradation, which occur in heated foods, especially those which are toasted or roasted in their preparation (*8*). Koehler and coworkers demonstrated the formation of amino carbonyls from the condensation of amino acid bound nitrogen with the carbonyl of a sugar, which in turn condense to form pyrazines (*9*). Pyrazines have been identified in various heat processed food products including nuts, soy, rice, egg, cocoa, cheese, bread, potato, vegetable, meat and seafood products and others (*10*). Therefore, pyrazines contribute, at least partially, to the overall flavor of nearly all heated foods. In particular, they have been reported as character-impact odorants in blanched peanut (*11*), roasted beef (*12*), french fries (*13*) and coffee (*14*).

Downloaded by OHIO STATE UNIV LIBRARIES on May 29, 2012 | http://pubs.acs.org
Publication Date (Web): May 29, 2012 | doi: 10.1021/bk-2012-1098.ch005

Determination of Alkylpyrazines in Foods

Pyrazines, as in the case of most volatile compounds, can be isolated from food systems by various methods. Steam distillation (atmospheric or vacuum) combined with solvent extraction has been commonly used (*15*, *16*). A main limitation of distillation, especially when conducted under atmospheric conditions, is the potential for artifact formation (*9*). This may be overcome by a mild and exhaustive distillation technique called solvent-assisted flavor evaporation (SAFE) (*17*). Other methods used without distillation include supercritical fluid extraction (*18*) and solvent free techniques such as headspace analysis (*19*) and solid-phase microextraction (SPME) (*20*).

In the identification of pyrazines, capillary gas chromatography (GC) coupling with a mass spectrometer has been the preferred method. The use of a nitrogen specific GC detector (e.g., nitrogen-phosphorus detector), has been used for the selective analysis of pyrazines (*15*). Other GC detectors used for the analysis of pyrazines include flame ionization and thermal conductivity detectors (*15*, *21*). The application of gas chromatography-olfactometry (GCO) techniques has enabled the identification of high (odor) potency pyrazines which exist in trace concentrations. For example, the roasty/nutty smelling compounds 2-ethyl-3,5-dimethylpyrazine and 2-ethyl-3,6-dimethylpyrazine, with low odor detection thresholds of 2.2 ng/g and 57 ng/g in oil (*13*), respectively, were identified as potent odorants in peanut based on GCO and molecular sensory analysis (*11*). This is in contrast to previous reports which indicated the more highly abundant methylpyrazine and 2,5-dimethylpyrazine were important aroma contributors in roasted peanut (*20*); however, these compounds have low odor-activity values (OAVs) because of their relatively high odor detection thresholds of 27 μg/g (methylpyrazine) and 17 μg/g (2,5-dimethylpyrazine) in oil (*22*).

Previous Methods Used for the Synthesis of Deuterium-Labeled Pyrazines

To our knowledge the first use of SIDA for the quantification of pyrazines was done by Schieberle and Grosch who determined the concentrations of acetylpyrazine and 2-methyl-3-ethylpyrazine in wheat and rye bread crusts (*23*). In that study, deuterated acetylpyrazine was prepared from pyrazinamide and magnesium [$^{2}H_{3}$]-methyl iodide. Labeled 2-methyl-3-ethylpyrazine was synthesized by the condensation of 2,3-pentanedione and [$^{2}H_{4}$]-ethylenediamine. This was followed by fractionation using column chromatography (aluminum oxide) and further purification by thin layer chromatography (TLC), which resulted in isolation of very low quantities of target compounds. In a later study by the same research group, two character-impact odorants 2,3-diethyl-5-methylpyrazine and 2-ethyl-3,5-dimethylpyrazine were quantified in roasted beef by SIDA (*12*). The deuterated isotopologues of the above compounds were synthesized by treating 2,3-diethylpyraizne or 2,6-dimethylpyraizne, respectively, with [$^{2}H_{3}$]-alkyl lithium. The labeled compounds were isolated by TLC and then purified by high performance liquid chromatography (HPLC). Three alkoxypyrazines, specifically 2-isobutyl-3-[$^{2}H_{3}$]-methoxypyrazine, 2-isopropyl-3-[$^2H_3$]-methoxypyrazine and 2-secbutyl-[$^2H_3$]-methoxypyrazine were synthesized by treating their unlabeled counterparts with hydrogen chloride to form the corresponding 2-alkyl-3-hydroxypyrazines. The hydroxy derivatives were then treated with gaseous [$^2H_2$]-diazomethane in [$^2H_3$]-methanol. Reaction mixtures were subjected to silica gel chromatography to obtain purified labeled compounds (*24*, *25*). Czerny and others prepared [$^2H_3$]-2-methoxy-3,5-dimethylpyrazine by refluxing 2,6-dimethylpyrazine with chlorine in carbon tetrachloride followed by treatment of the residue with sodium [$^2H_3$]-methoxide in [$^2H_3$]-methanol. TLC and preparative GC were applied for purification (*26*). Other deuterated alkylpyrazines, namely methylpyrazine, dimethylpyrazine and trimethylpyrazine have been prepared by neucleophilic addition via the organolithium reagent [$^2H_3$]-methyl lithium with either pyrazine, methylpyrazine or 2,5-dimethylpyrazine, respectively (*27*). The target compounds were isolated in low yields by TLC.

The main disadvantage of the above mentioned synthesis methods is the formation of numerous side products, thus resulting in low overall yields of the target compounds. Recently our group developed a convenient method for the synthesis of stable deuterium labeled alkylpyrazines. The synthesis involves the chlorination of an alkylpyrazine into a corresponding alkylchloropyrazine, followed by neucleophillic coupling of a deuterium labeled alkyl magnesium halide (Grignard reagent). The compounds [$^2H_3$]-2-methylpyrazine, [$^2H_5$]-2-ethylpyrazine, [$^2H_{10}$]-2,6-diethylpyrazine, [$^2H_3$]-2,3(6)-dimethylpyrazine, 2-methyl-3(6)-[$^2H_5$]-ethylpyrazine, [$^2H_3$]-trimethylpyrazine, [$^2H_5$]-2-ethyl-3,6-dimethylpyrazine, [$^2H_5$]-2-ethyl-3,5-dimethylpyrazine, and 2,3-diethyl-5-[$^2H_3$]-methylpyrazine have been successfully prepared in good yields (14-82%) and high purities (86-98%).

Application of SIDA for the Quantification of Selected Pyrazines in Commercial Peanut Butters

As previously mentioned, the primary prerequisite of SIDA is the availability of the isotope labeled internal standards. The following demonstration starts with the synthesis of labeled [$^2H_5$]-2-ethyl-3,6-dimethylpyrazine by an improved method as an example.

Synthesis of [$^2H_5$]-2-Ethyl-3,6-dimethylpyrazine ([$^2H_5$]-2E36DMP)

Organometallic reagents such as ethylmagnesium bromide (Grignard reagent) or ethyl lithium are highly reactive nucleophiles. They are often used in the organic synthesis for adding an alkyl group and are frequently used in the preparation of deuterated alkylpyrazines according to prvious literature. For example, in the reaction of 2,3-diethylpyraizne with [$^2H_3$]-methyl lithium only a small amount of 2,3-diethyl-5-[$^2H_3$]-methylpyrazine was found in reaction mixture, thus requiring further complex purification steps due to the low reaction yield (*12*). Although methyllithium is very reactive, this reaction only produces about 5% product due to the fact that an alkylpyrazine is not a good electrophilic substrate for the reactive

Downloaded by OHIO STATE UNIV LIBRARIES on May 29, 2012 | http://pubs.acs.org
Publication Date (Web): May 29, 2012 | doi: 10.1021/bk-2012-1098.ch005

Downloaded by OHIO STATE UNIV LIBRARIES on May 29, 2012 | http://pubs.acs.org
Publication Date (Web): May 29, 2012 | doi: 10.1021/bk-2012-1098.ch005

organometallic reagent. In order to overcome this problem, a chloroalkylpyrazine can be used as the substrate for the deuterium labeled alkyl Grignard reagent instead of an alkylpyrazine (*28*). The chlorine group (electrophile) on the pyrazine ring will be selectively and efficiently attacked by a deuterated alkyl group via Grignard reaction and the reaction yield could be nearly 100%. The following method was used to prepare [$^2H_5$]-2-ethyl-3,6-dimethylpyrazine in excellent yield. The general synthesis scheme is shown in figure 3.

Preparation of Grignard Reagent

Magnesium turnings [146 mg (6 mmol); 99.98% metals basis; Sigma-Aldrich Co., St. Louis, MO] was placed in a three-necked flask equipped with a magnet stir bar, a reflux condenser, rubber septa, and nitrogen purge line. Anhydrous diethyl ether [20 mL; 99.9%. Fisher Scientific, Fair Lawn, NJ] and a small crystal of iodine [Sigma-Aldrich] were added to give a yellow-brown clear solution. To the mixture was transferred (dropwise) a solution (720 mg (6.3 mmol) dissolved in 5 mL diethyl ether) of [$^2H_5$]-bromoethane [99 atom % D; Sigma-Aldrich] over a period of 20 min at room temperature with stirring (solution turned colorless and then cloudy). Stirring was continued for 2 h under nitrogen atmosphere and then the solution was cooled to 0 °C using an external ice bath.

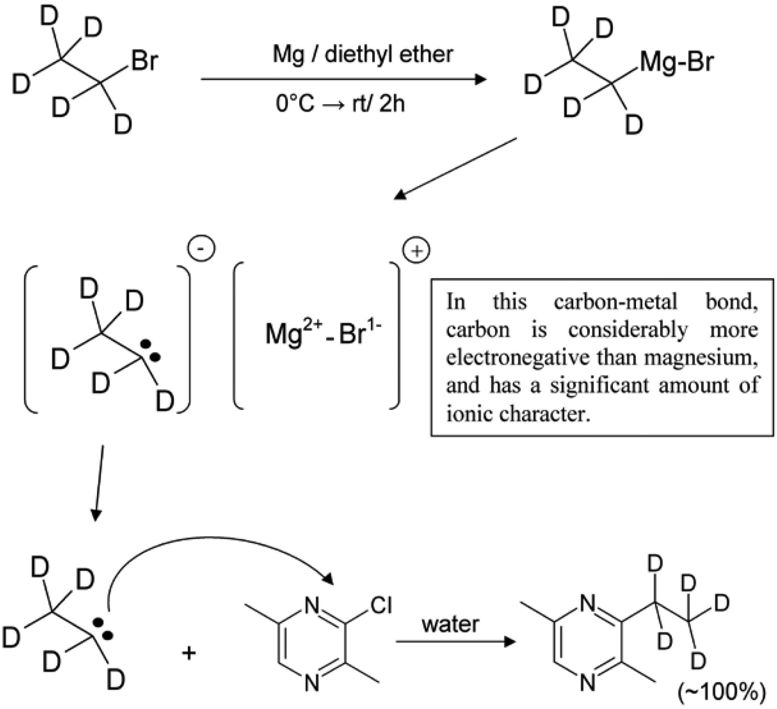

In this carbon-metal bond, carbon is considerably more electronegative than magnesium, and has a significant amount of ionic character.

Figure 3. Scheme for the synthesis of [$^2H_5$]-2-ethyl-3,6-dimethylpyraizne.

Downloaded by OHIO STATE UNIV LIBRARIES on May 29, 2012 | http://pubs.acs.org
Publication Date (Web): May 29, 2012 | doi: 10.1021/bk-2012-1098.ch005

Addition of Deuterium-Labeled Ethyl Group

[1,3-Bis (diphenylphosphino) propane] nickel (II) chloride [135 mg (5% mol equiv.); Sigma-Aldrich] (28) was added to the above Grignard reagent at 0°C. To the mixture was added dropwise of solution (713 mg (5 mmol) dissolved in 5 mL diethyl ether) of 3-chloro-2,5-dimethylpyrazine [98%. Sigma-Aldrich] with good stirring and the system was maintained at 0°C throughout the addition period of about 10 min (solution changed from red to black in color). The reaction mixture was removed from the ice bath and the temperature was allowed to rise to room temperature and then the mixture was stirred for 2 h.

Termination and Product Isolation

The mixture was chelated with 25 mL of ice-cold water and then stirred for 30 min at room temperature. The organic layer was separated, and the aqueous layer extracted twice with diethyl ether (20 mL). The combined organic layers were washed with brine and then concentrated (Vigreux column) to about 1 mL. The product was purified by column (1.5 cm i.d. x 20 cm length) chromatography (10 g; silica gel, grade 923, 100-200 mesh. Sigma-Aldrich] conditioned with a mixed solvent of pentane [Sigma-Aldrich]: diethyl ether (9:1, v/v). After loading of the reaction mixture, the column was washed with 70 mL of pentane: diethyl ether (9:1, v/v), and then with 70 mL of pentane: diethyl ether (7:3, v/v) to give 560 mg of the target compound (yield = 82%) [$^2H_5$]-2-ethyl-3,6-dimethylpyrazine, 98% purity by GC/FID. MS (EI): 141 (100, M^+), 139 (76), 140 (57), 42 (41), 61 (19), 39 (19), 110 (13), 109 (13), 40 (11), 108 (10).

Synthesis of Other Deuterated Pyrazines

[$^2H_5$]-2-Ethyl-3,5-dimethylpyrazine and 2,3-diethyl-5-[$^2H_3$]-methylpyrazine were prepared using a procedure similar to that described above for [$^2H_5$]-2-ethyl-3,6-dimethylpyrazine, except for the following: [$^2H_5$]-2-Ethyl-3,5-dimethylpyrazine was synthesized by reaction of 2-chloro-3,5-dimethylpyrazine with [$^2H_5$]-ethylmagnesium bromide and 2,3-diethyl-5-[$^2H_3$]-methylpyrazine was synthesized by reaction of 2,3-diethyl-5-chloropyrazine with [$^2H_3$]-methylmagnesium iodide.

Addition of Stable Isotopes, Equilibration, and Preparation of Volatile Extracts

Peanut butter was chosen for this demonstration since it is rich source of alkylpyrazines, is a homogeneous product, and represents a highly complex food matrix, typically being composed of 50% fat, 25% protein, 10% carbohydrates, ~1% water and ~1% emulsifiers.

The general procedure for quantification of pyrazines in peanut butter by SIDA is illustrated in figure 4. Peanut butter (100 g), 100 mL of a saturated aqueous sodium chloride solution and 150 mL diethyl ether were combined and thoroughly mixed using a magnetic stir bar. The isotope labeled internal standards ([$^{2}H_{5}$]-2-ethyl-3,5-dimethylpyraizne, [$^{2}H_{5}$]-2-ethyl-3,6-dimethyl-pyrazine, and 2,3-diethyl-5-[$^{2}H_{3}$]-methylpyrazine in diethyl ether) were then added (amounts added were based on preliminary data) and the mixture was stirred for 3 h to achieve equilibrium between the internal standards and unlabeled analytes. The mixture was centrifuged (2000xg) and the solvent layer collected. The residue was extracted (with 1 h stirring and centrifugation) two more times with 100 ml diethyl ether. The combined solvent extract was concentrated to 150 mL by (Vigreux column) distillation. The volatile compounds were subjected to SAFE and then fractionated into neutral/basic (NB) and acidic (AC) fractions (*29*). Only the NB fraction (containing the pyrazines) was analyzed by GC-MS.

Downloaded by OHIO STATE UNIV LIBRARIES on May 29, 2012 | http://pubs.acs.org
Publication Date (Web): May 29, 2012 | doi: 10.1021/bk-2012-1098.ch005

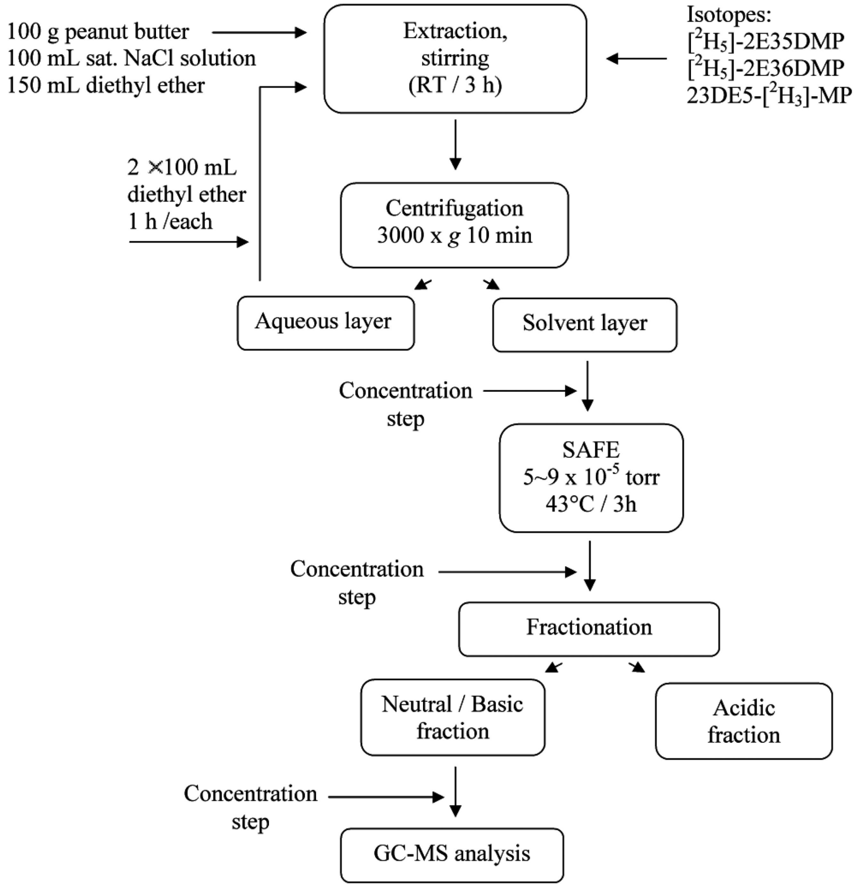
100 g peanut butter
100 mL sat. NaCl solution
150 mL diethyl ether
Extraction, stirring (RT / 3 h)
Isotopes:
[²H₅]-2E35DMP
[²H₅]-2E36DMP
23DE5-[²H₃]-MP
2 ×100 mL diethyl ether 1 h /each
Centrifugation 3000 x g 10 min
Aqueous layer
Solvent layer
Concentration step
SAFE 5~9 x 10⁻⁵ torr 43°C / 3h
Concentration step
Fractionation
Neutral / Basic fraction
Acidic fraction
Concentration step
GC-MS analysis

Figure 4. General procedure of SIDA for quantification of selected pyrazines in peanut butter.

Instrumental Analysis and Quantification Methods

As earlier mentioned, the accuracy of SIDA is assured because the ratio of the labeled and unlabeled isotopologues remains constant throughout the isolation and analysis steps. However, the nearly identical physical and chemical properties of the two isotopologues can results in peak overlap or co-elution during GC. Therefore, a MS detector is needed to distinguish the two isotopologues based on differences between certain mass ions which are unique for each compound. There were several important considerations for selecting ions for quantification. These include: 1) high mass, 2) no ion overlap between isotopologues and 3) high relative ion intensity. For example, figure 5 shows the mass spectra for (a) unlabeled 2-ethyl-3,6-dimethylpyraizne and (b) deuterated 2-ethyl-3,6-dimethylpyraizne. Several ion pairs could be chosen for quantification. The ion pair of 136 (unlabeled) versus 141 (labeled) is a good choice because it satisfies the aforementioned considerations.

Downloaded by OHIO STATE UNIV LIBRARIES on May 29, 2012 | http://pubs.acs.org
Publication Date (Web): May 29, 2012 | doi: 10.1021/bk-2012-1098.ch005

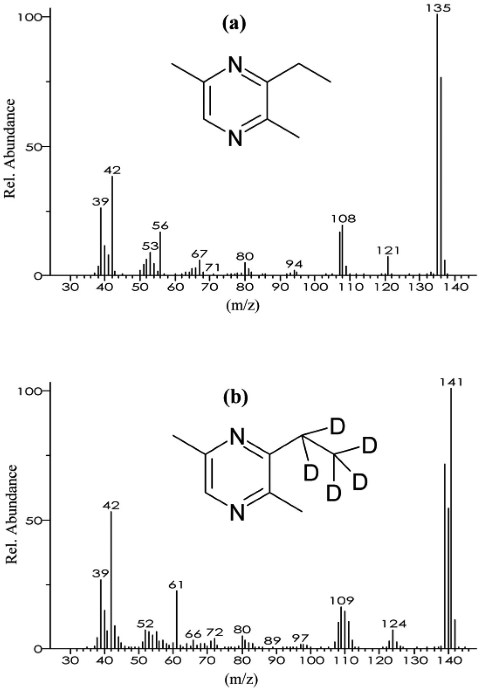

Figure 5. Mass spectra (electron impact) of (a) unlabeled and (b) [$^2H_5$]-labeled 2-ethyl-3,6-dimethylpyrazine.

Downloaded by OHIO STATE UNIV LIBRARIES on May 29, 2012 | http://pubs.acs.org
Publication Date (Web): May 29, 2012 | doi: 10.1021/bk-2012-1098.ch005

In addition, ions selected for the unlabeled and labeled compounds might have different signal responses depending on the type of ionization used during GC-MS analysis. It is, therefore, necessary to determine a response factors for the ion pair based on the relationship of the ion peak area ratio to that of the mass ratio of unlabeled to labeled compound. For example, five solutions of unlabeled 2-ethyl-3,6-dimethylpyraizne (2E36DMP) and [$^2H_5$]-2-ethyl-3,6-dimethylpyraizne ([$^2H_5$]-2E36DMP) were prepared with mass ratios of 1/10, 1/5, 1/1, 5/1 and 10/1 and these were analyzed by GC-MS. The response factor (Table I) was determined as the reciprocal slope of linear regression plot (slope = 0.926, intercept = 0.160, $r^2 = 0.99$) of mass ratio versus ion area ratio.

Table I. Selected Ions and Response Factors Used in Stable Isotope Dilution Analysis of Selected Pyrazines

pyrazine (analyte)	*labeled standard*	*mass ion (m/z)*		*response factor*
		analyte	*internal standard*	
2-ethyl-3,5-dimethylpyrazine	[$^2H_5$]-2E35DMP	136	141	0.913
2-ethyl-3,6-dimethylpyrazine	[$^2H_5$]-2E36DMP	136	141	1.080
2,3-diethyl-5-methyl pyrazine	23DE5-[$^2H_3$]-MP	150	153	1.088

Note: GC/MS was performed using a 6890 gas chromatograph-5973N mass selective detector (Agilent, Palo Alto, CA). Separations were performed on a Stabilwax column (30 m x 0.25 mm x 0.25 μm film thickness, Restek, Bellefonte, PA). Helium was the carrier at a constant flow of 1 mL/min. To minimize loss of any labile constituents, samples were injected using a PTV inlet in the cold splitless mode (-50°C for 0.1 min, then ramped at 12°C/sec and held at 260°C). GC oven temperature was programmed from 35 to 225°C at 6°C/min with initial and final hold times of 5 and 20 min, respectively. Other conditions were as follows: MSD interface temperature, 260°C; ionization energy, 70 eV; mass range, 35-350 a.m.u; EM voltage, Autotune + 165 V; scan rate, 4.45 scans/s.]

The concentrations of selected alkylpyrazines were calculated based on the extracted ion peak area ratios (extracted ion peak area of analyte / extracted ion peak area of labeled internal standard) corrected by the response factor (Table I). The labeled compounds (ion 141 or 153) eluted at retention times close to those of the unlabeled compounds (ion 136 or 150), but showed a distinct mass shift. Therefore, the analytes and internal standards can be identified by matching mass spectral information and GC retention characteristics.

Downloaded by OHIO STATE UNIV LIBRARIES on May 29, 2012 | http://pubs.acs.org
Publication Date (Web): May 29, 2012 | doi: 10.1021/bk-2012-1098.ch005

Table II. Concentrations and Odor-Activity Values (OAVs) for Selected Alkylpyrazines in Commercial Peanut Butters

alkylpyrazine	*Jif* [a]		*Planters* [b]		*Skippy* [c]		*Smucker's* [d]	
	Conc. [e]	*OAV* [f]	*Conc.*	*OAV*	*Conc.*	*OAV*	*Conc.*	*OAV*
23DE5MP	11.7 ± 0.2	23	26.2 ± 2.1	52	42.7 ± 4.8	85	40.0 ± 2.2	68
2E35DMP	79.9 ± 3.3	40	105 ± 7	52	139 ± 8	70	189 ± 10	94
2E36DMP	328 ± 2	6	598 ± 3	7	503 ± 6	9	421 ± 3	10

[a] Jif Creamy Peanut Butter 18 OZ; The J. M. Smucker Company, Orrville, OH. [b] New Planters Creamy Peanut Butter 16.3 OZ; Kraft Foods Global Inc., Northfield, IL. [c] Skippy Natural Creamy Peanut Butter Spread 15 OZ; Unilever Company, Englewood cliffs, NJ. [d] Smucker's Natural Creamy Peanut Butter 16 OZ; The J. M. Smucker Company, Orrville, OH. [e] Average Concentration (ng/g) ± standard deviation (n = 2). [f] Odor-activity value (OAV) = concentration / odor detection thresholds (in oil) from reference (*11*) [Threshold values: 23DE5MP, 0.5 ng/g; 2E35DMP, 2.2 ng/g; 2E36DMP, 57 ng/g]

Concentrations and OAVs of Selected Alkylpyrazines in Commercial Peanut Butters

Concentrations and odor active values (OAVs) for selected alkylpyrazines in commercial peanut butters are given in Table II. There are limited quantitative data in the literature concerning alkylpyrazines in peanut products, and most of these reports focused only on the highly abundant alkylpyrazines, such as 2,5-dimethylpyrazine and 2,6-dimethylpyrazine (*18*, *20*). As mentioned earlier, these highly abundant alkylpyrazines are not considered to be major contributors to roasted peanut flavor because of their relatively high odor detection thresholds. On the other hand, certain pyrazines with low odor detection thresholds, such as 2E35DMP, 2E36DMP and 23DE5MP, are reported to be important odorants despite their relatively low abundance in peanut products. Previously, 2E35DMP, 2E36DMP and 23DE5MP were reported to be present at 5534 ng/g, 352 ng/g and 2.2 ng/g (*9*), respectively, in blanched peanut and 23 ng/g, 196 ng/g and 13 ng/g, respectively, in pan roasted peanut (*27*). The above concentrations are close to those determined in the present study for the commercial peanut butters, although some differences due to peanut variety, processing and other factors are to be expected. Therefore, SIDA appears to a suitable means to accurately quantify of alkylpyrazines in peanut butters.

The precision of SIDA was also acceptable, with an average relative standard deviation (RSD) of 4.4%, which ranged from 0.6% to 11.2%. The higher RSD for 2,3-diethyl-5-methylpyrazine was probably due to the low concentration of the compound (~10 to 40 ng/g). Some other errors could have been caused the difficulty in precisely spiking of trace amounts of the labeled internal standards or by inconsistent integration of very small peaks during data analysis.

Conclusions

- A prerequisite of SIDA for alkylpyrazine analysis is the availability of stable isotopic labeled internal standards. This challenge was overcome by development of an improved and convenient synthesis method for deuterated alkylpyrazines, which involves the nucleophilic addition of a labeled alkyl Grignard reagent to a chloroalkylpyrazine resulting in the high yield and purity of the target compounds.
- Applications of SIDA for the determination of three important alkylpyrazines in four peanut butters demonstrated the great accuracy and precision of the method.
- The availability of chloroalkylpyrazines is the key of this improved synthesis. Typically, there are over ten alkylpyrazines in peanut products which are found in relatively high abundance. The synthesis of the isotope labeled counterparts of these pyrazines requires the availability of several different kinds of chloroalkylpyrazines. The synthesis of chloroalkylpyrazines by chlorination of alkylpyrazines or alkylpyrazine-N-oxides will be described by our group in a separate communication.

Downloaded by OHIO STATE UNIV LIBRARIES on May 29, 2012 | http://pubs.acs.org
Publication Date (Web): May 29, 2012 | doi: 10.1021/bk-2012-1098.ch005

References

1. Sweeley, C. C.; Elliott, W. H.; Fries, I.; Ryhage, R. *Ana. Chem.* **1966**, *38*, 1549–1553.
2. USFDA. *Detection and quantitation of acrylamide in foods.* 2002. http://www.fda.gov/Food/FoodSafety/FoodContaminantsAdulteration/ChemicalContaminants/Acrylamide/default.htm
3. Munch, P.; Schieberle, P. *J. Agric. Food Chem.* **1998**, *46*, 4695–4701.
4. Cai, Z.; Wang, D.; Ma, W. T. *Anal. Chim. Acta* **2004**, *503*, 263–270.
5. Fors, S. In *The Maillard reaction in Foods and Nutrition*; Waller, G. R., Feather, M. S., Eds.; ACS Symposium Series 215; American Chemical Society: Washington, D.C., 1983; pp 185−286.
6. Reichstein, T.; Staudinger, H. British patent GB246454, 1926.
7. Reichstein, T.; Staudinger, H. British patent GB260960, 1928.
8. Hwang, H.; Hartman, T. G.; Ho, C. *J. Agric. Food Chem.* **1995**, *43*, 179–184.
9. Koehler, P. E.; Mason, M. E.; Newell, J. A. *J. Agric. Food Chem.* **1969**, *17* (2), 393–396.
10. Maga, J. A. *Crit. Rev. Food Sci. Nutr.* **1982**, *16*, 1–48.
11. Schirack, A. V.; Drake, M. A.; Sanders, T. H.; Sandeep, K. P. *J. Food Sci.* **2006**, *71*, C513–C520.
12. Cerny, C.; Grosch, W. *Z. Lebensm.-Unters. Forsch.* **1993**, *196*, 417–422.
13. Wagner, R. K.; Grosch, W. *J. Am. Oil Chem. Soc.* **1998**, *75*, 1385–1392.
14. Blank, I.; Sen, A.; Grosch, W. *Z. Lebensm.-Unters. Forsch.* **1992**, *195*, 239–245.
15. Herent, M.; Collin, S. *J. Agric. Food Chem.* **1998**, *46*, 1975–1980.
16. Mussinan, C. J.; Wilson, R. A.; Katz, I. *J Agric. Food Chem.* **1973**, *21*, 871–872.
17. Engel, W.; Bahr, W.; Schieberle, P. *Eur. Food Res. Technol.* **1999**, *209*, 237–241.
18. Leunissen, M.; Davidson, V. J.; Kakuda, Y. *J. Agric. Food Chem.* **1996**, *44*, 2694–2699.
19. Warner, K. J. H.; Dimick, P. S.; Ziegler, G. R.; Mumma, R. O.; Hollender, R. *J. Food Sci.* **1996**, *61*, 469–472.
20. Baker, G. L.; Cornell, J. A.; Gorbst, D. W.; Okeefe, S. F.; Sims, C. A.; Talcott, S. T. *J. Food Sci.* **2003**, *68*, 394–400.
21. Manson, M. E.; Johnson, B. *J. Agric. Food Chem.* **1966**, *14*, 454–460.
22. Koehler, P. E.; Manson, M. E.; Odell, G. V. *J. Food Sci.* **1971**, *36*, 816–818.
23. Schieberle, P.; Grosch, W. *J. Agric. Food Chem.* **1987**, *35*, 252–257.
24. Semmelroch, P.; Grosch, W. *J. Agric. Food Chem.* **1996**, *44*, 537–543.
25. Masanetz, C.; Grosch, W. *Flavor Frag. J.* **1998**, *13*, 115–124.
26. Czerny, M.; Grosch, W. *J. Agric. Food Chem.* **2000**, *48*, 868–872.
27. Chetschik, I.; Granvogl, M.; Schieberle, P. *J. Agric. Food Chem.* **2010**, *58*, 11018–11026.
28. Sato, N.; Matsuura, T. *J. Chem. Soc., Perkin Trans.* **1996**, *1*, 2345–2350.
29. Rotsatchakul, P.; Chaiseri, S.; Cadwallader, K. R. *J. Agric. Food Chem.* **2008**, *56*, 528–536.

Downloaded by OHIO STATE UNIV LIBRARIES on May 29, 2012 | http://pubs.acs.org
Publication Date (Web): May 29, 2012 | doi: 10.1021/bk-2012-1098.ch005

Downloaded by CORNELL UNIV on May 30, 2012 | http://pubs.acs.org
Publication Date (Web): May 29, 2012 | doi: 10.1021/bk-2012-1098.ch006

Chapter 6

An LC/MS/MS Method for the Analysis of Furocoumarins in Citrus Oil

Richard Hiserodt* **and Li Chen**

International Flavors & Fragrances Inc., 1515 State Highway 36,
Union Beach, NJ 07735
***E-mail: richard.hiserodt@iff.com**

Furocoumarins are secondary plant metabolites commonly found in the families *Umbelliferae* and *Rutaceae*. The basic members of this class of compounds are psoralen and angelicin. Researchers have shown particular interest in alkoxy analogues of psoralen; particularly at the 5- and 8-positions. Bergapten (5-methoxypsoralen) and xanthotoxin (8-methoxypsoralen) have been found to be effective in the treatment of the skin diseases psoriasis and vitiligo when combined with the phototherapy technique, PUVA. A mode of action is thought to be mono-adduct formation with DNA but formation of di-adducts, leading to cross-linked DNA and potential carcinogenic side effects, is also a possibility. In response to this, the International Fragrance Association (IFRA) and the European Commission have agreed to ban the use of furocoumarins in cosmetic products except when they are part of natural essences. When present as the result of natural essences, the total furocoumarin concentration cannot exceed 5 ppm based on the analysis of seven marker furocoumarins. To ensure compliance, an LC/MS/MS method using electrospray ionization was developed for the analysis of the seven marker furocoumarins plus seven other furocoumarins. Various aspects of method development are discussed as well as conclusions from the analysis of citrus oils.

In Recent Advances in the Analysis of Food and Flavors; Toth, S., et al.;
ACS Symposium Series; American Chemical Society: Washington, DC, 2012.

Downloaded by CORNELL UNIV on May 30, 2012 | http://pubs.acs.org
Publication Date (Web): May 29, 2012 | doi: 10.1021/bk-2012-1098.ch006

Introduction

Background

Furocoumarins (also known as furanocoumarins or psoralens) are secondary plant metabolites commonly found in the families *Umbelliferae* / *Apiaceae* (angelica, carrot, celery, parsley, cumin, etc.) and *Rutaceae* (citrus) but found in other families also (*1*). The basic members of this class of compounds are psoralen and angelicin (see Figure 1) Psoralen is linear and toxic and angelicin is angular and thought to present little threat to human health (*2*, *3*).

The furocoumarins in which researchers have shown particular interest are alkoxy analogues of psoralen (see Figure 2); particularly at the 5- and 8-positions. Bergapten (5-methoxypsoralen, 5-MOP) and xanthotoxin (8-methoxypsoralen, 8-MOP) have been found effective in the treatment of the skin diseases psoriasis and vitiligo when combined with phototherapy; a combination of psoralen and UVA-radiation commonly referred to as PUVA. A mode of action of PUVA is thought to be the formation of mono-adducts with DNA; specifically the pyrimidine base thymine in thymine-adenine base pairs. Mono-adduct formation can occur by way of a cycloaddition reaction at the 3-4 double bond or the 4′-5′ double bond of psoralen or its alkoxy analogs (see Figure 1). Because there are two sites at which cycloaddition can occur, there is a potential for DNA cross-linking if the second DNA strand also contains a thymine-adenine base pair in close proximity. Di-adduct formation can lead to potential carcinogenic side effects. Psoralen has a greater tendency to form di-adducts than the methoxy analogues bergapten and xanthotoxin. Angelicin does not have a strong tendency to form di-adducts because of stearic hindrance (*2*–*5*).

The characteristics of furocoumarins that make them good drug candidates for the treatment of psoriasis and vitiligo are not desirable for ingredients used in cosmetics and sunscreens. Sunscreens containing bergapten, from the use of bergamot oil in these products, were marketed in the US and EU in the early 1980s (*6*). Early studies indicated the level of bergapten in sunscreens was too low to worry about phototoxicity but a study in 1982 by Walter, *et al.* (*7*) concluded that the concentration of bergapten was high enough to induce cutaneous phototoxicity. In 1987, Switzerland banned psoralen-containing sunscreens. In 1995, the first epidemiological study was published linking melanoma risk to bergapten and the EU banned suntan lotions containing >1 ppm total psoralen (*8*).

Legislation

Historically, the International Fragrance Association (IFRA) has limited bergapten to 15 ppm in finished consumer products that are applied to the skin and subsequently exposed to sunlight. Currently, European Cosmetics Directive 76/768/EEC (Entry 358, Annex II) prohibits the use of furocoumarins except for the normal content in natural essences and limits their concentration to < 1 ppm in sun protection and bronzing products. The Scientific Committee on Consumer Products (SCCP), now the Scientific Committee on Consumer Safety (SCCS), which advises the European Commission, proposed in 2001 to limit the furocoumarin concentration from natural essences to 1 ppm in all types of cosmetic products (SCCNFP/0932/00). This would greatly restrict the use of natural citrus oils in these products (*9–11*)

In response to this, the Research Institute for Fragrance Materials (RIFM), which evaluates the safety of fragrance raw materials in cosmetics and other consumer products, initiated a number of studies to evaluate the risk of furocoumarins in cosmetic products. The results of these studies were shared with the European Commission in 2007 in the form of a proposal to allow a total of 5 ppm of any combination of six marker furocoumarins (bergapten, bergamottin, byakangelicol, epoxybergamottin, isopimpinellin, and oxypeucedanin) in any type of leave-on product and 50 ppm for rinse-off products (*9–11*). The European Commission agreed with the stipulation that xanthotoxin be added to the list creating a total of seven marker furocoumarins. The restriction would therefore be no more than 5 ppm for leave-on products and 50 ppm for rinse-off products for any combination of the seven furocoumarin marker compounds with the added stipulation that no single furocoumarin be present at >1 ppm (*11*).

Downloaded by CORNELL UNIV on May 30, 2012 | http://pubs.acs.org
Publication Date (Web): May 29, 2012 | doi: 10.1021/bk-2012-1098.ch006

Analytical Methods

Few analytical methods have been reported in the literature on the quantitation of furocoumarins in citrus. The studies that have were limited in the number of furocoumarins studied or matrices investigated (*12–19*). Frerot, *et al.* published an elegant study of 15 furocoumarins (*19*). They utilized diode array detection (DAD) but reported several coelution problems using this detection system. They were able to resolve these issues by utilizing fluorescence and MS detection as well as the use of two mobile phases. Without these backup detection systems, these coelution problems might lead to misidentifications. This is the analytical method IFRA is currently evaluating, for general use, for the analysis of furocoumarins in citrus oils.

Purpose

The purpose of this work was to develop an LC/MS/MS method for the quantitative analysis and identification of the seven marker furocoumarins plus seven other furocoumarins at the 1 ppm level to be compliant with proposed IFRA and European Commission guidelines for the analysis of these compounds in citrus products used in cosmetics.

Materials and Methods

Analytical Standards

Analytical standards were purchased from ChromaDex (Irvine, CA, Grade P). Citrus oils were obtained from various sources and were predominately cold pressed oils.

Downloaded by CORNELL UNIV on May 30, 2012 | http://pubs.acs.org
Publication Date (Web): May 29, 2012 | doi: 10.1021/bk-2012-1098.ch006

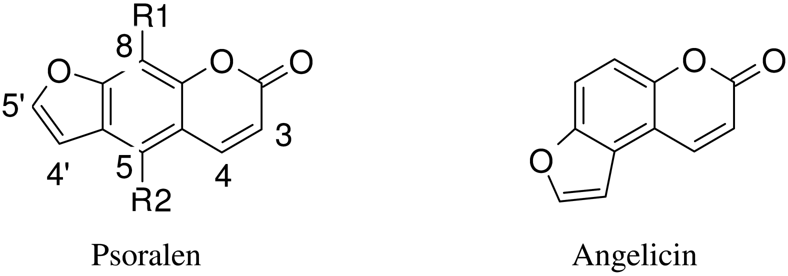
R1
8
O
O
O
5'
3
4'
5
4
R2
Psoralen
O
O
O
Angelicin

Figure 1. Structures of psoralen and angelicin.

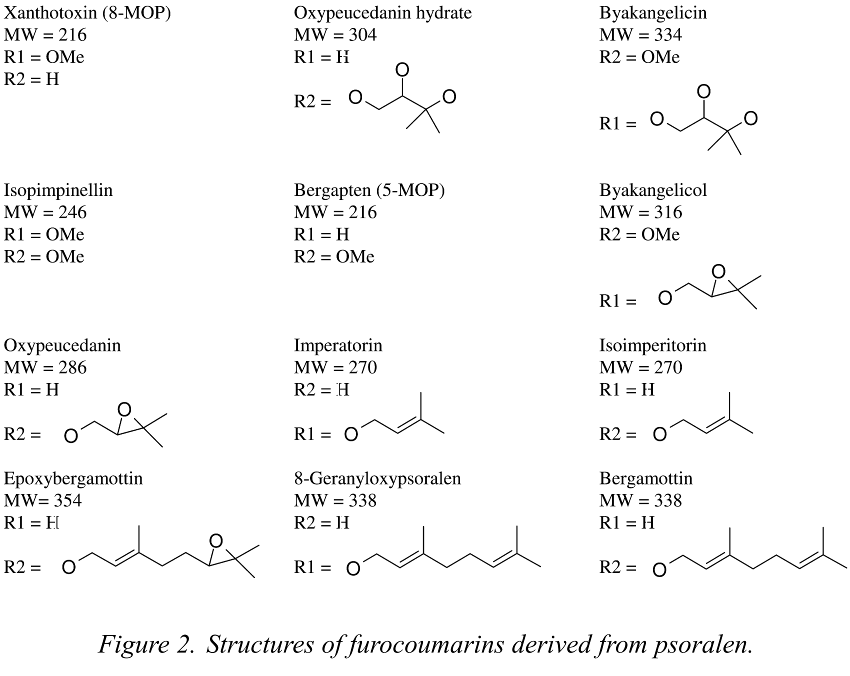
Xanthotoxin (8-MOP)
MW = 216
R1 = OMe
R2 = H
Oxypeucedanin hydrate
MW = 304
R1 = H
R2 =
Byakangelicin
MW = 334
R2 = OMe
R1 =
Isopimpinellin
MW = 246
R1 = OMe
R2 = OMe
Bergapten (5-MOP)
MW = 216
R1 = H
R2 = OMe
Byakangelicol
MW = 316
R2 = OMe
R1 =
Oxypeucedanin
MW = 286
R1 = H
R2 =
Imperatorin
MW = 270
R2 = H
R1 =
Isoimperitorin
MW = 270
R1 = H
R2 =
Epoxybergamottin
MW= 354
R1 = H
R2 =
8-Geranyloxypsoralen
MW = 338
R2 = H
R1 =
Bergamottin
MW = 338
R1 = H
R2 =

Figure 2. Structures of furocoumarins derived from psoralen.

Preparation of Standard Stock Solutions and Standards

Standard stock solutions of each furocoumarin (approximately 5 mg/mL ±0.01 mg) were prepared in acetonitrile and stored at -20 °C. Aliquots were taken from the individual stock solutions and diluted in methanol such that all standards contained equal concentrations of the furocoumarins from 1 to 1000 ng/mL equivalent to 1-1000 ppm based on a 1 mg/mL sample concentration. Fresh standards were prepared for every sequence of samples.

Downloaded by CORNELL UNIV on May 30, 2012 | http://pubs.acs.org
Publication Date (Web): May 29, 2012 | doi: 10.1021/bk-2012-1098.ch006

Table 1. LC/MS/MS analyte specific parameters for furocoumarins

Retention time (min.)	*Furocoumarin*	*CAS No.*	*Transitions (m/z > m/z)*	*CE (V)*	*S-Lens (V)*
3.52	Psoralen	66-97-7	187>131 187>77	27 42	99
3.64	Xanthotoxin (8-MOP)*	298-81-7	217>161 217>89	25 43	86
3.81	Angelicin	523-50-2	187>131 187>77	27 42	99
3.89	Oxypeucedanin hydrate	26423-85-8	305>203 305>147	27 38	105
3.92	Byakangelicin	482-25-7	335>233 335>231	16 20	78
4.35	Isopimpinellin*	482-27-9	247>217 247>95	27 27	102
4.49	Bergapten (5-MOP)*	484-20-8	217>202 217>89	23 42	93
5.20	Byakangelicol*	26019-79-2	317>233 317>231	14 18	92
5.31	Oxypeucedanin*	26091-73-6	305>203 305>147	20 35	97
6.37	Imperatorin	482-44-0	271>203 271>147	14 34	77
7.36	Isoimperatorin	482-445-1	271>203 271>147	14 34	67
7.40	Epoxybergamotin*	264234-04-0	355>203 355>147	30 42	73
8.64	8-Geranyloxypsoralen	7437-55-0	339>203 339>147	17 39	84
9.35	Bergamottin*	7380-40-7	339>203 339>147	17 39	79

* Marker furocoumarins

Preparation of Samples

Approximately 10 mg of citrus oil (±0.01 mg) were diluted to 10.0 mL with methanol.

Analytical Method

LC/MS/MS analysis was carried out with a Shimadzu LC-20AD Prominence HPLC system (Shimadzu Scientific Instruments, Columbia, MD) interfaced with

In Recent Advances in the Analysis of Food and Flavors; Toth, S., et al.;
ACS Symposium Series; American Chemical Society: Washington, DC, 2012.

Downloaded by CORNELL UNIV on May 30, 2012 | http://pubs.acs.org
Publication Date (Web): May 29, 2012 | doi: 10.1021/bk-2012-1098.ch006

a TSQ Vantage triple quadrupole mass spectrometer (ThermoElectron, San Jose, CA). The chromatographic separation was performed on an Eclipse Plus C18, 1.8 µm, 4.6 mm X 50 mm (Agilent Technologies, Wilmington, DE) which was maintained at room temperature. Mobile phase A consisted of water (5 mM $HCOOH.NH_3$ + 0.1% formic acid) and mobile phase B consisted of methanol (5 mM $HCOOH.NH_3$ + 0.1% formic acid). The gradient profile was 40% B to 100% B in 10 min. (hold for 2 min. at 100% B) and re-equilibrate at initial conditions for 2 min. The injection volume was 2 µL. The Ion Max source parameters were 5.0 kV HESI spray voltage, vaporizer temperature 300 °C, sheath gas 60, aux gas 25, and capillary temperature 300 °C. The analyte specific parameters are listed in Table 1.

Results and Discussion

Identification

LC/MS/MS is a very sensitive technique for multicomponent analysis. This sensitivity is achieved by monitoring two or three characteristic ions or transitions in an analyte's spectrum rather than the complete spectrum. When choosing the transitions to monitor, one has to be mindful of choosing ions that will give the best sensitivity while at the same time be characteristic of the analyte in question (*20–26*). For instance, the two most intense ions for monitoring the pesticide fenoxycarb are *m/z* 116 and *m/z* 256. These ions are generated from different parts of the molecule and therefore are characteristic of this analyte (see Figure 3).

This is not strictly the case for the furocoumarin oxypeucedanin. Here the alkoxy side chain fragments to yield the ion at *m/z* 203 which further fragments to yield the ion at *m/z* 147 (see Figure 4). In other words, both fragments originate from the same part of the molecule. This is generally the case with the other furocoumarins as well. Consequently, more emphasis was placed on monitoring ions that gave good sensitivity rather than ions that were strictly from different parts of the molecule.

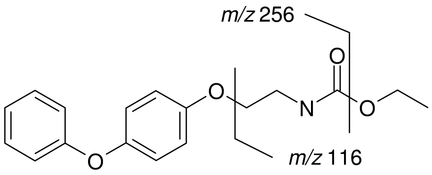

Figure 3. Transitions monitored for the pesticide fenoxycarb and their relationship to the molecule.

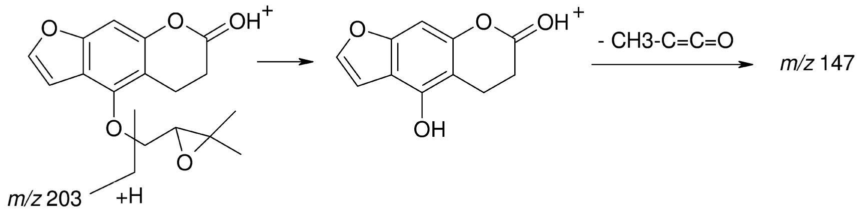

Figure 4. Transitions monitored for the furocoumarin oxypeucedanin and their relationship to the molecule.

It is important to exclude ions that are due to nonspecific loss of H_2O or NH_3 from the protonated molecule as candidates for ions to monitor. CH_3 is sometimes included in this list but loss of a methyl radical from a protonated molecule (an even-electron molecule) generates an odd-electron molecule which is a violation of the even-electron rule (*27*) and is not a common occurrence in an LC/MS/MS experiment. Loss of a methyl radical is seen in protonated molecules that have a methoxy group attached to an aromatic ring which can readily delocalize the odd electron. This is the case with bergapten. The transition *m/z* 217 > *m/z* 202 is due to the loss of a methyl radical from the protonated molecule. However, this was not the case for xanthotoxin.

Table 2. Acceptance criteria for agreement of analyte peak area ratios with standard peak area ratios

Relative Intensity (% of base peak)	*LC/MS/MS (relative)*
>50%	±20%
>20% to 50%	±25%
>10% to 20%	±30%
≤10%	±50%

In accordance with European Commission guidelines, two transitions were monitored for each furocoumarin and identification was based on the peak area ratio for the two transitions which leads to four identification points (see Figure 5). The agreement between the peak area ratios for the standards and samples depends on the relative intensity of the transitions monitored and are summarized in Table 2 (*21*).This is required to minimize the possibility of interference from coeluting matrix components.

Downloaded by CORNELL UNIV on May 30, 2012 | http://pubs.acs.org
Publication Date (Web): May 29, 2012 | doi: 10.1021/bk-2012-1098.ch006

Downloaded by CORNELL UNIV on May 30, 2012 | http://pubs.acs.org
Publication Date (Web): May 29, 2012 | doi: 10.1021/bk-2012-1098.ch006

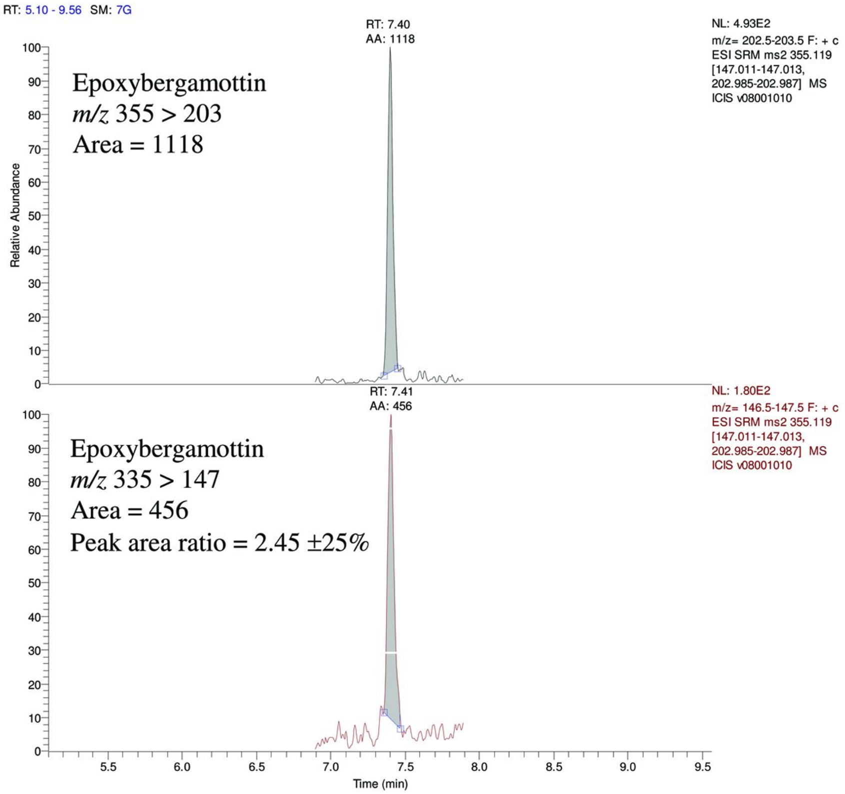

Figure 5. Evaluation of peak area ratio data for epoxybergamottin and generating four identification points.

Chromatography

There are four pairs of furocoumarin pairs that have the same nominal mass and transitions and must be separated to ensure accurate quantitation. They are psoralen/angelicin, xanthotoxin/bergapten, imperatorin/isoimperatorin, and 8-geranyloxypsoralen/bergamottin (see chromatogram in Figure 6).

Isoimperatorin and epoxybergamottin have different nominal masses but also have the same transitions and are not baseline resolved under the chromatographic conditions used in this study (retention time 7.36 min. and 7.40 min. respectively). Even though they are not chromatographically separated, good quantitation can be obtained because they can be separated in the mass spectrometer as long as cross-talk is not an issue.

Cross-talk can occur when you have two components with different masses but the same transitions and are coeluting or poorly resolved. This is the case with isoimperatorin (MW = 271) and epoxybergamottin (MW = 355). During this analysis, ions *m/z* 147 & *m/z* 203 are monitored for both compounds. Cross-talk can occur, for instance, when isoimperatorin is being monitored but the ions for epoxybergamottin have not cleared the collision cell leading to spurious results. The occurrence of cross-talk can be checked by making an injection of isoimperatorin while monitoring the transitions for both isoimperatorin and epoxybergamottin (see Figure 7). Since there is not a distinct peak in the bottom chromatogram for epoxybergamottin, there is no cross-talk.

Downloaded by CORNELL UNIV on May 30, 2012 | http://pubs.acs.org
Publication Date (Web): May 29, 2012 | doi: 10.1021/bk-2012-1098.ch006

Quantitation

Quantitative data were obtained using the external standard method and the weakest of the two transitions monitored for each furocoumarin. The weakest transition was chosen for quantitation to insure that the peak ratio can be evaluated at low concentrations. Standards were prepared in the 1-1000 ng/mL range (equivalent to 1-1000 ppm based on a 1 mg/mL sample concentration). Standards were run before and after a sample sequence of 25 samples. The resulting calibration curves were fitted to either linear or quadratic equations and weighted 1/X. There should be no more than a 15% deviation of the standards from the nominal concentration. A blank was run after the first standard sequence and before the last to ensure there was no carry-over.

Bergamot, lemon, grapefruit, orange, and Mandarin oils were spiked with 10 ng/mL of each furocoumarin (equivalent to 10 ppm each based on a sample concentration of 1 mg/mL, 1 replicate each citrus oil). Recoveries of furocoumarins were 86-112%. Recoveries from a folded oil (orange 5X) ranged from 73-115% with the exception of bergamottin which was 59% (see Table 3). To evaluate recovery at different levels, an orange oil was spiked 2, 10, 100, & 500 ng/mL equivalent to 2, 10, 100, & 500 ppm based on a 1 mg/mL sample concentration. The recovery for all furocoumarins at all levels ranged from 88-108% (data not reported).

A lemon oil was chosen as the control sample. It was analyzed with every sequence of samples as a check to see how well the method was performing. Data from the analysis of a control sample showed inter-day precision with an RSD of <12% for all of the furocoumarins examined (data not included) and ≤7% for the marker furocoumarins (Table 4). The data for the marker furocoumarins in the control control sample are summarized in Figure 8. The concentration was plotted on a log scale because of the wide range of furocoumarin concentration in this citrus oil.

Downloaded by CORNELL UNIV on May 30, 2012 | http://pubs.acs.org
Publication Date (Web): May 29, 2012 | doi: 10.1021/bk-2012-1098.ch006

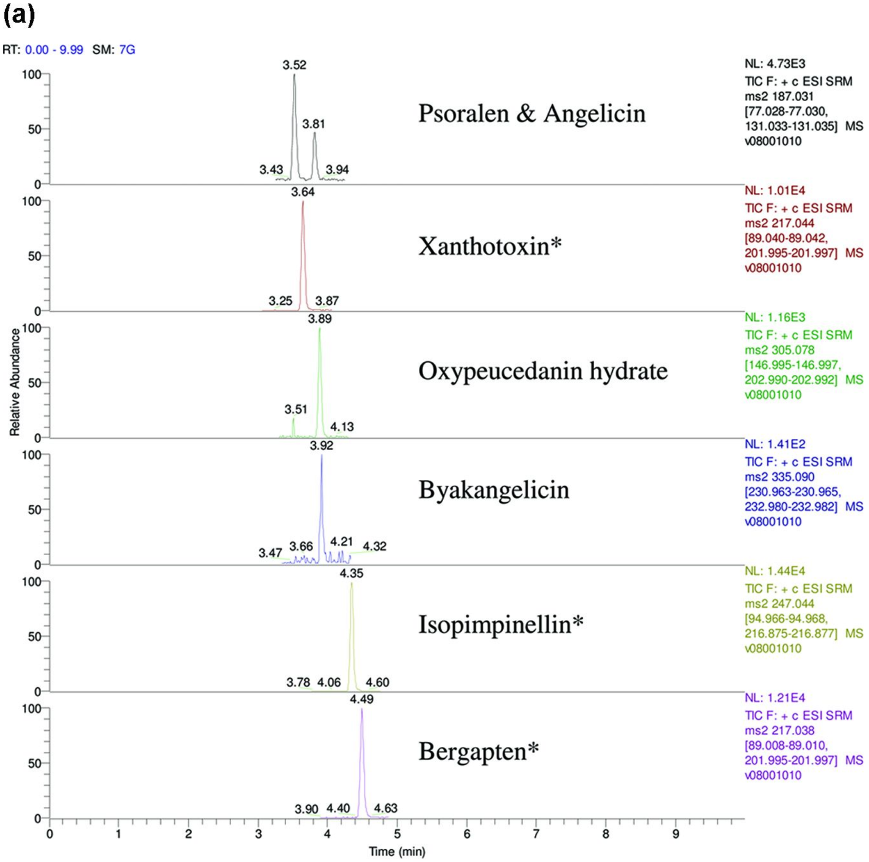

* marker furocoumarins

Downloaded by CORNELL UNIV on May 30, 2012 | http://pubs.acs.org
Publication Date (Web): May 29, 2012 | doi: 10.1021/bk-2012-1098.ch006

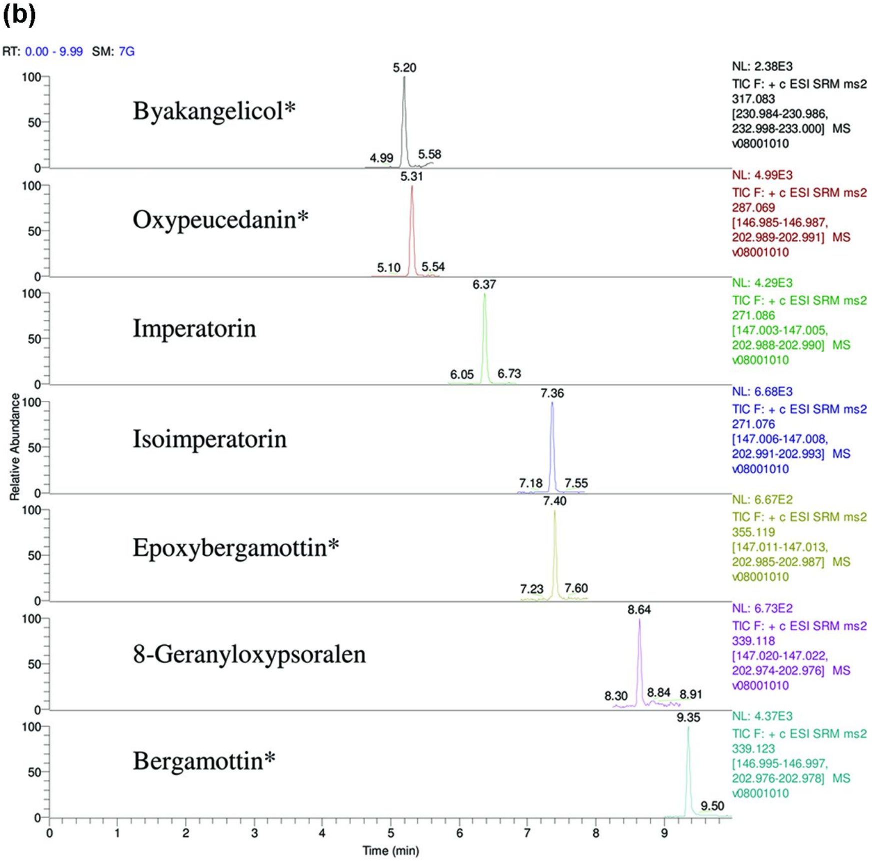

* marker furocoumarins

Figure 6. (a,b) TIC chromatograms for the furocoumarins.

Table 3. Recovery data for selected citrus oils

Furocoumarin	*Bergamot*	*Lemon*	*Grapefruit*	*Orange*	*5X Orange*	*Mandarin*
Psoralen	96	94	97	96	98	98
Xanthotoxin (8-MOP)*	95	98	99	100	101	101
Angelicin	95	94	95	99	98	100
Oxypeucedanin hydrate	98	99	100	104	97	97
Byakangelicin	100	97	101	104	106	98
Isopimpinellin*	95	97	99	100	103	101
Bergaptan (5-MOP)*	97	97	98	99	98	103
Byakangelicol*	110	102	100	108	101	98
Oxypeucedanin*	98	95	98	104	105	96
Imperatorin	100	99	106	86	75	97
Isoimperatorin	98	99	100	99	97	100
Epoxybergamotin*	95	100	96	104	103	99
8-Geranyloxypsoralen	98	96	99	110	115	101
Bergamottin*	95	96	96	97	59	94

* Marker furocoumarins

Downloaded by CORNELL UNIV on May 30, 2012 | http://pubs.acs.org
Publication Date (Web): May 29, 2012 | doi: 10.1021/bk-2012-1098.ch006

Downloaded by CORNELL UNIV on May 30, 2012 | http://pubs.acs.org
Publication Date (Web): May 29, 2012 | doi: 10.1021/bk-2012-1098.ch006

Table 4. Control sample (lemon oil) precision data for marker furocoumarins

Replicate	*Xanthotoxin*	*Bergapten*	*Byakangelicol*	*Oxypeucedanin*	*Isoimperatorin*	*Epoxybergamottin*	*Bergamottin*
1	15.0	66.0	60.0	102	6.41	2.28	317
2	13.9	64.7	58.6	97.2	6.21	2.38	301
3	14.6	64.5	58.6	103	6.67	2.24	316
4	15.1	70.9	62.4	108	6.95	2.52	336
5	14.5	66.7	59.6	100	6.51	2.32	315
6	14.1	65.2	58.6	97.4	6.44	2.07	305
7	14.1	65.8	58.8	100	6.54	2.23	313
8	14.0	66.0	57.4	98.4	6.50	2.51	314
9	13.9	64.4	59.8	98.5	6.67	2.36	303
10	13.5	61.8	55.5	94.9	6.07	2.48	295
11	13.4	62.0	56.2	93.4	6.01	2.08	288
12	14.2	64.8	59.9	98.4	6.54	2.39	311
13	16.7	74.8	65.7	111	7.40	2.62	360
14	14.5	67.6	56.4	102	6.73	2.31	324
15	15.7	70.0	62.6	105	6.83	2.57	325
16	14.0	61.9	58.0	90.0	6.04	2.32	262
17	13.4	60.5	55.2	87.9	6.07	1.97	279

Continued on next page.

Table 4. (Continued). Control sample (lemon oil) precision data for marker furocoumarins

Replicate	*Xanthotoxin*	*Bergapten*	*Byakangelicol*	*Oxypeucedanin*	*Isoimperatorin*	*Epoxybergamottin*	*Bergamottin*
18	15.1	68.6	60.8	101	6.94	2.35	303
19	15.6	71.3	64.2	105	7.17	2.53	341
20	14.1	64.4	57.4	98.3	6.65	2.36	319
Avg.	14.5	66.1	59.3	99.6	6.57	2.34	311
Std. Dev.	0.85	3.61	2.80	5.57	0.38	0.17	21.7
RSD (%)	5.86	5.46	4.72	5.60	5.77	7.31	6.96

Downloaded by CORNELL UNIV on May 30, 2012 | http://pubs.acs.org
Publication Date (Web): May 29, 2012 | doi: 10.1021/bk-2012-1098.ch006

Downloaded by CORNELL UNIV on May 30, 2012 | http://pubs.acs.org
Publication Date (Web): May 29, 2012 | doi: 10.1021/bk-2012-1098.ch006

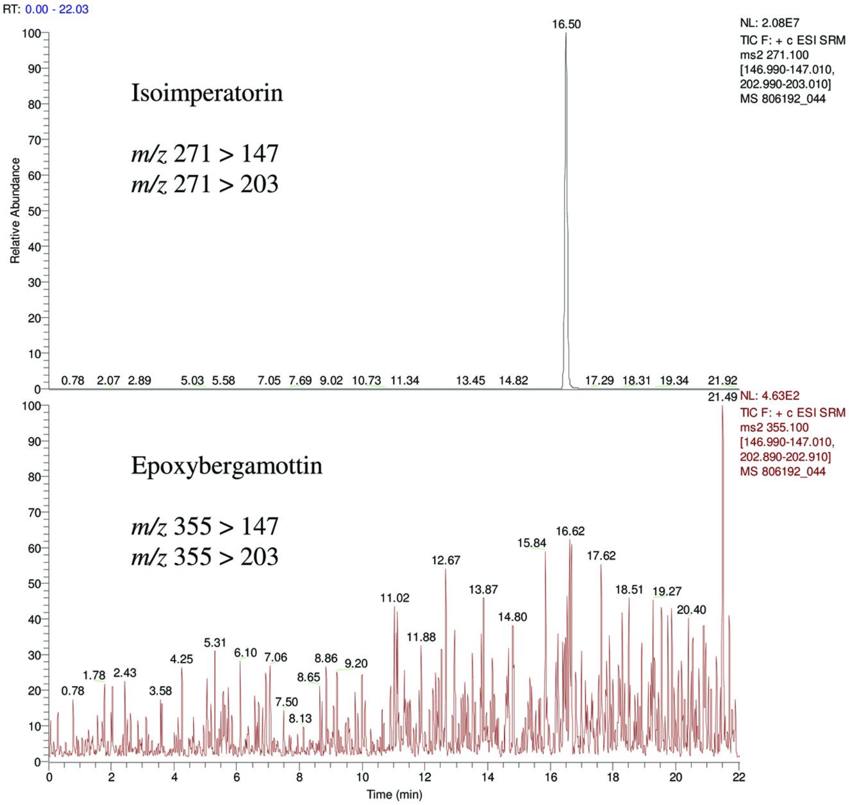

Figure 7. Chromatograms for isoimperatorin (top) and epoxybergamottin (bottom) after injecting isoimperatorin and monitoring the transitions for both furocoumarins to show there is no cross-talk.

Table 5. Correlation of marker furocoumarin concentration to the total furocoumarin (FC) concentration in selected citrus oils

	Lemon	*Lime*	*Bergamot*	*Grapefruit*	*Tangerine*
Total markers	3,469 ppm	25,597 ppm	13,701 ppm	4,263 ppm	31 ppm
Total FC	3,781 ppm	27,205 ppm	13,936 ppm	4,272 ppm	37 ppm
Marker % total	92%	94%	98%	99%	84%

Downloaded by CORNELL UNIV on May 30, 2012 | http://pubs.acs.org
Publication Date (Web): May 29, 2012 | doi: 10.1021/bk-2012-1098.ch006

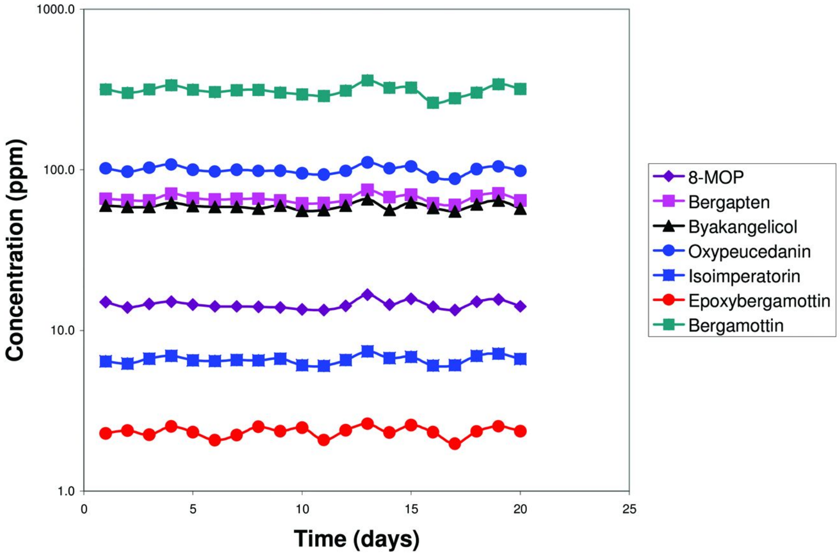

Figure 8. Plot of control sample (lemon oil) data for marker furocoumarins.

Conclusion

A fast and rigorous analytical method enabling the quantitative and qualitative assessment of the furocoumarin content in citrus oils was developed. This method is linear over the wide concentration range of furocoumarins in citrus. We have found there to be minimal matrix effects as evidenced by excellent recoveries from spiked samples. Our control data shows this method to be stable and rugged. The marker furocoumarins were selected as representative of the total furocoumarin concentration in a citrus oil (*9–11*). Table 5 shows the marker furocoumarins as a percent of the total furocoumarin concentration based on our analyses. The data for Bergamot and grapefruit oils shows that the marker furocoumarins represented 98% and 99% respectively of the total furocoumarin concentration. The data for lemon and lime oils shows that the marker furocoumarins represented 92% and 94% respectively of the total. Our data shows that if 8-geranyloxypsoralen was included as a marker furocoumarin, the percent of total furocoumarins for lemon and lime oils would increase to 98% and 97% respectively. The marker furocoumarins represented 84% of the total for tangerine oil but the total furocoumarin concentration was below levels of concern.

References

1. Peroutka, R.; Schulzova, V.; Botek, P.; Hajslova, J. Analysis of furocoumarins in vegetables (***Apiaceae***) and citrus fruits (***Rutaceae***). *J. Sci. Food Agric.* **2007**, *87*, 2152–2163.
2. Kitamura, N.; Kohtani, S.; Nakagaki, R. Molecular aspects of furocoumarin reactions: Photophysics, photochemistry, photobiology, and structural analysis. *J. Photochem. Photobiol., C* **2005**, *6*, 168–185.
3. Serrano-Perez, J. J.; Gonzalez-Luque, R.; Merchan, M.; Serrano-Andres, L. The family of furocoumarins: Looking for the best photosensitizer for phototherapy. *J. Photochem. Photobiol., A* **2008**, *199*, 34–41.
4. Bordin, F. Photochemical and photobiological properties of furocoumarins and homologues drugs. *Int. J. Photoenergy* **1999**, *1*, 1–6.
5. Bordin, F. Photochemical mechanisms of DNA damage induced by furocoumarins. In *Advances in Biomedical Applications of Photochemistry & Photobiology*; Vargas, F., Ed.; Research Signpost 37/661 (2): Kerala, India, 2002; pp 95−113.
6. Cartwright, L. E.; Walter, J. F. Psoralen-containing sunscreen is tumorigenic in hairless mice. *J. Am. Acad. Dermatol.* **1983**, *8*, 830–836.
7. Walter, J. F.; Gange, R. W.; Mendelson, I. R. Psoralen-containing sunscreen induces phototoxicity and epidermal ornithine decarboxylase activity. *J. Am. Acad. Dermatol.* **1982**, *6*, 1022–1027.
8. Autier, P.; Dore, J.-F.; Cesarini, J.-P.; Boyle, P. Should subjects who used psoralen suntan activators be screened for melanoma? *Ann. Oncol.* **1997**, *8*, 435–437.
9. Vey, M. Information Letter 799. International Fragrance Association, Brussels, Belgium. February 28, 2008.
10. Vey, M. Information Letter 832. International Fragrance Association, Brussels, Belgium. July 14, 2009.
11. Lecrenier, S. European Commission, Brussels, Belgium. In a letter to Houri, J.-P. International Fragrance Association, Brussels, Belgium. May 27, 2009.
12. Lin, Y.-K.; Sheu, M.-T.; Huang, C.-H.; Ho, H. O. Development of a Reversed-Phase High-Performance Liquid Chromatographic Method for Analyzing Furanocoumarin Components in Citrus Fruit Juices and Chinese Herbal Medicines. *J. Chromatogr. Sci.* **2009**, *47*, 211–215.
13. Prosen, H.; Kocar, D. Different sample preparation methods combined with LC-MS/MS and LC-UV for determination of some furocoumarin compounds in products containing citruses. *Flavour Fragr. J.* **2008**, *23*, 263–271.
14. Govindarajan, R.; Singh, D. P.; Singh, A. P.; Pandey, M. M.; Rawat, A. K. S. A Validated HPLC Method for Quantification and Optimization of Furocoumarins in Different Extracts of Fruits of *Heracleum candicans*. *Chromatographia* **2007**, *66*, 401–405.
15. Govindarajan, R.; Singh, D. P.; Singh, A. P.; Rawat, A. K. S. Validated Reversed-Phase Column High-Performance Liquid Chromatographic Method for Separation and Quantification of Polyphenolics and Furocoumarins in Herbal Drugs. *J. AOAC International* **2008**, *91*, 1020–1024.

Downloaded by CORNELL UNIV on May 30, 2012 | http://pubs.acs.org
Publication Date (Web): May 29, 2012 | doi: 10.1021/bk-2012-1098.ch006

Downloaded by CORNELL UNIV on May 30, 2012 | http://pubs.acs.org
Publication Date (Web): May 29, 2012 | doi: 10.1021/bk-2012-1098.ch006

16. Kang, J.; Zhou, L.; Sun, J.; Han, J.; Guo, D.-A. Chromatographic fingerprint analysis and characterization of furocoumarins in the roots of *Angelica dahurica* by HPLC/DAD/ESI-MS^n technique. *J. Pharm. Biomed. Anal.* **2008**, *47*, 778–785.
17. Singh, D. P.; Govindarajan, R.; Rawat, A. K. S. Comparison of Different Analytical HPLC Columns for Determination of Furocoumarins in Heracleum candicans Fruits. *J. Liq. Chromatogr. Relat. Technol.* **2008**, *31*, 421–427.
18. Frerot, E.; Decorzant, E. Quantification of Total Furocoumarins in Citrus Oils by HPLC Coupled with UV, Fluorescence, and Mass Detection. *J. Agric. Food Chem.* **2004**, *52*, 6879–6886.
19. Manthey, J. A.; Buslig, B. S. Distribution of Furanocoumarins in Grapefruit Juice Fractions. *J. Agric. Food Chem.* **2005**, *53*, 5158–5163.
20. Guidance for Industry – Bioanalytical Method Validation. U.S Department of Health and Human Services, Food and Drug Administration, Center for Drug Evaluation and Research (CDER), Center for Veterinary Medicine (CVM). May 2001. URL http://www.fda.gov/cder/guidance/index.htm.
21. Commission Decision of 12 August 2002 implementing Council Directive 96/23/EC concerning the performance of analytical methods and the interpretation of results. *Off. J. Eur. Commun.*. URL http://eur-lex.europa.eu/LexUriServ/LexUriServ.do?uri=OJ:L:2002:221:0008:0036:EN:PDF.
22. Rivier, L. Criteria for the identification of compounds by liquid chromatography-mass spectrometry and liquid chromatography-multiple mass spectrometry in forensic toxicology and doping analysis. *Chem. Acta* **2003**, *492*, 69–82.
23. Taverniers, I; De Loose, M.; Van Bockstaele, E. Trends in quality in the analytical laboratory. II. Analytical method validation and quality assurance. *Trends Anal. Chem.* **2004**, *23*, 535–552.
24. Guidance for Industry – Mass Spectrometry for Confirmation of the Identity of Animal Drug Residues. U.S. Department of Health and Human Services, Food and Drug Administration, Center for Veterinary Medicine. May 1, 2003. URL http://www.fda.gov/cvm/guidance/published.htm.
25. Method Validation and Quality Control Procedures for Pesticide Residues Analysis in Food and Feed. Document No. SANCO/3131/2007. URL http://ec.europa.eu/food/plant/protection/resources/qualcontrol_en.pdf.
26. IOFI Working Group on Methods of Analysis. Guidelines for LC-MS identifications of flavouring substances in nature, made by the Working Group on Methods of Analysis of the International Organization of the Flavor Industry (IOFI). *Flavour Fragr. J.* **2010**, *25*, 2–3.
27. McLafferty, F. W. and Turecek, F. *Interpretation of Mass Spectra*, 4th ed.; University Science Books: Mill Valley, CA, 1993; p 55.

Downloaded by CORNELL UNIV on May 29, 2012 | http://pubs.acs.org
Publication Date (Web): May 29, 2012 | doi: 10.1021/bk-2012-1098.ch007

Chapter 7

EU Essential Oils Hazard Classification

Quantitative Multicomponent GCMS Analysis

Joost Broekhans* **and Hans Leijs**

International Flavors & Fragrances Inc., Tilburg Analytical Services R&D,
Postbox 5021, 5004 EA Tilburg, The Netherlands
***E-mail: joost.broekhans@iff.com**

A quantitative analysis method has been developed for EU hazard classification requirements for essential oils. Method uses dual column GCMS to analyze for 77 analytes. Quantitation is based on full scan extracted ion technique and internal standards. A wide calibration range is needed to cover the range of concentrations observed in nature. Analytical data are processed automatically using a software routine. This paper demonstrates aspects of the method, including dual column approach, calibration, validation, identification criteria and automated data processing. Also, a comparison between full scan extracted ion and SIM quantitation is discussed.

Introduction

Within the European Union (EU) chemical substances have to be classified based on hazard risks and if dangerous, labeled accordingly. For single substance chemicals, hazard classification is normally based on available toxicological data which again is based on tests.

Article 6 of the Dangerous Substances Directive of the European Union (*1*) describes that manufacturers of dangerous substances are obliged to carry out investigation concerning the hazardous properties of such substances. Paragraph 1.7.2.1 of annex VI (*2*) of the same directive describes: "Where impurities, additives or individual constituents of substances have been identified, they shall be taken into account if their concentration is greater than or equal to the limits specified."

In Recent Advances in the Analysis of Food and Flavors; Toth, S., et al.;
ACS Symposium Series; American Chemical Society: Washington, DC, 2012.

Downloaded by CORNELL UNIV on May 29, 2012 | http://pubs.acs.org
Publication Date (Web): May 29, 2012 | doi: 10.1021/bk-2012-1098.ch007

Natural complex substances (e.g. essential oils, extracts from botanical and animal sources) require a special procedure for hazard classification as they might have variable chemical compositions. The classification of natural complex substances is based on levels of classifiable constituents and can differ for substances from same origin obtained by different production procedures (e.g. absolutes, concretes and distilled oils) and seasonal influences.

Based on risk assessment, a selection of classifiable constituents occurring in natural complex substances was made. A method was developed for analysis of 77 classifiable constituents from this selection. Method uses GC-MS operated in full scan mode. In order to minimize the influence of any co-eluting matrix component on identification or quantitation, each sample is sequentially injected on an apolar and a polar column. Quantitation is based on two internal standards and one extracted ion per analyte. Calibration is done using 8 standards. Identification is done by library search. Data is automatically processed after interpretation. A routine automatically compares the results for both columns, assigns the correct reporting limits and summarizes the results in an overview.

Method was validated by determination of the linearity of the calibration. For reproducibility and recovery validation, three matrices: Bergamot oil, Petitgrain oil and a simple self-prepared matrix were spiked with approximately 300 mg/kg of each analyte. Each non-spiked and spiked sample was freshly prepared and analyzed on eleven different days over a range of four weeks. Recoveries and relative standard deviations were calculated from the data afterwards.

Performance of the method operated in full scan mode was compared against operation in SIM mode. A random selection of analytes was spiked to the same three matrices as describes earlier. Spiked matrices were analyzed using method operated in SIM mode. Results were compared against full scan extracted ion results.

Materials and Methods

GC-MS Analysis

GC-MS analysis was performed on a Shimadzu QP2010 mass spectrometer coupled to a Shimadzu GC-2010 gas chromatograph equipped with an AOC-5000 autosampler. The system was equipped with two split/splitless injectors and two columns of different polarity. Both columns were connected to the MS interface. Autosampler was configured to sequentially inject on both columns. Details of equipment used are shown in Table 1.

Calibration Standards Preparation

Components and chemicals included in this method are shown in Table 2. The purity of each component was verified using GCFID area percent analysis with similar GC parameters. Purities were found to be < 90%, except for allyl isothiocyanate (88%), 1-heptanal (85%), octanal (85%), cis-β-ocimene (64%, contains app. 30% limonene), terpinolene (87%), α-terpineol (81%) and used in further calculations for calibration. Each month, 5 separate master mixtures each containing a subset of the total set of 77 analytes were prepared by weighing 0.05 g of each compound and diluting to 10 g total weight with acetone (~5000 mg/kg per compound). The 5 master mixtures were combined into one combined stock mixture by weighing 0.5 g of each master mixture and diluting it with 7.5 g acetone (~250 mg/kg per component). A calibration stock solution was prepared by diluting 2.8 g combined stock mixture to 20 g using acetone (~35 mg/kg).

Table 1. Equipment and settings

GCMS system	Shimadzu QP2010 MS Shimadzu GC-2010 Shimadzu AOC5000 autosampler
Injection	1 µl, 250°C, split 1:10
Carrier gas	He
Column 1	Agilent CPSil 5 CB 50 m x 0.25 mm x 0.25 µm
	170 kPa (51 min.)- 30 kPa/min. - 500 kPa (5 min.) – -100 kPa/min. - 170 kPa (58.6 min.)
Column 2	Agilent VF-Wax 50 m x 0.25 mm x 0.20 µm 170 kPa (113 min.) - 30 kPa/min. - 500 kPa (4.9 min)
Oven	50°C (2 min.) - 2°C/min - 150°C - 20°C/min. - 250°C (10 min.) – cool 200°C/min. - 50°C (6 min.) - 4°C/min. - 216°C - 10°C/min. - 250°C (10 min.)
MS solvent cut time	3 min. and filament off from 60 min. to 76.8 min.
MS detector gain	+ 0.20 kV relative to tuning result
MS parameters	Interface 250°C, Ion source 200°C Full scan m/z 40 – 260, scan time 0.20 s.

Downloaded by CORNELL UNIV on May 29, 2012 | http://pubs.acs.org
Publication Date (Web): May 29, 2012 | doi: 10.1021/bk-2012-1098.ch007

The internal standard solution was prepared by diluting 0.05 g 1,4-dibromobenzene and 0.05 g 9-bromophenanthrene into 100 ml methanol (~ 500 mg/l). Calibration standards were prepared by diluting the calibration stock solution to 0.3, 2, 5, 10, 15 and 18 mg/kg per compound using acetone. In order to add a repeating point in calibration, standard of 5 mg/kg was prepared in duplo. 100µl of internal standard solution was added to each standard. A blank containing only acetone and internal standard was also prepared.

Sample Preparation

All samples (i.e. essential oils) were diluted in acetone prior to analysis. For analysis of expected levels of 10 to 1700 mg/kg a 100 times sample dilution was applied. 0.1 gram of sample was weighed into a glass bottle. 100µl of internal standard solution was added. Mixture was diluted into 10 gram total using acetone and analyzed using acquisition settings as described earlier.

Downloaded by CORNELL UNIV on May 29, 2012 | http://pubs.acs.org
Publication Date (Web): May 29, 2012 | doi: 10.1021/bk-2012-1098.ch007

Table 2. Components and chemicals including CAS registry numbers

Name	*CAS*	*Name*	*CAS*
1,4-dibromobenzene [a]	106-37-6	isophorone	78-59-1
1,8-cineol (eucalyptol)	470-82-6	isophytol	505-32-8
1-heptanal	111-71-7	isopulegol	89-79-2
1-nonanal	124-19-6	l-carvone	6485-40-1
1-octanol	111-87-5	m-cresol	108-39-4
1-octen-3-ol	3391-86-4	menthol	89-78-1
1-octen-3-yl acetate	2442-10-6	menthyl acetate	89-48-5
2-methoxy-phenol	90-05-1	methyl anthranilate	134-20-3
2-phenyethylisothiocyanate	2257-09-2	methyl benzoate	93-58-3
2-undecanone	112-12-9	methyl salicylate	119-36-8
4-terpinenol	20126-76-5	myrcene	123-35-3
9-bromophenanthrene [a]	573-17-1	myristicin	607-91-0
acetone [b]	67-64-1	nerolidol	7212-44-4
acetonitrile, phenyl	140-29-4	n-hexanol	111-27-3
alloocimene	673-84-7	nicotine	54-11-5
allyl isothiocyanate	57-06-7	nonanoic acid	112-05-0
alpha phellandrene	4221-98-1	ocimene	13877-91-3
alpha pinene	80-56-8	o-cresol	95-48-7
alpha terpinene	99-86-5	octanal	124-13-0
alpha terpineol	98-55-5	p-cresol	106-44-5
benzaldehyde	100-52-7	p-cymene	99-87-6
benzene	71-43-2	phenol	108-95-2
beta-pinene	18172-67-3	phenylethyl acetate	103-45-7
butyl butyrate	109-21-7	phenylethyl alcohol	60-12-8
caffeine	58-08-2	sabinene	3387-41-5
camphor	76-22-2	sabinyl acetate	3536-54-7
carvacrol	499-75-2	safranal	116-26-7
citronellal	106-23-0	salicylaldehyde	90-02-8
cuminaldehyde	122-03-2	styrene	100-42-5
cuminyl alcohol	536-60-7	terpinolene	586-62-9
decanal	112-31-2	thymol	89-83-8
decanol	112-30-1	toluene	108-88-3

Continued on next page.

In Recent Advances in the Analysis of Food and Flavors; Toth, S., et al.;
ACS Symposium Series; American Chemical Society: Washington, DC, 2012.

Table 2. (Continued). Components and chemicals including CAS registry numbers

Name	*CAS*	*Name*	*CAS*
dihydro alpha ionone	31499-72-6	trans-2-hexenal	6728-26-3
dihydro beta ionone	17283-81-7	trans-anethole	4180-23-8
dodecanol	112-53-8	valencene	4630-07-3
furfural	98-01-1	β-ionone	79-77-6
furfuryl alcohol	98-00-0	γ-terpinene	99-85-4
heptanoic acid	111-14-8	δ-3-carene	13466-78-9
indole	120-72-9		

[a] Internal standard. [b] Used as solvent.

Downloaded by CORNELL UNIV on May 29, 2012 | http://pubs.acs.org
Publication Date (Web): May 29, 2012 | doi: 10.1021/bk-2012-1098.ch007

For expected levels up to ~5 % a higher sample dilution can be applied by weighing 0.1 gram of sample into a glass bottle, adding 3 ml of internal standard solution and diluting to 10 gram total using acetone. Mixture is further diluted by pipetting 30µl into 1000µl acetone.

Analysis

Calibration standards including a blank and samples were analyzed on both columns sequentially using the acquisition settings described earlier. Qualifier and quantifier ions were selected from the full scan data for each target analyte as shown in Table 3. As the method was operated in full scan mode, qualifier ions are only used for an initial automated screen of the chromatogram for analytes.

Results and Discussion

Calibration

Figure 1 shows full scan chromatogram of sequential injection of the calibration standard of 5 mg/kg. Most analytes were sufficiently separated (R_S < 1) on both columns and in all cases where no sufficient chromatographic separation was obtained on the CP-Sil 5 column, the analytes were separated on the VF-Wax MS column. Furthermore, quantitative analysis was still possible for co-eluting analytes due to selection of quantifier ions as displayed in Table 3.

Downloaded by CORNELL UNIV on May 29, 2012 | http://pubs.acs.org
Publication Date (Web): May 29, 2012 | doi: 10.1021/bk-2012-1098.ch007

Table 3. Qualifier and quantifier ions selected for analysis

Name	*Quantifier; qualifier ions (m/z)*
1,4-dibromobenzene [a]	235.7; 237.7, 233.7, 156.9 [b]
9-bromophenanthrene [a]	256; 258, 176.1, 177.1 [b]
1,8-cineol(eucalyptol)	154; 139, 108, 81
1-heptanal	81; 70, 55, 44
1-nonanal	98; 82, 70, 57
1-octanol	84; 70, 56
1-octen-3-ol	85; 72, 57
1-octen-3-yl acetate	128; 99, 43
2-methoxy-phenol	124; 109, 81
2-phenyethylisothiocyanate	163; 105, 91
2-undecanone	85; 58
4-terpinenol	154; 111, 93
acetonitrile, phenyl	117; 116, 90, 89
alloocimene, isomer 1	136; 121, 105, 79
alloocimene, isomer 2	136; 121, 105, 79
allyl isothiocyanate	99; 72
alpha phellandrene	136; 93, 91, 77
alpha pinene	136; 121, 93
alpha terpinene	136; 121, 105, 93
alpha terpineol	59; 93, 121, 136
benzaldehyde	106; 105, 77
benzene	78; 77
beta ionone	177; 135
beta pinene	136; 121, 93
butyl butyrate	89; 71, 56
caffeine	194; 109, 82, 67
camphor	152; 108, 95, 82
carvacrol	150; 135, 107, 91
citronellal	69; 95, 121, 154
cuminaldehyde	148; 133, 119, 105
cuminyl alcohol	150; 135, 119, 105
decanal	112; 82, 70, 57

Continued on next page.

Table 3. (Continued). Qualifier and quantifier ions selected for analysis

Name	*Quantifier; qualifier ions (m/z)*
decanol	97; 83, 70, 55
delta-3-carene	136; 121, 93
dihydro alpha ionone	176; 136, 121, 95
dihydro beta ionone	176; 161, 136, 121
dodecanol	140; 111, 97, 83
furfural	96; 95
furfuryl alcohol	98; 97, 81, 69
gamma terpinene	136; 121, 93, 77
heptanoic acid	60; 73, 87, 101
indole	117; 90, 89
isophorone	138; 82
isophytol	71; 123
isopulegol, isomer 1	136; 121, 81, 154
isopulegol, isomer 2	136; 121, 154
l-carvone	150; 108, 82, 54
m-cresol	108; 107, 79
menthol	138; 95, 81, 71
menthyl acetate	138; 123, 95, 81
methyl anthranilate	151; 119, 92
methyl benzoate	136; 105, 77
methyl salicylate	152; 120, 92
myrcene	69; 93, 121, 136
myristicin	192; 161, 131, 91
nerolidol, isomer 1	69; 93, 161
nerolidol, isomer 2	69; 93, 107, 161
n-hexanol	56; 69
nicotine	84; 162, 133
nonanoic acid	129; 115, 73, 60
ocimene	93; 121, 105, 77
o-cresol	108; 107, 79, 77
octanal	84; 57, 100
p-cresol	108; 107, 79, 77

Continued on next page.

Downloaded by CORNELL UNIV on May 29, 2012 | http://pubs.acs.org
Publication Date (Web): May 29, 2012 | doi: 10.1021/bk-2012-1098.ch007

Table 3. (Continued). Qualifier and quantifier ions selected for analysis

Name	*Quantifier; qualifier ions (m/z)*
p-cymene	119; 91, 134
phenol	94; 66, 65
phenylethyl acetate	104; 91
phenylethyl alcohol	91; 92, 122
sabinene	93; 136, 77
sabinyl acetate	91; 119, 108, 92
safranal	150; 121, 107, 91
salicylaldehyde	122; 121, 93, 65
styrene	104; 78, 51
terpinolene	136; 121, 105, 93
thymol	150; 135, 115, 91
toluene	91; 92
trans-2-hexenal	83; 69, 55, 98
trans-anethole	148; 147, 117, 105
valencene	204; 189, 161, 133

[a] Internal standard [b] m/z values in 1 decimal numbers for brominated compounds

Downloaded by CORNELL UNIV on May 29, 2012 | http://pubs.acs.org
Publication Date (Web): May 29, 2012 | doi: 10.1021/bk-2012-1098.ch007

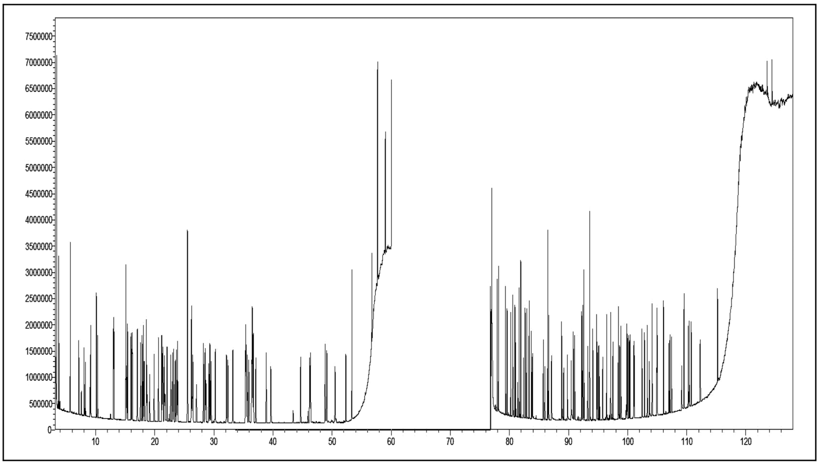

Figure 1. Full scan chromatogram of calibration standard 5 mg/kg.

Calibration lines were set up according to the internal standard method. Each analyte is calibrated using the nearest eluting internal standard being either 1,4-dibromobenzene or 9-bromophenanthrene. Peak integration was checked and corrected manually where needed. Correlation coefficients of all analytes were above 0.995 indicating sufficient linearity of the calibrated range. For unclear reasons, exceptions were the calibration lines of 1-nonanal and nonanoic acid on CP-Sil 5 column which both had correlation coefficients slightly below 0.995. Linearity of these calibration lines was assumed not to be sufficient for accurate quantification and therefore the calibration of these analytes on the CP-Sil 5 column was excluded. Stability of the calibration was determined by repetitive injection of the 5 mg/kg standard over ten days. Average relative standard deviation of the area ratio (analyte / internal standard) of all analytes was determined to be 4% with a maximum of 10%. Examples of calibration lines are shown in Figure 2.

Downloaded by CORNELL UNIV on May 29, 2012 | http://pubs.acs.org
Publication Date (Web): May 29, 2012 | doi: 10.1021/bk-2012-1098.ch007

Potential Issues

Complex samples such as essential oils require sufficient chromatographic separation in order to be able to correctly identify and quantify target analytes. Any occurring coelutions can be overcome as long as the MS spectra of the coeluting components provide distinctive information. Subject target analytes do not always provide spectra which are distinctive enough to overcome coelutions with matrix components. In these cases a second GC run on a column with different polarity which overcomes the coelution is needed.

Similar multi-target analytical methods based on GCMS have been published (*3*, *4*). These methods analyze for potential fragrance allergens in perfume oils. Identification is based on retention time and the ratio of selected ions acquired in SIM mode. Quantification is done using one ion. Multiple SIM windows, each containing app. 3 ions are needed in order not to lose sensitivity. Therefore, a separate acquisition window as small as 0.1 min is needed per one or two analytes. This works well for clean matrices where retention times are stable. For multi-component analysis of 77 analytes it is very complex to set up separate SIM windows for each analyte. Acquisition windows would have to be very small. When analyzing complex matrices as essential oils, retention time shifts are common and may cause an analyte to shift out of its acquisition window. This might then cause false negatives or the need of repetition of the analysis. The acquisition in full scan mode avoids this. Also when doing acquisition in SIM mode, coelution of matrix components containing isobaric ions used for identification and quantitation may cause false positives, negatives or incorrect quantification. In this case, using full scan mode and allowing full scan library searches for identification as published earlier (*5*) may be more suitable.

Examination of Table 3 shows that chosen quantifier ion is not always the most abundant ion from the spectrum of the analyte. In order to minimize the chance of coelution with an isobaric ion, less abundant ions were chosen in some cases. Up to three qualifier ions were chosen for an initial automated screen of the chromatogram for target analytes.

Downloaded by CORNELL UNIV on May 29, 2012 | http://pubs.acs.org
Publication Date (Web): May 29, 2012 | doi: 10.1021/bk-2012-1098.ch007

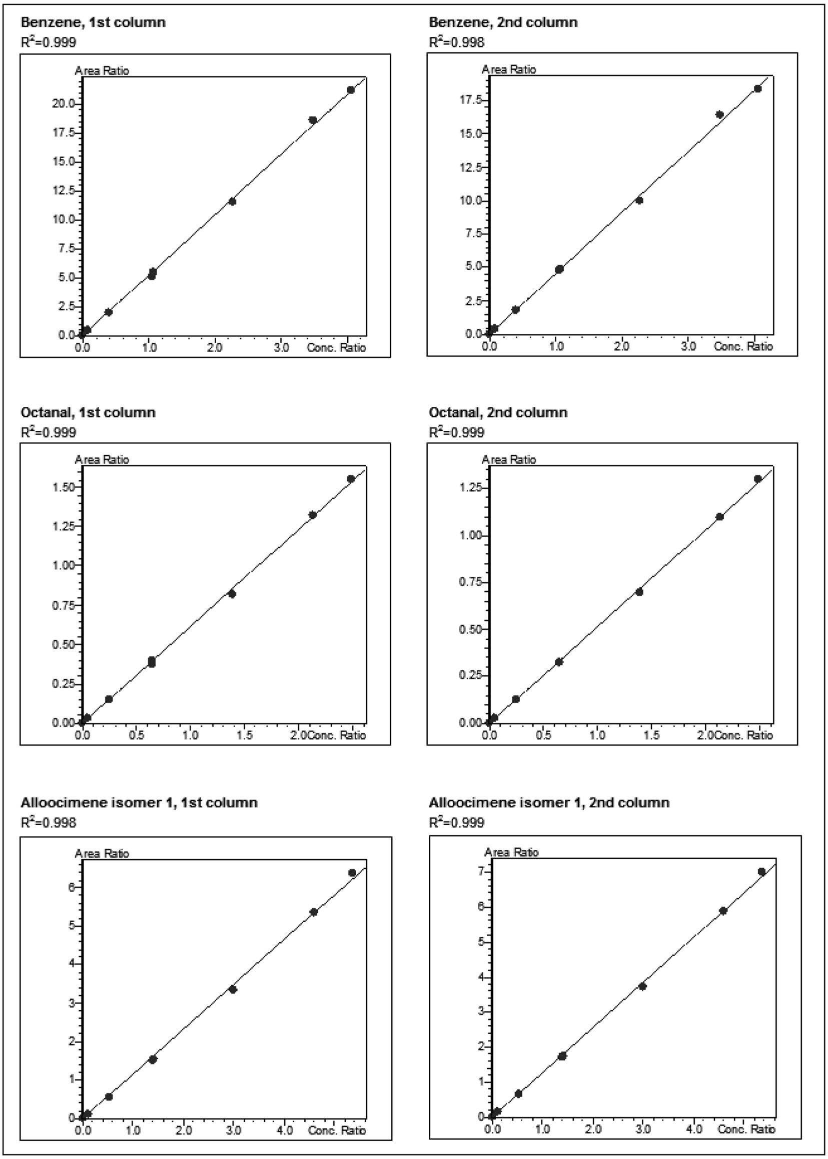

Figure 2. Example calibration lines.

Data Interpretation and Automatic Processing

Analytical data of samples were interpreted by an analyst. Interpretation included manual identification of positive analytes and manual correction of peak integration. Two commercial mass spectral library's (Wiley Registry of Mass Spectral Data, 8th edition, by John Wiley & Sons, Inc. and NIST/EPA/NIH

Downloaded by CORNELL UNIV on May 29, 2012 | http://pubs.acs.org
Publication Date (Web): May 29, 2012 | doi: 10.1021/bk-2012-1098.ch007

Mass Spectral Library NIST 08, 2008 edition) and a private library containing all subject analytes were used for identification based on library search similarity index.

An analyte was assumed to be identified positively when library search similarity index was above 70% and the result was above the reporting limit. Reporting limits were set to 10 mg/kg in sample. The average signal to noise ratio for the target ion in the lowest standard of 0.3 mg/kg (equal to 30 mg/kg in sample) still was 100.

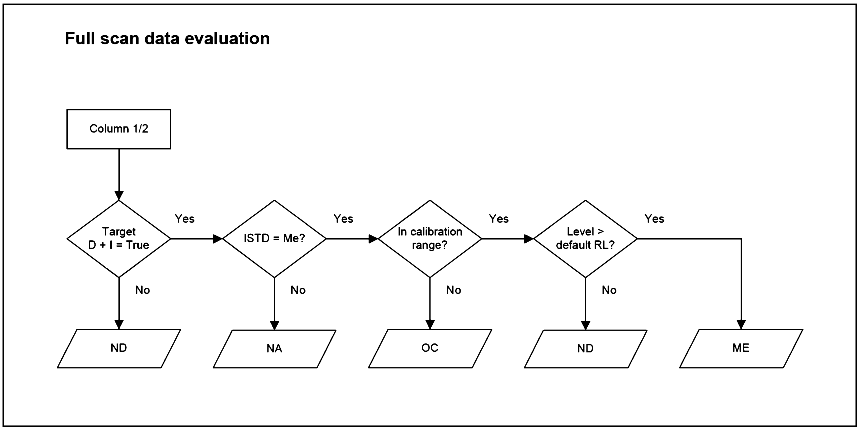

Figure 3. Automated data processing flowchart.

Table 4. Decision scheme for combining two column results

		Column 1 result			
		ND	*NA*	*OC*	*ME*
Column 2 result	ND	ND	NA	OC	ME
	NA	NA	NA	OC	ME
	OC	OC	OC	OC	ME
	ME	ME	ME	ME	ME

As subject analysis includes analysis of each sample on two analytical columns, two analytical results are generated. After interpretation by the analyst, an software routine automatically evaluates both analytical results and combines them into one result for each analyte. Routine assigns certain ‘exception values’ to each result, both from the first and second column. Exception values can be ‘NA’, which means that subject analyte on subject column could not be analyzed. This may be the case where an analyte was identified but cannot be quantified as the corresponding internal standard was coeluting. Exception value ‘ND’ indicates that subject analyte was either not detected or quantified level was below the reporting limit. ‘OC’ indicates that the quantified level for an analyte was above the calibration range. ‘ME’ as exception value means that subject analyte was identified by the analyst and level was quantified. If for subject analyte the exception value on the other column also was ‘ME’, the quantified levels are compared. The average level is reported when the difference is below 10%. If the difference is above, the lowest values is reported. The highest quantified level is reported in the case where one of the column results is below the reporting limit and the other column results was above. A flowchart of the software routine is shown in Figure 3. Table 4 shows the decision scheme for combining results from column 1 and 2 into one final result.

If for example an analyte was not identified on the first column due to coelution with matrix, the automated data processing routine would have generated a ND exception value. The second column would have exception value ME and a quantified level if the analyte was identified and the observed level was within the calibration range. The routine would generate ME as exception value and the level of the second column after combining the results from both columns. A report is generated once all decisions are taken. The format of the report is suitable for further upload to a LIMS.

Downloaded by CORNELL UNIV on May 29, 2012 | http://pubs.acs.org
Publication Date (Web): May 29, 2012 | doi: 10.1021/bk-2012-1098.ch007

Reproducibility and Recovery

To validate the method, the recovery and reproducibility were determined. Three different matrices were spiked with all analytes at nominal levels of approximately 300 mg/kg. One of the matrices was a self-prepared simple matrix of 5 components: limonene, linalool, ethyl decanoate, dipropylene glycol and methyl dihydrojasmonate. The other two matrices were distilled Italian Bergamot oil and Petitgrain citronnier oil, which is a steam distilled essential oil from lemon tree leaves and twigs. Both matrices are commercially available and were obtained from International Flavors and Fragrances (Tilburg, The Netherlands). In order to maximize variation, spiked and non-spiked samples were analyzed once a day for eleven different days over a period of five weeks. Four analysts sequentially prepared the samples during that period. Also, after two weeks (five out of eleven analyses done) new injection liners and septa were installed as instrument maintenance. Mass spectrometer was tuned and system was re-calibrated using freshly prepared calibration standards.

Table 5 shows confidence intervals of the recoveries for each analyte in the three different matrices based on eleven measurements. The data shows that overall recovery was good for most analytes in each matrix. Exceptions were heptanoic acid and nonanoic acid in Bergamot oil. These analytes show a lower recovery, probably due to matrix interference. Observed level of methyl anthranillate in Petitgrain oil measured on the first and second day was close to nominal but was decreasing to approximately 50% recovery during the rest of the test period. This might indicate instability of the component in Petitgrain matrix but needs further examination to confirm. Spiked levels of some analytes could not be determined as these analytes were already present at higher levels in the non-spiked oils or were co-eluting with matrix components. Small confidence intervals indicate that reproducibility was excellent.

Downloaded by CORNELL UNIV on May 29, 2012 | http://pubs.acs.org
Publication Date (Web): May 29, 2012 | doi: 10.1021/bk-2012-1098.ch007

Table 5. Confidence intervals of spiked analytes in various matrices (spiked at 300-400 mg/kg)

	Recovery confidence interval % (n=11, α=0.05)		
Name	*Self-prepared matrix*	*Bergamot oil*	*Petitgrain citronnier oil*
benzene	96 - 102	93 - 100	96 - 103
toluene	93 - 104	94 - 104	93 - 101
furfural	94 - 100	94 - 100	98 - 103
trans-2-hexenal	102 - 111	102 - 106	102 - 106
furfuryl alcohol	101 - 105	93 - 100	97 - 100
n-hexanol	99 - 104	74 - 110	102 - 108
allyl isothiocyanate	95 - 101	97 - 101	98 - 102
styrene	101 - 105	95 - 102	97 - 104
1-heptanal	99 - 103	100 - 108	98 - 105
alpha pinene	84 - 96	[a]	[a]
benzaldehyde	94 - 98	93 - 97	100 - 104
1-octen-3-ol	98 - 102	82 - 114	99 - 104
sabinene	84 - 102	[a]	[a]
phenol	92 - 102	78 - 89	75 - 83
butyl butyrate	104 - 107	101 - 106	108 - 113
octanal	104 - 109	[a]	102 - 109
beta pinene	96 - 101	[a]	[a]
myrcene	[a]	[a]	[a]
alpha phellandrene	83 - 93	85 - 99	[a]
delta-3-carene	95 - 103	83 - 105	[a]
alpha terpinene	99 - 105	77 - 110	[a]
p-cymene	96 - 105	[a]	[a]
salicylaldehyde	85 - 100	74 - 85	96 - 101
1,8-cineol(eucalyptol)	109 - 115	112 – 117 [b]	[a] [b]
ocimene	105 - 112	101 – 112	[a]
o-cresol	97 - 105	95 - 100	98 - 103
gamma terpinene	102 - 106	[a]	[a]
1-octanol	96 - 102	127 - 143	96 - 108
p-cresol	89 - 98	93 - 99	100 - 102

Continued on next page.

Table 5. (Continued). Confidence intervals of spiked analytes in various matrices (spiked at 300-400 mg/kg)

	Recovery confidence interval % (n=11, α=0.05)		
Name	*Self-prepared matrix*	*Bergamot oil*	*Petitgrain citronnier oil*
m-cresol	94 - 98	89 - 95	105 - 109
2-methoxy-phenol	101 - 105	92 - 98	104 - 107
heptanoic acid	78 - 84	45 - 66	83 - 91
methyl benzoate	105 - 108	74 - 112	106 - 110
terpinolene	97 - 113	97 - 113	[a]
1-nonanal	90 - 96 [b]	89 – 100 [b]	89 - 113 [b]
phenylethyl alcohol	95 - 105	96 - 102	100 - 105
isophorone	82 - 93	68 - 103	106 - 110
acetonitrile, phenyl	101 - 105	102 - 106	102 - 105
1-octen-3-yl acetate	101 - 106	60 - 109	101 - 105
alloocimene, isomer 1	97 - 102	93 - 105	77 - 95
camphor	101 - 105	76 - 113	[a]
isopulegol, isomer 1	100 - 103	78 - 108	94 – 101
alloocimene, isomer 2	99 - 113	65 - 102	66 - 110
citronellal	94 - 100	66 - 99	[a]
isopulegol, isomer 2	103 - 106	78 - 108	98 - 103
menthol	98 - 103	74 - 111	98 - 105
4-terpinenol	98 - 108	94 - 110	0 - 0
methyl salicylate	104 - 113	91 - 96	105 - 115
alpha terpineol	104 - 111	[a]	[a]
safranal	102 - 115	102 - 107	97 - 106
decanal	94 - 99	92 - 105	92 - 103
cuminaldehyde	101 - 111	97 - 107	101 - 109
l-carvone	100 - 113	60 - 111	[a]
phenylethyl acetate	98 - 110	99 - 103	101 - 108
nonanoic acid	80 - 86 [b]	55 - 61 [b]	96 - 103 [b]
decanol	92 - 101	83 - 94	106 - 110
indole	96 - 107	96 - 105	103 - 106
trans-anethole	100 - 112	102 - 107	101 - 110

Continued on next page.

Downloaded by CORNELL UNIV on May 29, 2012 | http://pubs.acs.org
Publication Date (Web): May 29, 2012 | doi: 10.1021/bk-2012-1098.ch007

Downloaded by CORNELL UNIV on May 29, 2012 | http://pubs.acs.org
Publication Date (Web): May 29, 2012 | doi: 10.1021/bk-2012-1098.ch007

Table 5. (Continued). Confidence intervals of spiked analytes in various matrices (spiked at 300-400 mg/kg)

	Recovery confidence interval % (n=11, α=0.05)		
Name	*Self-prepared matrix*	*Bergamot oil*	*Petitgrain citronnier oil*
cuminyl alcohol	100 - 110	96 - 104	106 - 112
sabinyl acetate	97 - 105	92 - 104	99 - 106
2-undecanone	95 - 102	57 - 106	100 - 108
thymol	97 - 110	99 - 104	101 - 109
menthyl acetate	101 - 112	74 - 111	108 - 114
carvacrol	96 - 104	92 - 101	108 - 113
methyl anthranilate	91 - 105	70 - 105	[c]
nicotine	87 - 98	78 - 87	73 - 83
dihydro alpha ionone	100 - 106	91 - 104	100 - 108
dihydro beta ionone	99 - 108	73 - 110	101 - 106
2-phenyethylisothiocyanate	91 - 97	93 - 97	93 - 99
dodecanol	98 - 110	91 - 102	103 - 113
beta ionone	95 - 104	71 - 106	101 - 108
valencene	95 - 108	91 - 97	92 - 100
myristicin	91 - 98	68 - 103	99 - 105
nerolidol, isomer 1	93 - 99	70 - 105	103 - 109
nerolidol, isomer 2	94 - 100	71 - 106	99 - 106
caffeine	106 - 108	94 - 98	102 - 107
isophytol	102 - 106	73 - 110	109 - 115

[a] Recovery could not be determined as component was present at higher levels in matrix. [b] Confidence interval based on second column only. [c] Analyte showed decreasing recoveries.

The recovery study described showed some examples of advantages by using the two column approach. The analysis of Bergamot and Petitgrain oils showed coelution of 1,8-cineol (eucalyptol) with limonene from the matrix on the first column. Quantitation was not possible on this column as the analyte spectrum does contain a distinctive ion ($^{m}/_{z}$ 154) but the overloaded signal of limonene was interfering correct quantitation. In this case the quantitation was done using the second column analysis.

Downloaded by CORNELL UNIV on May 29, 2012 | http://pubs.acs.org
Publication Date (Web): May 29, 2012 | doi: 10.1021/bk-2012-1098.ch007

Full Scan versus SIM Quantitation

In order to compare full scan with SIM based results several analytes were randomly selected and a method was set up for acquisition in SIM mode. Based on Table 3 one quantifier ion and up to three qualifier ions were acquired for each analyte. Gas chromatographic settings were kept identical to method described earlier.

Method was calibrated using internal standard method and the same calibration standards as used earlier. After calibration, the three matrices from previous experiment were spiked with selected analytes at nominal levels of approximately 300 mg/kg. Spiked matrices were analyzed once a day for eleven different days over a period of three weeks. During this period, after one week (four analysis done) mass spectrometer was tuned and instrument was re-calibrated using fresh prepared calibration standards.

As acquisition was performed in SIM mode, ion ratios were now used as identification criteria rather than the spectrum library search used earlier for the full scan method. Commission decision 2002/657/EC of the European Parliament (*6*) describes an identification system based on identification points (IP's). The system requires a minimum of four ions (equals 4 IP's) to be acquired per analyte for SIM based methods. An analyte is assumed positively identified when the actual ion ratio of all four ions falls within the tolerance window as described in Table 6.

Table 6. Ion ratio tolerances applied for SIM based method. Source: Commission Decision 2002/657/EC of the European Parliament (*6*)

Rel. intensity (% of quantifier ion)	*Tolerance ($^{+}/_{-}$ %)*
< 50	10
< 20 to 50	15
< 10 to 20	20
≤ 10	50

For subject method, acquisition of four ions for some analytes is difficult to achieve. The mass-spectra of those analytes do not contain enough distinctive ions and therefore only two or three IP's can be obtained.

Table 7 shows confidence intervals of the recoveries for each analyte in the three different matrices obtained using the SIM acquisition method. As can be seen, recoveries are excellent for each selected analyte and reproducibility is again also sufficient.

Downloaded by CORNELL UNIV on May 29, 2012 | http://pubs.acs.org
Publication Date (Web): May 29, 2012 | doi: 10.1021/bk-2012-1098.ch007

Table 7. Confidence intervals of spiked analytes in various matrices acquired in SIM-mode (spiked at 300-400 mg/kg)

	Recovery confidence interval % (n=11, α=0.05)		
Name	*Self-prepared matrix*	*Bergamot oil*	*Petitgrain citronnier oil*
toluene	89 - 99	94 - 101	90 - 99
furfural	91 - 98	80 - 89	92 - 106
trans-2-hexenal	94 - 97	92 - 95	89 - 92
allyl isothiocyanate	92 - 100	91 - 99	93 - 109
alpha pinene	83 - 95	[a]	[a]
benzaldehyde	87 - 94	87 - 95	99 - 114
1-octen-3-ol	90 - 97	95 - 104	105 - 118
sabinene	81 - 89	[a]	[a]
phenol	90 - 94	75 – 94 [d]	83 - 86 [d]
beta pinene	93 - 99	[a]	[a]
alpha phellandrene	99 - 111	97 - 101	[a]
alpha terpinene	95 - 101	95 - 101	[a]
p-cymene	88 - 92	[a]	[a]
salicylaldehyde	86 - 94	83 - 91	87 - 95
1,8-cineol(eucalyptol)	106 - 113	107 - 113	[a]
ocimene	98 - 103	93 - 104	[a]
o-cresol	94 - 96	91 – 96 [c]	80 - 98
1-octanol	92 - 99	114 – 125	93 - 102
p-cresol	89 - 92	91 – 95 [c]	91 - 95
2-methoxy-phenol	95 - 100	93 - 98	100 - 105
terpinolene	97 - 102	100 - 104	[a]
phenylethyl alcohol	91 - 96	87 - 92	97 - 100
acetonitrile, phenyl	95 - 101	98 - 105	96 - 103
1-octen-3-yl acetate	93 - 101	90 - 98	99 - 106
4-terpinenol	101 - 111	101 - 109	[a]
alpha terpineol	98 - 103	[a]	[a]
safranal	100 - 110	94 - 110	90 – 104 [a]
phenylethyl acetate	97 - 106	91 - 103	96 - 104
nonanoic acid	86 – 98 [b]	56 – 72 [b]	104 - 127 [b]

Continued on next page.

Table 7. (Continued). Confidence intervals of spiked analytes in various matrices acquired in SIM-mode (spiked at 300-400 mg/kg)

Name	*Recovery confidence interval % (n=11, α=0.05)* *Self-prepared matrix*	*Bergamot oil*	*Petitgrain citronnier oil*
trans-anethole	98 - 109	94 - 108	94 - 108
thymol	94 - 104	94 - 107	92 - 103
nicotine	92 - 100	90 - 98	85 - 101
2-phenyethylisothiocyanate	91 - 97	91 - 95	89 - 102
valencene	96 - 105	86 - 98	89 - 99

[a] Recovery could not be determined as component was present at higher levels in matrix. [b] Confidence interval based on second column only. Calibration on first column excluded. [c] Confidence interval based on second column only due to failing ion ratio on other column. [d] Confidence interval based on first column only due to failing ion ratio on other column.

Downloaded by CORNELL UNIV on May 29, 2012 | http://pubs.acs.org
Publication Date (Web): May 29, 2012 | doi: 10.1021/bk-2012-1098.ch007

Comparison of Table 5 (full scan) and 7 (SIM) shows that both acquisition modes produce comparable results. In some cases an analyte was not positively identified using the SIM based method as the actual ion ratio was not within the tolerance window. Ortho- and para-cresol for example were only positively identified on the second column as analysis of the spiked Bergamot matrix on the first column showed a failing ratio of two ions due to coelution with a matrix component. Second example is safranal of which the ratio of one ion failed in analysis of the spiked Petitgrain matrix on the second column. For both cases, the full scan method clearly showed similarity search indices above 85% and positively identified the analytes. These examples demonstrate the value of the two column approach applied in the method as well as the advantage of using full scan library search for identification.

The full scan method is also preferred as it complies with the identification points system (*6*). System describes that the usage of library search as identification criterion can be applied using a set minimum similarity index. The SIM based method does not comply with the identification points system as only two or three ions were acquired for several analytes. The spectra of those analytes do not contain ions which are distinctive enough.

Data presented clearly show the excellent performance of the full scan method for quantitative analysis of 77 selected analytes for EU essential oils hazard classification. Reanalysis is not needed in cases of coeleution on one column as the usage of a second column allows quantification in most cases. A data processing routine automatically combines results from both columns and generates a report. Quality of the quantitative data is high. The excellent performance of the method was demonstrated by the recovery and reproducibility data in various matrices. Quantitative results from the full scan extracted ion versus SIM based method were demonstrated to be comparable. However, the full scan method has the clear advantage of library search for identification.

Downloaded by CORNELL UNIV on May 29, 2012 | http://pubs.acs.org
Publication Date (Web): May 29, 2012 | doi: 10.1021/bk-2012-1098.ch007

Acknowledgments

We thank Michalina Troc, Katja Filonova, Jos Smeets, and Luc Alders for their skillful technical assistance.

References

1. Directive 92/32/EEC of the European Parliament and of the Council of 30 April 1992 amending Council Directive 67/54/EEC on the approximation of the laws, regulations and administrative provisions relating to the classification, packaging and labeling of dangerous substances. *Off. J. Eur. Union* **1992**, *L154*, 1−29.
2. Annex VI of the Dangerous substances directive 67/54/EEC of the European Parliament. *Off. J. Eur. Union* **2001**, *L225*, 263−314.
3. Analytical procedure for the GC/MS quantitation of potential fragrance allergens in fragrance compounds; version 1. *Analytical Procedures*; International Fragrance Association: Brussels, Belgium, 2003; pp 1−10.
4. Chaintreau, A; Joulain, D.; Marin, C.; Schmidt, C.; Vey, M. GC-MS quantitation of fragrance compounds suspected to cause skin reactions. 1. *J. Agric. Food Chem.* **2003**, *51*, 6398–6403.
5. Leijs, H.; Broekhans, J.; Van Pelt, L.; Mussinan, C. Quantitative analysis of the 26 allergens for cosmetic labelling in fragrance raw materials and perfume oils. *J. Agric. Food Chem.* **2005**, *53*, 5487–5491.
6. Commission Decision 2002/657/EC of the European Parliament and of the Council of 12 August 2002 implementing Council Directive 96/23/EC concerning the performance of analytical methods and the interpretation of results. *Off. J. Eur. Union* **2002**, *L221*, 8−36.,

Chapter 8

Analysis of Haloanisoles in Corks and Wines

Thomas S. Collins, Anna Hjelmeland, and Susan E. Ebeler[*]

Department of Viticulture and Enology, Graduate Group in Agricultural and Environmental Chemistry, and Food Safety and Measurement Facility, University of California, Davis, One Shields Avenue, Davis, California 95616
[*]E-mail: seebeler@ucdavis.edu

Downloaded by UNIV OF GUELPH LIBRARY on May 30, 2012 | http://pubs.acs.org
Publication Date (Web): May 29, 2012 | doi: 10.1021/bk-2012-1098.ch008

Haloanisoles (*e.g.,* 2,4,6-trichloroanisole, TCA; 2,4-dichloroanisole, 2,4-DCA; 2,6-dichloroanisole, 2,6-DCA; 2,3,4,6-tetrachloroanisole, TeCA; pentachloroanisole, PCA; and 2,4,6-tribromoanisole, TBA) cause musty off-aromas in many consumer products, including wine. In wines, the most common source of haloanisole contamination is cork closures, although barrels and other winery sources may also be sources of contamination. Human sensory thresholds for many haloanisoles are in the low ng L^{-1} level, therefore analytical methods for identification and quantification of these compounds requires limits of detection and quantitation at similar levels or lower. Gas chromatography-mass spectrometry is commonly used for analysis of haloanisoles and numerous sample preparation techniques have been reported. This chapter will briefly review information about sources of haloanisole contamination in consumer products and then review analytical approaches for measuring these important compounds in wines.

2,4,6-Trichloroanisole (TCA) has been identified as a trace contaminant producing a musty off-aroma in a wide range of food products and beverages, including broiler chickens (*1*), essential oils (*2*), wine (*3*), water (*4*, *5*), grains (*6*), potatoes (*7*), raisins (*8*), sake (*9*) and others. Similarly, 2,3,4,6-tetrachloroanisole (TeCA) has been identified as a contaminant in broiler chickens (*10*), pharmaceuticals (*11*) and in wine (*12*). Additionally, the bromine analogue to TCA, 2,4,6-tribromoanisole (TBA) has been identified in marine products (*13*),

In Recent Advances in the Analysis of Food and Flavors; Toth, S., et al.;
ACS Symposium Series; American Chemical Society: Washington, DC, 2012.

and in wine (*14*) and has been shown to produce a musty off aroma in raisins exposed to TBA (*13*). Recently, TBA contamination of Tylenol® and other over-the-counter medications resulted in numerous consumer complaints of a musty aroma in the products and ultimately product recalls (*15*).

Sensory thresholds for the haloanisoles are generally quite low. In water, the detection threshold varies from 30 pg L^{-1} (*16*) to 7.4 ng L^{-1} (*17*), while in wine detection thresholds of 1.4 ng L^{-1} (*18*), 2.5 ng L^{-1} (*19*) and 4 ng L^{-1} (*20*) have been reported. Prescott et al. (*21*) reported a detection threshold of 2.1 ng L^{-1} and a consumer rejection threshold of 3.1 ng L^{-1} in Chardonnay wine, but also pointed out that a significant number of panelists did not reject the wine even at much higher levels, suggesting that a proportion of the population may be relatively insensitive to the presence of TCA

In most cases involving food products and beverages, TCA and other anisoles are present as contaminants, *i.e.,* the TCA was introduced to the product from another source. In wine, for example, contaminated cork closures are often the source (*3*, *22*), although Chatonnet (*14*) also demonstrated that oak barrels used for wine storage can be a source of TCA as well. Several studies have shown that packaging materials for food products can be a source of contamination as well, particularly wood based packaging (*8*, *23*). Ramstad (*11*) found that a musty odor present in some contaminated pharmaceuticals came from the cardboard boxes used as packaging for the plastic bottles containing the pharmaceuticals. Contamination can also occur during shipping or storage of food products. A sampling of timber samples from six shipping containers involved in alleged contamination of food products was analyzed for chlorophenols and chloroanisoles. All of the wood samples were found to contain trichlorophenol (TCP), tetrachlorophenol (TeCP), and pentachlorophenol (PCP) and in all but one case, the corresponding chloroanisoles were found as well (*24*). Shipping pallets are thought to be the source of contamination in recent cases of TBA contamination of pharmaceuticals (*15*).

The kinetics of the transfer of TCA from packaging materials and through packaging materials has been evaluated as well. Rij et al. (*25*) studied the sorption and desorption behavior of TCA and polyethylene films, as well as the transfer of TCA across a polyethylene film and was able to establish a temperature dependence for these phenomena. Similarly, Jickells et al. (*26*) evaluated gas phase transfer rates for a range of potential contaminants, including TCA as well as the ability of different packaging materials and formats to provide a barrier to contamination of food products by TCA.

Numerous studies have focused on the formation of TCA and other chloroanisoles in wood, cork and other materials that are the demonstrated sources of contamination. In the study of shipping containers cited above, Hill et al. (*24*) isolated 38 fungal species from the wood samples, 19 of which could methylate chlorophenols to the corresponding chloroanisoles; each individual sample had at least three fungal species capable of the biomethylation reaction. Similarly, Ramstad (*11*) isolated six biomethylation-capable fungal species from the cardboard shipping containers associated with the contaminated pharmaceuticals. In cork closures, chloroanisole contamination can arise from fungal activity in and on the cork bark while it is still on the tree or by fungal activity on cork

Downloaded by UNIV OF GUELPH LIBRARY on May 30, 2012 | http://pubs.acs.org
Publication Date (Web): May 29, 2012 | doi: 10.1021/bk-2012-1098.ch008

slabs or cork cylinders which have been treated with chlorine based bleaches during the cork production process (*27*). The location of the contamination on the closure and the mix of chlorophenols and anisoles present can in some cases provide insight into the source of the contamination. In certain cases, the food product can be contaminated with a chlorophenol, which can be subsequently converted to the anisole during food processing. Miki et al. (*9*) found that rice koji used in the production of sake had been contaminated with TCP by wooden tools that contained TCP; during the processing of the koji, organisms present in the koji converted the TCP to TCA. The presence of TCP in the wooden tools was attributed to reaction of chlorine from sanitizers used to clean the tools with phenolic compounds present in the wooden tools. Similarly, off-aromas in potatoes from Nova Scotia were found to result from the application of chlorinated pesticides to the soil in which the potatoes were grown. The pesticides were converted to chloroanisoles by microorganisms associated with the soils and the surface of the potato tubers (*7*).

The very low sensory thresholds of the haloanisoles have necessitated development of highly sensitive and specific analytical methods for identification and quantification. The objective of this paper is to review methods of analysis for haloanisoles in corks and wines. The focus will be on sample preparation procedures used widely with gas chromatographic (GC) analyses. We also discuss several different GC detectors that have been commonly employed for haloanisole analysis, including recent applications in our laboratory using GC-tandem quadrupole MS. Although other approaches for haloanisole analysis have been described, including immunassays and various sensor systems or electronic noses (*e.g.,* semiconductor sensor arrays, direct mass spectrometry detection) (*28*–*32*) they are beyond the scope of this chapter.

Downloaded by UNIV OF GUELPH LIBRARY on May 30, 2012 | http://pubs.acs.org
Publication Date (Web): May 29, 2012 | doi: 10.1021/bk-2012-1098.ch008

Extraction of Haloanisoles

Early analyses of haloanisoles in food products typically involved solvent extraction or steam distillation extraction (*e.g.,* Likens-Nickerson extraction) of large quantities of sample (*e.g.,* 25-500 g) over several hours or with multiple isolation steps (*3*, *8*, *13*, *33*). These methods, when combined with GC-MS, are highly sensitive and typically give limits of detection in the 2-5 ng L^{-1} range for TCA (*3*). More recently, solventless extraction procedures (*e.g.,* solid phase microextraction (SPME) and stir bar sorptive extraction (SBSE or Twister®)) and liquid microextraction methods have been proposed for analysis of haloanisoles in wines and corks and these procedures will be briefly reviewed below.

Sorptive Extractions

Solid phase microextraction (SPME) was introduced in the early 1990's and is now widely used for a range of flavor and off-flavor analyses. SPME offers many advantages over traditional solvent extraction including the elimination of hazardous solvents, rapid extraction times (typically ~30 min), and easy automation. SPME sampling can occur either from the headspace (HS) or by insertion of the fiber into the liquid sample (direct immersion or DI-SPME), but most published applications have involved headspace sampling. Evans et al. (*34*) and Fisher and Fisher (*35*) were the first to report application of HS-SPME for haloanisole analysis in corks and wines. Fischer and Fischer (*35*) showed that headspace sampling of TCA in wine gave extraction efficiencies (determined by comparing peak areas) that were up to four times greater than those of liquid sampling for the same extraction times. These authors also observed that direct SPME analysis of ground, moistened cork samples did not give reliable quantitation due to very slow extraction kinetics. Therefore most SPME methods for analysis of corks involve soaking the corks for several hours in solvent (usually ethanol, methanol, or a wine matrix) followed by SPME analysis of the extract (*36–38*). Carasek et al. (*39*) proposed an interesting modification for direct HS-SPME analysis of haloanisoles in cork using an internally cooled solid-phase microextraction fiber, which increases analyte partitioning to the fiber coating. By cooling the SPME fiber to 10°C, the cork sample could be heated to 130°C and analyte recoveries of >75% were obtained with only 10 min of extraction. Detection and quantification limits were also lower for the cold-fiber extraction compared to regular HS-SPME (Table 1).

Optimization of HS-SPME methods involves evaluation of several parameters including the fiber type, extraction time and temperature conditions, use of salts to alter solvent ionic strength and solute partitioning to the headspace, and selection of an internal standard. In an overview of selected published protocols that describe the optimization of various SPME parameters, most optimized methods describe similar extraction temperature, time, and ionic strength conditions (Table 1). Generally, nonpolar PDMS fibers have been most widely used for haloanisole analysis. Recently, Bianco et al. (*49*) reported that PDMS fibers gave better extraction efficiencies for most haloanisoles (2,3,6-TCA, TeCA, PCA, and TBA) compared to DVB/CAR/PDMS fibers. These authors further reported that TCA was extracted more efficiently with the DVB/CAR/PDMS fiber, however the mixed phase fibers tended to swell when exposed to the headspace of ethanolic solutions and therefore had shorter lifetimes.

SPME extraction efficiencies can be influenced by matrix conditions (*50*). To account for these matrix effects, SPME quantitation is usually performed by either standard addition procedures or by addition of internal standards (IS). Stable isotope dilution analysis is generally recognized as an effective way to minimize matrix effects (*51*) and Pollnitz et al. (*52*) were the first to report use of a stable isotope labeled TCA analog ($^2H_5$-TCA) for analysis of TCA in wines. This compound is now frequently used as an IS for HS-SPME analyses (Table 1). The presence of ethanol tends to increase the reported limits of detection and quantitation for most haloanisoles but in general most reported HS-SPME methods for alcoholic beverages still report LODs and LOQs near sensory threshold levels (Table 1).

Downloaded by UNIV OF GUELPH LIBRARY on May 30, 2012 | http://pubs.acs.org
Publication Date (Web): May 29, 2012 | doi: 10.1021/bk-2012-1098.ch008

Downloaded by UNIV OF GUELPH LIBRARY on May 30, 2012 | http://pubs.acs.org
Publication Date (Web): May 29, 2012 | doi: 10.1021/bk-2012-1098.ch008

Table 1. Selected references describing HS-SPME optimization for analysis of haloanisoles in water, wines and corks (listed chronologically)

Sample	*Haloanisoles Measured*	*Fiber type*	*Extraction Time and Temperature*	*Salt Addition*	*Internal Standard Used*	*Detector (Ionization mode)*	*Reported LOQ/LOD*	*Reference*
Wine	TCA	PDMS	25 min/45°C	Sat'd NaCl	$[^2H_5]$TCA	MS—SIM mode (EI)	5 ng L^{-1} LOQ	(*34*)
Wine and Cork	TCA	PDMS	30 min/20°C	Sat'd NaCl	None reported (quantitation by Standard Addition)	MS—SIM mode (EI)	2.9 ng L^{-1} LOD	(*35*)
Wine	TCA	PDMS	30 min/25°C	5 M NaCl	None reported (quantitation by Standard Addition for red wines)	ECD	5-8 ng L^{-1} LOQ/1 ng L^{-1} LOD	(*40*)
Wine	TCA	PDMS	20 min/ 30°C	Sat'd NaCl	TBA	ECD	2.9-18 ng L^{-1} LOD	(*41*)
Cork (1 g cork in 9 mL water)	TCA; 2,4-DCA; 2,6-DCA	Carboxen-PDMS	40 min/75°C	None reported	None reported	Ion-trap MS/MS (CI and EI mode)	None reported	(*42*)
Water	TCA	DVB/CAR/PDMS	30 min/50°C	30% (w/v) NaCl	3-isobutyl-2-methoxy-pyrazine	Ion-trap MS—SIM mode (EI)	0.40-0.47 ng L^{-1}	(*43*)

Continued on next page.

Downloaded by UNIV OF GUELPH LIBRARY on May 30, 2012 | http://pubs.acs.org
Publication Date (Web): May 29, 2012 | doi: 10.1021/bk-2012-1098.ch008

Table 1. (Continued). Selected references describing HS-SPME optimization for analysis of haloanisoles in water, wines and corks (listed chronologically)

Sample	*Haloanisoles Measured*	*Fiber type*	*Extraction Time and Temperature*	*Salt Addition*	*Internal Standard Used*	*Detector (Ionization mode)*	*Reported LOQ/LOD*	*Reference*
Wine	TCA; 2,6-DCA; TBA	PDMS	40 min/50°C	4.8 M NaCl	None reported	ECD and ICP-MS	TCA: 1.3 ng L^{-1} LOD DCA: 3.1 ng L^{-1} LOD; TBA: 4.0 ng L^{-1} LOD	(*44*)
Water	TCA	PDMS	30 min/40°C	Sat'd Na_2SO_4	None reported	ECD	0.7 ng L^{-1} LOD/2.3 ng L^{-1} LOQ	(*45*)
Cork (0.2 g in 25 mL water)	TCA; 2,4-DCA; 2,6-DCA; TeCA; PCA	DVB/CAR/ PDMS	90 min/65°C	None reported	2,3,6-trichloro-toluene	ECD	0.2-2.6 ng g^{-1} LOD/0.6-8.6 ng g^{-1} LOQ	(*46*)
Wine	TCA; TBA	PDMS	30 min/21°C	30% NaCl	2,3,6-trichloro-anisole	Low resolution MS—SIM (CI); High resolution—SIM (EI)	Low res.: 0.2-0.3 ng L^{-1} LOQ; High res.: 0.03 ng L^{-1} LOQ	(*47*)

Downloaded by UNIV OF GUELPH LIBRARY on May 30, 2012 | http://pubs.acs.org
Publication Date (Web): May 29, 2012 | doi: 10.1021/bk-2012-1098.ch008

Sample	*Haloanisoles Measured*	*Fiber type*	*Extraction Time and Temperature*	*Salt Addition*	*Internal Standard Used*	*Detector (Ionization mode)*	*Reported LOQ/LOD*	*Reference*
Cork (0.2 g in 8 mL water or dry)	TCA; 2,4-DCA; 2,6-DCA; PCA	DVB/PDMS	75 min/85°C; Cold (10°C) fiber: 10 min/130°C	None reported	None reported	TOF-MS (scan mode)	1.2-1.8 ng g^{-1} LOD/3.9-6 ng g^{-1} LOQ; Cold Fiber: 0.25-0.49 ng g^{-1} LOD/ 0.83-1.62 ng g^{-1} LOQ	(*39*)
Wine	TCA	PDMS	45 min/30°C	0.2 g L^{-1} NaCl	None reported	Ion-trap MS—scan mode (EI)	2 ng L^{-1} (lowest standard evaluated)	(*48*)
Wine	TCA; 2,3,6-TCA; TeCA; PCA; TBA	PDMS	30 min/40°C	Sat'd NaCl	$[^2H_5]$TCA	MS—SIM mode (EI)	0.2-0.4 ng L^{-1} LOD/ 0.5-1.5 ng L^{-1} LOQ	(*49*)

Downloaded by UNIV OF GUELPH LIBRARY on May 30, 2012 | http://pubs.acs.org
Publication Date (Web): May 29, 2012 | doi: 10.1021/bk-2012-1098.ch008

The above methods generally involve extractions under equilibrium or near-equilibrium conditions (*i.e.*, analyte equilibrium between matrix, headspace, and fiber is obtained). Multiple HS-SPME (MHS-SPME) under non-equilibrium conditions has also been proposed in order to minimize matrix effects that have frequently been observed in equilibrium HS-SPME analysis of wines (*53*, *54*). MHS-SPME is based on repeated extraction of the sample headspace until the analyte is exhaustively extracted (usually after 2-5 extractions) and the total peak area from the successive extractions is used for quantitation. Using MHS-SPME, Martinez-Urunuela (*53*) successfully analyzed haloanisoles in wines, including, TCA, TeCA and PCA with limits of quantitation and detection of 5 ng L^{-1} and 1.5 ng L^{-1}, respectively. MHS-SPME of haloanisoles in different wine matrices gave results that were equivalent to those obtained with HS-SPME quantitation using the method of standard addition. Ezquerro and Tena (*55*) observed that MHS-SPME for direct analysis of ground cork stoppers using three successive HS-SPME extractions (45 min each at 75°C) gave results that were equivalent to those obtained by 16 h Soxhlet extractions using pentane as an extracting solvent.

Stir bar sorptive extraction (SBSE or Twister®) is a solventless extraction technique, similar to SPME, where the polymeric sorptive material is coated on the outside of a magnetic stir bar. Like SPME, sampling can take place from either the headspace or the liquid phase, however extraction capacities for SBSE are typically greater than those for SPME since the amount of sorbent is significantly greater (*56*). Extraction times for analysis of haloanisoles in water and wine samples using SBSE are also generally ≥ 1 h, although full equilibration of the analytes between the sample matrix and the sorptive material during extraction is not required for accurate quantitation (*57–61*). Unlike SPME analysis, sampling via SBSE is not fully automated. Following extraction, analytes are usually thermally desorbed from the Twister® stir bar in a specially designed GC inlet followed by cryofocusing on the front of the GC column prior to separation and detection. Maggi et al. (*60*) compared haloanisole analysis in wine samples using HS-SPME, direct immersion-SPME and Twister® extraction from the liquid phase. SBSE was more sensitive than SPME for all analytes (Table 2); reported LOD and LOQ values for HS-SPME sampling however, were generally higher than others reported in the literature.

As an inexpensive alternative to SBSE, Montes et al. (*62*) utilized bulk PDMS rods to extract chloroanisoles from the liquid or headspace of water and wine samples. Following extraction (2.5 h at room temperature), the analytes were desorbed by sonicating the rods in pentane and the solvent was injected into a GC with detection by ECD or MS-ion trap in the MS/MS mode. Extraction efficiency using headspace sampling was approximately two times that obtained with direct immersion sampling. Limits of quantitation were lower using GC-ion trap MS/MS, compared to the ECD, and ranged from 0.5-1.5 ng L^{-1} depending on the chloroanisole studied. The amount of PDMS sorbent (31 µL) used was similar to that in Twister® bars and overall results were comparable for both types of extraction.

Downloaded by UNIV OF GUELPH LIBRARY on May 30, 2012 | http://pubs.acs.org
Publication Date (Web): May 29, 2012 | doi: 10.1021/bk-2012-1098.ch008

Table 2. Comparison of Limits of Detection and Quantitation for SBSE and SPME analysis of haloanisoles in wines[1]

	LOQ (ng L^{-1})			*LOD (ng L^{-1})*		
Analyte	*SBSE*[2]	*DI-SPME*[3]	*HS-SPME*[4]	*SBSE*[2]	*DI-SPME*[3]	*HS-SPME*[4]
TCA	0.10	0.56	285.50	0.03	0.46	87.40
TeCA	1.27	1.14	351.20	0.71	0.66	107.40
PCA	0.08	1.39	796.40	0.05	0.88	243.10

[1] Adapted with permission from reference (*60*). Copyright 2008 Elsevier. GC-ion trap MS/MS analysis conditions were the same for all sampling procedures. A 5 mL sample size was used and γ-hexalactone was added as an internal standard prior to extraction. [2] SBSE extraction conditions: PDMS coated stir bar, 0.5 mm film thickness, 10 mm length; sampling in liquid phase at room temperature for 60 min with stirring at 700 rpm [3] DI-SPME extraction conditions: 100 μm PDMS fiber; fiber immersed in sample liquid phase at room temperature for 60 min with shaking at 700 rpm. [4] HS-SPME extraction conditions: 100 μm PDMS fiber; sampling from headspace at 35°C for 60 min with shaking at 700 rpm.

In addition to the sorptive extraction methods discussed above, solid phase extraction (SPE) has been used for isolation and extraction of haloanisoles. While not solventless, like SPME and SBSE, SPE methods typically require less solvent compared to most liquid-liquid extraction procedures and SPE can be highly effective in removing matrix interferences and concentrating the analytes. Soleas et al. (*63*) isolated TCA from wines and cork extracts using C18 SPE cartridges; a 125-fold concentration of the original sample was achieved by eluting the TCA in <0.5 mL of dichloromethane solvent. These authors report limits of quantification and detection of 2 ng L^{-1} and 0.1 ng L^{-1}, respectively using GC-MS in SIM mode. The SPE method of Soleas et al. was modified by Alvarez-Rodriguez et al. (*64*) to include analysis of TeCA and PCA from cork extracts although no detection or quantification limits were reported. Martinez-Urunuela et al. (*65*) reported enrichment factors of up to 500-fold for TCA, TeCA and PCA extracted from wines using a polymeric reverse phase SPE sorbent (Oasis HLB) and elution with methanol and hexane. Using this procedure, GC-MS detection limits using a large volume injection (9 μL) and an MS ion trap detector in MS/MS mode were 0.3, 0.4, and 2.4 ng L^{-1}, for TCA, TeCA and PCA respectively. Similar detection limits for TCA and TBA were also reported by Insa et al. (*66*) using LiChrolut EN SPE cartridges to isolate the haloanisoles; the extract was analyzed by GC with large volume injections (50 μL) and ion trap MS in selected ion storage mode. Recently, Schmarr et al. (*67*) reported a multi-step extraction using LiChrolut EN SPE cartridges followed by filtration on a basic aluminum oxide (Al_2O_3) column. The polarity filtration on Al_2O_3, when combined with large volume injections and multidimensional GC separations and detections, were successful in removing matrix interferences and allowed detection and quantification at sub-ng L^{-1} levels.

Jonsson et al. (*68*) proposed the miniaturization of traditional SPE using only 4 mg of C18 sorbent packed into a 100 µL syringe; this is compared to traditional SPE cartridges that use 60 mg or more of the stationary phase. Sample sizes of 100-1000 µL were used and analytes were eluted in 10 µL of solvent. Limits of detection for TCA and TBA depended on the type of detector used and ranged from 0.17-0.40 µg L^{-1} for GC-ECD to 0.22-0.75 ng L^{-1} for GC with high resolution MS in SIM mode.

Finally, dispersive solid phase extractions (often called QuEChERS since these extractions are quick, easy, cheap, effective, rugged, and safe) is a relatively new sample preparation technique combining both liquid-liquid extraction and solid phase extraction (see reviews by (*69–71*)). Using this technique, the sample is extracted with solvent, a salt is added to separate the phases, and finally a sorbent is added to remove matrix interferences prior to GC-MS analysis. Recently, Patil et al. (*72*) described isolation of TCA from wines using toluene, $MgSO_4$/NaCl, and a primary secondary amine sorbent. The authors reported that the method was effective at removing matrix interferences, however, some matrix signal enhancement was still observed, particularly when the extract was analyzed by GC-TOF compared to tandem GC-MS.

Downloaded by UNIV OF GUELPH LIBRARY on May 30, 2012 | http://pubs.acs.org
Publication Date (Web): May 29, 2012 | doi: 10.1021/bk-2012-1098.ch008

Liquid Microextractions

Liquid microextraction procedures are of increasing interest for analysis of volatiles in foods and beverages due to their high enrichment factors, use of only a few microliters of solvent for extraction, and compatibility with GC separations. These techniques, including single drop extractions, membrane extractions, and dispersive liquid-liquid microextractions have been reviewed (*56*, *73*, *74*). Recently, Marquez-Sillero et al. (*75*) described a single drop ionic liquid extraction combined with ion mobility spectrometry (IMS) detection for analysis of TCA in wines. A 2 µL drop of the ionic liquid extracting solvent (1-hexyl-3-methylimidazolium bis(trifluoromethylsulfonyl)-imide was exposed to the headspace above 2 mL of the wine sample for 30 min at 30°C. After the extraction, the syringe plunger was retracted and the sample directly injected into the multicolumn IMS inlet. The limit of detection and quantitation were 0.01 ng L^{-1} and 0.05 ng L^{-1}, respectively. Wine samples had to be diluted to less than 5% ethanol to avoid dissolution of the extracting solvent by the ethanol.

Montes et al. (*76*) described a microporous polypropylene membrane extraction system for analysis of several haloanisoles in water. The membrane was either used dry for headspace sampling or soaked in solvent to immobilize ~6.5 µL nonane to use for immersion sampling. Samples (80-115 mL) were extracted for 2-4 hours and following extraction, the membranes were rinsed with 250 µL hexane to isolate the haloanisoles. Using GC with ECD detection, the reported limit of quantitation was between 0.3-16 ng L^{-1} for TCA, 2,4-DCA, TeCA, PCA, and TBA in water.

Dispersive liquid-liquid microextractions use a ternary component solvent system to extract analytes into small volumes of extracting solvent (*i.e.*, the ternary system consists of the liquid (usually aqueous) sample, dispersing solvent, and extracting solvent). When combined, the solvent system forms a haze with

Downloaded by UNIV OF GUELPH LIBRARY on May 30, 2012 | http://pubs.acs.org
Publication Date (Web): May 29, 2012 | doi: 10.1021/bk-2012-1098.ch008

small droplets of the extracting solvent dispersed through the sample. Analyte extraction is enhanced by the small droplet size of the solvent and extractions are very rapid, essentially occurring in less than 5 min. Several reports of dispersive liquid-liquid extractions for haloanisole analysis in wines have been described (*77–79*). These methods generally use acetone as the dispersing solvent for the extraction of wine samples and the extracting solvent is carbon tetrachloride or chloroform. A brief centrifugation step (usually < 2 min) is required to disrupt the emulsion and separate the phases. Reported limits of detection ranged from 2-111 ng L^{-1} depending on the haloanisole studied. Fontana et al. (*80*) recently reported a modification to dispersive liquid-liquid microextractions where rather than adding a dispersing solvent, ultrasound radiation was used to emulsify and disperse fine droplets of extracting solvent into the aqueous bulk phase. Analytes were rapidly extracted into the solvent and a short centrifugation was used to disrupt the emulsion. As reported by Fontana et al. (*80*), ultrasonification of 5 mL of wine for 5 min and using 25 μL of trichloroethene as the extracting solvent provided enrichment factors of ≥ 400 and a limit of detection (using GC-ion trap MS/MS) of 0.7 ng L^{-1} for TCA.

As these studies indicate, the use of liquid-liquid microextraction for analysis of haloanisoles holds much promise for the rapid and sensitive analysis of haloanisoles in corks and wines. However, these techniques are still relatively new, and further work is needed to fully evaluate them in a range of matrices and to compare them to other traditional extraction procedures.

Alternative Cork Extraction Approaches

As noted previously, extraction kinetics of haloanisoles from cork material can be very slow and solvent extractions of up to 24 hours are often used prior to analysis (*81*). In addition, many methods for analysis of haloanisoles do not yield a quantitative extraction, providing instead an estimate of the amount of analyte that is released into the extracting phase in a given time period (sometimes called “releasable” haloanisoles; (*36–38*)). Soxhlet extractions using a low boiling solvent require several hours for extraction and are often used for quantitative extraction of cork material (*82*, *83*). However, approaches that use less solvent and allow for faster extraction times have recently been proposed, including supercritical fluid extraction, microwave assisted extraction and pressurized fluid extraction. Supercritical fluids have diffusivity properties similar to those of gases and density and solvating properties similar to those of liquids. As a result, they can rapidly diffuse through porous solids, like cork, to solubilize and extract analytes. Using supercritical fluid extraction (SFE), recovery of TCA from ground cork material was greater than 97% and comparable to recoveries obtained with Soxhlet extraction (*82*). However, the SFE method was much more rapid than Soxhlet extractions, requiring only 20 min/sample compared to 24 h/sample.

Pressurized liquid extractions operate under similar principles as supercritical fluid extractions since the solvent is heated under pressure and approaches the supercritical region (*84*). With SFE the solvent is often CO_2, while with pressurized liquid extractions the solvent is typically an organic solvent (*e.g.*, hexane, pentane, pentane/ether) (*85*, *86*). Pressurized liquid extractions of TCA, 2,6-DCA, and PCA from cork stoppers with extraction times of less than 4 min were reported by Gomez-Ariza et al. (*85*). Analyte recoveries were >92% and were comparable to those obtained with 24 h Soxhlet extractions. Ezquerro et al. (*87*) observed that pressurized liquid extraction of TCA from cork stoppers gave results that were equivalent to multiple headspace-SPME and Soxhlet extractions.

Finally, microwave heating of samples in closed vessels allows extractions at temperatures above the boiling point of the solvent so that extraction efficiency can be improved and analysis times decreased compared to traditional extraction procedures. Pizarro et al. (*88*) found that microwave assisted sampling for analysis of TCA, TeCA, PCA, and TBA in cork gave recoveries that were similar to Soxhlet extractions (~90%) with limits of detection and quantitation ranging from 0.30-0.68 ng g^{-1} and 0.98-2.28 ng g^{-1}, respectively (GC with an electron capture detector was used for the analysis). As opposed to quantitative extraction, Vestner et al. (*61*) proposed that microwave assisted extraction could also be used to provide a rapid estimate of "releasable" TCA from corks. Microwave assisted extractions of whole corks for 120 min using 10% ethanol (at 40°C) as the solvent and combined with SBSE of the final extract provided results that were comparable to those obtained by soaking the corks for 24 h in 10% ethanol (at room temperature) prior to SBSE.

While super critical fluid extraction, pressurized solvent extraction and microwave assisted extraction all provide rapid extractions and the potential for excellent recoveries of haloanisoles from solid cork materials, they do require use of specialized equipment. As a result, simple solvent extractions at room temperature for several hours or days are still widely used for haloanisole analysis of corks, as discussed previously.

GC Detection Methods

Early attempts to identify and quantify TCA in tainted wines and food products were limited by the very low concentrations at which it is typically present and the use of non-selective GC detectors, such as FID, since other compounds present at higher concentrations frequently co-eluted with TCA (*3*, *89*). By taking advantage of the very low human sensory threshold for this compound, application of GC with Olfactometric detection allowed successful identification of a narrow chromatographic region associated with the characteristic musty aroma of TCA tainted wines and other food products (*3*, *89*). Further analysis of this region by GC-MS in scan and then in selected ion monitoring mode was then used to identify and quantify this compound in tainted samples. From these early studies it is clear that selective and sensitive chemical detectors are needed for accurate quantitation of haloanisoles.

The most common detectors for analysis of haloanisoles in corks and wines are electron capture detectors (ECD), which are highly selective for analytes containing halogens, and GC-MS detectors (Table 1). To achieve the needed selectivity and sensitivity GC-MS detectors are typically operated in the selected ion monitoring (SIM) mode, or tandem MS techniques are used (either with an ion trap or triple quadrupole instruments). Principles of each of these detector

Downloaded by UNIV OF GUELPH LIBRARY on May 30, 2012 | http://pubs.acs.org
Publication Date (Web): May 29, 2012 | doi: 10.1021/bk-2012-1098.ch008

types have been reviewed (*90–95*). Comparisons of sensitivity of the different detectors for haloanisole analysis are difficult to make due to differences in matrix (cork or wine), sample preparation and fold-concentrations during extractions, as well as to differences in injection volumes. Two reports have directly compared detection or quantitation limits of ECD and tandem MS-ion trap detectors for analysis of selected haloanisoles extracted from corks or water samples (Table 3). For these studies, both detectors generally provided sensitivities near or below sensory thresholds, however the results were not consistent in showing that one detector provides better response than the other.

Downloaded by UNIV OF GUELPH LIBRARY on May 30, 2012 | http://pubs.acs.org
Publication Date (Web): May 29, 2012 | doi: 10.1021/bk-2012-1098.ch008

Table 3. Comparison of ECD and GC-ion trap MS/MS detectors for analysis of haloanisoles

	LOD reported by (44)[1]		*LOQ reported by (62)*[2]	
Compound	*GC-µECD*	*GC-ion trap MS/MS*	*GC-µECD*	*GC- ion trap MS/MS*
TCA	1.1 µg L^{-1}	5.5 µg L^{-1}	2.5 ng L^{-1}	0.8 ng L^{-1}
2,4-DCA	--	--	20 ng L^{-1}	0.5 ng L^{-1}
2,6-DCA	2.3 µg L^{-1}	5.3 µg L^{-1}	--	--
TBA	2.2 µg L^{-1}	5.4 µg L^{-1}	1.3 ng L^{-1}	1.5 ng L^{-1}
TeCA	--	--	1.5 ng L^{-1}	0.5 ng L^{-1}
PCA	--	--	0.8 ng L^{-1}	0.5 ng L^{-1}

[1] Pressurized liquid extraction of fortified cork; 1 µL splitless injection of extract [2] Fortified water sample extracted with PDMS rod; analytes desorbed with pentane; 2 µL splitless injection of pentane extract.

However, co-elutions and matrix interferences have been reported with GC-ECDs (*67*). Tandem MS detection, particularly with ion-trap MS/MS instruments, is becoming widely accepted for haloanisole analysis (*42*, *43*, *48*, *54*, *60*, *79*, *80*, *96–98*).

Tandem MS/MS involves several steps whereby precursor ions generated in the MS source are selected, transferred to a collision or reaction cell where they are further fragmented by bombarding with high energy reaction gases, and finally detected (see also reviews by (*92–95*)). Tandem MS/MS experiments can be performed to monitor the precursor ions, product ions, and/or neutral loss fragments in a variety of ways offering a high degree of selectivity and sensitivity since many background ions are not detected. Two types of instruments are available, ion trap and quadrupole instruments. Ion trap instruments trap the precursor ions and sequentially manipulate them in time; as noted above these instruments have been widely used for haloanisole analysis in corks and wines. With quadrupole instruments, ions travel through space and are sequentially transferred through a series of three quadrupoles where ion selection,

Downloaded by UNIV OF GUELPH LIBRARY on May 30, 2012 | http://pubs.acs.org
Publication Date (Web): May 29, 2012 | doi: 10.1021/bk-2012-1098.ch008

collision/reaction and monitoring are performed. Patil et al. (*72*) recently used quadrupole tandem MS to analyze TCA in wines and reported sub ng L^{-1} detection limits using a dispersive solid phase extraction to isolate the analyte from the wine. However, while extensively used for multiresidue pesticide analysis, applications of triple quadrupole MS/MS for targeted analysis of haloanisoles remains limited.

We recently developed a high throughput triple quadrupole MS method for simultaneous analysis of TCA, TeCA, PCA, and TBA in wines (*99*). Using HS-SPME-GC with minimal sample preparation (*i.e.,* no salt addition), limits of detection were 0.1 ng L^{-1} for TCA, TeCA, and PCA and 0.5 ng L^{-1} for TBA, values that are lower than previously reported (Table 1). Using this method, TCA concentrations in five wines reported to have off-aromas associated with cork taint were 2.4 – 43 ng L^{-1}.

Time-of-flight (TOF) detectors are increasingly used for metabolomics applications (see also review (*74*)). These detectors provide faster acquisition rates than quadrupole detectors, which aids in analyte resolution, quantitation, and identification. Carasek et al. (*39*) combined HS-SPME with GC-TOF analysis in scan mode and reported limits of detection and quantitation similar to those using GC-MS with selected ion monitoring (SIM) or with tandem MS/MS (Table 1). More recently, GC-TOF combined with dispersive solid phase extraction of TCA from wine was used to achieve a very low detection limit of 0.008 ng mL^{-1} (*72*). While most GC-TOF applications use instruments with unit mass resolution, at least two reports detailing analysis of TCA and TBA in wines using a high resolution instrument (10,000 resolving power) have emerged (*47*, *68*). Sub-ng L^{-1} detection limits were reported by these authors which were lower than the detection limits obtained from the same samples analyzed with a low resolution quadrupole MS detector; both instruments were operated in selected ion monitoring mode (Table 1).

The ionization method can also influence the results and while most reports use Electron Ionization (EI) for haloanisole analysis, chemical ionization (CI) has also been used (*e.g.,* Table 1). Jonsson et al. (*47*, *68*) indicated that CI can be more sensitive than EI for haloanisole analysis, although no direct comparisons with the same sample sizes and instruments were reported.

Finally, Schmarr et al. (*67*) have proposed a novel multidimensional separation and detection system for haloanisole analysis. Analytes are initially separated in Column 1 and detected using an FID detector. Selected chromatographic regions are then heart-cut and transferred to Column 2 where they undergo additional separation and detection with a quadrupole MS. Schmarr et al. proposed that the multidimensional separation and detection eliminates matrix interferences that are observed with some samples. When combined with injection volumes of up to 20 µL using a large volume injector and applied to analysis of extracts from cork soaks and wine samples, limits of detection and quantitation for TCA, TeCA, and TBA ranged from 0.05-0.09 ng L^{-1} and 0.19-0.34 ng L^{-1}, respectively.

Downloaded by UNIV OF GUELPH LIBRARY on May 30, 2012 | http://pubs.acs.org
Publication Date (Web): May 29, 2012 | doi: 10.1021/bk-2012-1098.ch008

Summary

Haloanisole contamination results in undesirable off-aromas in wines and other consumer products. Gas chromatographic separations combined with mass spectrometry detection are commonly used for analysis of these compounds. To achieve limits of detection and quantitation in the low ng L^{-1} range, consistent with sensory threshold values, sample preparation techniques that result in high concentration factors are necessary. Due to its ease of use and elimination of toxic solvents, HS-SPME has become one of the most commonly used sample preparation techniques for haloanisole analysis. Highly sensitive and selective GC detectors, such as triple quadrupole tandem MS also provide significant enhancements in sensitivity, selectivity, and speed compared to other commonly available detectors. While there have been significant improvements in analytical tools for analysis of haloanisoles in the past ~15 years, research efforts continue to provide new approaches for analysis of these compounds and the limits with respect to analysis speed and sensitivity continue to be surpassed with new improvements in instrumentation and extraction techniques.

References

1. Curtis, R. F.; Dennis, C.; Gee, J. M.; Gee, M. G.; Griffiths, N. M.; Land, D. G.; Peel; Robinson, D. *J. Sci. Food Agric.* **1974**, *25*, 811–828.
2. Stoffelsma, J.; De Roos, K. *J. Agric. Food Chem.* **1973**, *21*, 738–739.
3. Buser, H.-R.; Zanier, C.; Tanner, H. *J. Agric. Food Chem.* **1982**, *30*, 359–362.
4. Hodin, F.; Borén, H.; Grimvall, A.; Karlsson, S. *Water Sci. Technol.* **1991**, *24*, 403–410.
5. Nystrom, A.; Grimvall, A.; Krantz-Ruilcker, C.; Savenhed, R.; Åerstrand, K. *Water Sci. Technol.* **1992**, *25*, 241–249.
6. Seitz, L. M.; Ram, M.; Rengarajan, R. *J. Agric. Food Chem.* **1999**, *47*, 1051–1061.
7. Daniels-Lake, B. J.; Prange, R. K.; Gaul, S. O.; McRae, K. B.; de Antueno, R.; McLachlan, D. *J. Am. Soc. Hortic. Sci.* **2007**, *132*, 112–119.
8. Aung, L. H.; Smilanick, J. L.; Vail, P. V.; Hartsell, P. L.; Gomez, E. *J. Agric. Food Chem.* **1996**, *44*, 3294–3296.
9. Miki, A.; Isogai, A.; Utsunomiya, H.; Iwata, H. *J. Biosci. Bioeng.* **2005**, *100*, 178–183.
10. Engel, C.; De Groot, A.; Weurman, C. *Science* **1966**, *154*, 270.
11. Ramstad, T.; Walker, J. S. *Analyst* **1992**, *117*, 1361–1366.
12. Chatonnet, P.; Guimberteau, G.; Dubourdieu, D.; Boidron, J. *J. Int. Sci. Vigne Vin.* **1994**, *28*, 131–151.
13. Whitfield, F. B.; Hill, J. L.; Shaw, K. J. *J. Agric. Food Chem.* **1997**, *45*, 889–893.
14. Chatonnet, P.; Bonnet, S.; Boutou, S.; Labadie, M. D. *J. Agric. Food Chem.* **2004**, *52*, 1255–1262.
15. McCoy, M. *C&E News* **2010** Jan.25, *88* (4), 18.
16. Griffiths, N. M. *Chem. Senses Flavour* **1974**, *1*, 187–195.

17. Guadagni, D. G.; Buttery, R. G. *J. Food Sci.* **1978**, *43* (4), 1346–1347.
18. Duerr, P. In *Proceedings of the International Symposium on Cool Climate Viticulture and Enology*; Heatherbell, A., Lombard, P. D., Bodyfelt, F. W., Price, S. F., Eds.; Oregon State University, Depts. of Food Science and Technology, Horticulture, and Extension Service, in cooperation with the Oregon Winegrowers Association and Oregon Wine Advisory Board: Corvallis, OR, 1985; pp 257−266.
19. Liacopoulos, D.; Skouroumounis, G.; Pollnitz, A.; Sefton, M. 1999. In *Proceedings of the Tenth Australian Wine Industry Technical Conference*, Sydney, New South Wales, 2-5 August, 1998; Blair, R. J., Sas, A. N., Hayes, P. F., Høj, P. B., Eds.; Australian Wine Industry Technical Conference Inc.: Sydney, NSW, Australia, 1999; pp 261
20. Amon, J.; Vandepeer, J.; Simpson, R. *Wine Ind. J.* **1989**, *4*, 62–69.
21. Prescott, J.; Norris, L.; Kunst, M.; Kim, S. *Food Qual. Pref.* **2005**, *16* (4), 345–349.
22. Simpson, R. F. *Aust. N. Z. Wine Ind. J.* **1990**, *5*, 286–296.
23. Crosby, K. I; Greve, P. A.; Korte, F.; Still, G. G.; Vonk, J. W. *Pure Appl. Chem.* **1981**, *53*, 1051–1080.
24. Hill, J. L.; Hocking, A. D.; Whitfield, F. B. *Food Chem.* **1995**, *54* (2), 161–166.
25. Rij, R. E.; Fong, L. S.; Aung, L. H. *J. Stored Prod. Res.* **1996**, *32* (4), 303–306.
26. Jickells, S. M.; Poulin, J.; Mountfort, K. A.; Fernandez-Ocana, M. *Food Addit. Contam.* **2005**, *22* (8), 768–782.
27. Simpson, R. F.; Sefton, M. A. *Aust. J. Grape Wine Res.* **2007**, *13* (2), 106–116.
28. Marti, M. P.; Boque, R.; Riu, M.; Busto, O; Guasch, J. *Anal. Bioanal. Chem.* **2003**, *376*, 497–501.
29. Moore, E.; Pravda, M.; Guilbault, G. G. *Anal. Chim. Acta* **2003**, *484* (1), 15–24.
30. Santos, J. P.; Lozano, J.; Aleixandre, M.; Sayago, I.; Fernandez, M. J.; Ares, L.; Gutierrez, J.; Horrillo, M. C. *Sens. Actuators, B* **2004**, *103*, 98–103.
31. Sanvicens, N.; Moore, E. J.; Guilbault, G. G.; Marco, M. P. *J. Agric. Food Chem.* **2006**, *54*, 9176–9183.
32. Lausterer, R.; Sanvicens, N.; Marco, M. P.; Hock, B. *Anal. Lett.* **2003**, *36* (4), 713–729.
33. Whitfield, F. B.; Nguyen, T. L.; Shaw, K. J.; Last, J. H.; Tindale, C. R.; Stanley, G. *Chem. Ind.* **1985**, *19*, 661–663.
34. Evans, T. J.; Butzke, C. E.; Ebeler, S. E. *J. Chromatogr., A* **1997**, *786*, 293–298.
35. Fischer, C.; Fischer, U. *J. Agric. Food Chem.* **1997**, *45* (6), 1995–1997.
36. Hervé, E.; Price, S.; Burns, G.; Weber, P. *Chemical Analysis of TCA as a Quality Control Tool for Natural Corks*. 2000. Presented at the ASEV Annual Meeting, July 1999, Reno NV. http://www.corkqc.com/currentresearch/CorkTaint/ETS%20CQC-SPME.pdf (accessed on-line Dec. 29, 2011).

Downloaded by UNIV OF GUELPH LIBRARY on May 30, 2012 | http://pubs.acs.org
Publication Date (Web): May 29, 2012 | doi: 10.1021/bk-2012-1098.ch008

37. ISO 20752:2007. Cork stoppers—determination of releasable 2,4,6-trichloroanisole (TCA).
38. Macku, C.; Gonzalez, L.; Schleussner, C.; Mesquita, A. C.; Herwatt, J. W.; Kirch, L. C.; Schwartz, R. J. *J. Agric. Food Chem.* **2009**, *57*, 7962–7968.
39. Carasek, E.; Cudjoe, E.; Pawliszyn, J. *J. Chromatogr., A* **2007**, *1138*, 10–17.
40. Riu, M.; Mestres, M.; Busto, O.; Guasch, J. *J. Chromatogr., A* **2002**, *977*, 1–8.
41. Alzaga, R.; Ortiz, L.; Sachez-Baeza, F.; Marco, M. P.; Bayona, J. M. *J. Agric. Food Chem.* **2003**, *51* (12), 3509–3514.
42. Bianchi, F.; Careri, M.; Mangia, A.; Musci, M. *J. Sep. Sci.* **2003**, *26*, 369–375.
43. Sung, Y. H.; Li, T. Y.; Huang, S. D. *Talanta* **2005**, *65* (2), 518–524.
44. Gomez-Ariza, J. L.; Garcia-Barrera, T.; Lorenzo, F. *J. Anal. At. Spectrom.* **2005**, *20* (9), 883–888.
45. Pinheiro, P. B. M.; Esteves da Silva, J. C. G. *Anal. Bioanal. Chem.* **2005**, *382* (2), 341–346.
46. Riu, M.; Mestres, M.; Busto, O.; Guasch, J. *Anal. Chim. Acta.* **2006**, *563*, 310–314.
47. Jonsson, S.; Uusitalo, T.; van Bavel, B.; Gustafsson, I.-B.; Lindstrom, G. *J. Chromatogr., A* **2006**, *111*, 71–75.
48. Viera Neto, P.; Rocha, S. M.; Silvestre, A. J. D. *J. Sci. Food Agric.* **2007**, *87*, 632–640.
49. Bianco, G.; Novario, G.; Zianni, R.; Cataldi, T. R. I. *Anal. Bioanal. Chem.* **2009**, *393* (8), 2019–2027.
50. Pawliszyn, J. *Solid Phase Microextraction—Theory and Practice*; Wiley−VCH: New York, 1997.
51. Polaskova, P.; Herszage, J; Ebeler, S. E. Wine flavor: Chemistry in a glass. *Chem. Soc. Rev.* **2008**, *37*, 2478–2489.
52. Pollnitz, A. P.; Pardon, K. H.; Liacopoulos, D.; Skouroumounis, G. K.; Sefton, M. A. *Aust. J. Grape Wine Res.* **1996**, *2*, 184–190.
53. Martinez-Urunuela, A.; Gonzalez-Saiz, J.; Pizarro, C. *J. Chromatogr., A* **2005**, *1089*, 31–38.
54. Pizarro, C.; Perez-del-Notario, N.; Gonzalez-Saiz, J. M. *J. Chromatogr., A* **2007**, *1166*, 1–8.
55. Ezquerro, O.; Tena, M. T. *J. Chromatogr. A.* **2005**, *1068*, 201–208.
56. Kloskowski, A.; Chrzanowski, W.; Pilarczyk, M.; Namiesnik, J. *Crit. Rev. Anal. Chem.* **2007**, *37*, 15–38.
57. Ochiai, N.; Sasamoto, K.; Takino, M.; Yamashita, S.; Daishima, S.; Heiden, A.; Hoffman, A. *Analyst* **2001**, *126* (10), 1652–1657.
58. Benanou, D.; Acobas, F.; de Roubin, M. R.; Sandra, F. D. P. *Anal. Bioanal. Chem.* **2003**, *376* (1), 69–77.
59. Benanou, D.; Acobas, F.; de Roubin, M. R. *Water Sci. Technol.* **2004**, *49* (9), 161–170.
60. Maggi, L.; Zalacain, A.; Mazzoleni, V.; Alonso, G. L.; Salinas, M. R. *Talanta* **2008**, *75*, 753–759.
61. Vestner, J.; Fritsch, S.; Rauhut, D. *Anal. Chim. Acta.* **2010**, *660*, 76–80.

Downloaded by UNIV OF GUELPH LIBRARY on May 30, 2012 | http://pubs.acs.org
Publication Date (Web): May 29, 2012 | doi: 10.1021/bk-2012-1098.ch008

Downloaded by UNIV OF GUELPH LIBRARY on May 30, 2012 | http://pubs.acs.org
Publication Date (Web): May 29, 2012 | doi: 10.1021/bk-2012-1098.ch008

62. Montes, R.; Rodriguez, I.; Rubi, E.; Bollain, M. H.; Cela, R. *Anal. Chim. Acta.* **2007**, *599*, 84–91.
63. Soleas, G. J.; Yan, J.; Seaver, T.; Goldberg, D. M. *J. Agric. Food Chem.* **2002**, *50*, 1032–1039.
64. Alvarez-Rodriguez, M. L.; Recio, E.; Coque, J. J. R. *Eur. Food Res. Technol.* **2009**, *230*, 135–143.
65. Martinez-Urunuela, A.; Rodriguez, I.; Cela, R.; Gonzalez-Saiz, J. M.; Pizarro, C. *Anal. Chim. Acta.* **2005**, *549*, 117–123.
66. Insa, S.; Antico, E.; Ferreira, V. *J. Chromatogr., A.* **2005**, *1089*, 235–242.
67. Schmarr, H.-G.; Koschinski, S.; Sang, W.; Slabizki, P. *J. Chromatogr., A* **2011**, DOI: 10.1016/j.chroma.2011.10.033.
68. Jonsson, S.; Hagberg, J.; van Bavel, B. *J. Agric. Food Chem.* **2008**, *56*, 4962–4967.
69. Majors, R. E. *LC-GC* **2007**, *25*, 436–446.
70. Lehotay, S. J.; Anastassiades, M.; Majors, R. E. *LC-GC* **2010**, *28*, 504–516.
71. Fenik, J.; Tankiewicz, M.; Biziuk, M. *Trends Anal. Chem.* **2011**, *30*, 814–826.
72. Patil, S. H.; Banerjee, K.; Utture, S. C.; Fontana, A. R.; Altamirano, J. C.; Oulkar, D. P.; Wagh, S. S.; Dasgupta, S.; Patil, S. B.; Jadhav, M. R.; Ugare, B. R.; Adsule, P. G.; Deshmukh, M. B. *Food Chem.* **2011**, *124* (4), 1734–1740.
73. Pena-Pereira, F.; Lavilla, I.; Bendicho, C. *Spectrochim. Acta, Part B* **2009**, *54*, 1–15.
74. Ebeler, S. E. In *Handbooks in Separation Science: Gas Chromatography*; Poole, C. F., Ed.; Elsevier: Amsterdam, 2012; in press.
75. Marquez-Sillero, I.; Cardenas, S.; Valcarcel, M. *J. Chromatogr., A* **2011**, *1218*, 7574–7580.
76. Montes, R.; Rodriguez, I.; Rubi, E.; Ramil, M.; Cela, R. *J. Chromatogr., A* **2008**, *1199*, 21–26.
77. Campillo, N.; Viñas, P.; Cacho, J. I.; Peñalver, R.; Hernández-Córdoba, M. *J. Chromatogr., A* **2010**, *1217*, 7323–7330.
78. Pizarro, C.; Saenz-Gonzalez, C.; Perez-del-Notario, N.; Gonzalez-Saiz, J. M. *J. Chromatogr., A* **2010**, *1217*, 7630–7637.
79. Pizarro, C.; Saenz-Gonzalez, C.; Perez-del-Notario, N.; Gonzalez-Saiz, J. M. *J. Chromatogr., A* **2011**, *1218*, 1576–1584.
80. Fontana, A. R.; Patil, S. H.; Banerjee, K.; Altamirano, J. C. *J. Agric. Food Chem.* **2010**, *58*, 4576–4581.
81. Callejon, R. M.; Troncoso, A. M.; Morales, M. L. *Talanta* **2007**, *71*, 2092–2097.
82. Taylor, M. K.; Young, T. M.; Butzke, C. E.; Ebeler, S. E. *J. Agric. Food Chem.* **2000**, *48* (6), 2208–2211.
83. Chatonnet, P.; Labadie, D.; Boutou, S. *J. Int. Sci. Vigne Vin.* **2003**, *37*, 181–193.
84. Schantz, M. M. *Anal. Bioanal. Chem.* **2006**, *386*, 1043–1047.
85. Gomez-Ariza, J. L.; Garcia-Barrera, T.; Lorenzo, F.; Gonzalez, G. A. *Anal. Chim. Acta.* **2005**, *540*, 17–24.
86. Wright, J.; DePhillipo, T. *LC-GC.* **2010**; http://chromatographyonline.findanalytichem.com/lcgc/Articles/Comparison-of-

In Recent Advances in the Analysis of Food and Flavors; Toth, S., et al.;
ACS Symposium Series; American Chemical Society: Washington, DC, 2012.

Supercritical-Fluid-Extraction-SFE-a/ArticleStandard/Article/detail/727860 (accessed on-line, Dec. 31, 2011).

87. Ezquerro, O.; Garrido-Lopez, A.; Tena, M. T. *J. Chromatogr. A.* **2006**, *1102*, 18–24.
88. Pizarro, C.; Perez-del-Notario, N.; Gonzalez-Saiz, J. M. *J. Chromatogr. A.* **2007**, *1149*, 138–144.
89. Spadone, J.-C.; Takeoka, G.; Liardon, R. *J. Agric. Food Chem.* **1990**, *38*, 226–233.
90. Poole, C. F. *J. High Res. Chromatogr.* **1982**, *5*, 454–471.
91. Morris, P. J. T.; Ettre, L. S. *LC-GC.* **2007**; http://chromatographyonline.findanalytichem.com/lcgc/article/articleDetail.jsp?id=409516 (accessed on-line, Jan. 1, 2012).
92. Gross, J. H. *Mass Spectrometry. A Textbook*; Springer-Verlag: Berlin, 2004.
93. de Hoffmann, E.; Stroobant, V. *Mass Spectrometry: Principles and Applications*, 3rd ed.; Wiley and Sons: West Sussex, England, 2007.
94. McMaster, M. C. *GC/MS. A Practical User's Guide*, 2nd ed.; Wiley and Sons: New Jersey, 2008.
95. Hübschmann, H. J. *Handbook of GC/MS. Fundamentals and Applications*, 2nd ed.; Wiley-VCH Verlag GmbH & Co: Weinheim, Germany, 2009.
96. Gomez-Ariza, J. L.; Garcia-Barrera, T.; Lorenzo, F. *J. Chromatogr., A* **2004**, *1049*, 147–153.
97. Gomez-Ariza, J. L.; Garcia-Barrera, T.; Lorenzo, F. *J. Chromatogr., A* **2004**, *1056*, 243–247.
98. Gomez-Ariza, J. L.; Garcia-Barrera, T.; Lorenzo, F. *Anal. Chim. Acta.* **2004**, *516*, 165–170.
99. Hjelmeland, A.; Collins, T. S.; Mitchell, A. E.; Ebeler, S. E. *Analysis of haloanisoles in wines using solid phase microextraction and gas chromatography triple quadrupole mass spectrometry.* 2012, in preparation.

Downloaded by UNIV OF GUELPH LIBRARY on May 30, 2012 | http://pubs.acs.org
Publication Date (Web): May 29, 2012 | doi: 10.1021/bk-2012-1098.ch008

Downloaded by CORNELL UNIV on May 30, 2012 | http://pubs.acs.org
Publication Date (Web): May 29, 2012 | doi: 10.1021/bk-2012-1098.ch009

Chapter 9

Comparative Studies on the Generation of Acrolein as Well as of Aroma-Active Compounds during Deep-Frying with Different Edible Vegetable Fats and Oils

Alice Ewert,[§] Michael Granvogl,[*,#] and Peter Schieberle[§,#]

[#]Technical University of Munich, Chair for Food Chemistry
[§]German Research Center for Food Chemistry Lise-Meitner-Straße 34,
D-85354 Freising, Germany
[*]E-mail: Michael.Granvogl@lrz.tum.de

It is well-known that high temperature cooking of food can lead to the generation of several decomposition compounds, which may either provide desirable qualities, like taste and flavor, or undesirable properties showing adverse effects on human health. Therefore, the present study investigated the influence of different oils on the generation of desirable aroma-active compounds and the undesirable food-borne toxicant acrolein during frying. For this purpose, six edible fats and oils varying in their fatty acid composition were used for deep-frying of thin potato slices. After the frying process, first, the key aroma compounds of the chips were quantified by means of stable isotope dilution assays. Secondly, acrolein was quantified in chips as well as in the frying medium. For this purpose, two quantitation methods for acrolein using stable isotopically labeled [$^{13}C_3$]-acrolein as internal standard were newly developed. The results clearly showed that the use of a frying medium mainly consisting of mono-unsaturated or saturated fatty acids led to significantly lower amounts of (*E*,*E*)-2,4-decadienal and (*E*,*Z*)-2,4-decadienal in chips. In contrast, acrolein generation in chips seemed not to be affected by the type of frying medium. However, significantly elevated acrolein concentrations were generated in those oils containing higher amounts of linolenic acid (e.g., rapeseed or linseed oil).

In Recent Advances in the Analysis of Food and Flavors; Toth, S., et al.;
ACS Symposium Series; American Chemical Society: Washington, DC, 2012.

Downloaded by CORNELL UNIV on May 30, 2012 | http://pubs.acs.org
Publication Date (Web): May 29, 2012 | doi: 10.1021/bk-2012-1098.ch009

Introduction

During deep-frying, fats and oils are repeatedly exposed to elevated temperatures in the presence of atmospheric oxygen and receive maximum oxidative and thermal abuse. Such extended thermal oxidative conditions can lead to the generation of several decomposition compounds of the frying fat. On one hand, these products are responsible for desirable properties, like taste, flavor, and browning, on the other hand some of these degradation products, e.g., acrolein, can have adverse effects on human health due to its irritating power and ability for depressing the respiratory immune response (*1*). Acrolein is considered as a priority pollutant according to the U.S. Environmental Protection Agency (EPA) (*2*) and is classified in group 3 by the International Agency for Research on Cancer (IARC) (*3*). Additionally, in recent years, acrolein was analyzed in various foodstuff, biological samples or tobacco smoke (*4–6*). Its formation is dependent on several factors, such as temperature, heating time, oxygen concentration, and the type of oil (*7–9*). However, analysis of low-molecular aldehydes, such as acrolein, is complicated due to their high volatility and reactivity as well as the lack of a chromophore in the structure.

Therefore, the aim of the study was to investigate the generation of desirable (key aroma compounds) and undesirable (acrolein) food constituents during frying of potato slices using six different fats and oils varying in their fatty acid composition. Quantitation of acrolein was on the basis of two newly developed methods using stable isotopically labeled [$^{13}C_3$]-acrolein as internal standard.

Methods

Oil Heating Process (Model System)

Oil samples (30 g) were weighed into open glass tubes and heated in a metal block (24 h/180 °C). Immediately after cooling to room temperature, the internal standard [$^{13}C_3$]-acrolein (120-900 µg, dissolved in methanol; amount depending on the respective experiments) was added to the samples.

Deep-Frying of Potatoes

Thin slices of potatoes were deep-fried at 180 °C in pre-heated oil (2.3 L) for 2.5 min in a commercial deep-fryer. In total, the frying time did not exceed 2 h. According to general deep-frying instructions, the chips were rotated repeatedly during the frying process, leading to an even browning. For acrolein quantitation in oils, after 3, 6, and 9 frying cycles, aliquots (10 mL) were removed and the internal standard [$^{13}C_3$]-acrolein (5 – 35 µg) was added. For acrolein quantitation in chips, to an aliquot (10 g; powdered in liquid nitrogen using a blender), water (10 mL) and the internal standard (5 – 10 µg) were added.

Downloaded by CORNELL UNIV on May 30, 2012 | http://pubs.acs.org
Publication Date (Web): May 29, 2012 | doi: 10.1021/bk-2012-1098.ch009

Quantitation of Acrolein by Headspace GC-MS (Method I)

After the samples were stirred for 20 min at room temperature, aliquots of the headspace volume (500 µL) were injected into a Trace GC equipped with an HP-5 MS column. The effluent was monitored by an ion trap mass spectrometer running in the chemical ionization mode with methanol as reagent gas. Acrolein and [$^{13}C_3$]-acrolein were identified by means of their retention times and their protonated molecular ions (*m/z* 57 for acrolein and *m/z* 60 for [$^{13}C_3$]-acrolein, respectively).

Quantitation of Acrolein by GC-MS after Derivatization with Pentafluorophenyl hydrazine (PFPH) (Method II)

To aliquots of the samples (either 3 g of oil or 10 g of chips), PFPH solution (0.5 mL; 2 mg dissolved in 0.1 mol/L HCl) was added and, after dilution with dichloromethane (50 mL), the mixture was stirred for 20 min at room temperature. Then, the PFPH derivatives of acrolein and [$^{13}C_3$]-acrolein were separated from the sample by solvent assisted flavor evaporation (SAFE) technique (*10*) at 48 °C under vacuum. Aliquots of the solution (2 µL) were analyzed by GC-MS (CI) using an FFAP column. The acrolein and [$^{13}C_3$]-acrolein hydrazones were again characterized by their retention times and their protonated molecular ions obtained in the full scan mode (*m/z* 237 for acrolein and *m/z* 240 for [$^{13}C_3$]-acrolein, respectively).

Quantitation of Key Aroma Compounds in Potato Chips

In preliminary trials based on aroma extract dilution assays (AEDA), several key aroma compounds were identified, e.g., (*E*,*E*)-2,4-decadienal, (*E*,*Z*)-2,4-decadienal, 2-ethyl-3,5-dimethylpyrazine, 2-methylbutanal, 3-methylbutanal, and 3-(methylthio)propionaldehyde. These compounds were quantified by stable isotope dilution assays (SIDA): to aliquots of chips (20 - 50 g; depending on the amount of the respective analyte), dichloromethane (200 mL) as well as the corresponding stable isotopically labeled internal standards were added. After stirring for 3 h at room temperature, the volatile compounds were separated from the non-volatiles using SAFE technique (*10*). Quantitation of 2-methylbutanal and 3-methylbutanal was performed by headspace GC-MS (CI), all other odorants by GC-MS (CI).

Results and Discussion

Generation of Acrolein during Thermal Processing of Oils

The crucial factor of headspace GC-MS analysis of low molecular weight compounds like acrolein is the low specifity of the mass traces. Regarding the toxicological relevance of acrolein, an additional method, which was not on the basis of a direct measurement, but on a derivatization of the analyte prior to GC-MS measurement, was developed. Preliminary studies showed that pentafluorophenyl hydrazine (PFPH) is prone to convert acrolein into a stable

Downloaded by CORNELL UNIV on May 30, 2012 | http://pubs.acs.org
Publication Date (Web): May 29, 2012 | doi: 10.1021/bk-2012-1098.ch009

hydrazone (*11*). For both methods, determination of LODs and LOQs was performed by adding different amounts of acrolein (2, 5, 10, 25, and 50 µg/kg) to unheated oilve oil, which was proven to be free of acrolein in preliminary trials. After workup and analysis by GC-MS, LODs (5 µg/kg, method I; 10 µg/kg, method II) and LOQs (15 µg/kg, method I; 30 µg/kg, method II) were calculated on the basis of the signal-to-noise ratio of 3:1 and 9:1, respectively.

Quantitative results obtained for six different oils heated at 180 °C for 24 h in a metal block using open glass tubes provided very similar data by both methods (Figure 1) demonstrating that the direct headspace measurement can be performed without any interference of co-eluting compounds (*m/z* 57 and *m/z* 60; MS-CI). Further, it was observed that heating of oils containing higher levels of linolenic acid (rapeseed and linseed oil) resulted in the generation of significantly higher amounts of acrolein. The correlation of acrolein generation and linolenic acid concentration was also reported by da Silva and Pereira as well as Katragadda et al., who independently investigated acrolein emission rates during heating of various fats and oils (*12*, *13*). The considerable lower acrolein concentrations from coconut and olive oil may be explained by its high degree of saturated or mono-unsaturated fatty acids generally providing a higher stability vs. thermal oxidation.

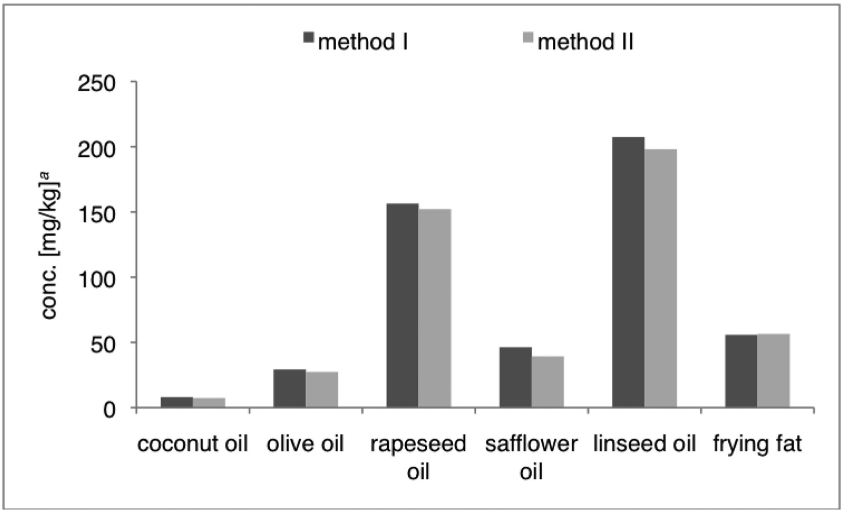

Figure 1. Comparison of acrolein concentrations in different oil samples after heating at 180 °C for 24 h (model system). [a]Mean values are based on two independent heat-processes.

In a further series of experiments, thin slices of potatoes were fried in these oils using a commercial deep-fryer. Afterwards, acrolein concentrations were quantified in the chips as well as in the frying medium. As shown in Table I, acrolein was detected in all chips samples, but compared to the heated oil samples (Figure 1), much lower acrolein concentrations were analyzed. Similar results were obtained for different frying mediums, e.g., 23.3 µg/kg for chips fried in rapeseed oil and 17.2 µg/kg for chips fried in a common frying fat. Thus, the type of frying medium seemed not to influence the acrolein generation in the chips in a significant way.

Table I. Generation of Acrolein in Potato Chips using Different Frying Mediums

chips prepared in	*acrolein conc. (µg/kg)*[a, b]
rapeseed oil	23.3 (22.0 – 24.9)
safflower oil	15.1 (13.3 – 17.9)
frying fat	17.2 (15.8 – 18.9)
commercial chips (sunflower oil)[c]	18.3 (16.9 – 19.7)

[a] Quantified by headspace GC-MS (method I). [b] Data are mean values of triplicates; concentration ranges in parenthesis. [c] For comparison.

The next series of frying experiments investigated the influence of heating time/number of frying cycles on acrolein formation in the frying oil. In contrast to chips, acrolein generation in oils after a certain number of frying cycles with potato slices was found to be highly influenced by the choice of oil. Similar to the results obtained for the model system (Figure 1), oils containing mainly saturated or mono-unsaturated fatty acids resulted in lower acrolein amounts of only 0.39 mg/kg (coconut oil) or 0.46 mg/kg (olive oil) after 9 frying cycles, respectively, whereas oils with a higher degree of unsaturation revealed amounts of 2.42 mg/kg (rapeseed oil) and 2.72 mg/kg (linseed oil), respectively (Figure 2). A prolonged time decreased the acrolein concentration of the oil gradually, e.g., in rapeseed oil from 4.31 mg/kg (3 frying cycles) to 2.42 mg/kg (9 frying cycles) (Figure 2). A possible explanation is the reaction of acrolein (or precursors of acrolein) with degradation products, which were formed during the frying process. Again, linseed and rapeseed oil generated the highest amounts of acrolein.

Further, it seemed that the free acrolein content was obviously lowered in the presence of a frying food. Oil samples heated under the same conditions, but without potato slices, showed much higher acrolein concentrations, e.g., 2.94 mg/kg in comparison to 0.65 mg/kg (with potato slices) for the frying fat or 7.72 mg/kg in comparison to 2.72 mg/kg (with potato slices) for linseed oil, respectively (Figure 2).

Downloaded by CORNELL UNIV on May 30, 2012 | http://pubs.acs.org
Publication Date (Web): May 29, 2012 | doi: 10.1021/bk-2012-1098.ch009

Downloaded by CORNELL UNIV on May 30, 2012 | http://pubs.acs.org
Publication Date (Web): May 29, 2012 | doi: 10.1021/bk-2012-1098.ch009

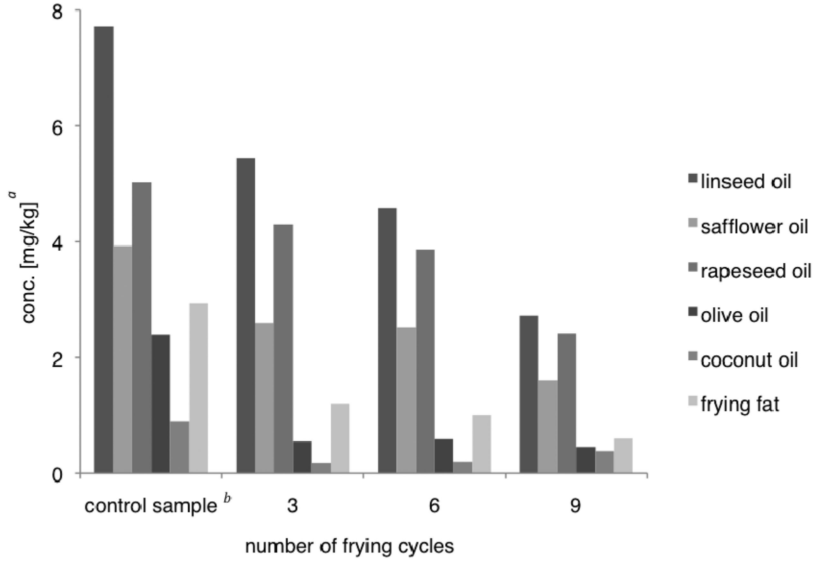

Figure 2. Concentrations of acrolein in different fats and oils after frying of potato chips affected by the number of frying cylces (analyzed by headspace GC-MS; method I). [a]*Mean values of triplicates.* [b]*Oil samples heated under similar frying conditions, but without any food.*

Generation of Key Aroma Compounds during Deep-Frying of Potato Chips

To investigate the impact of the frying medium on the generation of desirable odorants, several key aroma compounds of chips were quantified: (*E*,*E*)-2,4-decadienal, (*E*,*Z*)-2,4-decadienal, 2-ethyl-3,5-dimethylpyrazine, 2,3-diethyl-5-methylpyrazine, 3-ethyl-2,5-dimethylpyrazine as well as the *Strecker* aldehydes 2-methylbutanal, 3-methylbutanal, and 3-(methylthio)propionaldehyde. This selection was on the basis of detailed studies by Wagner and Grosch (*14*) about key aroma compounds in fried potatoes from. In Figure 3, a typical GC-MS chromatogram is exemplarily shown for the quantitation of (*E*,*E*)- and (*E*,*Z*)-2,4-decadienal in chips prepared in safflower oil using stable isotope dilution analysis (SIDA) .

In comparison to the other aroma compounds, the amount of generated (*E*,*E*)-2,4-decadienal and (*E*,*Z*)-2,4-decadienal was significantly influenced by the type of frying medium. A clear correlation between the total amount of linoleic acid (coconut oil < 1%; rapeseed oil ≈ 20%; safflower oil ≈ 80%) and the concentration of the generated 2,4-decadienals was present. Consequently, the concentrations in chips of (*E*,*E*)-2,4-decadienal were 347 µg/kg, 1354 µg/kg, and 3901 µg/kg as well as of (*E*,*Z*)-2,4-decadienal 56.1 µg/kg, 207 µg/kg, and 797 µg/kg prepared in coconut, rapeseed, and safflower oil, respectively. These results clearly indicated linoleic acid as precursor for (*E*,*E*)-2,4-decadienal, which was

Downloaded by CORNELL UNIV on May 30, 2012 | http://pubs.acs.org
Publication Date (Web): May 29, 2012 | doi: 10.1021/bk-2012-1098.ch009

already reported by Grosch (*15*). On the basis of the molecular sensory science concept, odor activity values (OAV; ratio of concentration of an odorant and its odor threshold) were exemplarily calculated for (*E*,*E*)-2,4-decadienal proving this odorant as an important contributor to the overall aroma of potato chips fried in rapeseed oil (OAV = 15) in contrast to chips prepared in coconut oil (AW = 1). The concentrations of the other key aroma compounds were not significantly influenced by different frying mediums (data not shown).

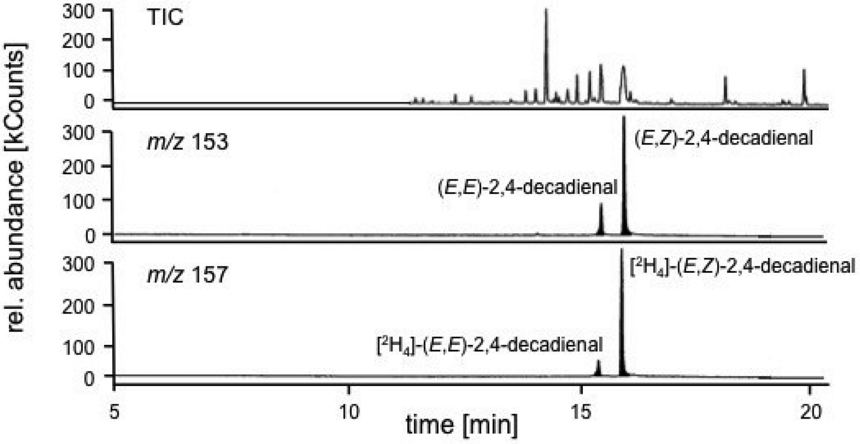

Figure 3. Mass chromatogram (MS-CI) for the quantitation of (E,E)-2,4-decadienal and (E,Z)-2,4-decadienal in potato chips using SIDA.

In summary, the results proved the successful application of the newly developed methods on the quantitation of acrolein in different frying oils as well as in fried potato chips. Furthermore, the data suggest that obviously linolenic acid is an important precursor for acrolein formation during heat-processing of oils. However, oils heated with potato slices generally yielded significant lower acrolein concentrations in the frying medium compared to oils heated without any frying food, independently from the type of frying oil. Regarding the key aroma compounds of chips, no evident influence of the type of frying medium was observed, except for (*E*,*E*)-2,4-decadienal and (*E*,*Z*)-2,4-decadienal, which both showed great differences in their concentrations depending on the frying medium and, therefore, on the resulting overall aroma. The results indicated that it will not be an easy challenge to reduce the amounts of undesirable food-borne toxicants, e.g., acrolein, without changing the usual concentration of desirable aroma-active compounds, e.g., (*E*,*E*)-2,4-decadienal, by replacing commonly used frying fats.

Downloaded by CORNELL UNIV on May 30, 2012 | http://pubs.acs.org
Publication Date (Web): May 29, 2012 | doi: 10.1021/bk-2012-1098.ch009

References

1. Li, L.; Holian, A. Acrolein: a respiratory toxin that suppresses pulmonary host defence. *Rev. Environ. Health* **1998**, *13*, 99–108.
2. *Health effects assessment for acrolein*. U.S. Environmental Protection Agency, Chicago, IL, 1987; EPA/600/8-88/013.
3. *IARC Monographs on the evaluation of carcinogenic risks to humans*. Vol. 1–102, 17.06.2011. (http://monographs.iarc.fr/ENG/Classification/ClassificationsAlphaOrder.pdf).
4. Kataoka, H.; Kondo, T.; Sumida, A. Gas chromatographic determination of aldehydes in combustion smoke samples. *Anal. Chim. Acta* **1998**, *358*, 269–275.
5. Singer, B. C.; Hodgson, A. T. Gas-phase organics in environmental tobacco smoke. 1. Effects of smoking rate, ventilation, and furnishing level on emission factors. *Environ. Sci. Technol.* **2002**, *5*, 846–853.
6. Gilbert, N. L.; Guay, M.; Miller, J. D.; Judek, S.; Chan, C. C.; Dales, R. E. Levels and determinants of formaldehyde, acetaldehyde, and acrolein in residential indoor air in Prince Edward Island, Canada. *Environ. Res.* **2005**, *99*, 11–17.
7. Fujisaki, M.; Mohri, S.; Endo, Y.; Fujimoto, K. The effect of oxygen concentration on oxidative deterioration in heated high-oleic safflower oil. *J. Am. Oil Chem. Soc.* **2000**, *77*, 231–234.
8. Fujisaki, M.; Endo, Y.; Fujimoto, K. Retardation of volatile aldehyde formation in the exhaust of frying oil by heating under low oxygen atmospheres. *J. Am. Oil Chem. Soc.* **2002**, *79*, 909–914.
9. Committee on Aldehydes. Health effects of some other aldehydes. In *Formaldehyde and other aldehydes*; National Research Council; National Academy Press: Washington, DC, 1981; p 18.
10. Engel, W.; Bahr, W.; Schieberle, P. Solvent assisted flavour evaporation – a new and versatile technique for the careful and direct isolation of aroma compounds from complex food matrices. *Eur. Food Res. Technol.* **1999**, *209*, 237–241.
11. Ewert, A.; Granvogl, M.; Schieberle, P. Development of two stable isotope dilution assays for the quantitation of acrolein in heat-processed fats. *J. Agric. Food Chem.* **2011**, *59*, 3582–3589.
12. Da Silva, T. O.; Pereira, P. A. Influence of time, surface-to-volume ratio, and heating process (continous or intermittent) on the emission rates of selected carbonyl compounds during thermal oxidation of palm and soybean oils. *J. Agric. Food Chem.* **2008**, *56*, 3129–3135.
13. Katragadda, H. R.; Fullana, A.; Sidhu, S.; Carbonell-Barrachina, A. A. Emissions of volatile aldehydes from heated cooking oils. *Food Chem.* **2010**, *120*, 59–65.
14. Wagner, R. K.; Grosch, W. Key odorants of French fries. *J. Am. Oil Chem.* **1998**, *75*, 1385–1392.
15. Grosch, W. New concepts of lipid oxidation. *Lebensmittelchem. Gerichtl. Chem.* **1984**, *38*, 81–87.

Downloaded by UNIV OF GUELPH LIBRARY on May 30, 2012 | http://pubs.acs.org
Publication Date (Web): May 29, 2012 | doi: 10.1021/bk-2012-1098.ch010

Chapter 10

Application of Two-Dimensional Orthogonal Reversed-Phase Liquid Chromatography for Taste Compound Analysis

Deshou Jiang,* Yuan Huang, and Devin G. Peterson

**Department of Food Science, University of Minnesota,
1334 Eckles Ave., Saint Paul, MN 16802
*E-mail: jiang295@umn.edu**

The discovery of taste compounds in foodstuffs is challenged by traditional one-dimensional liquid chromatographic techniques that have inadequate resolving power to facilitate identification of target analytes. The purpose of this study was to investigate the development and application of an off-line two-dimensional high pressure liquid chromatographic (2D HPLC) system for taste analysis. A simple geometric approach was applied to characterize the practical orthogonality of the analytical system for column selection. This mathematical prediction of resolving power correlated well with the experimental findings. A highly orthogonal 2D HPLC system was developed for the analysis of bitter compounds in whole wheat bread.

Introduction

Historically flavor analysis has focused mainly on volatile flavor compounds and consequently advancements in methodology for flavor research have largely involved techniques specific for volatile analytes. Because taste compounds are primarily viewed as non-volatile compounds that interact with taste receptors in the oral cavity, LC techniques are typically utilized for separation and analysis. Generally, taste analysis is considered more analytically challenging than volatile analysis for two main reasons. Firstly, there is no single LC/MS library as powerful as GC/MS in terms of identification. Secondly, LC is behind GC in terms of the practical resolving power. The lack of resolving power of traditional one dimensional LC for taste analysis becomes a limiting factor when dealing

In Recent Advances in the Analysis of Food and Flavors; Toth, S., et al.;
ACS Symposium Series; American Chemical Society: Washington, DC, 2012.

Downloaded by UNIV OF GUELPH LIBRARY on May 30, 2012 | http://pubs.acs.org
Publication Date (Web): May 29, 2012 | doi: 10.1021/bk-2012-1098.ch010

with complex materials such as food products for adequate separation to facilitate identification. Ideally LC techniques for the identification of 'taste-active' compounds should provide adequate resolution for separation and subsequent fractionation of the target compound.

The intrinsic separation power of a separation system can be characterized by the peak capacity. Peak capacity is defined as the maximum number of equally resolved peaks that can fit in the separation space (*1*). This value is a theoretical construct and should not be understood as practical maximum numbers of peak that separation systems can resolve. Since peak widths in gradient elution are more or less the same for all of peaks, Snyder defined peak capacity as the gradient time window divided by peak width (*2*). Typical peak capacities for one dimensional HPLC range from 20 to 400 (*3*), which is much lower than the number of components in a complex food sample or for that mater a simple Maillard reaction model system.

Two dimensional separation systems can dramatically increase the peak capacity. The ideal peak capacity is defined as the product of first dimensional peak capacity and second dimensional peak capacity. For example, when combining orthogonal columns with the peak capacities of 100 and 100, the resulting peak capacity for this 2D system will be 10,000. However, in reality, the practical peak capacity is also determined by their orthogonality (*4*) and can be mathematically derived as (*5*),

$$n^{*}_{p,2D} = {}^{1}n_c \times {}^{2}n_c \times f_{Coverage} \qquad (1)$$

Column selection is based on the 'predicted' analytes physico-chemical properties. For research on bitterness, most compounds of interest are considered to be relatively hydrophobic. Consequently, a RP-RP 2D system is a logical choice to develop an efficient separation system for bitter compounds analysis because the analytes need to be retained (albeit uniquely) by the RPLC columns for separation. In addition to phase selection, mobile phase conditions are also important considerations as co-eluted ionic compounds can often be resolved by a pH change in the second dimension; however, co-eluted neutral components represent a more challenging situation for RP-RP 2D separation systems. A column comparison function F_S(-C) has been developed by Snyder and Dolan in order to develop a suitable two-dimensional separation for neutral compounds (*6*). Bonus RP is considered to be one of the most orthogonal columns paired with conventional C18 column (*6*).

The objective of this study was to investigate the resolving power of a RP-RP 2D HPLC system utilizing two RP columns with pH modification (C18/Bonus-RP, mobile phase pH 2.8 and 5.0 for first and second dimension, respectively). A whole grain wheat bread crust extract was used as a sample in this paper. This HPLC system was directly compared to another 2D HPLC system without a Bonus-RP or pH modification (C18/C18 system at pH 2.8). C18/Bonus RP offline system was termed system A, while C18/C18 system was system B in the following sections.

Downloaded by UNIV OF GUELPH LIBRARY on May 30, 2012 | http://pubs.acs.org
Publication Date (Web): May 29, 2012 | doi: 10.1021/bk-2012-1098.ch010

Materials and Methods

Chemicals

All the chemicals were purchased from Sigma-Aldrich Co. (St Louis, MO). High performance liquid chromatography (HPLC) solvents were purchased from EMD Chemicals (Gibbstown, NJ). Whole grain bread extract was prepared according to Jiang and Peterson (*7*).

HPLC Analysis

A preparative HPLC system was used and consisted of: a binary pumping system (LC-8A), a manual injector (SIL-10vp), a column heater, a variable-wavelength UV-Vis detector 254 nm (Shimadzu, SPD-10A). The analytical HPLC system consisted of a binary pumping system (LC-10 ADvp), a in-line degasser (DGU-14A), an autosampler (SIL-10vp), a water column heater (TCM model, Waters), a variable-wavelength UV-Vis detector 254 nm) (Shimadzu, SPD-10A).

HPLC – First Dimension

The whole grain sample extract was taken up in a mixture (1/9; v/v) of methanol and aqueous formic acid (0.2%; pH 2.1), and aliquots (2ml) of sample were separated by HPLC using a preparative C18 column (150 mm×21.2 mm, pursuit 5, Varian, USA) at a flow rate of 20ml/min. Monitoring the effluent at 254 nm, chromatography was performed starting with a mixture (90/10, v/v) of aqueous formic acid (0.1%, pH 2.8) and methanol for 5 minutes, thereafter increasing the methanol content to 90% (linear gradient) within 15 min. The effluent was collected in 20 fractions with 0.75minutes per fraction (Fig 1). And all of these fractions were freeze-dried and the residues obtained were then taken up in a 2ml mixture of (1/9; v/v) of methanol and water then used for second dimensional separation in both systems.

HPLC – Second Dimension

The individual first dimensional HPLC fractions were further separated by one of two analytical columns a C18 column (pursuit 5, Varian, USA) or a polar embedded group column (Bonus-RP, Agilent, USA) with the same dimensions at 150×2.1mm. For system A, the mobile phase consisted of ammonium acetate (10mM, pH =5) as A and methanol as B; whereas for system B, the mobile phase consisted of formic acid (0.1%, pH 2.8) as A and methanol as B. Gradient for C18 started at 10% B, hold for 5 minutes and then increased to 50% B within 25 minutes with flow rate at 0.2ml/min. Gradient for Bonus-RP started at 0% B, hold for 5 minutes and then increased to 50% B within 25minutes with a flow rate at 0.2ml/min.

Downloaded by UNIV OF GUELPH LIBRARY on May 30, 2012 | http://pubs.acs.org
Publication Date (Web): May 29, 2012 | doi: 10.1021/bk-2012-1098.ch010

Data Analysis

Three-dimensional chromatograms were visualized using a home-coded Matlab program that contained peak detection algorithms.

Results and Discussion

The resolving power of chromatographic system A (C18/Bonus RP column combination, with pH modification) and system B (C18/C18 column combination, without pH modification) are illustrated in Figure 1. Comparison of the 3D plots easily reveals the enhanced resolving power of system A versus system B, indicating the high orthogonality of system A in comparison to system B. For system B, almost all of peaks are located at the diagonal of 2D HPLC separation space, which is typical of a separation system with low orthogonality; additional column length (a second column) did not provide a practical improvement in the resolution.

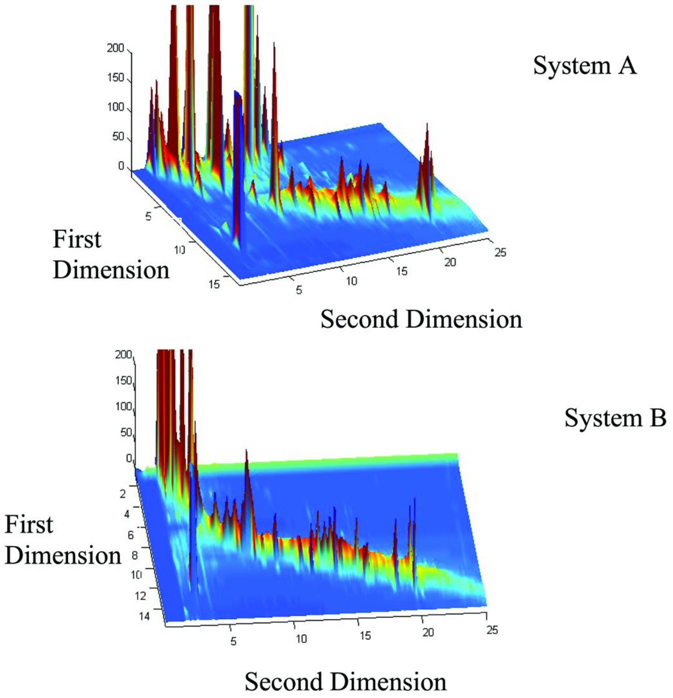

Figure 1. 3D 2D-HPLC chromatograms of whole grain bread crust from system A and B.

Downloaded by UNIV OF GUELPH LIBRARY on May 30, 2012 | http://pubs.acs.org
Publication Date (Web): May 29, 2012 | doi: 10.1021/bk-2012-1098.ch010

To further illustrate the enhanced resolving power of a 2D HPLC system with appropriate orthogonal column selection, the chromatograms from the second dimension obtained for the same fraction from the first dimension of each 2D HPLC system A and B are illustrated in Figure 2. System A reported at least seventeen peaks that were integrated in comparison to system B with only two main peaks observed.

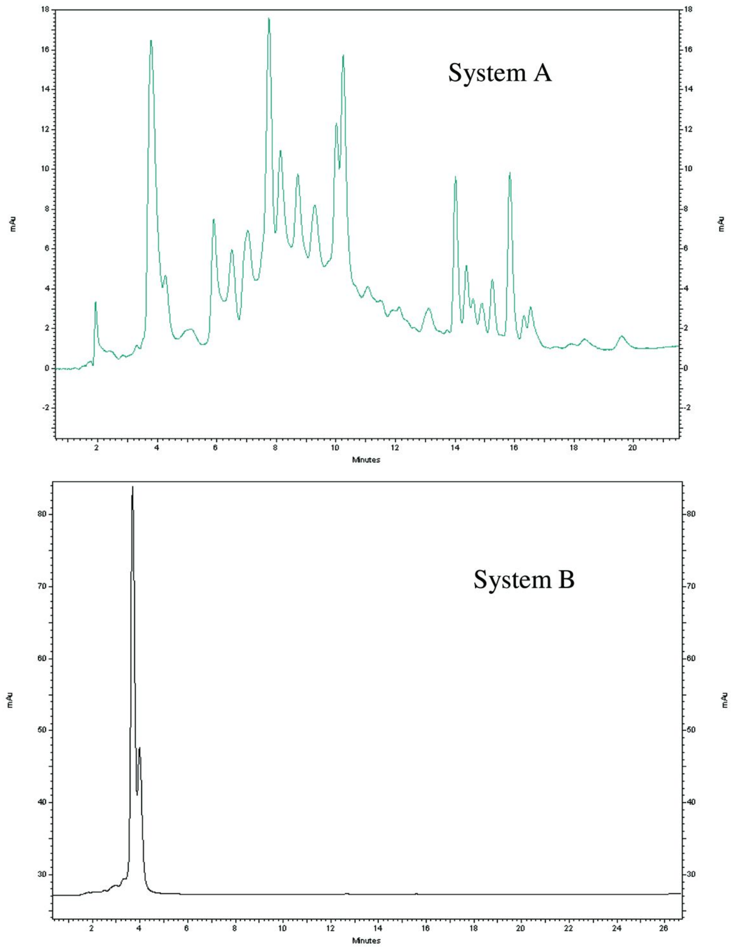

Figure 2. Second dimensional chromatogram of HPLC system A and B; same fraction analyzed from first dimension.

Downloaded by UNIV OF GUELPH LIBRARY on May 30, 2012 | http://pubs.acs.org
Publication Date (Web): May 29, 2012 | doi: 10.1021/bk-2012-1098.ch010

The difference in resolving power between these 2D LC systems can be attributed to orthogonal phase chemistry of the second column. The unique Bonus-RP column for system A consisted of an amide group embedded in a long alkyl chain. This column is a very good hydrogen acceptor, which enables the retention of more hydrophilic compounds with hydrogen bonding donor groups such as hydroxyl group and thiol group. These types of hydrogen bonding interaction provided unique analyte-column interactions in comparison to the C-18 phase.

The orthogonality and practical peak capacity of these 2D HPLC systems were further quantified by a simple geometric method (*5*). Both 2D separation spaces were equally separated into bins. The 'f coverage or f-c values', used to define orthogonality, were calculated based on the percentage of bins occupied by peaks. Occupied areas were highlighted in both systems as illustrated in Figure 3. For system A, out of 75 bins, 47 bins were included in the occupied region. Therefore, f value was calculated as 63%. Only 36% was obtained for system B. The peak capacity of each 2D HPLC system was also calculated according to Equation 1-5 listed below (*5*). Peak capacity of each dimension was calculated by occupied gradient time divided by average baseline peak width. These results also agreed with Dolan and Snyder (*6*) who indicated the Bonus-RP column is an orthogonal column when combined any conventional C18 column.

Equation 1 - Peak capacity for first dimensional separation

$$^{1}n_{c} = (t_{last} - t_{first})/W = (15\,\mathrm{min} - 0.89\,\mathrm{min})/0.75\,\mathrm{min} = 18$$

Equation 2 - Peak capacity for second dimensional separation of system A

$$^{1}n_{c} = (t_{last} - t_{first})/W = (25\,\mathrm{min} - 1.53\,\mathrm{min})/0.82\,\mathrm{min} = 29$$

Equation 3 - Peak capacity for second dimensional separation of system b

$$^{1}n_{c} = (t_{last} - t_{first})/W = (25\,\mathrm{min} - 0.89\,\mathrm{min})/0.75\,\mathrm{min} = 32$$

Equation 4 - Peak capacity for 2D System A

$$n^{*}_{p,2D} = {}^{1}n_{c} \times {}^{2}n_{c} \times f_{Coverage} = 18 \times 29 \times 0.63 = 329$$

Equation 5 - Peak capacity for 2D System B

$$n^{*}_{p,2D} = {}^{1}n_{c} \times {}^{2}n_{c} \times f_{Coverage} = 18 \times 32 \times 0.36 = 207$$

Downloaded by UNIV OF GUELPH LIBRARY on May 30, 2012 | http://pubs.acs.org
Publication Date (Web): May 29, 2012 | doi: 10.1021/bk-2012-1098.ch010

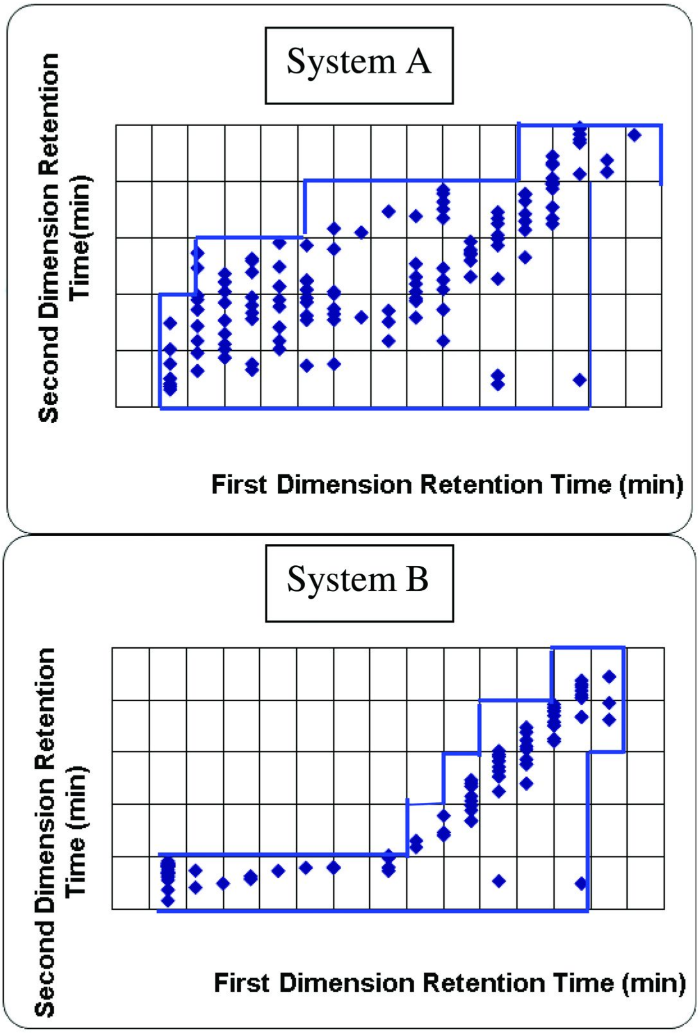

Figure 3. Peak distributions of the 2D HPLC System A and B.

In summary an orthogonal 2D HPLC system was developed for the analysis of bitter compounds in food. This chromatographic system was utilized in a subsequent study (*6*) and demonstrated the adequate resolution for the identification of bitter compounds in whole grain wheat bread curst.

Downloaded by UNIV OF GUELPH LIBRARY on May 30, 2012 | http://pubs.acs.org
Publication Date (Web): May 29, 2012 | doi: 10.1021/bk-2012-1098.ch010

References

1. Giddings, J. C. Maximum number of components resolvable by gel filtration and other elution chromatographic methods. *Anal. Chem.* **1967**, *39* (8), 1027–1028.
2. Dolan, J. W.; Snyder, L. R.; Djordjevic, N. M.; Hill, D. W.; Waeghe, T. J. Reversed-phase liquid chromatographic separation of complex samples by optimizing temperature and gradient time I. Peak capacity limitations. *J. Chromatogr., A* **1999**, *857* (1-2), 1–20.
3. Gilar, M.; Daly, A. E.; Kele, M.; Neue, U. D.; Gebler, J. C. Implications of column peak capacity on the separation of complex peptide mixtures in single-and two-dimensional high-performance liquid chromatography. *J. Chromatogr., A* **2004**, *1061* (2), 183–192.
4. Gilar, M.; Olivova, P.; Daly, A. E.; Gebler, J. C. Orthogonality of separation in two-dimensional liquid chromatography. *Anal. Chem.* **2005**, *77* (19), 6426–34.
5. Huang, Y.; Gu, H.; Filgueira, M.; Carr, P. W. An experimental study of sampling time effects on the resolving power of on-line two-dimensional high performance liquid chromatography. *J. Chromatogr., A* **1218** (20), 2984–94.
6. Dolan, J.; Snyder, L. Selecting an "orthogonal" column during high-performance liquid chromatographic method development for samples that may contain non-ionized solutes. *J. Chromatogr., A* **2009**, *1216* (16), 3467–3472.
7. Jiang, D.; Peterson, D. G. Charaterization of Bitter Compounds in Whole Wheat Bread: Strategies of Flavor Improvement. Submitted for publication.

Downloaded by STANFORD UNIV GREEN LIBR on May 30, 2012 | http://pubs.acs.org
Publication Date (Web): May 29, 2012 | doi: 10.1021/bk-2012-1098.ch011

Chapter 11

Anacardic Acid Profiling in Cashew Nuts by Direct Coupling of Preparative High-Speed Countercurrent Chromatography and Mass Spectrometry (*prep*HSCCC-ESI-/APCI-MS/MS)

Gerold Jerz,*,[1] Josué A. Murillo-Velásquez,[2] Irina Skrjabin,[1] Recep Gök,[1] and Peter Winterhalter[1]

[1]Institute of Food Chemistry, Technische Universität Braunschweig, Schleinitzstrasse 20, 38106 Braunschweig, Germany
[2]Universidad De El Salvador, Escuela de Química, El Salvador
***E-mail: g.jerz@tu-bs.de. Fax: +49-531-3917230**

In many subtropical and tropical countries the cashew nut production (*Anacardium occidentale* L., Anacardiaceae) is a valuable food crop and of high agroeconomical interest. Anacardic acids are phenolic lipids which have shown a wide spectrum of biological effects, such as antibacterial, and anti-tumor activities. In this preparative separation experiment *high-speed countercurrent chromatography* (HSCCC) was directly coupled to an electrospray and atmospheric pressure chemical ionization mass spectrometry device (*prep*HSCCC/ESI-APCI-MS-MS) and used as a metabolic profiling tool to investigate commercial cashew nuts for the occurrence and semiquantitative measurement of different anacardic acids. Immediate structural data were retrieved throughout the countercurrent chromatographic run. For higher and lower concentrated compounds all molecular ion signals and complete MS/MS-fragmentation data of anacardic acids were obtained. Twenty anacardic acids in the mass range between *m/z* 163 and *m/z* 657 were detected. Co-elution effects were monitored by selective mass traces and detection of novel minor concentrated anacardic acids with even numbered

In Recent Advances in the Analysis of Food and Flavors; Toth, S., et al.;
ACS Symposium Series; American Chemical Society: Washington, DC, 2012.

alkyl chains was achieved. Tentatative structures of novel dicarboxylic- and one dimeric anacardic acids will be presented.

Downloaded by STANFORD UNIV GREEN LIBR on May 30, 2012 | http://pubs.acs.org
Publication Date (Web): May 29, 2012 | doi: 10.1021/bk-2012-1098.ch011

Most of the known plant polyphenols are generally not recognized to cause any toxic effects to human health. Nevertheless, there are some highly bioactive and potentially cytotoxic phenolic lipids, such as alkyl-resorcinols, and alkyl-salicylates which are chemotaxonomical markers for the plant family Anacardiaceae (*1*). One important representative for human nutrition is the popular cashew nut (*Anacardium occidentale* L.) frequently consumed in large amounts, as well as cashew fruits (mainly used for juices, jams, chutneys). All cashew products are commerciall important agricultural crops grown in sub-tropical and tropical regions of the world, with main production in Brazil, India and Vietnam (*2*, *3*).

In this study a preparative metabolite profiling using HSCCC with on-line coupling to ESI-/ and -APCI-MS/MS was performed in order to monitor the occurrence of anacardic acids, so far not sufficiently documented in cashew nuts. These phenolic lipids are 6-alkyl substituted salicylic acids with differing chain lengths and degree of unsaturation (saturated, mono-enoic, di-enoic, tri-enoic) having isolated *cis*-configured double bonds (DB). Up to now, these phenolic acids with a certain lipid character had been identified in *Anacardium occidentale* with C-13, C-15, and C-17 alkyl-chain lengths (*4*, *5*).

Since the 1950s, cashew nut shell oil liquid (CNSL) was used as a rich source for anacardic acid recovery applied in industrial processes. Also, various interesting biological activity profiles had been found by *in-vitro* screenings. Out of these properties, the anti-tumor (breast cancer BT-20-, HeLa-cells) (*6*), and also antibacterial activities of anacardic acids such as against methicillin-resistant *Staphylococcus aureus* (MRSA) (*7–12*), and against the pathogene *Helicobacter pylori* - responsible for upper gastrointestinal tract infections - should be mentioned (*13*, *14*).

In recent literature, some promising aspects of using anacardic acids as naturally grown therapeutics for the potential treatment of so-called '*neglected diseases'*, such as the tropical protozoan related infections Chagas Disease (*Trypanosoma cruzi*) (*15*, *16*), Leishmaniosis (*Leishmania* sp.) (*17–19*), and Malaria (*Plasmodium falciparum*) were documented (*20*). The anacardic acid bioactivities seem to be strongly related to the amphiphilic character (polar phenol 'head-group' – lipophilic alkyl 'side-chain') causing protein-interactions, and membrane-disruptions (*21*).

In the presented study, *Countercurrent Chromatography* (CCC) was used as a very efficient preparative separation methodology to fractionate the complex anacardic acid metabolite profile occurring in cashew nuts. These phenolic lipids are characterized by very similar polarity properties, and would require multi-step conventional solid phase chromatographic separation steps. CCC-devices are operated with immiscible biphasic solvent systems and omit undesired chemisorptive effects of analytes. A large number of already evaluated solvent mixtures generating two-phase systems can be applied (*22*, *23*). The mode of separation during CCC can be explained by fast mixing and settling processes of the sample analytes in a rapidly changing centrifugal force field which will be generated by a so-called J-type centrifuge with serially connected coil columns rotating in a planetary-type system. Principally, the used separation columns are very long Teflon tubes wrapped around these rotating coil-bobbins. Further detailed informations about CCC techniques are available in literature (*23*).

Time efficiency, economic aspects and the use of environmental friendly solvents are a large issue in todays natural product recovery and could enforce the search for novel pharmaceutical leads and target substances. Purifcations in the range of 500 mg – 1000 g can be accomplished by low- and larger scale CCC-equipments (*24*, *25*).

To monitor the elution of components we coupled the HSCCC device directly to the mass spectrometer with ESI-, and APCI-ion desolvation unit (*prep*HSCCC-ESI-/APCI-MS/MS) (cf. Figure 1). This preparative approach was first performed for the detection of polyphenols in sea buckthorn juice (*26*). Since then, various natural product separations using preparative HSCCC (*27–32*), and centrifugal partioning chromatography (CPC) with MS-detection have been published (*33*).

Preparative HSCCC with ESI- and APCI-MS/MS detection displaying selected single ion-traces (Figure 2A.-D.), visualize strongly overlaid and co-eluting compound peaks. Hence, specific compounds can still be recognized in complex matrices (*target-guided*-screening). Therefore, this methodology is a valuable tool in the field of preparative natural product isolation and for immediate on-line structure elucidation approaches.

Downloaded by STANFORD UNIV GREEN LIBR on May 30, 2012 | http://pubs.acs.org
Publication Date (Web): May 29, 2012 | doi: 10.1021/bk-2012-1098.ch011

Experimental Procedure

Extraction Process

White cashew nuts (slightly roasted, organic quality, 500 g, Neuform company, Germany) were blended in a lab-mixer and extracted 3 times with a mixture of *n*-hexane and acetonitrile (1:1 v/v). In the first step, the extracts were filtered through a cheese cloth and then finally through a paper filter. After pooling of extracts, organic solvents were removed in vacuo. Final lyophilisation yielded 70 g of oil extract. The solvent mixture was chosen for extraction due to excellent solubility of anacardic acids and the later use as specific biphasic solvent system for preparative HSCCC with the already evaluated good detection properties for ESI- and APCI-MS.

Experimental of HSCCC-ESI-/APCI-MS/MS

The preparative HSCCC instrument was a multilayer coil planet centrifuge model CCC 1000 (Pharma-Tech Research Corp., U.S.A.), equipped with three preparative coil columns connected in series (polytetrafluorethylene (PTFE) tubing-volume: 850 mL). A manual sample injection valve with a 25 mL loop was used to introduce the sample into the coil system. The mobile phase was delivered with a Biotronik BT 3020 HPLC pump (Jasco, Grossumstadt, Germany) (for details of the HSCCC apparatus cf. (*34*)).

In Recent Advances in the Analysis of Food and Flavors; Toth, S., et al.;
ACS Symposium Series; American Chemical Society: Washington, DC, 2012.

Downloaded by STANFORD UNIV GREEN LIBR on May 30, 2012 | http://pubs.acs.org
Publication Date (Web): May 29, 2012 | doi: 10.1021/bk-2012-1098.ch011

For the preparative experiment, 500 mg of the *n*-hexane/acetonitrile crude extract of cashew nuts was re-dissolved in the system *n*-hexane - acetonitrile (1:1 *v/v*) and injected to the countercurrent chromatographic system.

The experimental set-up of the HSCCC/ESI-/APCI-MS-MS hyphenation is presented in Figure 1. The continuous acquisition of mass spectrometric data was done by using a LC-MS ion trap multiple mass-spectrometer (Bruker Daltonics, Bremen, Germany) and negative ionization mode analyzed ions from *m/z* 100 to 2000 using ESI-, and APCI-desolvation units, respectively.

The CCC-equipment was operated in the '*head-to-tail*' mode using the upper solvent layer as the stationary phase. The mobile phase was pumped at a flow rate of 3.0 mL/min, and rotation velocity of the centrifuge coil rotor was set to 1000 rpm. After passing through a UV/Vis detector (λ 210 nm, chromatogram not presented here), the eluate was directed to a variable low pressure micro-splitter valve (UpChurch Scientific®, Oak Harbour, WA, U.S.A.) where a split ratio of 1 : 600 was adjusted. The divided micro flow rate of 5 µL/min was guided to the ESI-MS/MS interface during the *elution* mode of chromatography. The main effluent stream with separated compounds was collected in the test tubes of the fraction collector. For the *extrusion* mode (sequential recovery of the separated compounds from the coil-system) the ion-source was changed to an APCI-desolvation unit, stationary phase (*n*-hexane) was pumped with 6.0 mL/min flow rate, and spinning velocity of the HSCCC centrifuge was 700 rpm.

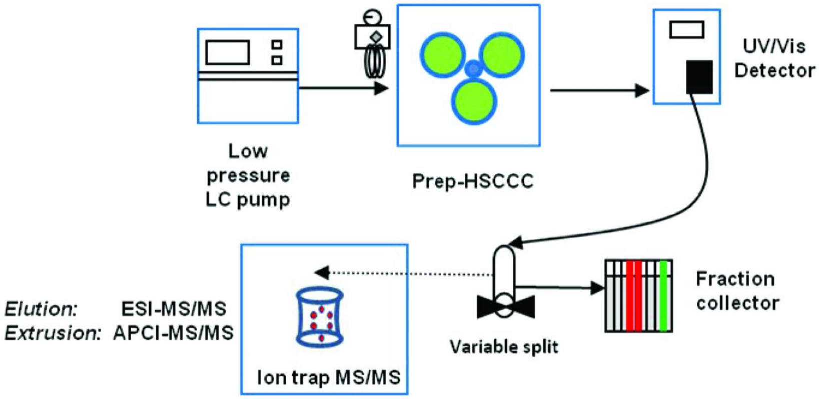

Figure 1. Schematic diagram of the preparative HSCCC instrument (850 mL coil volume) coupled to ESI-/APCI-MS/MS ion trap multiple mass-spectrometer. Negative ionization mode for ion detection: scan range m/z 100-2000.

HSCCC-*elution* mode ESI-MS-MS parameters: drying gas was nitrogen (flow 5.0 L min^{-1}, 310 °C), and nebulizer pressure was set to 8 psi. ESI-MS-MS parameters (neg. mode): capillary +3700 V, end plate +3200 V, capillary exit -113 V, skim 1 -38 V, trap drive 58.0, target mass range *m/z* 500, compound stability 100%, trap drive level 120%, ICC target 50000, max. accumulation time 200 ms, charge control on, threshold auto MS/MS 500, MS/MS experiments afforded a fragmentation amplitude value of 1.2 V.

Detection of components during the *extrusion* process with *n*-hexane and potentially more lipophilic components was done by the exchange to an APCI-MS interface. HSCCC-*extrusion* mode APCI-MS/MS (only differing parameters to ESI are presented): drying gas (flow 3.0 L min^{-1}, 350°C), APCI temperature 400°C, nebulizer pressure 5 psi. APCI-MS-MS parameters (neg. mode): capillary +900 V, end plate +400 V, capillary exit -107 V, skim 1 -34 V, trap drive 55.0.

During the hyphenation experiment (chromatographic *elution* and *extrusion*), the continuous isolation of five precursor ions was achieved and resulted in the recovery of MS/MS fragmentation data of all co-eluting compounds. In case of already *in-source* ESI generated fragment ions of anacardic acids, the MS-MS mode delivered also the stage MS^3 fragmentations of these compounds.

The collected HSCCC fractions were combined according to the collected on-line MS results and were dried in a SpeedVac (ThermoSavant SC210 A, U.S.A.) for recovery of the separated anacardic acids and gravimetric calculation.

Downloaded by STANFORD UNIV GREEN LIBR on May 30, 2012 | http://pubs.acs.org
Publication Date (Web): May 29, 2012 | doi: 10.1021/bk-2012-1098.ch011

Results and Discussion

Separation and Structure Elucidation of Anacardic Acids from Cashew Nuts

In the past, various investigations dealt with the mass-spectrometrical identification of anacardic acids, and structurally related compounds such as cardanols, and cardols from CNSL using electron impact (EI-MS, 70eV), and electrospray techniques (CE-ESI-TOF-MS/MS) (*4*, *35*).

For the *on-line* coupling of preparative HSCCC with ESI-MS/MS and direct monitoring of the eluting components from the coil-column system, the negative ionization mode was applied for the chromatographic *elution* and APCI detection was used for the *extrusion* section (cf. Fig 2., 3.). All acquired mass-spectrometrical data of the presented structures were measured in *on-line* mode during the preparative HSCCC separation (cf. Figure 2A.-D.).

The negative ionization polarity guaranteed best detection sensitivities for the phenolic lipids resulting in abundant [M-H]$^-$ quasimolecular ion signals and daughter fragment ions [M-44]$^-$ from the cleavage of CO_2 from the phenolic carboxyl group. The observed ion abundancies for further fragmentations in the alkyl/ alkenyl chains were rather small, and locations of double bonds cannot be clearly elucidated due to induced double bond migrations during ESI-MS-ionization.

C15-Chain Anacardic Acids (Main Phenolic Lipids in Cashew Nuts)

The preparative coupling of HSCCC and ESI-MS/MS delivered all mass-spectrometrical data (MS, MS^2, and MS^3-signals) of the typical major concentrated C15-chain anacardic acids by extraction of selected and specific molecular ion traces (**7**: *m/z* 341, 3 DB; **8**: *m/z* 343, 2 DB; **9**: 345, 1 DB; **10**: *m/z* 347, 0 DB) (cf. Figure 2A., Table I). Anacardic acids as phenolic lipids are well documented in literature (*21*). (*Abbreviation: 'double bond'* = DB)

Downloaded by STANFORD UNIV GREEN LIBR on May 30, 2012 | http://pubs.acs.org
Publication Date (Web): May 29, 2012 | doi: 10.1021/bk-2012-1098.ch011

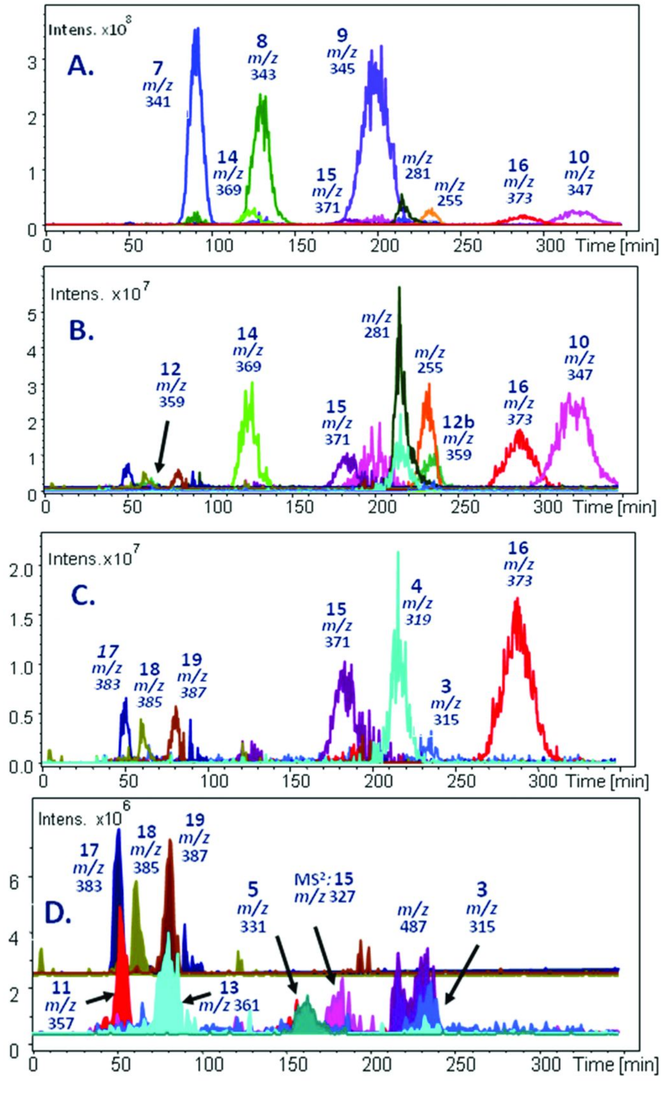

*Figure 2. prepHSCCC-ESI-MS data (elution mode): injection amount 500 mg. **A:** Base peak chromatogram (neg. ESI-MS mode resulting in $[M-H]^-$ signals, scan-range: m/z 100-2000) with major concentrated anacardic acids in cashew nuts and selected single ion traces m/z 341 (**7**), m/z 343 (**8**) and m/z 345 (**9**) (structures cf. Figure 4). **B and C:** minor concentrated anacardic acids; **D:** very minor concentrated anacardic acids (peak signals smoothened with Gaussian function).*

Our 1D-NMR spectroscopy data confirmed isolated double bonds in *cis*-configuration for the mono-enoic, di-enoic and tri-enoic alkyl chains in anacardic acids. Previously, these pure compounds were isolated from CNSL (data not presented here). In case of 7, NMR showed an overlapped ^{1}H-signal (δ_H: 5.35 ppm, *m*, 4H, *J* ~5Hz) with a small coupling constant and indicated the *cis*-double bonds and also an additional exomethylene-function. Also the $^{2,3}J$-CH-long range correlation signals (HMBC) unambiguously confirmed the constitution of **7**. Respective ESI-MS-MS fragmentation data of **7 - 10** are given in Table I. All these phenolic lipids with carboxyl-functions had presented under ESI-condititions already *in-source* MS-fragmentations leading to indicative neutral loss fragment-ions ([M-H-44]$^-$) due to the cleavage of CO$_2$. These already stage MS^2 signals (indentical to molecular weights of respective cardanols) were automatically isolated and fragmented during the coupling experiment by the ion-trap MS deector and delivered indirectly MS^3-data of anacardic acids **7-10** (cf. Table I).

Interestingly, the phenolic acid lipids **7-10** were completely base-line separated by the HSCCC approach without the use of acidic solvent modifiers (cf. Figure 2A.). Polarity and retention times seemed to be highly influenced by the amount of *cis*-configured double bonds in the alkyl chain of the anacardic acids. Slightly differing compound polarities could not explain the excellent separation results. A proposed mechanism for the elution order of the anacardic acids will be discussed in a separate section. The detected ions at *m/z* 281 and *m/z* 255 were interpreted as free oleic- and palmitic- acid, respectively (cf. Figure 2B.).

The ESI-MS, and MS/MS identified compounds **7-10** were directly recovered from the respective tubes of the fraction collector for a gravimetric quantification. Basis of the calculation was the cashew nut weight for extraction, the total amount of resulting oily extract, the injection amount to HSCCC (cf. Exp.) and this resulted in the concentration values for the anacardic acids and are in accordance with literature data: **7** (1.3 mg, 318 ppm), **8** (0.9 mg, 221 ppm), **9** (0.1 mg, 24 ppm), **10** (1.7 mg, 416 ppm) (*35*). The total amount of anacardic acids in cashew nuts can be estimated to be about 800-1000 ppm including the lower concentrated substances (cf. Figure 4).

For differing geoclimatical origins and existing diversities of *Anacardium occidentale* varieties, anacardic acid contents may be a variable. In the respective mass-traces, the observed ion intesities do not reflect the real anacardic acid concentrations in the measured extract. Obviously, the specific ion-responses are also dependent on the amount of unsaturated positions in the alkyl chain. Therefore, purified and identified anacardic acids from the HSCCC-MS approach can be used as authentic reference materials for substance quantifications by LC-ESI-MS analysis.

Various ginkgolic acids occurring in *Ginkgo biloba* leaves (used for tea infusions), and the respective extracts (food additives) are structurally identical or similar to known anacardic acids from cashew material. In the case of pharmaceutically used *Ginkgo biloba* extracts, the group of ginkgolic acids was classified as toxic and a maximum content of 5 ppm ginkgolic acids had been established (*36*). This safety value seemed to be originated from toxicological and technological issues but will be largely overrun by the consumption of cashew nuts containing anacardic acids as shown here (approx. 800-1000 ppm).

Downloaded by STANFORD UNIV GREEN LIBR on May 30, 2012 | http://pubs.acs.org
Publication Date (Web): May 29, 2012 | doi: 10.1021/bk-2012-1098.ch011

Downloaded by STANFORD UNIV GREEN LIBR on May 30, 2012 | http://pubs.acs.org
Publication Date (Web): May 29, 2012 | doi: 10.1021/bk-2012-1098.ch011

C17-Chain Anacardic Acids (Minor Phenolic Lipids in Cashew Nuts)

The HSCCC-ESI-MS run also detected lower concentrated anacardic acids with a C17-chain in cashew nuts, which were only decribed as part of the cashew nut shell oil liquid (*4*, *5*). The selected ion traces for **14**-**16** were recognized by a mass value increase of Δ*m/z* 28 indicating two additional methylene-groups in the alkyl/alkenyl chains (cf. Figure 2B.-C., amplified ESI-MS traces). The chain extensions resulted in increased lipophilic chromatographic characteristics and moved the components to longer retention times during the HSCCC run. As observed for **7**-**10**, a complete base-line separation for C17- structures was also achieved. The MS^2-, and MS^3-signals confirmed the C17-chain anacardic acids with the respective selected precursor MS-ion traces (**14**:*m/z* 369, 3 DB; **15**: *m/z* 371, 2 DB; **16**: *m/z* 373, 1 DB). The anacardic acid with a complete saturation in the alkyl chain - theoretically expected with [M-H]- at *m/z* 375 (0 DB) – and known for CNSL oil was not present in the cashew nuts.

The observed MS^3 fragment-ion pattern generated from the ESI *in-source* MS^2 fragment ions appeared to be very similar to the MS^3 spectra of the C15 compounds **7**-**10** (cf. Table I). Soley, in the higher mass area different fragment ions occurred. The structures given in Figure 4 are tentative, so far 1D/2D-NMR data are not available. Therefore we can only assume that the positions of the double bonds are as presented and that in case of **14** an exomethylene-double bond function is present similar to compound **7**.

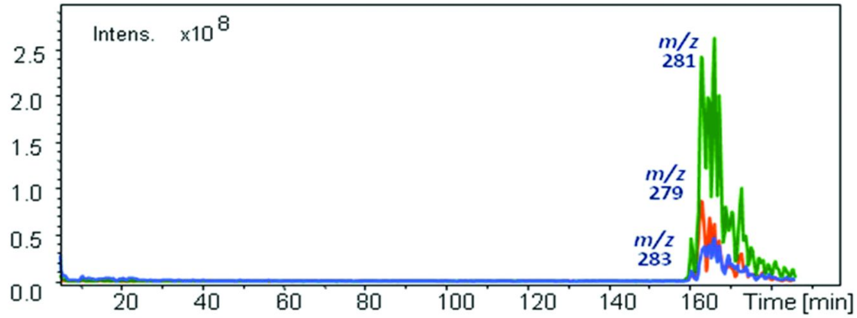

Figure 3. Base peak chromatogram of the HSCCC-extrusion with negative APCI mode and $[M-H]^-$ signals: scan-range: m/z 100-2000. Triacylglycerides were detected as molecular ion signals of free fatty acids as direct in-source APCI-fragments: m/z 279 (linoleneic acid), m/z 281 (linolic acid), m/z 283 (oleic acid) (ion-traces smoothened with Gaussian function).

Overlaid selective ESI-mass traces of C15- and C17 compounds revealed partly strong co-elution effects (cf. Figure 2A.-B.) such as for the pairs **8** (C15, 2 DB) and **14** (C17, 3 DB), as well as for **9** (C15, 1DB) and **15** (C17, 2 DB). As observed for C15-compounds, the identical elution sequence was seen as for the C17 derivatives that an increasing number of cis-double bonds led to shorter retention times (R_t: **14** < **15** < **16**). Hence, the lipophilic effect of an additional methylene-group in the chain (C17) has been completely compensated by the presence of an additional *cis*-double bond in the chain.

Here, the clear advantage of a preparative coupling of HSCCC and MS became obvious. Chromatographic co-elution effects can be visualized by selected MS-traces and fractionation of pure targets is achieveable in a more precise way, and further clean-up procedures can be omitted.

The search for calculated ESI-MS ion traces of suspected C19-type anacardic acids at *m/z* 397 (3 DB), *m/z* 399 (2 DB), *m/z* 401 (1 DB), *m/z* 403 (0 DB) was negative for cashew nuts.

In respect of bioactivity, anacardic acid **16** had been isolated and characterized before from *Viola websteri* (Violaceae) as one of the anti-malaria principles showing activity against chlorquine-sensitve *Plasmodium falciparum* (*20*).

Anacardic Acids with C2-, C5-, C13-, C14-, C16-Alkyl/Alkenyl-Functionalities (Trace Phenolic Lipids)

The anacardic acid with the highest polarity eluting first from the HSCCC system and also showing a strong chromatographic broadening was detected by the selective ESI-MS mass trace at *m/z* 163 ($[M-H]^-$). The neutral loss of Δ*m/z* 44 (cleavage of CO_2) leading to ion *m/z* 119 corroborated our structural suggestion of a vinyl-substituted salicylic acid **1**. This assigned compound could be a very reactive species as known from vinyl-substituted polyphenols.

For the anacardic acid **2** at *m/z* 205, two neutral loss cleavages were observed, first with Δ*m/z* 42 (allyl-fragmentation), and second with Δ*m/z* 44 leading to *m/z* 119 as observed for component **1** (cf. Table I, Figure 4). For anacardic acid **2** we proposed a C5-chain at the salicylic acid backbone, and an exomethylene double bond.

The structural proposals for C13-type anacardic acids were made on the basis of molecular ion signals at *m/z* 315 (2 DB) **3,** and *m/z* 319 (0 DB) **4** and MS-MS fragmentation (cf. Figure 4, Table I). C13-type anacardic acids were isolated before from *Pistacia vera* nuts (*37*).

In the same manner two C14- and three C16 anacardic acids were recognized by $[M-H]^-$ at *m/z* 331 (1DB) **5**, and *m/z* 333 (0 DB) **6**, and three C16-anacardic acids were detected at *m/z* 357 (2 DB) **11** , *m/z* 359 (1 DB) **12**, *m/z* 361 (0 DB) **13** including the characteristic neutral loss cleavages of Δ*m/z* 44 for carboxyl functions (cf. Figure 2D.).

Additionally to the C16-type compound **12** (retention time window of 50-80 min), surprisingly another ion peak with the same $[M-H]^-$ -signal occurred at *m/z* 359 of much higher ion abundancy (R_t ~236 min) (cf. Figure 2B.). In this case we postulated for compound **12b** (also Δ*m/z*44 cleavage) a single *trans*-configured double bond, and therefore a stonger affinity to the stationary phase or teflon tube material. To the best of our knowledge the tentative structures **1**-**6** and **11**-**13** with the detected molecular weights are indicating novel natural products for cashew material. Detailed 1D/2D-NMR data, still have to be acquired for structural confirmation.

Downloaded by STANFORD UNIV GREEN LIBR on May 30, 2012 | http://pubs.acs.org
Publication Date (Web): May 29, 2012 | doi: 10.1021/bk-2012-1098.ch011

Dicarboxy-Substituted C15 Anacardic Acids (Trace Constituents)

Shortly, after the so-called countercurrent chromatographic *break-through* of mobile phase (R_t ~35min) (cf. Figure 2C.-D.), three polar and so far not known minor concentrated C15 anacardic acids were detected by their selected ion traces $[M-H]^-$: *m/z* 383 (4 DB) (**17**), *m/z* 385 (3 DB) (**18**), and *m/z* 387 (2 DB) (**19**) (cf. Figure 4, cf. Table I). All compounds revealed the neutral loss of Δ*m/z* 44 with the respective abundant fragment ions indicating the cleavage of CO_2 originated from a carboxyl-functions. In case of substance **18** the MS-MS cleavage showed fragment ion *m/z* 341 identical to the detected molecular weight of **7**, in case of **19** resulted the ion *m/z* 343 indicative for **8**.

The MS-MS fragmentation of anacardic acid **17** resulted in *m/z* 339 where we had postulated an anacardic acid backbone with four double bonds, so far not seen in cashew material. In the MS-MS spectras of **17**-**19** also low abundant fragment ions were visible indicating the loss of a second carboxyl-function, respectively (cf. Table I). Tentative structural assignments are presented in Figure 4, nevertheless by means of ESI-MS-MS the substitution pattern and the location of the additional carboxyl-functions at the phenol-system cannot be determined. Larger amounts of **17**-**19** have to be isolated to investigate the substitution pattern by $^1H/^1H$-couplings in the phenol ring by NMR spectroscopy. The concentrations of the dicarboxy-substituted anacardic acids **17**-**19** are much lower than the principal components of the type C15-alkyl-/alkenyl (cf. Figure 2, ESI-MS detection abundancies) in cashew nuts. Assuming the lower retention time of **17** on the HSCCC coil system, the additional double bond is most likely to be in a *cis*-configuration. The position of double bonds cannot be safely derived from MS-MS data. ESI-MS conditions (soft ionization) still seemed to induce double-bond migrations and not clear fragment ion differences for the aliphatic chain cleavages resulted (cf. Table I). For absolute classification of double bond locations, the dimethyldisulfide/ I_2-derivatization would yield the respective di-thio-ethers which then result in exact EI-MS fragmentions thus allowing determination of the double bond locations (*38*).

Anacardic Acid Dimer – Tentative Structure by ESI-MS-MS

Compound **20** eluted very early during the *prep*HSCCC-ESI-MS coupling (cf. Figure 5, R_t 45 min). The direct ESI-MS and-MS-MS data revealed a dimeric structure of two different anacardic acids. The MS-MS fragmentation of the molecular ion peak $[M-H]^-$ at *m/z* 657 (**20**) resulted in the most abundant daughter ion at *m/z* 613 (int. 100%) showing a neutral loss of Δ*m/z* 44 (cleavage CO_2) from a carboxyl group (cf. Figure 4). The second neutral loss Δ*m/z* 44 to *m/z* 569 of much smaller ion intensity indicated the existence of an additional acidic function. A dimeric nature of **20** consisted of two different anacardic acids which was supported by the neutral loss of Δ*m/z* 344, and also a fragment ion at *m/z* 343 giving the idea of an anacardic acid moiety such as for substance **8** (C15 alk-dienyl chain). Fragment ion at *m/z* 313, and a respective neutral loss cleavage of Δ*m/z* 314 ($[M-343]^-$) indicated an anacardic acid with an C13 alk-dienyl chain (cf. substance **3**).

Downloaded by STANFORD UNIV GREEN LIBR on May 30, 2012 | http://pubs.acs.org
Publication Date (Web): May 29, 2012 | doi: 10.1021/bk-2012-1098.ch011

Downloaded by STANFORD UNIV GREEN LIBR on May 30, 2012 | http://pubs.acs.org
Publication Date (Web): May 29, 2012 | doi: 10.1021/bk-2012-1098.ch011

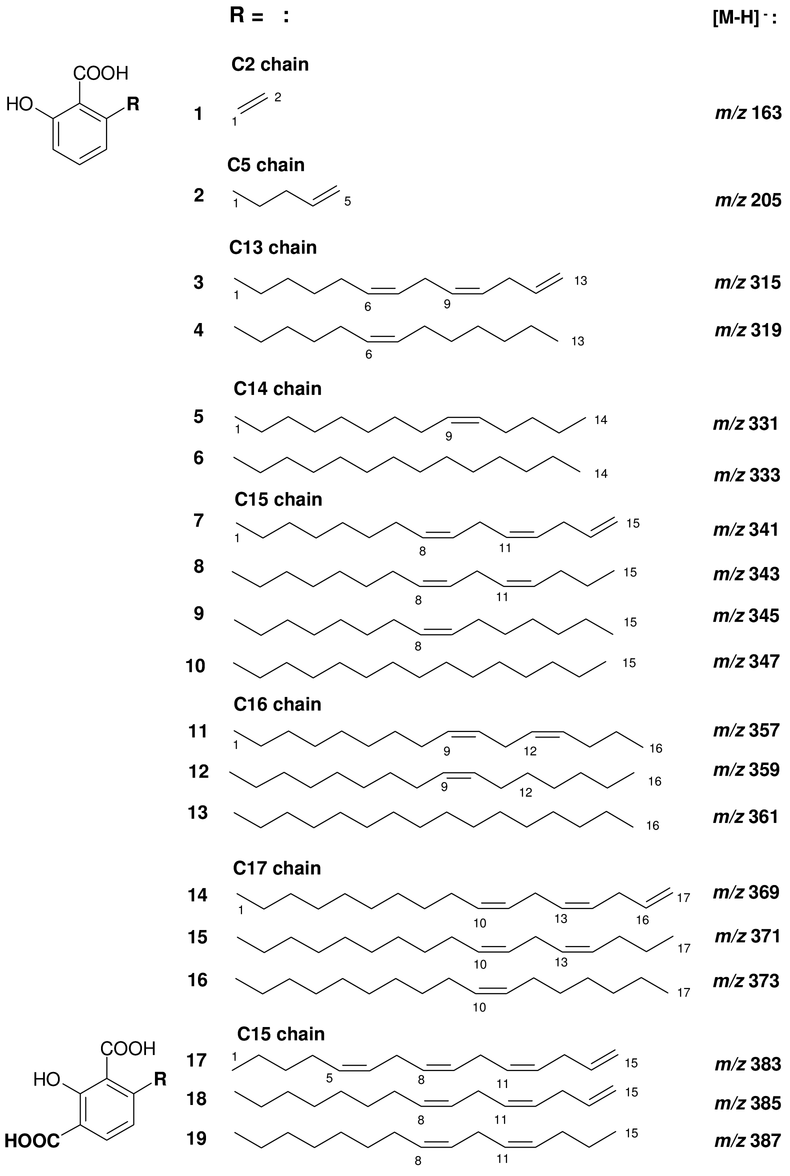
R = :
[M-H]⁻:
COOH
HO
R
C2 chain
1
m/z 163
C5 chain
2
m/z 205
C13 chain
3
m/z 315
4
m/z 319
C14 chain
5
m/z 331
6
m/z 333
C15 chain
7
m/z 341
8
m/z 343
9
m/z 345
10
m/z 347
C16 chain
11
m/z 357
12
m/z 359
13
m/z 361
C17 chain
14
m/z 369
15
m/z 371
16
m/z 373
C15 chain
COOH
HO
R
HOOC
17
m/z 383
18
m/z 385
19
m/z 387

*Figure 4. Tentatively assigned anacardic acid structures **1-19** detected by direct coupling of preparative HSCCC-ESI-MS/M presented with increasing molecular weigths and carbon numbers in the alkyl/ alkenyl-chains.*

Noticing two CO_2-exits, we assumed that the carboxyl groups should exist in non-esterified form, and hence a linkage between the phenolic systems was postulated (cf. Figure 4). Only the recovery of larger amounts would give the opportunity to perform 1D/2D-NMR spectroscopy of **20**, such as HMBC, HMQC to confirm the proposed constitution.

Theoretically, a carbon-linkage between the aliphatic chains would be possible by a former reaction of activated positions in the *cis*-configured polyunsaturated double-bond systems. Of interest, is the low elution time of compound **20** in respect of all other anacardic acids. We assumed that the more bulky appearance of the anacardic acid dimer has caused a less active *van-der-Waals* interaction with the lipophil teflon surface of the HSCCC coil tubings and hence the reversible desorption/elution processes occurred faster.

The formation of carbon-linked dimers could be an enzymatic reaction between the anacardic acids already acting in the plant tissue material. Semi-synthetic approaches using horseradish peroxidase and H_2O_2 and resulted in oligomers and polymers of anacardic acids with coating and resin characteristics (*39*, *40*). During high temperature roasting process, oxidative C-C coupling of phenolic rings could as well be initiated in the cashew nuts. Then dimeric anacardic acids could be of value as marker substances to assess thermal impacts of cashew roasting. Biological evaluation of antibacterial properties of dimeric anacardic acids would be of interest, as well as the investigation of anacardic acid based bioplastics/ co-polymers for prevention of dangerous biofilm growth in products for clinical uses.

Downloaded by STANFORD UNIV GREEN LIBR on May 30, 2012 | http://pubs.acs.org
Publication Date (Web): May 29, 2012 | doi: 10.1021/bk-2012-1098.ch011

Unidentified Compounds

Two low abundant ion signals - not completely resolved - with the selected mass trace at *m/z* 487 were detected and had shown also identical MS-MS fragmentation pattern (cf. Table I, Figure 2D.). Unfortunately, the *on-line* HSCCC derived data were not supporting an idea for a structural proposal of these minorly concentrated and potentially isomeric compounds.

Extrusion HSCCC Mode with APCI-MS-MS Detection

The *elution-extrusion* HSCCC, or two column volume ($2V_C$)-methodology suggested by Bethod et al. was implemented to the presented HSCCC-ESI-/ APCI-MS/MS anacardic acid coupling experiment (*41*). After termination of the *elution* process (pumping of mobile phase), the *extrusion* was started by stationary phase pumping (*n*-hexane) using a lower spinning velocity of the HSCCC centrifuge. This procedure removed the potentially fractionated components from the three coil-column-system and extruded them sequentially to the fraction collector. This approach is able to fractionate the full polarity range of natural products injected to the CCC-device without undesired chemisorption. In case of the presented HSCCC-MS coupling, the content of highly volatile *n*-hexane in the extruded stationary phase required the exchange of the ESI-interface to an APCI-source to maintain ionization of target components. The important fact is, that for anacardic acid detection and the use of acetonitrile, the negative ionization mode of APCI has to be chosen, otherwise highly altered MS spectra will be obtained. Immediately, anacardic acids decarboxylate under positive APCI conditions (results not presented), and the addition of a molecule acetonitrile to the fragment ions resulted in quasimolecular ions of the nature $[M-44+41]^+$, which had complicated the mass-spectrum interpretation.

Downloaded by STANFORD UNIV GREEN LIBR on May 30, 2012 | http://pubs.acs.org
Publication Date (Web): May 29, 2012 | doi: 10.1021/bk-2012-1098.ch011

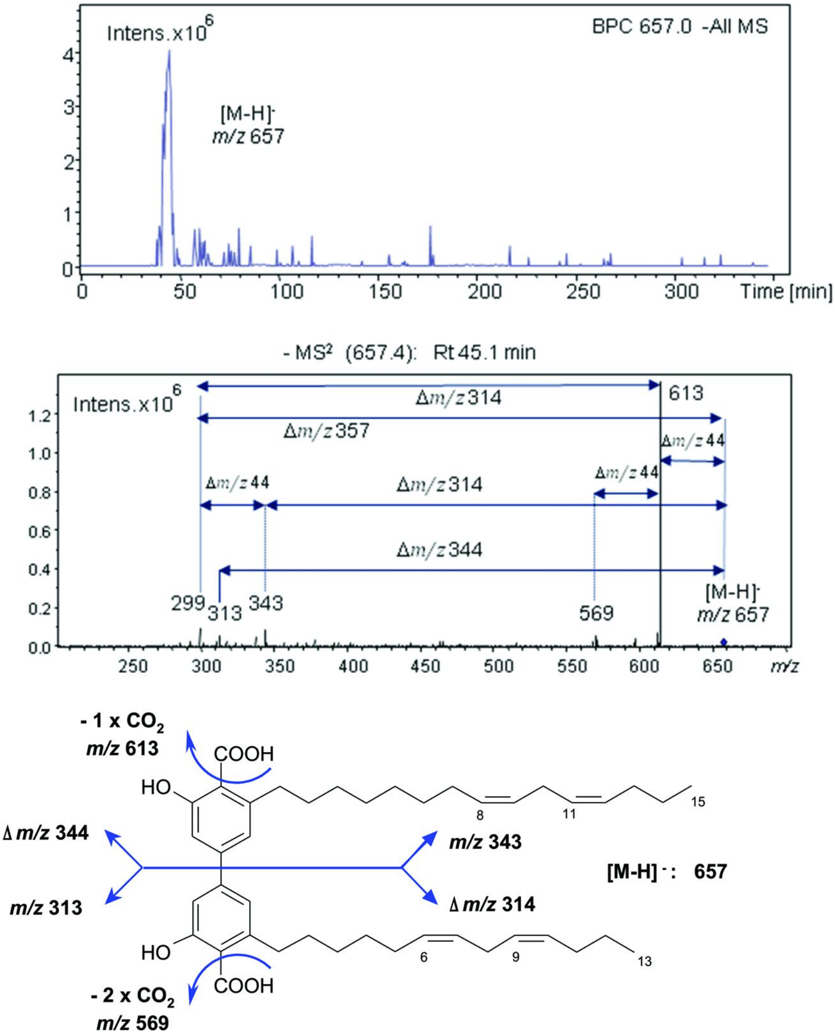

Figure 5. HSCCC-ESI-MS selected molecular ion peak of anacardic acid dimer ***20*** *at m/z 657 with a proposed C-C- linkage over the phenolic ring systems (DB = double bond). MS-MS fragments and neutral loss differences determined two different anacardic acids (C15 2DB + C13 2DB).*

Negative APCI-MS mass traces of the HSCCC-*extrusion* process are shown in Figure 3 and detected by their respective [M-H]$^-$ ion signals of three co-extruding compounds interpreted as free fatty acids (stearic acid: *m/z* 283, oleic acid: *m/z* 281, linoleic acid: *m/z* 279). Free fatty acids do have a medium polarity and this late recovery from the HSCCC column would be very unusual for this compound mixture. Beside the observed base-peak signals, molecular ion-clusters of very low abundances in the range of *m/z* 880-885 indicated the presence of triacylglycerides. Hence, we assumed that here the rather strong negative APCI conditions already initiated *in-source* MS-MS fragmentations of the very lipohilic triacylglycerides and cleaved fatty acids ion species.

Table I. Anacardic acids MS- and MS^n-data from the *elution*-process

ESI-MS *$[M-H]^-$:*	*Chain length* *Double bond amount*	*Neutral loss Δm/z*	*MS/MS*
	C2 chain		
1: *m/z* 163 *	Vinyl-salicylic acid 1 DB	44	119
	C5 chain		
2: *m/z* 205 *	1 DB exo-ethylene	42, 44	163, 119
m/z 281	Oleic acid	18	275, 263
m/z 255	Palmitinic acid	18	237
m/z 297 **	fragment of 7 3 DB		MS^3 *** 281, 267, 253, 239, 225, 211, 205, 197, 191, 185, 177, 163, 149, 121, 107
m/z 299 **	fragment of **8** 2 DB		MS^3 *** 293,257, 243, 229, 215, 197, 187, 175, 163, 143, 133, 119, 107
m/z 301 **	fragment of **9** 1 DB		MS^3 *** 273, 259, 245,231,217, 203,189,175, 161, 147,133,119, 106
m/z 303 **	fragment of **10** 0 DB		MS^3 *** 273, 133, 119, 106
	C13 chain		
3: *m/z* 315 *	2 DB	44	271, 255, 171
4: *m/z* 319 *	0 DB	44	275
m/z 325 **	fragment of **14** 3 DB		MS^3 *** 309, 295, 281, 267, 253, 239, 233, 225, 219, 211, 205, 197, 191, 183, 177, 163, 143 , 119, 106
m/z 327 **	fragment of **15** 2 DB		MS^3 *** 273, 231, 215, 203, 189, 183, 143, 133, 119, 108

Continued on next page.

Downloaded by STANFORD UNIV GREEN LIBR on May 30, 2012 | http://pubs.acs.org
Publication Date (Web): May 29, 2012 | doi: 10.1021/bk-2012-1098.ch011

Downloaded by STANFORD UNIV GREEN LIBR on May 30, 2012 | http://pubs.acs.org
Publication Date (Web): May 29, 2012 | doi: 10.1021/bk-2012-1098.ch011

Table I. (Continued). Anacardic acids MS- and MS^n-data from the *elution*-process

ESI-MS $[M-H]^-$:	***Chain length Double bond amount***	***Neutral loss Δm/z***	***MS/MS***
m/z 329 **	fragment of **16** 1 DB		MS^3 *** 259, 211, 199, 185, 177, 163, 147, 133 , 119, 106
	C14 chain		
5: *m/z* 331 *	1 DB	44	287
6: *m/z* 333 *	0 DB, trace	44	289
	C15 chain		
7: *m/z* 341	3 DB	44	297
8: *m/z* 343	2 DB	44	299
9: *m/z* 345	1 DB	44	301
10: *m/z* 347	0 DB	44	303
	C16 chain		
11: *m/z* 357 *	2 DB	44, 18	313, 295
12: *m/z* 359 *	1 DB	44, 18	315, 297
13: *m/z* 361 *	0 DB	44, 18	317, 299
12b: *m/z* 359 *	1 *trans* DB	44	315
	C17 chain		
14: *m/z* 369	3 DB	44	325, 295
15: *m/z* 371	2 DB	44	327
16: *m/z* 373	1 DB	44	329
	C15 chain	**dicar-boxy**	
17: *m/z* 383 *	4 DB	18, 44, 44	365, 339, 295
18: *m/z* 385 *	3 DB	18, 44, 44	367, 341, 297
19: *m/z* 387 *	2 DB	18, 44, 44	369, 343, 299
m/z 487	unknown	179	308, 249, 207, 188, 178
	Dimer		
20: *m/z* 657 *	C15 2 DB + C13 2 DB	44, 44	613, 569, 343, 313, 299

* Tentative structural assignment DB = *cis*-configured double bond ** *In-source* fragment ions (cardanols) generated in ESI-desolvation unit, observed for higher concentrated anacardic acids, direct loss of CO_2 as neutral loss cleavage. *** MS^2 fragment ions of respective *in-source* generated cardanols **) are equivalent to stage MS^3 fragment ions of respective anacardic acids.

The already detected ions in the *elution* mode at *m/z* 255 and *m/z* 281 were interpreted as free palmitic- and oleic acid, respectively (cf. Figure 2B.).

This specific fraction of the extrusion process (Rt 160-180 min) was recovered and the total content of triacylglycerides containing a mixture of stearic, oleic, linoleic acid was calculated as 11.5 % (m/m) of total vegetable oil in dried cashew nuts.

Retention Time of Anacardic Acids during Preparative HSCCC

The different selected ESI-MS single ion traces of anacardic acids (**1** – **20**) clearly indicated that compound separation during HSCCC was strongly depending on alkyl chain lengths attached to the salicylic acid backbone and their amount of *cis*-configured double bonds.

In the chosen *head-to-tail* mode with the *n*-hexane phase as the stationary phase, the more unsatured compounds eluted first and appeared to be much more polar than the more saturated ones. In the case of anacardic acids with C15-alkyl substitution (**7-10**): R_t (*m/z* 341) < R_t (*m/z* 343) < R_t (*m/z* 345) < R_t (*m/z* 347) the retention time differences were quite large (cf. Figure 2).

Countercurrent chromatography is frequently reported as a liquid-liquid separation technique without using solid phases. Specific partition factors of analytes between the used immiscible solvent phases generally give the chromatographic selectivity. The impact of the solid support, such as the long Teflon tubing, seemed to be neglected in the past but the evaluation of the compound elution sequence in the hyphenation experiment led to the conclusion that reversible and fast sorption/-desorption processes of anacardic acids at the Teflon material surface occurred and lately enabled the separation of these phenolic lipids. A slightly differing compound polarity cannot be the origin of this excellent chromatographic resolution. It is most likely the geometry of the alkyl/ alkenyl chains. Every *cis*-configured double bond will deliver a bending of a 30° degree to the aliphatic-chain. Due to our theory, *van-der-Waals* force interactions between the anacardic acids and the Teflon tube surface were weaker with increasing amounts of isolated *cis*-double bonds. A completely saturated alkyl chain such as **10** resulted in a rather long retention time in comparison to the early eluting *cis*-tri-enoic derivative **7** (cf. Figure 2A.). Principally, two molecules of the saturated compound **10** could better aggregate over the hydroxyl-carboxyl-function to form a dimer, directly masking the polar influence of the phenolic-head. For similar compounds such as alkyl *p*-hydroxy-benzoates – also with a polar-head and a lipophilic side chain - adsorptive interactions to Teflon were described before (*42*, *43*). Therefore, in our case of anacardic acid separation, Teflon material cannot be seen as an inert solid support. Nevertheless, adsorptive effects of Teflon might be strongly dependent on the amount of incorporated CF_2-functions in the material and the selected biphasic solvent system. Supporting this observation of retention time shifts influenced by *cis*- and *trans*-configured double bonds are one pair of anacardic acids (**12** and **12b**) with the same molecular ion signal $[M-H]^-$ at *m/z* 359. A double bond *trans*-configuration was suspected to be causing the strong retention time shift

Downloaded by STANFORD UNIV GREEN LIBR on May 30, 2012 | http://pubs.acs.org
Publication Date (Web): May 29, 2012 | doi: 10.1021/bk-2012-1098.ch011

difference of 170 min in the case of **12b** (substance not drawn in Figure 4, cf. Table I).

Conclusions

The *on-line* coupling of preparative HSCCC in combination with ESI-/APCI-MS/MS is an excellent metabolite profiling tool and allowed the monitoring of a complex component mixture during the separation procedure (500 mg injection). In the case of an achieved chromatographic base-line separation, the identified peaks can be recovered and contents can be calculated by simple gravimetry. The MS- and MS-MS identified substances could directly be implemented as an authentic reference materials to more accurate LC-MS quantification studies or evaluation of compound activities in biological assays.

During a HSCCC-MS run very important structural informations are obtained in real-time and can directly assist in the elucidation process of metabolites or summarizing full profiles of unknown crude extracts. Specific natural products of interest can directly be isolated and recognized in a complex matrix during the preparative (*target-guided*) isolation. In certain cases the purity control by off-line LC-ESI/APCI-MS-MS of HSCCC-fractions containing principal components could be omitted to save mass spectrometry experimental time. The intention of a preparative HSCCC-MS coupling is a rapid metabolite screening approach and is not very useful for a high sensitivity MS-detection. Illustrating that, higher concentrated anacardic acid, such as compound **7**, the relatively high mass transfer during the CCC-separation to the ESI-MS device was calculated from the recovered gravimetric amount, the elution time frame, the split ratio, and resulted in about 0.11 µg/ min.

Definitely, the re-investigation of evaporated CCC-fractions by a second chromatographic dimension, such as C_{18}-HPLC, and using off-line LC-ESI-MS-MS analysis would deliver much lower detection limits, and could reveal further extremely low concentrated compounds.

Anacardic acids are chemotaxonomical markers and typical for cashew nuts and all *Anacardium occidentale* plant materials such as CNSL, and could be of use as specific marker substances for identification of cashew nut products in other processed foods.

The result of this hyphenation study was that anacardic acids are minor concentrated phenolic lipids in respect of the total content of triacylglycerides. The *elution*-process concentrated and separated the minor anacardic acids during the chromatographic run, and the main amount of triacylglycerides was recovered in the *extrusion* process. The ratio of anacardic acids to triglycerides was calculated ~0.85 : 100. Nevertheless, from aspects of toxicology, the total content of approx. 1000 ppm of anacardic acids in nuts is far above the European safety value of identical or similar ginkgolic acids in *Ginkgo biloba* products (*36*).

Downloaded by STANFORD UNIV GREEN LIBR on May 30, 2012 | http://pubs.acs.org
Publication Date (Web): May 29, 2012 | doi: 10.1021/bk-2012-1098.ch011

Downloaded by STANFORD UNIV GREEN LIBR on May 30, 2012 | http://pubs.acs.org
Publication Date (Web): May 29, 2012 | doi: 10.1021/bk-2012-1098.ch011

Acknowledgments

We are indebted to Prof. Dr. Heiko Cammenga for helpful discussions (Institute of Physical and Theoretical Chemistry, Technische Universität Braunschweig). One of the authors (J.M.V.) is grateful for the research funding provided by the Project ALFA-partnership Latin-America - European Commission, LAGROTECH. AML/B7-311/97/0666/II-0451-FA-FCD-FI-FC.

References

1. Aguilar-Ortigoza, C. J.; Sosa, V.; Aguilar-Ortigoza, M. Toxic phenols in various Anacardiaceae species. *Econ. Bot.* **2003**, *57*, 354–364.
2. Morton, J. F. The Cashew's brighter future. *Econ. Bot.* **1961**, *15*, 57–78.
3. de Paiva, J. R.; de M. Barros, L.; Cavalcanti, J. J. V. Cashew (*Anacardium occidentale* L.) Breeding: A Global Perspective. In *Breeding Plantation Tree Crops: Tropical Species*; Jain, S. M., Priyadarshan, P. M., Eds.; Springer Science + Business Media LLC: New York, 2009; Chapter 9, pp 287−324.
4. Česla, P.; Blomberg, L.; Hamberg, M.; Jandera, P. Characterization of anacardic acids by micellar electrokinetic chromatography and mass spectrometry. *J. Chromatogr., A* **2006**, *1115*, 253–259.
5. Gellerman, J. L.; Schlenk, H. Methods for isolation and determination of anacardic acids. *Anal. Chem.* **1968**, *40*, 739–743.
6. Kubo, I.; Ochi, M.; Vieira, P. C.; Komatsu, S. Antitumor agents from the cashew *(Anacardium occidentale)* apple juice. *J. Agric. Food Chem.* **1993**, *41*, 1012–1015.
7. Himejima, M.; Kubo, I. Antibacterial agents from the cashew *Anacardium occidentale* (Anacardiaceae) nut shell oil. *J. Agric. Food Chem.* **1991**, *39*, 418–421.
8. Kubo, I.; Muroi, H.; Himejima, M.; Yamagiwa, Y.; Mera, H.; Tokushima, K.; Ohta, S.; Kamikawa, T. Structure-antibacterial activity relationships of anacardic acids. *J. Agric. Food Chem.* **1993**, *41*, 1016–1019.
9. Kubo, I.; Muroi, H.; Kubo, H. Structural functions of antimicrobial long-chain alcohols and phenols. *Bioorg. Med. Chem.* **1995**, *3*, 873–880.
10. Muroi, H.; Kubo, I. Bactericidal effects of anacardic acids and totarol on methicillin-resistant *Staphylococcus aureus* (MRSA). *Biosci. Biotech. Biochem.* **1994**, *58*, 1925–1926.
11. Kubo, I.; Nihei, K. I.; Tsujimoto, K. Antibacterial action of anacardic acids against methicillin resistant *Staphylococcus aureus* (MRSA). *J. Agric. Food Chem.* **2003**, *51*, 7624–7628.
12. Muroi, H.; Nihei, K.-I.; Tsujimoto, K.; Kubo, I. Synergistic effects of anacardic acids and methicillin against methicillin resistant *Staphylococcus aureus*. *Bioorg. Med. Chem.* **2004**, *12*, 583–587.
13. J. Kubo, J.; Lee, J. R.; Kubo, I. Anti-*Helicobacter pylori* agents from the cashew apple. *J. Agric. Food Chem.* **1999**, *47*, 533–537.
14. Castillo-Juárez, I.; Rivero-Cruz, F.; Celis, H.; Romero, I. Anti-*Helicobacter pylori* activity of anacardic acids from *Amphipterygium adstringens*. *J. Ethnopharmacol.* **2007**, *114*, 72–77.

15. Pereira, J. M.; Severino, R. P.; Vieira, P. C.; Fernandes, J. B.; da Silva, M.; Zottis, A.; Andricopulo, A. D.; Oliva, G.; Correa, A. G. Anacardic acid derivatives as inhibitors of glyceraldehydes-3-phosphate dehydrogenase from *Trypanosoma cruzi*. *Bioorg. Med. Chem.* **2008**, *16*, 8889–8895.
16. Freitas, R. F.; Prokopczyk, I. M.; Zottis, A.; Oliva, G.; Andricopulo, A. D.; Trevisan, M. T. S.; Vilegas, W.; Silva, M. G. V.; Montanari, C. A. Discovery of novel *Trypanosoma cruzi* glyceraldehyde-3-phosphate dehydrogenase inhibitors. *Bioorg. Med. Chem.* **2009**, *17*, 2476–2482.
17. Franca, F.; Lago, E. L.; Marsden, P. D. Plants used in the treatment of leishmanial ulcers due to *Leishmania* (Viannia) *braziliensis* in an endemic area of Bahia, Brazil. *Rev. Soc. Bras Med. Trop.* **1996**, *29*, 229–232.
18. Braga, F. G.; Bouzada, M. L. M.; Fabri, R. L.; de Matos, M. O.; Moreira, F. O.; Scio, E.; Coimbra, E. S. Antileishmanial and antifungal activity of plants used in traditional medicine in Brasil. *J. Ethnopharmacol.* **2007**, *111*, 396–402.
19. Silva, M. I. G.; de Melo, C. T. V.; Vasconcelos, L. F.; de Carvalho, A. M. R.; Sousa, F. C. F. Bioactivity and potential therapeutic benefits of some medicinal plants from the Caatinga (semi-arid) vegetation of Northeast Brazil: a review of the literature. *Rev. Bras. Farmcogn./Braz. J. Pharmcogn.* Epub Sep 16, 2011. Print version ISSN 0102-695X. http://dx.doi.org/10.1590/S0102-695X2011005000171.
20. Lee, S. J.; Park, W. H.; Moon, H. I. Bioassay-guided isolation of antiplasmodial anacardic acids derivatives from the whole plants of *Viola websteri* Hemsl. *Parasitol. Res.* **2009**, *104*, 463–466.
21. Stasiuk, M.; Kozubek, A. Biological activity of phenolic lipids. *Cell. Mol. Life Sci.* **2010**, *67*, 841–860.
22. Ito, Y., Conway, W. D. (Editors). *High-Speed Countercurrent Chromatography*. Chemical Analysis 132; Wiley: New York, 1996.
23. Ito, Y. Golden rules and pitfalls in selecting optimum conditions for high-speed counter-current chromatography. *J. Chromatogr., A* **2005**, *1065*, 145–168.
24. Du, Q.; Jerz, G.; He, Y.; Li, L.; Xu, Y.; Zhang, Q.; Zheng, Q.; Winterhalter, P.; Ito, I. Semi-industrial isolation of salicin and amygdalin from plant extracts using slow rotary counter-current chromatography. *J. Chromatogr., A* **2005**, *1074*, 43–46.
25. Sutherland, I.; Hewitson, P.; Ignatova, S. New 18-l process-scale counter-current chromatography centrifuge. *J. Chromatogr., A* **2009**, *1216*, 4201–4205.
26. Gutzeit, D.; Winterhalter, P.; Jerz, G. Application of Preparative High-speed counter-current chromatography / electrospray ionization mass spectrometry for a fast screening and fractionation of polyphenols. *J. Chromatogr., A* **2007**, *1172*, 40–46.
27. Fajardo-Oliveros, A.; Winterhalter, P.; Jerz, G. Investigation of the Colombian fruit ‘Cocona’ (*Solanum sessiliflorum*) by direct coupling of preparative high-speed countercurrent chromatography/ electrospray ionization mass spectrometry (*prep*HSCCC-ESI-MS/MS). *Lebensmittelchemie* **2010**, *64*, 41.

Downloaded by STANFORD UNIV GREEN LIBR on May 30, 2012 | http://pubs.acs.org
Publication Date (Web): May 29, 2012 | doi: 10.1021/bk-2012-1098.ch011

28. Macke, S.; Gutzeit, D.; Voigt, C. C.; Winterhalter, P.; Jerz, G. Application of preparative high-speed countercurrent chromatography/ electrospray ionization mass spectrometry for a fast target-guided screening of steroid alkaloid oligoglycosides in fruits of *Solanum rugosum*. *Lebensmittelchemie* **2010**, *64*, 42.
29. Jerz, G.; Wybraniec, S.; Gebers, N.; Winterhalter, P. Target guided separation of *Bougainvillea glabra* betacyanins by direct coupling of preparative ion-pair high-speed countercurrent chromatography and electrospray ionization mass-spectrometry. *J. Chromatogr., A* **2010**, *1217*, 4544–4554.
30. Jerz, G.; Gutzeit, D.; Winterhalter, P. Characterization of acylated flavonoid glycosides from sea buckthorn juice concentrate (*Hippophaë rhamnoides*) by preparative high-speed countercurrent chromatography/ electrospray ionization mass spectrometry hyphenation. In *Flavor and Health Benefits of Small Fruits*; Qian, M. C., Rimando, A. M., Eds.; ACS Symposium Series 1035; American Chemical Society: Washington, DC, 2010; Chapter 16, pp 253−265, ISBN13: 9780841225497.
31. Inoue, K.; Hattori, Y.; Hino, T.; Oka, H. An approach to on-line electrospray mass spectrometric detection of polypeptide antibiotics of enramycin for high-speed counter-current chromatographic separation. *J. Pharm. Biomed. Anal.* **2010**, *51*, 1154–1160.
32. Inoue, K.; Hattori, Y.; Horie, M.; Hino, T.; Oka, H. Preparative purification of gentamicin components using high-speed countercurrent chromatography coupled with electrospray mass spectrometry. *J. Sep. Sci.* **2011**, *34*, 1484–1488.
33. Toribio, A.; Destandau, E.; Elfakir, C.; Lafosse, M. Hyphenation of centrifugal partition chromatography with electrospray ionization mass spectrometry using an active flow-splitter device for characterization of flavonol glycosides. *Rapid Commun. Mass Spectrom.* **2009**, *23*, 1863–1870.
34. de Beer, D.; Jerz, G.; Joubert, E.; Wray, V.; Winterhalter, P. Isolation of isomangiferin from honeybush (*Cyclopia subternata*) leaves using high-speed countercurrent chromatography. *J. Chromatogr., A* **2009**, *1216*, 4282–4289.
35. Trevisan, M. T. S.; Pfundstein, B.; Haubner, R.; Würtele, G.; Spiegelhalder, B.; Bartsch, H.; Owen, R. W. Characterization of alkyl phenols in cashew (*Anacardium occidentale*) products and assay of their antioxidant capacity. *Food Chem. Toxicol.* **2006**, *44*, 188–197.
36. European Pharmacopoeia 6, Council of Europe, Strasbourg, Supplement 6.1., ISBN: 978-92-871-6057-7, Monograph 04/2008:1827; pp 3461−3463.
37. Yalpani, M; Tyman, J. H. P. The phenolic acids of *Pistacia vera*. *Phytochemistry* **1983**, *22*, 2263–2266.
38. Liu, Y.; Abreu, P. J. M. Long chain alkyl and alkenyl phenols from the roots of *Ozoroa insignis*. *J. Braz. Chem. Soc.* **2006**, *17*, 527–532.
39. Shridhara Alva, K.; Nayak, P. L.; Jayant Kumar, J.; Tripathy, S. K. Enzymatic polymerization of phenolic biomonomers derived from cashew nut shell liquid. *J. Macromol. Sci., Part A* **1997**, *34*, 665–674.

Downloaded by STANFORD UNIV GREEN LIBR on May 30, 2012 | http://pubs.acs.org
Publication Date (Web): May 29, 2012 | doi: 10.1021/bk-2012-1098.ch011

40. Tyman, J. H. P. Long chain phenols, XII. Compositional studies: the polymeric material in the unsaturated phenols of *Anacardium occidentale*. *J. Chromatogr.* **1978**, *156*, 255–266.
41. Berthod, A.; Ruiz-Angel, M. J.; Carda-Broch, S. Elution-extrusion countercurrent chromatography. Use of the liquid nature of the stationary phase to extend the hydrophobicity window. *Anal. Chem.* **2003**, *75*, 5886–5894.
42. Loh, W.; Volpe, P. L. O. Adsorption of alkyl *p*-hydroxybenzoates from aqueous solution onto teflon. *J. Colloid Interface Sci.* **1996**, *179*, 322–323.
43. Conder, J. R. Teflon, a noninert chromatographic support. *Anal. Chem.* **1971**, *43*, 367–370.

Downloaded by STANFORD UNIV GREEN LIBR on May 30, 2012 | http://pubs.acs.org
Publication Date (Web): May 29, 2012 | doi: 10.1021/bk-2012-1098.ch011

Downloaded by STANFORD UNIV GREEN LIBR on May 30, 2012 | http://pubs.acs.org
Publication Date (Web): May 29, 2012 | doi: 10.1021/bk-2012-1098.ch012

Chapter 12

Novel Insights into Flavor Chemistry of Asafetida

Andreas Degenhardt,[*] Margit Liebig, Birgit Kohlenberg, Beate Hartmann, Michael Roloff, Stefan Brennecke, Laurence Guibouret, Berthold Weber, and Gerhard Krammer

**Symrise AG, Flavor & Nutrition, Research & Innovation,
Mühlenfeldstrasse 1, 37603 Holzminden, Germany
[*]E-mail: andreas.degenhardt@symrise.com**

Asafetida is an important condiment based on an oleogum resin with an onion-like aroma obtained from various plants of the genus Ferula (family Umbelliferae), which are cultivated in countries like India. Since the flavor of Asafetida is significantly dominated by sulfur compounds, a combination of specific analytical and sensorial techniques was selected to investigate the flavor profile. In particular the combination of high-temperature liquid chromatography with preparative GC isolation of the volatile compounds has been employed. Newly identified substances are reported and sensory attributes of isolated sulphur-containing aroma compounds are described.

Introduction

Asafetida (*Ferula assa-foetida* L.) is obtained from various plants of the genus Ferula (family Umbelliferae). It is especially valued by its onion-like aroma. The content of oil is in the range of 6-20%. The samples which are available on the market are often ground samples with added gum arabic or rice flour (up to 50%). The essential oil of raw asafetida contains sulphur-bearing aroma compounds, terpenes as well as sesquiterpene coumarins (*1*, *2*). A recent investigation of the nature of the most potent aroma compounds of asafetida cannot be found in the literature, therefore we decided to perform a study into the aromatic composition of this important condiment.

In Recent Advances in the Analysis of Food and Flavors; Toth, S., et al.;
ACS Symposium Series; American Chemical Society: Washington, DC, 2012.

Downloaded by STANFORD UNIV GREEN LIBR on May 30, 2012 | http://pubs.acs.org
Publication Date (Web): May 29, 2012 | doi: 10.1021/bk-2012-1098.ch012

Results and Discussion

We have used a sensory-guided fractionation approach for the identification of the long lasting sulfury aroma notes of asafetida. We have started with a GC-olfactometry-MS identification of potent volatile aroma compounds. The extraction of asafoetida resin was followed by an extensive fractionation in order to separate taste-aroma contributions. We have used high-temperature liquid chromatography (HTLC) for screening of taste effects (*5*). With the use of preparative GC, we have isolated potent aroma compounds directly from LC fractions. By doing so, we have obtained a more relevant correlation of taste and aroma impression. Figure 1 shows the experimental protocol.

The extract obtained by diethylether/n-pentane has been analyzed by GC/MS and simultaneous GC-O screening. The results are shown in Figure 2. Compounds 1-7 are known from the literature, whereas compounds U1-U4 have not been in our database so far.

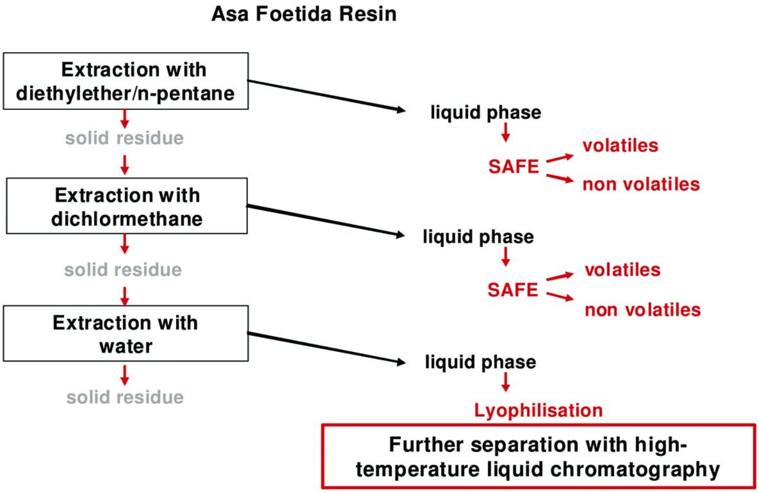
Asa Foetida Resin
Extraction with diethylether/n-pentane
solid residue
Extraction with dichlormethane
solid residue
Extraction with water
solid residue
liquid phase
SAFE
volatiles
non volatiles
liquid phase
SAFE
volatiles
non volatiles
liquid phase
Lyophilisation
Further separation with high-temperature liquid chromatography

Figure 1. Experimental protocol for the extraction of asafetida resin.

The polar phase (cf. Figure 1, right bottom, after lyophilisation) has been subjected to high-temperature liquid chromatography. This type of chromatography allows the use of water and ethanol as solvents for the chromatographic separation. After drying of the fractions, the samples have been reconstituted with water and tasted in a small panel and descriptive profiling has been performed. Figure 3 shows the separation and the sensorial evaluation results of the panel. Especially fractions 2 and 3 as well as fraction 11 have evoked our interest due to longlasting and powerful taste impressions. After the sequential extraction steps with solvents of decreasing polarity, this residue should only contain traces of volatile compounds but low-volatile or non-volatile components remain in the residue.

Downloaded by STANFORD UNIV GREEN LIBR on May 30, 2012 | http://pubs.acs.org
Publication Date (Web): May 29, 2012 | doi: 10.1021/bk-2012-1098.ch012

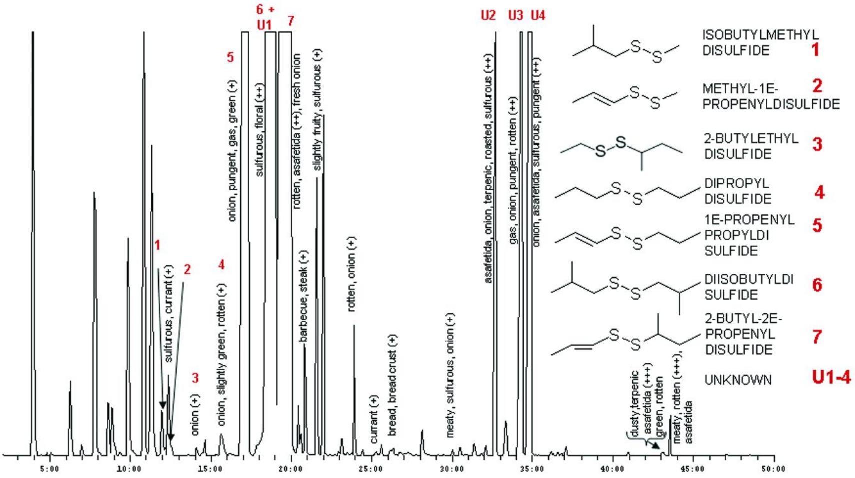

Figure 2. GC/MS chromatogram with sensorial attributes obtained by GC-O analysis of the diethylether/n-pentane extract.

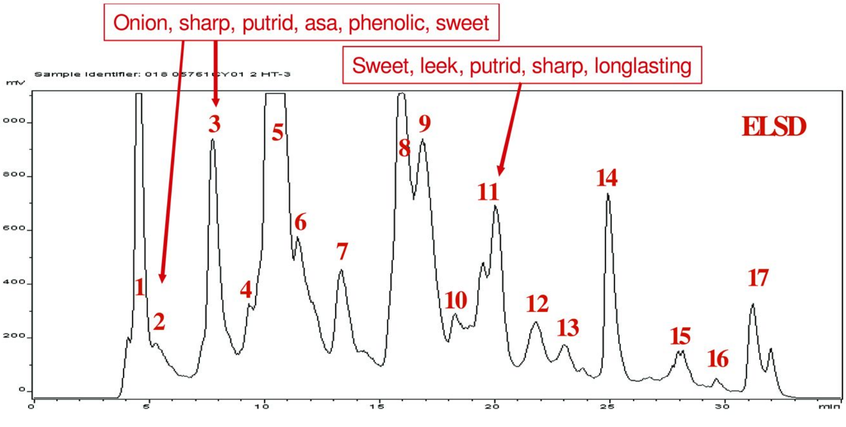

ELSD = evaporative light scattering detection

Figure 3. High-temperature liquid chromatography (HTLC) of the polar phase from the extraction procedure, numbers denote fractions not compounds.

However, the sensory descriptors indicate the presence of higher levels of aroma-active components. Therefore, we decided to subject the fractions 2,3 and 11 to further GC-O analysis. The volatile aroma compounds have been extracted from the aqueous fractions by solvent extraction with diethyl ether/pentane. Figure 4 shows the GC-O analysis of the fraction 2. The compound highlighted has been isolated using preparative gas chromatography

In Recent Advances in the Analysis of Food and Flavors; Toth, S., et al.;
ACS Symposium Series; American Chemical Society: Washington, DC, 2012.

in order to obtain more material for the NMR measurement. The sensory descriptors were dusty, sweet, tobacco and balsamic. The structure has been elucidated using NMR as trans-3,4,5-trimethoxycinnamic alcohol (3-(3,4,5-trimethoxyphenyl)-2-propen-1-ol, 9). The compound is known as a constituent of mace (*3*). The same procedure has been followed in case of fraction 3 from the HTLC separation (Figure 3). Figure 5 shows the results. The compound shown has again been isolated using preparative GC and shown to be 4-oxo-2,5,5,8a-tetramethyl-1-methylen-2,3-dehydro-decalin (10), a compounds which has been previously described in asafetida (*4*).

Downloaded by STANFORD UNIV GREEN LIBR on May 30, 2012 | http://pubs.acs.org
Publication Date (Web): May 29, 2012 | doi: 10.1021/bk-2012-1098.ch012

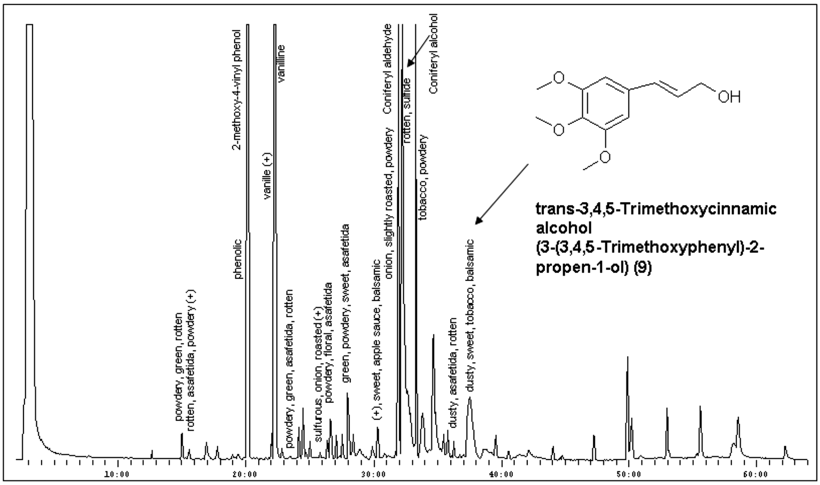

Figure 4. GC-O analysis of solvent extract from fraction 2 of the HTLC separation of the liquid polar phase.

Our further interest was focused on sulphur-containing aroma compounds in asafetida. Figure 2 indicates that all compounds marked with U1-U4 have not been previously reported in our database and other commercial available databases. Therefore, we have used another extraction protocol aimed at enriching the sulphur-containing aroma compounds. The work-up scheme was as follows: starting with pentane/diethyl ether extraction of asafetida gum, SAFE extraction of volatiles, and followed by silica gel column fractionation with pentane/ether step gradients from 100/0 to 0/100. A sensory guided isolation of potent aroma molecules has been carried out by a combination of GC-O and preparative GC. A summary of the compounds isolated is depicted in Figure 6.

Downloaded by STANFORD UNIV GREEN LIBR on May 30, 2012 | http://pubs.acs.org
Publication Date (Web): May 29, 2012 | doi: 10.1021/bk-2012-1098.ch012

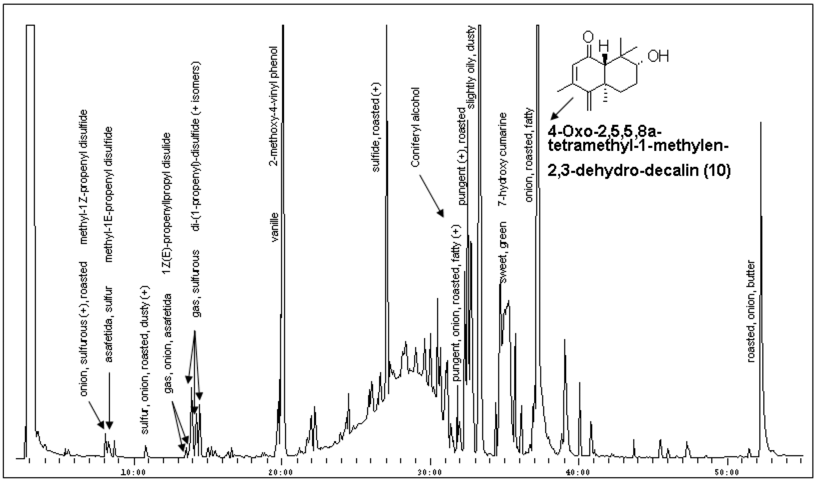

Figure 5. GC-O analysis of solvent extract from fraction 3 of the HTLC separation of the liquid polar phase.

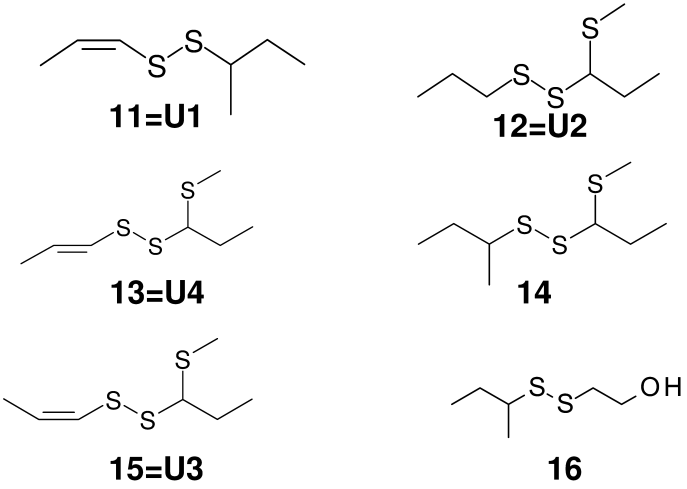

Figure 6. Isolated sulphur-containing aroma compounds.

Compounds 11, 12 and 13 are known constituents of asafetida. 11: cis-1-propenyl-sec-butyl-disulfide; 12: Propyl-1-methylthiopropyl-disulfide; 13: trans-1-propenyl-1-methylthiopropyl-disulfide; 14: sec-butyl-1-methylthiopropyl-disulfide (2 diastereomeres) ca.1:1; 15: cis-1-propenyl-1-methylthiopropyl-disulfide; 16: 2-butyl-(2-hydroxyethyl)disulfide.

Among the isolated compounds shown in Figure 6 three substances have not been reported before as natural compounds. To the best of our knowledge, compounds 14, 15 and 16 have been identified for the first time.

We were then interested in a sensory evaluation of the compounds. Since prep. GC only provided small quantities of the compounds, we decided to use a GC-O approach to evaluate the compounds. For this purpose, a mixture of the compounds has been injected and the individual sensorial properties have been obtained (cf. Figure 7). The compounds 11-15 showed roasty, onion-like, fatty/oily and sulfury aroma impressions.

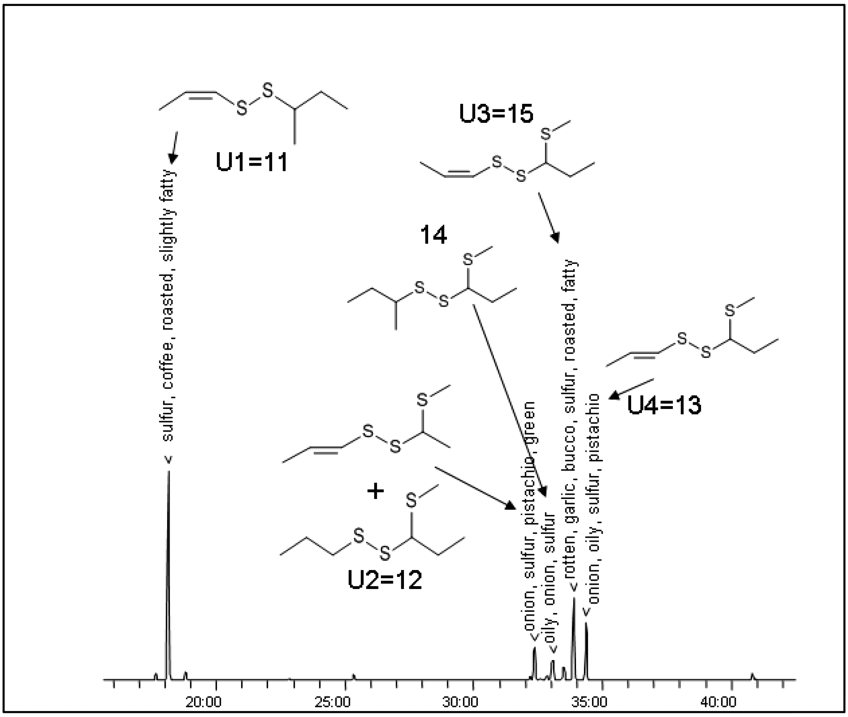

Figure 7. GC-O sensorial evaluation of isolated disulfide compounds.

Conclusions

Asafetida resin showed interesting sensorial effects: long lasting, mouth coating and strong roasty/onion-type notes. HTLC allows to directly screen and isolate/identify semi-volatile compounds besides non-volatile compounds.

Downloaded by STANFORD UNIV GREEN LIBR on May 30, 2012 | http://pubs.acs.org
Publication Date (Web): May 29, 2012 | doi: 10.1021/bk-2012-1098.ch012

Downloaded by STANFORD UNIV GREEN LIBR on May 30, 2012 | http://pubs.acs.org
Publication Date (Web): May 29, 2012 | doi: 10.1021/bk-2012-1098.ch012

HTLC is often favored over conventional LC because there is no need to use toxic solvents for the separation (*5*). Three novel disulfides have been found in asafetida which show strong sulfury, roasted sensorial properties.

Experimental Section

High-Temperature Liquid Chromatography (HTLC)

HTLC was carried out according to Reichelt et al. (*5*)

Preparative GC

GC HP5890II + Gerstel MCS + Gerstel PFC (30m DBWAX 0.53mm i.D. 1µm film thickness; 60-3-230°C, 5ml/min helium)

GC-MS and GC-O

GC Agilent 6890N; MS Finnigan MAT SSQ 7000; Gerstel OPD2 (60m ZB-WAX 0.32mm i.D. 0.25µm film thickness; 60-3-240°C, 2.4ml/min helium; Mass range 25-450)

GC-O: 60m ZB1 0.32mm i.d., 0.25µm film thickness; 80-4-280°C 2.4ml/min helium

Extraction

An experimental protocol shown in Fig. 1 has been used for the successive extraction of the asafetida resin. Solvent assisted flavour evaporation (SAFE) has been used to separate the volatile compounds from the non-volatile part.

Sensory Evaluation

The sensory evaluation of the HTLC separations has been performed as previously described (*5*).

NMR and MS Data of Compounds

400 MHz NMR Spectrometer, UNITY Inova, Varian; Solvent: benzene-d6, chloroform-d1

Mass Spectrometer: SSQ700, finnigan MAT, GC/EI-MS, 60m ZB-1

Spectral Data of Isolated Compounds

trans-3,4,5-Trimethoxycinnamic Alcohol (9)

^{1}H NMR (400 MHz,) δ 6.53 (s, 2H), 6.42 (dt, *J* = 15.8, 1.6 Hz, 1H), 6.07 (dt, *J* = 15.9, 5.5 Hz, 1H), 3.99 (td, *J* = 5.6, 1.6 Hz, 2H), 3.85 (s, 3H), 3.41 (s, 6H).

^{13}C NMR (100 MHz, $CDCl_3$) δ 153.3 s, 137.9 s, 132.5 s, 131.1 d, 128.1 d, 103.6 d, 63.6 t, 60.9 q, 56.1 q.

MW: 224 ($C_{12}H_{16}O_4$)

Naphthalin-1-on, (4AR,7R*,8AS*)-7-hydroxy-3,4A,8,8-tetramethyl-4-methylen (4-oxo-2,5,5,8a-tetramethyl-1-methylen-2,3-dehydro-decalin, 10)*

^{1}H NMR (400 MHz, C_6D_6) δ 5.79 (s, 1H), 4.89 (d, *J* = 0.7 Hz, 1H), 4.81 (d, *J* = 1.7 Hz, 1H), 2.84 (dt, *J* = 9.8, 4.6 Hz, 1H), 2.01 (s, 1H), 1.52 (d, *J* = 1.3 Hz, 3H), 1.51 – 1.35 (m, 4H), 1.40 (s, 3H), 1.34 (s, 3H), 0.98 (s, 3H), 0.83 (d, *J* = 5.1 Hz, 1H).

^{13}C NMR (100 MHz, C_6D_6) δ 197.8 s, 155.6 s, 148.6 s, 128.9 s, 111.5 t, 78.5 d, 60.4 d, 42.6 s, 38.5 s, 35.9 t, 28.5 q, 27.2 t, 23.4 q, 19.8 q, 15.4 q.

MW: 234 ($C_{15}H_{22}O_2$)

cis-1-Propenyl-sec-butyl-disulfid (11)

^{1}H NMR (400 MHz, C_6D_6) δ 6.14 (dq, *J* = 9.4, 1.6 Hz, 1H), 5.36 (dq, *J* = 9.4, 6.9 Hz, 1H), 2.55 (ddq, *J* = 6.7 Hz, 1H), 1.66 – 1.50 (m, 1H), 1.58 (dd, *J* = 6.9, 1.6 Hz, 3H), 1.44 – 1.24 (m, 1H), 1.15 (d, *J* = 6.8 Hz, 3H), 0.80 (t, *J* = 7.4 Hz, 3H).

^{13}C NMR (100 MHz, C_6D_6) δ 131.7 d, 125.9 d, 48.3 d, 28.8 t, 20.1 q, 14.3 q, 11.5 q.

MW: 162 ($C_7H_{14}S_2$)

Propyl-1-methylthiopropyl-disulfid (12)

^{1}H NMR (400 MHz, C_6D_6) δ 3.51 (dd, *J* = 8.0, 5.3 Hz, 1H), 2.54 – 2.45 (m, 2H), 2.13 – 2.00 (m, 1H), 1.86 (s, 3H), 1.79 – 1.68 (m, 1H), 1.59 – 1.48 (m, 2H), 0.98 (t, *J* = 7.3 Hz, 3H), 0.79 (t, *J* = 7.3 Hz, 3H).

MW: 196 ($C_7H_{16}S_3$)

trans-1-Propenyl-1-methylthiopropyl-disulfid (13)

^{1}H NMR (400 MHz, C_6D_6) δ 6.00 (dq, *J* = 14.8, 1.5 Hz, 1H), 5.76 (dq, *J* = 14.7, 6.7 Hz, 1H), 3.57 (dd, *J* = 8.2, 4.8 Hz, 1H), 2.06 (dqd, *J* = 14.6, 7.4, 4.9 Hz, 1H), 1.85 (s, 3H), 1.75 (ddq, *J* = 14.6, 8.2, 7.3 Hz, 1H), 1.39 (dd, *J* = 6.7, 1.6 Hz, 3H), 0.96 (t, *J* = 7.3 Hz, 3H).

^{13}C NMR (100 MHz, C_6D_6) δ 130.0 d, 126.9 d, 61.4 d, 28.5 t, 18.3 q, 14.5 q, 11.7 q.

MW: 194 ($C_7H_{14}S_3$)

Downloaded by STANFORD UNIV GREEN LIBR on May 30, 2012 | http://pubs.acs.org
Publication Date (Web): May 29, 2012 | doi: 10.1021/bk-2012-1098.ch012

sec-Butyl-1-methylthiopropyl-disulfid (1:1 Diastereomere) (14)

^{1}H NMR (400 MHz, C_6D_6) δ 3.55 (dd, *J* = 8.1, 5.0, Hz, 1H), 3.54 (dd, *J* = 8.1, 5.0 Hz, 1H), 2.70 (tq, *J* = 6.8 Hz, 1H), 2.69 (tq, *J* = 6.7 Hz, 1H), 2.16 – 2.04 (m, 2H), 1.89 (s, 3H), 1.89 (s, 3H), 1.82 – 1.51 (m, 4H), 1.45 – 1.28 (m, 2H), 1.18 (d, *J* = 6.8 Hz, 3H), 1.15 (d, *J* = 6.8 Hz, 3H), 0.99 (t, *J* = 7.3 Hz, 6H), 0.83 (t, *J* = 7.5 Hz, 6H).

MW: 210 ($C_8H_{18}S_3$)

cis-1-Propenyl-1-methylthiopropyl-disulfid (15)

^{1}H NMR (400 MHz, C_6D_6) δ 6.17 (dq, *J* = 9.4, 1.6 Hz, 1H), 5.39 (dq, *J* = 9.3, 6.9 Hz, 1H), 3.52 (dd, *J* = 8.1, 4.9 Hz, 1H), 2.03 (dqd, *J* = 14.6, 7.3, 4.9 Hz, 1H), 1.84 (s, 3H), 1.72 (ddq, *J* = 14.5, 8.1, 7.3 Hz, 1H), 1.57 (dd, *J* = 6.9, 1.6 Hz, 3H), 0.95 (t, *J* = 7.3 Hz, 3H).

^{13}C NMR (100 MHz, C_6D_6) δ 130.8 d, 126.8 d, 61.7 d, 28.1 t, 14.3 q, 14.0 q, 11.3 q.

MW: 194 ($C_7H_{14}S_3$)

2-Butyl-2(2-hydroxyethyl)-disulfid (16)

^{1}H NMR (400 MHz, C_6D_6) δ 3.54 (dt, *J* = 6.1 Hz, 2H), 2.50 (tq, *J* = 6.7 Hz, 1H), 2.45 (t, *J* = 6.1 Hz, 2H), 1.62 – 1.49 (m, 1H), 1.31 (ddq, *J* = 14.1, 7.3 Hz, 1H), 1.22 (t, *J* = 6.3 Hz, 1H), 1.11 (d, *J* = 6.8 Hz, 3H), 0.79 (t, *J* = 7.4 Hz, 3H).

MW: 166 ($C_6H_{14}OS_2$)

References

1. Takeoka, G. *Volatile constituents of asafetida.* ACS Symposium Series 826; American Chemical Society: Washington D.C., 2002, p 33-44.
2. Noleau, I.; Richard, H.; Peyroux, A.-S. Volatile compounds in leek and asafetida. *J. Essent. Oil Res.* **1991**, *3*, 241–256.
3. Hattori, M.; Yang, X. W.; Shu, Y. Z.; Kakiuchi, N.; Tezuka, Y.; Kikuchi, T.; Namba, T. Constituents of mace. Part IV. New constituents of the aril of Myristica fragrans. *Chem. Pharm. Bull.* **1988**, *36*, 648–53.
4. Appendino, G.; Maxia, L.; Bascope, M.; Houghton, P. J.; Sanchez-Duffhues, G.; Muñoz, E.; Sterner, O. A Meroterpenoid NF-κB Inhibitor and Drimane Sesquiterpenoids from Asafetida. *J. Nat. Prod.* **2006**, *69*, 1101–1104.
5. Reichelt, K. V.; Peter, R.; Paetz, S.; Roloff, M.; Ley, J. P.; Krammer, G. E.; Engel, K.-H. *J. Agric. Food Chem.* **2010**, *58*, 458−464. Correction: *J. Agric. Food Chem.* **2010**, *58*, 3241−3242.

Downloaded by STANFORD UNIV GREEN LIBR on May 30, 2012 | http://pubs.acs.org
Publication Date (Web): May 29, 2012 | doi: 10.1021/bk-2012-1098.ch012

Downloaded by OHIO STATE UNIV LIBRARIES on May 30, 2012 | http://pubs.acs.org
Publication Date (Web): May 29, 2012 | doi: 10.1021/bk-2012-1098.ch013

Chapter 13

Comparison of Fast Gas Chromatography−Surface Acoustic Wave Sensor (FGC-SAW) and Capillary GC-MS for Determining Strawberry and Orange Juice Volatiles

Xiaofen Du and Russell Rouseff[*]

University of Florida, Institute of Food and Agricultural Sciences,
Citrus Research and Education Center, 700 Experiment Station Road,
Lake Alfred, Florida 33850 U.S.A.
[*]E-mail: rrouseff@ufl.edu

Fast gas chromatography with surface acoustic wave detection (FGC-SAW) is a new instrumental approach which employs a polymer based volatile trap coupled to a short (1 m) capillary column and a single quartz SAW detector. Typically FGC-SAW headspace volatile analyses take less than 1 min, whereas a typical GC-MS run will take 30-60 min. The tradeoff for such rapid analysis is less chromatographic resolution but the resolution is often adequate for major components. For strawberries, 19 peaks were observed in 20 sec with the FGC-SAW and 80 peaks in 43 min for the GC-MS. For orange juice, 15 peaks were observed in 18 sec with the FGC-SAW and 60 peaks in 43 min for the GC-MS. The entire single analysis time for headspace sampling, GC analysis and instrumental recycling was 51 sec for strawberry and 46 sec for orange juice. Matching retention index values of standards, the major volatiles in strawberry using FGC-SAW were identified as esters, whereas terpenes and esters were the major volatiles identified in orange juice. The identifications were confirmed using GC retention index values and MS fragmentation patterns of standards. Although the chromatographic resolution of fruit volatiles from FGC-SAW was inferior to GC-MS, the

Downloaded by OHIO STATE UNIV LIBRARIES on May 30, 2012 | http://pubs.acs.org
Publication Date (Web): May 29, 2012 | doi: 10.1021/bk-2012-1098.ch013

usefulness of the data to distinguish strawberry varieties and orange juice quality was surprisingly equivalent. When GC-MS and FGC-SAW chromatographic data from identical samples were analyzed using principle component analysis, PCA, both could clearly differentiate 10 strawberry cultivars as well as between fresh and storage abused orange juice from concentrate.

Introduction

High resolution capillary gas chromatograph (HRGC) is the most widely used technique for the separation of volatile compounds in food because foods are typically complex mixtures and HRGC has exceptional separating powers. In highly complex cases, normal HRGC may not provide adequate resolution but resolution can be enhanced through the use of selected ion monitoring or multi-dimensional GC (GC × GC). Many types of GC detectors are commercially available. Flame ionization detector, FID, is a non-specific mass detector and the most commonly used detector for general volatile analysis. Sometimes selective detectors such as NPD (alkali flame ionization) are employed to specifically facilitate detection of nitrogen-containing compounds. For similar reasons a flame photometric detector (FPD) used to analyze sulfur-containing compounds. Mass spectrometry (MS) is generally used in volatile analysis to either identify an unknown or to quantify trace components using selective ion monitoring. It is exceptionally well adapted to flavor research since it is readily coupled to the GC and provides more rapid identification and compositional information about volatile compounds than any other detection method. Although capillary GC-MS is a powerful volatile analysis tool and can achieve precise, reliable and abundant information in food volatile analysis, instrumentation is costly, time-consuming, and limited to well-equipped laboratories. It does not typically allow for on-line measurements which may be required in the field and/or in processing plants.

The development of rapid, simple and low cost analytical techniques for volatile analysis has been an active area of research during the last two decades. Fast gas chromatograph-surface acoustic wave detector (FGC-SAW) is a new instrumental approach developed in the last decade. It typically consists of a sensor head and a support chassis but other designs are possible. The sensor head contains the hardware used to concentrate, separate and detect sample headspace volatiles. This hardware includes: a volatile concentrating trap, a sampling valve, a GC oven, short capillary column, and a SAW detector. The support chassis contains a pneumatic controller and electronic support. The chassis typically has a processor (system controller), which can be connected to a laptop computer via blue tooth or built into the chassis. Software is used to control the system, store and display the data. These units can often be made portable. The advantages of FGC-SAW include simplicity, portability, fast analysis (generally less than 1 min per sample), and relatively low instrumentation costs.

Several studies have employed FGC-SAW for the analysis of drugs and explosives (*1*, *2*), monitoring environmental pollutants (*3*), and quality assurance of food and beverage (*4–6*). In food and flavor analyses, FGC-SAW has been employed in the detection and discrimination of lard and vegetable oil aroma, monitoring the storage stability, and detecting adulteration with different sources of oils (*4*, *7–10*). FGC-SAW has also been used for the classification of honey types based on the aromas from different flower sources and the detection of sugar adulteration (*5*, *11*, *12*). Detecting and discriminating cultivar, species, and geographical differences of lilac blossom and *thymus* medical plants were also fulfilled by FGC-SAW (*13*, *14*). Aroma compounds in grapes and other plant volatiles have also been analyzed by FGC-SAW (*15*, *16*).

However, the application of FGC-SAW in food volatile analysis has not been fully exploited. FGC-SAW has never been used to determine strawberry and orange volatiles. The objective of the current study was to compare the information obtained using FGC-SAW with that of conventional capillary GC-MS from the analyses of fresh strawberries and orange juice volatiles.

Downloaded by OHIO STATE UNIV LIBRARIES on May 30, 2012 | http://pubs.acs.org
Publication Date (Web): May 29, 2012 | doi: 10.1021/bk-2012-1098.ch013

Materials and Methods

Chemicals

Pure standards of ethyl acetate, methyl butanoate, ethyl butanoate, methyl hexanoate, ethyl hexanoate, butyl butanoate, hexyl butanoate, linalool (3, 7-dimethylocta-1, 6-dien-3-ol), carvone (2-methyl-5-(1-methylethenyl)-2-cyclohexenone), (*E*)-2-hexenal, mesifurane (2, 5-dimethyl-4-methoxy-3(2*H*)-furanone), and γ-dodecalactone (5-octyloxolan-2-one) were obtained from Aldrich Chemical Co. Inc. (Milwaukee, WI). Valencene (4a, 5-dimethyl-3-prop-1-en-2-yl-2,3,4,5,6,7-hexahydro-1H-naphthalene), α-terpineol (2-(4-methyl-1-cyclohex-3-enyl) propan- 2-ol), and β-myrcene (7-methyl-3-methylene-1, 6-octadiene) were supplied from Sunpure (Lakeland, FL). Limonene (1-methyl-4-(1-methylethenyl)-cyclohexene) was acquired from Fluka Chemical (Milwaukee, WI). Geraniol (3, 7-dimethylocta-2, 6-dien-1-ol) was purchased from Acros Organics (Fair Lawn, NJ).

Strawberry and Orange Samples

'Strawberry Festival', the most popular commercialized strawberry cultivar in Florida, along with 'Rosa Linda', 'Winter Dawn', 'Sweet Charlie', 'Dover', 'Carmine', 'Earlibrite', '06-38', '05-85', and '05-107' were obtained from the University of Florida Gulf Coast Research and Education Center, Wimauma, Florida on March 7, 2011. Fruit from each cultivar was hand-harvested at the fully mature stage (full-red). Berries were washed with distilled water and dried on paper towels on the day of harvest. All straw-berries were visually sorted for uniform coloration and free of defects. Two hundred g of strawberries were pureed in a Waring blender (Waring Products, New Hartford, CO), with an equal weight of freshly distilled water and 20% (w/w) sodium chloride (Fisher Scientific, Fair Lawn, NJ). Sodium chloride was added to inhibit enzyme activity and to produce a salting-out effect during headspace volatile analysis. Blending

Downloaded by OHIO STATE UNIV LIBRARIES on May 30, 2012 | http://pubs.acs.org
Publication Date (Web): May 29, 2012 | doi: 10.1021/bk-2012-1098.ch013

was performed in the high speed pulse mode for 20 sec and the puree was immediately placed into individual glass vials and stored at -20 °C until analysis.

‘Valencia’ orange, the most broadly planted orange in Florida, was hand-harvested from trees in Winter Haven, Florida on March 31, 2011. Fruit were thoroughly washed with distilled water and allowed to dry on paper towels. Ten oranges were cut in half (equatorially) and extracted by hand with an electric reamer type juice extractor (Sunkist Growers. Inc., Ontario, CA). The juice was immediately collected in individual glass vials and stored at -20 °C until analysis. A lot of commercial shelf stable orange juice reconstituted from concentrate (Minute Maid® Kids$^+$, Coca-cola company, USA) in individual 200 mL (6.75 FL oz) Tetra-Pak containers were purchased in a local supermarket and left at room temperature (24±1 °C) for 10 months to intentionally produce off flavors. Volatiles of this storage abused orange juice were compared to the fresh ‘Valencia’ orange juice.

FGC-SAW Volatile Analysis

Five grams of strawberry puree or orange juice were weighed into 20-mL glass vials with silicone / PTFE septa (clean pack, Gerstel Inc., Linthicum, MD, USA) sealed with aluminum crimp caps. Prior to headspace sampling, strawberry samples were equilibrated at 40 °C in a water-bath for 20 min. Equilibration/ sampling temperature for orange juice was room temperature (24 °C±1 °C) for 5 min.

FGC-SAW used in this study was a zNose™ 4500 ultrafast GC analyzer (Electronic Sensor Technology, EST, New Bury Park, CA, USA). It consisted of a GC sensor head, a support chassis, and a system controller (software). The sensor head was equipped with a heated inlet nozzle, six-port valve, Tenax-trap, a short GC column and SAW detector. The support chassis contained a pump, a small helium gas cylinder and battery to power the electronics. The chassis also had a built-in processor, which was connected to a laptop via blue tooth. Analysis consisted of two steps: headspace sampling/concentration and injection/separation/detection. In sampling, a bent needle connected to the inlet nozzle (200 °C) was inserted through the septum of the sample vial and headspace vapor was withdrawn at 30 mL/min. A 10 gauge stainless steel sparging needle was also separately inserted through the septum until the end was just above the bottom of the solution in order to allow outside gases to balance the headspace gases pulled out by the pump. Sampling time was 10 s for strawberry and 5 s for orange juice. After being removed from the sample vial, headspace gases passed through a heated valve (160 °C) and onto a Tenax®-trap (0.7 mm O. D. × 51 mm long containing approximate 2 mg of Tenax®). The valve was then rotated to put the trap in line with the GC column to prepare for injection. The Tenax®-trap was quickly heated to 225 °C to release absorbed volatiles. The helium carrier gas transported the desorbed volatiles to a capillary column (DB5, 0.25 mm I. D. x 1 m length x 0.25 μm film thickness) at a rate of 3 mL/min. Initial GC oven temperature was 40 °C and immediately heated to 180 °C at a rate of 10 °C/s. A SAW crystal detected the volatiles exiting from the column.

Downloaded by OHIO STATE UNIV LIBRARIES on May 30, 2012 | http://pubs.acs.org
Publication Date (Web): May 29, 2012 | doi: 10.1021/bk-2012-1098.ch013

All the analytical parameters had been optimized prior to data collection. The entire sample analysis was 51.3 s for strawberry and 46.3 s for orange juice. This included: headspace sampling (10 s for strawberry and 5 s for orange juice), FGC-SAW analysis (26.3 s), and instrumental recycling (15 s). Between each sample measurement at least one blank was run to ensure a clean system and eliminate the possibility of sample carryover. Each sample was analyzed in duplicate.

Peak identifications were determined by matching "Kovats" standardized retention index values (LRI, using standard n-alkanes of C_6-C_{22} in methanol, supplied by Electronic Sensor Technology) with that from GC-MS identification using the same type of column. Confirmation of peak identifications was achieved by matching LRI values with authentic standards in both systems. Chromatographic peak areas were used for data analysis.

SPME-GC-MS Volatile Analysis

Ten grams of strawberry puree or orange juice was added into a 40-mL glass vial with a Teflon coated septum screw cap. A 4-mm Teflon stir bar was added and the container flushed with nitrogen. Each sample was equilibrated at 40 °C in a water-bath for 20 min. After equilibration, a fiber coated with divinylbenzene / carboxen / polydimethylsiloxane (DVB / CAR / PDMS, 2 cm, 50 / 30 µm film thickness, Supelco, Bellefonte, PA) was exposed to the vial headspace for 40 min at 40 °C. The fiber was then introduced into a heated GC injection for a 3-min desorption.

GC-MS analyses were performed using a PerkinElmer Clarus 500 gas chromatograph and quadropole mass spectrometer (PerkinElmer, Waltham, MA). Compound separation was achieved with an Rtx-5 column (60 m × 0.25 mm i.d., crossbond 5% diphenyl - 95% dimethyl polysiloxane × 0.50 μm film thickness, Restek Corp., Bellefonte, PA). Column flow rate was 2.0 mL/min. Initial oven temperature was 40 °C and held for 1 min, then increased to 190 °C at a rate of 4 °C/min, and finally to 250 °C at a rate of 8 °C/min, with a 5 min hold at the final temperature. Injection, MS transfer line, and ion source temperature was 230, 240, and 180 °C, respectively. Electron ionization was 70 eV. Mass spectrometric data from 30-300 *m/z* were collected and analyzed using TurboMass software (Perkin Elmer). Compound identifications were obtained by comparing mass fragmentation patterns with that from the NIST or Wiley 275.L (G1035) databases and confirmed in most cases with comparisons with authentic standards. Linear retention index (LRI) values were calculated using standard n-alkanes of C_5-C_{25} to assist in the identification peaks in FGC-SAW chromatograms.

Statistical Analysis

The Unscrambler version 10.0.1 software (CAMO ASA. Oslo, Norway) was used to perform Principle Component Analysis (PCA) of volatiles in ten strawberry cultivars.

Results and Discussion

Analysis Time versus Chromatographic Resolution

With chromatographic separations in less than 20 s, the most prominent feature of FGC-SAW is its extremely high analytical speed. Total analysis times are typically under 60s including headspace sampling, FGC-SAW analysis, and instrumental recycle times. One of the key components of this system is the SAW detector which consists of a SAW crystal and a small thermoelectric cooler. The crystal is mounted internally with the small thermoelectric cooler, which can provide cooling needed instantly during vapor adsorption and heating needed to clean the crystal when required. Typically FGC-SAW analysis of headspace volatiles of a sample will take less than 1 min, whereas a typical GC-MS run will take 30-60 min. As demonstrated in Figure 1 (A & B), total chromatograph run time for FGC-SAW of a strawberry sample was 26.3 sec, compared to 51 min to separate the identical volatile compounds using GC-MS.

The tradeoff for such rapid FGC-SAW chromatographic separations is a reduction of chromatographic resolution. As shown in Figure 1, 19 peaks were observed with the FGC-SAW (Figure 1 A) and around 80 peaks for the GC-MS (Figure 1 B) for the identical strawberry sample. In the case of fresh orange juice 15 peaks were observed with the FGC-SAW (Figure 2 A) and around 60 peaks for the GC-MS (Figure 2 B). Since identical samples were analyzed, it may therefore be inferred that each FGC-SAW peak contained more than a single compound. For example, in the strawberry sample, peaks 17 and 18 in GC-MS chromatogram (Figure 1 B) may co-elute as peak 17 in FGC-SAW chromatogram (Figure 1 A). In the case of fresh orange juice (Figure 2 B), peaks 7 and 8 in GC-MS probably co-elute as peak 8 in FGC-SAW chromatogram (Figure 2 A). However, only MS has the means to determine if more than a single compound is present in a chromatographic peak. There is no way to directly identify coelution in FGC-SAW peaks. The fact that far fewer peaks were observed using FGC-SAW would suggest that coelution was common. Peaks which elute close to each other in the longer GC-MS capillary column were unlikely to be resolved in the FGC-SAW. It should be mentioned that the sampling techniques used in both systems were slightly different and could be a minor contribution to the fewer peaks observed in the FGC-SAW chromatogram. The FGC-SAW system employed dynamic headspace sampling where volatiles were sucked out by vacuum and concentrated on a Tenax trap. In contrast, the GC-MS protocol employed SPME to concentrate and extract headspace volatiles. SPME is a static (equilibrium) based system and any differences between dynamic and static headspace sampling would be reflected in the respective chromatograms. Since different volatile sampling techniques were used in FGC-SAW and GC-MS procedures, the smaller number of peaks observed in FGC-SAW chromatograms cannot completely attributed to coeluted peaks observed in GC-MS chromatograms. However, coelution must be expected in the case of many if not most of the FGC-SAW chromatographic peaks.

Downloaded by OHIO STATE UNIV LIBRARIES on May 30, 2012 | http://pubs.acs.org
Publication Date (Web): May 29, 2012 | doi: 10.1021/bk-2012-1098.ch013

Downloaded by OHIO STATE UNIV LIBRARIES on May 30, 2012 | http://pubs.acs.org
Publication Date (Web): May 29, 2012 | doi: 10.1021/bk-2012-1098.ch013

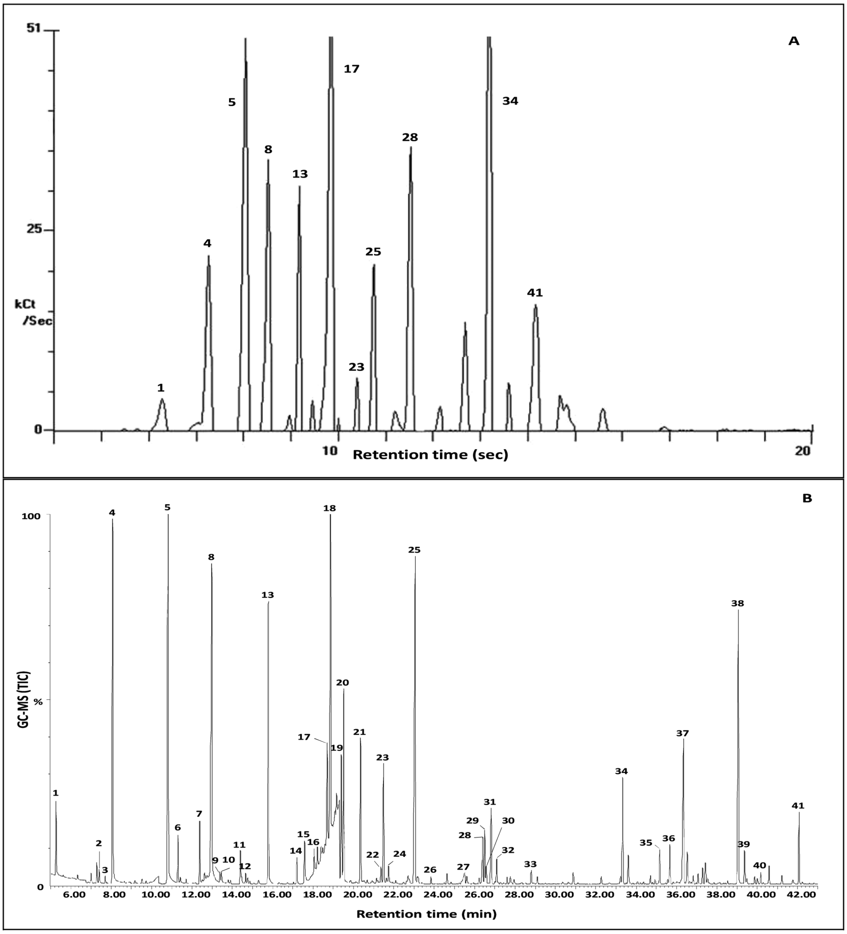

*Figure 1. FGC-SAW (**A**) and GC-MS (**B**) chromatograms of headspace volatiles for 'Strawberry Festival' strawberry. Key: 1. ethyl acetate; 2. methyl thioacetate; 3. ethyl propanoate; 4. methyl butanoate; 5. ethyl butanoate; 6. butyl acetate; 7. isopropyl butanoate; 8. (E)-2-hexenal; 9. (E)-2-hexenol; 10. hexanol; 11. 2-heptanone; 12. propyl butanoate; 13. methyl hexanoate; 14. (Z)-2-heptenal; 15. benzaldehyde; 16. 2-ethylhexenol; 17. butyl butanoate; 18. ethyl hexanoate; 19. hexyl acetate; 20. (E)-2-hexenyl acetate; 21. isopropyl hexanoate; 22. (E)-2-octenal; 23. mesifurane; 24. octanol; 25. linalool; 26. methyl octanoate; 27. octanoic acid; 28. hexyl butanoate; 29. (E)-2-hexenyl butanoate; 30. ethyl octanoate; 31. α-terpineol; 32. 2-ethylhexyl butanoate; 33. nerol; 34. octyl butanoate; 35. perillyl acetate; 36. farnesene; 37. γ-decalactone; 38. nerolidol, 39. octyl hexanoate; 40. p-menth-3-en-1-ol; 41. γ-dodecalactone.*

Downloaded by OHIO STATE UNIV LIBRARIES on May 30, 2012 | http://pubs.acs.org
Publication Date (Web): May 29, 2012 | doi: 10.1021/bk-2012-1098.ch013

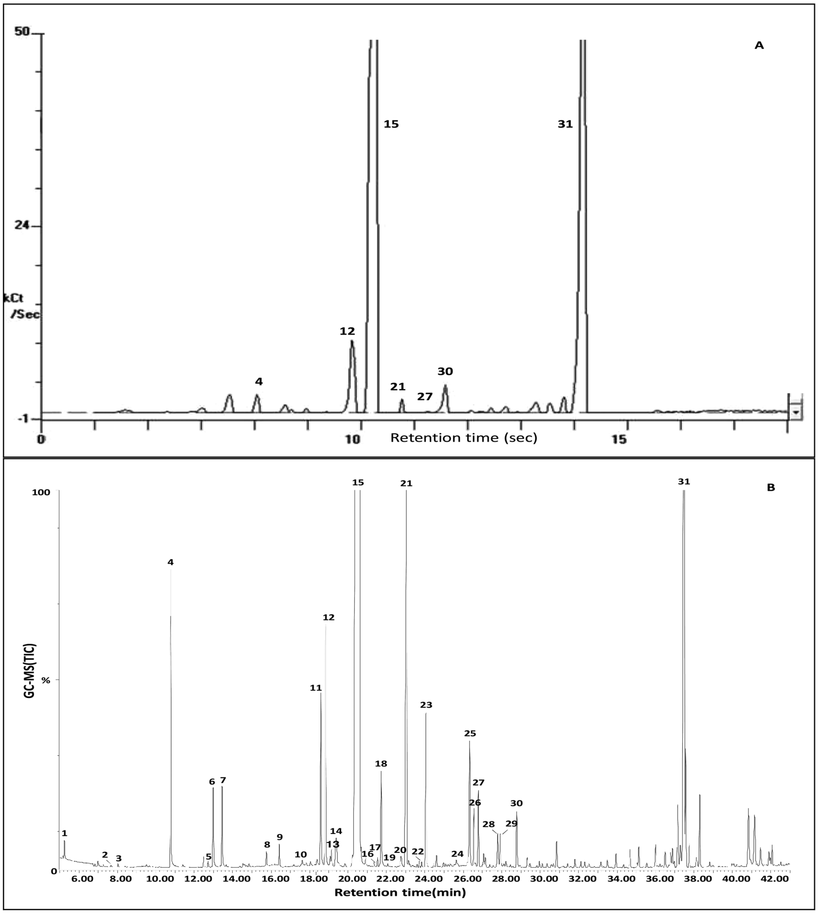

*Figure 2. FGC-SAW (**A**) and GC-MS (**B**) chromatograms of headspace volatiles for fresh 'Valencia' orange juice. Key: 1. ethyl acetate; 2. ethyl propanoate; 3. methyl butanoate; 4. ethyl butanoate; 5. ethyl 2-methylbutanoate; 6. (Z)-3-hexenol; 7. hexanol; 8. methyl hexanoate; 9. α-pinene; 10. heptanol; 11. β-myrcene; 12. ethyl hexanoate; 13. (Z)-3-hexenyl acetate; 14. hexyl acetate; 15. limonene; 16. (E)-2-octenal; 17. α-terpinene; 18. octanol; 19. (E)-linalool oxide; 20. α-terpinolene; 21. linalool; 22. methyl octanoate; 23. ethyl 3-hydroxyhexanoate; 24. decanal; 25. 4-terpineol; 26. ethyl octanoate; 27. α-terpineol; 28. β-citronellol; 29. nerol; 30. geraniol; 31. valencene.*

Peak Identifications

In the case of GC-MS, chromatographic peaks can be identified primarily from comparing the observed fragmentation pattern with that from standards or library standards and then confirmed by comparing the observed retention with standardized retention index values from standards or the literature. In the case of FGC-SAW identifications are based soley on comparison of calculated retention index values with standards or the literature and must therefore be considered as tentative. Many of the FGC-SAW tentative identifications were confirmed from the GC-MS identifications.

As listed in the caption for Figure 1, the major compounds identified in strawberry using FGC-SAW were esters including ethyl acetate, methyl butanoate, ethyl butanoate, methyl hexanoate, butyl butanoate, hexyl butanoate, and octyl butanoate. The major chemical classes identified in orange juice using FGC-SAW were esters, alcohols and terpenes such as ethyl butanoate, ethyl hexanoate, limonene, linalool, α-terpineol, geraniol, and valencene (Figure 2). Overall the results were consistent with GC-MS identifications, although the FGC-SAW chromatograms for orange juice were not particularly satisfactory because orange juice volatiles are typically composed of 90% or more of limonene. The huge amount of limonene in orange juice easily overload the capacity of the solid absorbent used in the FGC-SAW system. The partial solution to this problem was to reduce the dynamic headspace sampling time to reduce the total amount of volatiles exposed to the resin trap. However, in doing so the amounts of the other orange juice volatiles were also reduced, thus making them more difficult to detect.

Downloaded by OHIO STATE UNIV LIBRARIES on May 30, 2012 | http://pubs.acs.org
Publication Date (Web): May 29, 2012 | doi: 10.1021/bk-2012-1098.ch013

Strawberry Cultivar Principle Component Analysis

Although the qualitative analyses of fruit volatiles using FGC-SAW was inferior to GC-MS, the usefulness of the data to distinguish strawberry varieties and orange juice quality was equivalent. The resulting PCA score plots from both FGC-SAW and GC-MS strawberry data are compared in Figure 3. The PCA score plots were constructed from peak areas of the headspace volatiles from 10 strawberry cultivars analyzed in duplicate. In the case of FGC-SAW (Figure 3 A) 15 peak area values were employed. In the case of GC-MS (Figure 3 B) 66 peak area values were used. Even though fewer variables were used in the case of FGC-SAW, the resulting PCA score plots were roughly equivalent and the 10 strawberry cultivars could be differentiated in both cases. In FGC-SAW PCA score plot from Figure 3 A, the first two PCs accounted for 65% of the total variance. PC1 alone accounted for 42% of the total variance and was the major axis which differentiated strawberry cultivars. PC1 separated 10 strawberry cultivars into three groups: ‘Sweet Charlie’, ‘Rosa Linda’, ‘Festival’ and ‘Winter Dawn’ on the left-hand side (negative PC1 values), a large group consisting of ‘Carmine’, 05-85, 06-38, 05-107 and ‘Earlibrite’ just to the right of the central axis with small positive PC1 values. ‘Dover’ was separated so far from any others that it must be considered as a class in itself. ‘Sweet Charlie’ was further separated from ‘Rosa Linda’, ‘Festival’ and ‘Winter Dawn’ in PC2 and could be considered as a separate group as well. A very similar pattern was obtained from the GC-MS score plot (Figure 3 B) even though it used many more peak area values. It is worth noting that FGC-SAW explained more of the variance than GC-MS in these 10 strawberry cultivars. The first two GC-MS principal components only accounted for 46%, compared to 65% from the first two

Downloaded by OHIO STATE UNIV LIBRARIES on May 30, 2012 | http://pubs.acs.org
Publication Date (Web): May 29, 2012 | doi: 10.1021/bk-2012-1098.ch013

principal components from the FGC-SAW data. These results also suggest that 'Rosa Linda' and 'Winter Dawn' had similar volatile profile to 'Festival', which is the dominant strawberry cultivar in Florida. FGC-SAW has been reported to successfully classify honey from seven different floral sources (*11*) and *thymus* medicinal plant from different botanical and geographical origin (*13*). Thus, in the case of strawberry volatiles both techniques provide roughly equivalent information.

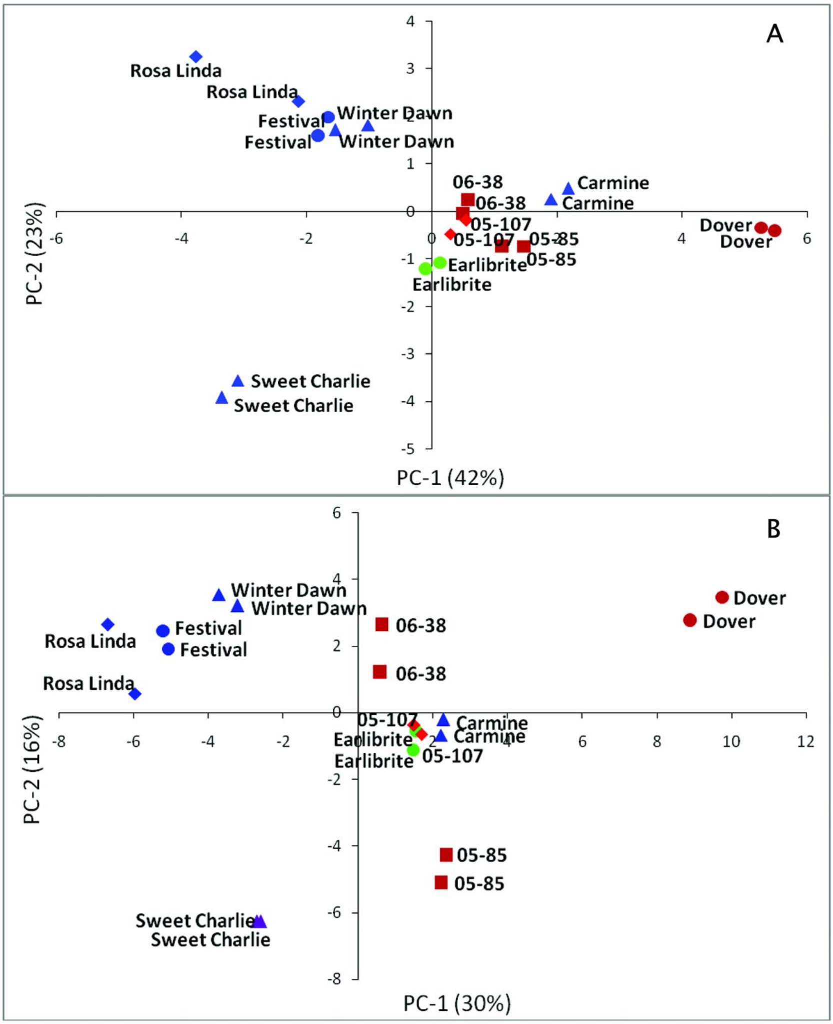

*Figure 3. PCA score plots of mean peak area of headspace volatiles for 10 strawberry cultivars analyzed using FGC-SAW (**A**) and GC-MS (**B**).*

Downloaded by OHIO STATE UNIV LIBRARIES on May 30, 2012 | http://pubs.acs.org
Publication Date (Web): May 29, 2012 | doi: 10.1021/bk-2012-1098.ch013

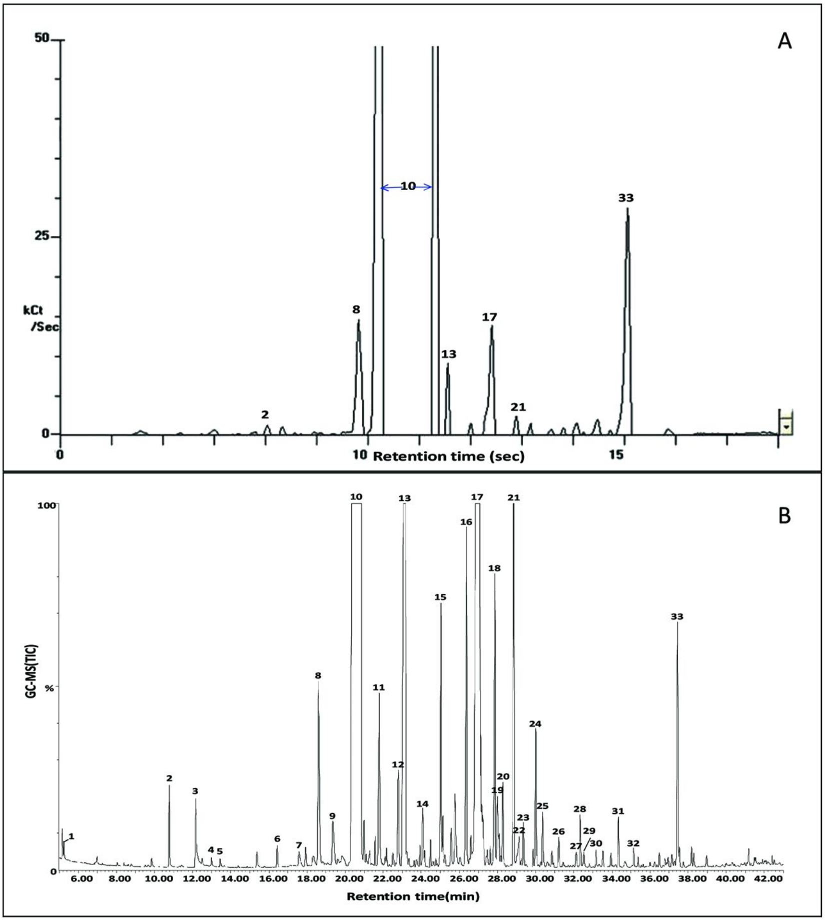

*Figure 4. FGC-SAW (**A**) and GC-MS (**B**) chromatograms of headspace volatiles for a commercial temperature abused orange juice. Key: 1. ethyl acetate; 2. ethyl butanoate; 3. furfural; 4. (Z)-3-hexenol; 5. hexanol; 6. α-pinene; 7. benzylaldehyde; 8. β-myrcene; 9. γ-terpinene; 10. limonene; 11. octanol; 12. α-terpinene; 13. linalool; 14. ethyl 3-hydroxyhexanoate; 15. p-menth-8-en-ol; 16. 4-terpineol; 17. α-terpineol; 18. (Z)-carvenol; 19. nerol; 20. (E)-carveol; 21. carvone; 22. nonanoic acid; 23. decanol; 24. perillaldehyde; 25. perilla alcohol; 26. 4-vinylguaiacol; 27. citronellyl acetate; 28. α-terpineol acetate; 29. neryl acetate; 30. geranyl acetate; 31. perillyl acetate; 32. caryophyllene; 33. valencene.*

Fresh and Storage Abused Orange Juice

Fresh orange juice and storage abused orange juice from concentrate could also be differentiated using FGC-SAW. Unfortunately, orange juice provides an example where the FGC-SAW does not perform particularly well. Extremely high amounts of limonene in orange juice diminished the ability to detect other volatiles due to the limited capacity of the volatile trap. It should be realized that there were major differences in the volatile composition of the two orange juices examined in this study. These two juice types were chosen as extreme examples to demonstrate the proof of concept. The fresh squeezed 'Valencia' orange juice represents optimal juice quality whereas the storage abused juice should represent a poor quality juice. In addition, the storage abused juice was reconstituted from concentrate which meant it was heated at least twice; once during the concentration process and once when the concentrate was reconstituted with water. In addition, the samples were over five months past their shelf life and additional volatiles can be expected due to storage abuse. Many thermally generated artifacts are typically generated in this intentionally abusive situation. These artifacts are more clearly shown in GC-MS than in the FGC-SAW. The presence of quality degrading artifacts such as carvone, α-terpineol and 4-vinylguaiacol can clearly be seen in the GC-MS chromatogram. However, two of these three major artifacts (carvone and α-terpineol) could also be detected in the FGC-SAW chromatogram.

In comparing the FGC-SAW chromatograms in Figure 2 (A) and Figure 4 (A) the major difference is due to the large limonene peak which actually saturated the detector in Figure 4 A giving the false appearance of two limonene peaks. Other qualitative and quantitative differences were observed between two samples. Fresh orange juice had higher levels of ethyl butanoate, ethyl hexanoate, geraniol and valencene (Figure 2 A), which generally provide fresh fruit and citrus flavor. The storage abused orange juice had higher levels of α-terpineol and carvone (Figure 4 A), which were mainly generated by thermal processing and storage abuse. The volatile difference of these two orange juices could be confirmed by GC-MS chromatograms as shown in Figure 2 B and Figure 4 B. Volatile compounds such as ethyl hexanoate and geraniol only existed in fresh orange juice, while storage abused orange juice had huge amount of limonene, α-terpineol, carvenol and carvone. The higher level of limonene in the juice reconstituted from concentrate was probably due to the addition of cold pressed orange oil to help restore the volatiles lost during the concentration process.

Downloaded by OHIO STATE UNIV LIBRARIES on May 30, 2012 | http://pubs.acs.org
Publication Date (Web): May 29, 2012 | doi: 10.1021/bk-2012-1098.ch013

Conclusions

The FGC-SAW technology is capable of analyzing headspace volatiles in less than 1 min. whereas a typical GC-MS will take 30-60 min. However, FGC-SAW had considerably less chromato-graphic resolution than capillary GC-MS. Examples for comparison between FGC-SAW and GC-MS were given for strawberry and orange juice volatiles. FGC-SAW could differentiate among 10 strawberry cultivars as well as between fresh orange juice and storage abused orange juice. The results from both instrumental approaches provided roughly equivalent PCA results in the case of strawberry volatiles.

Downloaded by OHIO STATE UNIV LIBRARIES on May 30, 2012 | http://pubs.acs.org
Publication Date (Web): May 29, 2012 | doi: 10.1021/bk-2012-1098.ch013

Funding Sources

This project was funded in part by a United States Department of Agriculture Specialty Crops Research Initiative USDA NIFA Award (#2009-51181-05783) entitled, "Increasing Consumption of Fresh Fruits & Vegetables by Enhancing Their Quality and Safety" as a joint research project with the University of California, Davis and the University of Florida.

References

1. Staples, E. J. Contract No. DTRS-57-89-C-00126. Department of Transpiration, Transportation Systems Center, Kendall Square, Cambridge, MA, 1991.
2. Watson, G. W.; McGuire, D. S. Presented at the 35th American Chemical Society Western Regional Meeting, Ontario, California, October 1999.
3. Staples, E. J. In *Dioxin/Furan detection and analysis using a SAW based electronic nose*; IEEE Ultrasonics Symposiu; Schneider, S. C., Levy, M., McAroy, B. R., Eds.; Sendai, Miyagi, Japan, 1998; pp 2−25.
4. Che Man, Y. B.; Gan, H. L.; NorAini, I.; Nazimah, S. A. H.; Tan, C. P. *Food Chem.* **2005**, *90* (4), 829–835.
5. Veraverbeke, E. A.; Irudayaraj, J.; Lammertyn, J. *J. Sci. Food Agric.* **2005**, *85* (2), 243–250.
6. Staples, E. J. In *The zNose™, a new electronic nose using acoustic technology*; Acoustical Society of America: Melville, New York, 2000.
7. Nurjuliana, M.; Che Man, Y. B.; Mat Hashim, D. *J. Am. Oil Chem. Soc.* **2011**, *88* (1), 75–82.
8. Gan, H. L.; Che Man, Y. B.; Tan, C. P.; NorAini, I.; Nazimah, S. A. H. *Food Chem.* **2005**, *89* (4), 507–518.
9. Gan, H. L.; Tan, C. P.; Che Man, Y. B.; NorAini, I.; Nazimah, S. A. H. *Food Chem.* **2005**, *89* (4), 271–282.
10. Biswas, S.; Heindselmen, K.; Wohltjen, H.; Staff, C. *Food Control* **2004**, *15* (1), 19–26.
11. Tewari, J. C.; Irudayaraj, J. M. K. *J. Agric. Food Chem.* **2005**, *53* (18), 6955–6966.
12. Lammertyn, J.; Veraverbeke, E. A.; Irudayaraj, J. *Sens. Actuators, B* **2004**, *98*, 54–62.
13. Oh, S. Y.; Kob, J. W.; Jeonga, S.-Y.; Hong, J. *J. Chromatogr., A* **2008**, *1205* (1-2), 117–127.
14. Oh, S. Y.; Shinc, H. D.; Kimc, S. J.; Hong, J. *J. Chromatogr., A* **2008**, *1183* (1-2), 170–178.
15. Watkins, P.; Wijesundera, C. *Talanta* **2006**, *70*, 595–601.
16. Kunert, M.; Biedermann, A.; Koch, T.; Boland, W. *J. Sep. Sci.* **2002**, *25* (10-11), 677–684.

Downloaded by OHIO STATE UNIV LIBRARIES on May 30, 2012 | http://pubs.acs.org
Publication Date (Web): May 29, 2012 | doi: 10.1021/bk-2012-1098.ch014

Chapter 14

The Power Law and Dynamic Rheology in Cheese Analysis

Michael H. Tunick* **and Diane L. Van Hekken**

Dairy & Functional Foods Research Unit, Eastern Regional Research Center, Agricultural Research Service, U.S. Department of Agriculture,
600 E. Mermaid Lane, Wyndmoor, PA 19038
***E-mail: michael.tunick@ars.usda.gov. Phone: 215-233-6454**

The protein networks of food such as cheese are investigated nondestructively by small amplitude oscillatory shear analysis, which provides information on elastic modulus (G′) and viscous modulus (G″). Relationships between frequency and viscoelastic data may be obtained from frequency sweeps by applying the power law, in which G′ and G″ are related to a power of frequency. The power law was applied to the investigation of Queso Fresco cheeses stored at 4 or 10°C for up to 12 wk. The equations revealed changes during aging that were evidently due to leakage of whey from the cheese matrix. Viscous dissipation of energy was not as pronounced as elastic energy storage in the samples. The results demonstrate that a great deal of data may be simplified into two equations that provide insight into the rheological behavior of a food.

Not subject to U.S. Copyright. Published 2012 by American Chemical Society
In Recent Advances in the Analysis of Food and Flavors; Toth, S., et al.;
ACS Symposium Series; American Chemical Society: Washington, DC, 2012.

Downloaded by OHIO STATE UNIV LIBRARIES on May 30, 2012 | http://pubs.acs.org
Publication Date (Web): May 29, 2012 | doi: 10.1021/bk-2012-1098.ch014

All viscoelastic materials display a mixture of elastic solid and viscous liquid behavior. At sufficiently small deformations, the sample may exhibit linear viscoelasticity, in which the properties measured are independent of the magnitude of the stress or strain applied (*1*). In this linear viscoelastic region (LVR), dynamic rheological analyses may be performed by varying stress and strain harmonically with time. This nondestructive test, small amplitude oscillatory shear analysis (SAOSA), provides information on protein networks in food. The equation used is

$$G^* = \sqrt{(G')^2 + (G'')^2}$$

where G*, the complex modulus, is a measure of the deformation of the sample; G', the elastic (or storage) modulus, is a measure of the energy stored and recovered per oscillation; and G", the viscous (or loss) modulus, is a measure of the energy dissipated and lost as heat per oscillation.

In SAOSA, strain sweeps are performed at a constant oscillation frequency ω, such as 1 Hz (resulting in an experimental time of 1 s) or 10 Hz (experimental time of 0.1 s). A strain is selected from the LVR, which is a relatively linear region of the curve of log G' vs. log strain. Using the selected strain, a frequency sweep over at least 2 decades of ω is then conducted to observe the response of the structure (bond-making, bond-breaking, polymer strand entanglements, etc.) to the different experimental times (*1*).

Cheese is a viscoelastic material, and cheese rheology has been studied in a systematic way since the 1930s (*2*). Our laboratory has performed SAOSA of a number of cheese varieties, comparing imitation, full-fat, and low-fat Mozzarella (*3*, *4*), Cheddar and Cheshire (*5*), hard and soft goat's milk cheeses (*6*, *7*), and the Hispanic cheeses Queso Chihuahua (*8*) and Queso Fresco (*9*). Queso Fresco is often eaten fresh (the name means "fresh cheese"), but many consumers in the U.S. would like the option of refrigerating the product for a few weeks (*9*). Tests such as SAOSA are therefore needed to determine the effects of refrigeration on the protein structure of Queso Fresco. The results consist of columns of numbers that are not easily interpreted. Comparisons are sometimes made by selecting values at a particular frequency, which does not give the entire picture of the rheological behavior. A simple equation would allow for examination of huge amounts of data over the entire frequency range.

The power law, a mathematical model in which the frequency of an event varies with the power of an attribute of the event, reduces data to an equation:

$$f(x) = ax^k$$

The power law has been applied to diverse phenomena such as earthquake intensity, population of cities, and sizes of power outages (*10*). The power law can also be used to determine relationships between moduli and oscillatory frequencies

Downloaded by OHIO STATE UNIV LIBRARIES on May 30, 2012 | http://pubs.acs.org
Publication Date (Web): May 29, 2012 | doi: 10.1021/bk-2012-1098.ch014

in SAOSA by substituting values for G′, G″, and ω in the equation. Nolan et al. applied the power law to SAOSA of natural and imitation Mozzarella in 1989 (*3*), and others have since employed it to evaluate data for Mozzarella (*11*, *12*), the Turkish cheese Gaziantep (*13*), the Spanish cheese Arzúa-Ulloa (*14*), pasteurized process cheese (*15*), and frozen low-fat soft cheese (*16*). The application of the power law is still relatively uncommon in SAOSA research, however, despite its usefulness. This chapter will show how the power law is applied to SAOSA of Queso Fresco that has been refrigerated at 4 and 10°C, and how the results are interpreted.

Materials and Methods

Queso Fresco cheeses were manufactured from milk obtained locally. Milk (180 kg) was pasteurized (72°C, 15 s), homogenized in two stages (6.9, 3.5 MPa), and poured into a stainless steel vat and adjusted to 32°C. No starter culture was added. The curd was coagulated with chymosin (14 mL Chy-Max, Chr. Hansen, Milwaukee, WI; diluted in 200 mL water), cooked (39°C, 30 min), and wet salted with 2.63 kg NaCl. The drained curds were then chilled, milled into small pieces, and hand-packed into molds for storage overnight at 4°C. Cheeses were removed from the molds the next day, sliced into smaller blocks, and vacuum packaged. Samples were stored for up to 12 wk at 4 or 10°C. The composition of the cheeses at 1 wk was 53-56% moisture, 15-17% protein, 22-23% fat, 3% lactose, 3% ash, and 1.6% NaCl. The pH was around 6.3. Only the moisture decreased significantly during storage.

SAOSA were conducted at room temperature using an AR-2000 rheometer (TA Instruments, New Castle, DE) with 25-mm parallel aluminum plates. Specimens were sliced from cheese blocks with piano wire and cut with a cork borer into disks measuring 25 mm diameter and around 4 mm thick. The outer edge of each specimen was coated with mineral oil to prevent drying. Strain sweeps were run from 0.1 to 2.0% strain and frequency sweeps were run in triplicate from 1 to 100 rad/s. Microsoft Excel was used to generate plots of G′ and G″ vs. ω, and power law equations.

Results and Discussion

The LVR of each Queso Fresco sample was around 0.6-1.0% strain, and 0.8% strain was selected for all of the frequency sweeps. Table 1 shows the data obtained from a frequency sweep of Queso Fresco stored for 1 wk at 4°C. A set of data at one frequency, for example 10 rad/s, merely provides a glimpse into the behavior of the specimen without taking the rest of the frequency range into account.

By using the power law, G′ and G″ are related to ω:

$$G' = a\omega^{x} \qquad G'' = b\omega^{y}$$

where *a* and *b* are the magnitudes of G′ and G″ at a given ω, and *x* and *y* are the relative degree of viscoelasticity of the gels. To obtain *a, b, x,* and *y* from the data in Table 1, G′ and G″ were plotted vs. ω on an Excel spreadsheet, and regression lines with the "power" option were added along with the equations and R^2 values (Figure 1). In Excel, the regression equations are in the form $y = cx^k$, so the power law values are a = 7138 Pa·s, x = 0.122, b = 1983 Pa·s, and y = 0.134. The 63 numbers in Table 1 were thus reduced to four, plus the two R^2 values, and offer a more complete depiction of the rheological responses.

Downloaded by OHIO STATE UNIV LIBRARIES on May 30, 2012 | http://pubs.acs.org
Publication Date (Web): May 29, 2012 | doi: 10.1021/bk-2012-1098.ch014

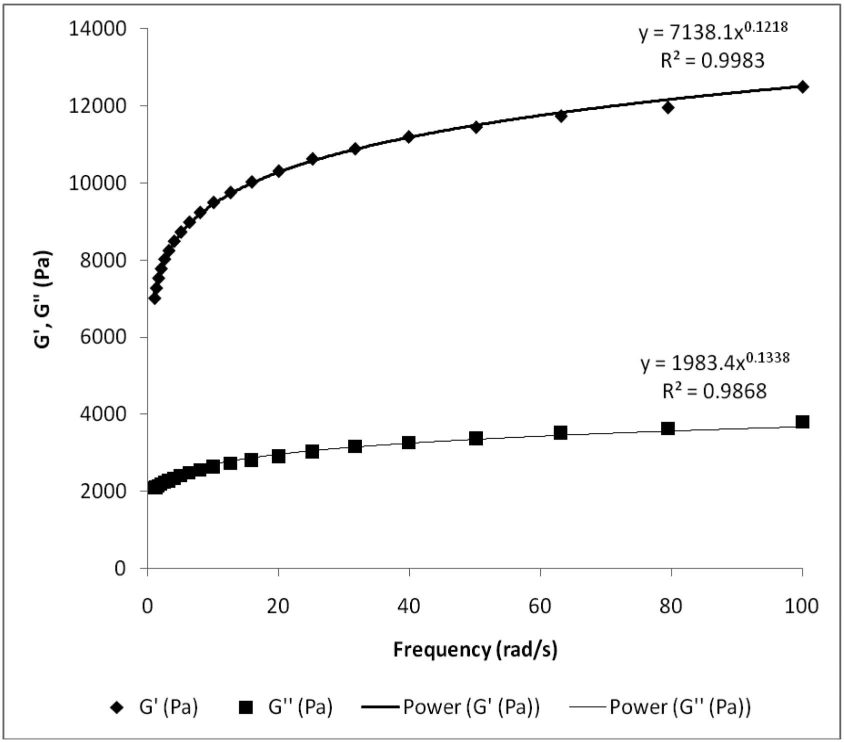

Figure 1. Fitting of power law regression lines to Table 1 data.

Downloaded by OHIO STATE UNIV LIBRARIES on May 30, 2012 | http://pubs.acs.org
Publication Date (Web): May 29, 2012 | doi: 10.1021/bk-2012-1098.ch014

Table 1. Raw data for frequency sweep at 0.8% strain of Queso Fresco sample after 1 wk of storage at 4°C. ω = frequency, G′ = elastic modulus, and G″ = viscous modulus

ω (rad/s)	*G′ (Pa)*	*G″ (Pa)*
1.000	7009	2090
1.259	7273	2106
1.586	7530	2143
1.995	7778	2188
2.512	8025	2240
3.163	8246	2275
3.980	8490	2335
5.011	8730	2408
6.309	8984	2480
7.943	9238	2558
10.000	9497	2640
12.590	9756	2727
15.840	10030	2817
19.950	10310	2914
25.120	10630	3027
31.630	10890	3169
39.810	11200	3261
50.110	11450	3374
63.090	11740	3515
79.430	11960	3632
100.000	12500	3804

The averages for *a, b, x,* and *y* for the cheeses in the study are shown in Table 2. The values of *a* were always greater than the corresponding values of *b*, demonstrating that the elastic response was higher than the viscous response, which is typical for cheese.

Downloaded by OHIO STATE UNIV LIBRARIES on May 30, 2012 | http://pubs.acs.org
Publication Date (Web): May 29, 2012 | doi: 10.1021/bk-2012-1098.ch014

Table 2. Rheological values derived from power law equations for Queso Fresco cheeses stored at 4 and 10 °C for up to 12 wk. Elastic modulus equals $a\omega^x$ and viscous modulus equals $b\omega^y$, where ω is frequency. Averages of three replicates

	1 wk		*4 wk*		*8 wk*		*12 wk*	
	4°C	*10°C*	*4°C*	*10°C*	*4°C*	*10°C*	*4°C*	*10°C*
a	9155	9944	9572	10441	11460	12752	12218	15493
x	0.1278	0.1220	0.0972	0.1125	0.1125	0.1431	0.1295	0.1553
R^2	0.9976	0.9952	0.9956	0.9961	0.9962	0.9977	0.9989	0.9990
b	2562	2675	2916	3013	3237	3506	3331	4149
y	0.1504	0.1544	0.1315	0.1414	0.1549	0.1695	0.1628	0.1677
R^2	0.9871	0.9881	0.9711	0.9727	0.9868	0.9917	0.9893	0.9912

The values for y were always greater than those of x, indicating that G″ displayed greater frequency dependence than G′; as experimental times grew shorter, the ability to dissipate energy grew increasingly greater than the ability to store energy. The x and y values were between 0.09 and 0.17, which are relatively low compared with other natural hard or semi-hard cheese varieties.

The x values of Mozzarella and Gaziantep have been reported in the 0.17-0.21 range and the y values in the 0.19-0.24 range (*3*, *11–13*). The a and b ranges for Gaziantep were reported as 3000-9760 Pa and 1000-3390 Pa, respectively (*13*), but the ranges for Mozzarella were 22700-88400 Pa for a and 10300-30900 Pa for b (*3*, *11*, *12*). The low values for Queso Fresco are due to a combination of milk homogenization, high NaCl content, and curd milling, which prevents the formation of a structure with long-range interactions and resulting in a characteristic granular and crumbly texture.

Downloaded by OHIO STATE UNIV LIBRARIES on May 30, 2012 | http://pubs.acs.org
Publication Date (Web): May 29, 2012 | doi: 10.1021/bk-2012-1098.ch014

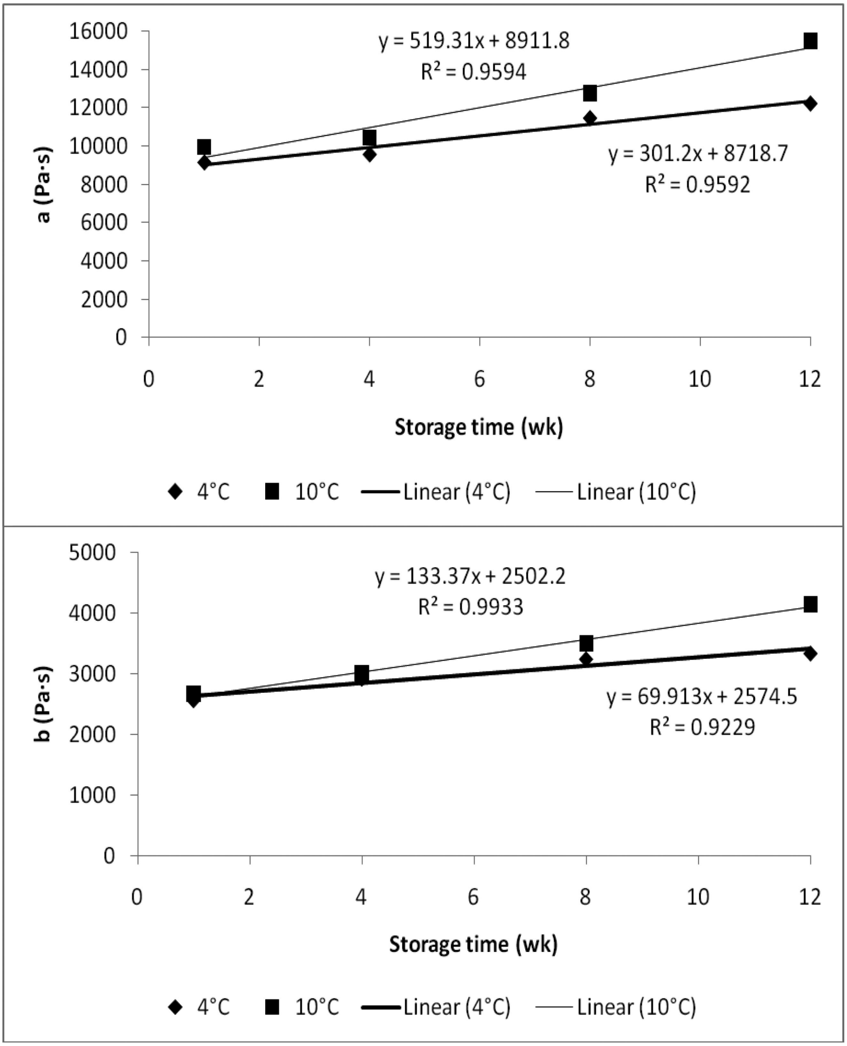

Figure 2. Fitting of linear regression lines to Table 2 data, comparing Queso Frescos stored at 4 °C and 10 °C for up to 12 wk. a and b are measures of elastic modulus and viscous modulus, respectively.

All samples exhibited increases in *a* and *b* over the 12 wk of aging, corresponding to increases in G′ and G″. Proteolysis of casein in cheeses made with starter culture microorganisms causes degradation of the protein network by enzymatic action, which reduces both storage and dissipation of energy (*16*, *17*), which is reflected by decreases in *a* and *b* with storage time. Queso Fresco is not made with a starter, however, and undergoes limited proteolysis from bacteria that either survived pasteurization or contaminated the cheese during processing.

The increases in *a* and *b* may have resulted in leakage of excess whey, which is common for this variety (*9*). Some whey loss lessens the ability for casein strands to slide past each other, thereby increasing G′ and G″. The averages for *a* and *b* were higher for cheeses stored at the higher storage temperature since whey leakage was higher at 10°C. With one exception, *x* and *y* were higher at 10°C than at 4°C. The *x* and *y* values were fairly steady throughout the 12 wk, implying that the responses did not vary greatly with frequency. All of the R^2 values were greater than 0.97, demonstrating the excellent fit of the power law curves.

Graphs of *a* and *b* vs. storage time reveal that G′ and G″ increased linearly with age (Figure 2). The close fits to the regression lines ($R^2 > 0.92$) indicate that whey loss continued at a linear rate.

Downloaded by OHIO STATE UNIV LIBRARIES on May 30, 2012 | http://pubs.acs.org
Publication Date (Web): May 29, 2012 | doi: 10.1021/bk-2012-1098.ch014

Conclusions

Small amplitude oscillatory shear analysis presents a picture of the behavior of protein matrices in cheese. The large amount of data generated by this technique may be converted into power law equations that provide a model for the response of cheese to strain over a range of frequencies. The calculation of these equations simplifies the results and facilitates the comparison of sample properties.

Acknowledgments

The authors thank Ray Kwoczak for preparing the cheeses and James Shieh for performing compositional analyses. Mention of trade names and commercial products in this publication is solely for the purpose of providing information and does not imply recommendation or endorsement by the U.S. Department of Agriculture. USDA is an equal opportunity provider and employer.

References

1. Tunick, M. H. *J. Agric. Food Chem.* **2011**, *59*, 1481–1486.
2. Tunick, M. H.; Nolan, E. J. In *Physical Chemistry of Food Processes*; Baianu, I. C., Ed.; Van Nostrand Reinhold: New York, 1992; Vol. 1, pp 273−297.
3. Nolan, E. J.; Holsinger, V. H.; Shieh, J. J. *J. Texture Stud.* **1989**, *20*, 179–189.
4. Tunick, M. H.; Mackey, K. L.; Shieh, J. J.; Smith, P. W.; Cooke, P.; Malin, E. L. *Int. Dairy J.* **1993**, *3*, 649–662.
5. Tunick, M. H.; Nolan, E. J.; Shieh, J. J.; Basch, J. J.; Thompson, M. P.; Maleeff, B. E.; Holsinger, V. H. *J. Dairy Sci.* **1990**, *73*, 1671–1675.
6. Van Hekken, D. L.; Tunick, M. H.; Park, Y. W. *J. Agric. Food Chem.* **2004**, *52*, 5372–5377.
7. Van Hekken, D. L.; Tunick, M. H.; Park, Y. W. *J. Dairy Sci.* **2005**, *88*, 1966–1972.
8. Van Hekken, D. L.; Tunick, M. H.; Tomasula, P. M.; Molina Corral, F. J.; Gardea, A. A. *Int. J. Dairy Technol.* **2007**, *60*, 5–12.
9. Tunick, M. H.; Van Hekken, D. L. *J. Food Qual.* **2010**, *33*, 204–215.
10. Clauset, A.; Shalizi, C. R.; Newman, M. E. J. *SIAM Rev.* **2009**, *51*, 661–703.

11. Diefes, H. A.; Rizvi, S. S. H.; Bartsch, J. A. *J. Food Sci.* **1993**, *58*, 764–769.
12. Subramanian, R.; Muthukumarappan, K.; Gunasekaran, S. *J. Texture Stud.* **2003**, *34*, 361–380.
13. Kahyaoglu, T.; Kaya, S. *Int. Dairy J.* **2003**, *13*, 867–875.
14. Tovar, C. A.; Cerdeiriña, C. A.; Romaní, L.; Prieto, B.; Carballo, J. *J. Texture Stud.* **2003**, *34*, 115–129.
15. Subramanian, R.; Muthukumarappan, K.; Gunasekaran, S. *Int. J. Food Prop.* **2006**, *9*, 377–393.
16. Meza, B.; Verdini, R. A.; Rubiolo, A. C. *Int. Dairy J.* **2011**, *21*, 346–351.
17. Ak, M. M.; Gunasekaran, S. *J. Food Sci.* **1996**, *61*, 566–576.

Downloaded by OHIO STATE UNIV LIBRARIES on May 30, 2012 | http://pubs.acs.org
Publication Date (Web): May 29, 2012 | doi: 10.1021/bk-2012-1098.ch014

Subject Index

A

- 4-Acetylthio-2-alkanones
  - capillary gas chromatography, 30, 32*f*
  - chromatographic data, 36
  - diastereoisomers
    - capillary gas chromatography separation, 37*f*
    - odor properties, 38*t*
  - enantiomers
    - capillary gas chromatographic separation, 32*f*
    - GC separation, 32
    - GC-elution, 34*f*
    - odor thresholds, 35*f*
  - enzyme-catalyzed hydrolysis, 30
  - gas chromatography-mass spectrometry, 31
  - gas chromatography-olfactometry, 31, 35*f*
  - high-performance liquid chromatography, 31, 35*f*
  - ^{1}H-NMR anisotropy method, 32
  - lipase-catalyzed kinetic resolution, 32
  - overview, 27
  - sensory data, 36
  - sensory properties assessment, 35
  - synthesis, 28
- Acrolein versus aroma-active compounds
  - concentrations, 132*f*, 134*f*
  - deep-frying, potatoes, 130
  - generation
    - key aroma compounds, 134
    - oil thermal processing, 131, 133*t*
  - oil heating process, 130
  - overview, 129
  - quantitation
    - headspace GC-MS, 131
    - key aroma compounds, 131, 135*f*
- Alternative cork extraction, haloanisoles, 119
- Anacardic acid profiling, cashew nuts
  - alkyl/alkenyl-functionalities, 153
  - APCI-MS-MS detection, 156
  - C15-chain, 149
  - C17-chain, 152
  - concentrated, 150*f*
  - dicarboxy-substituted C15, 154
  - dimer, 154, 157*f*
  - elution-process, 158*t*
  - extraction process, 147
  - extrusion HSCCC mode, 156
  - HSCCC-ESI-/APCI-MS/MS, 147
  - overview, 145
  - retention time, 160
  - separation, 149
  - structure elucidation, 149
  - structures, 155*f*
  - unidentified compounds, 156
- Analyte peak area ratios, furocoumarins, 77*t*
- Angelicin, 74*f*
- Asafetida
  - extraction, 168*f*
  - GC/MS chromatogram, 169*f*
  - GC-O analysis, 170*f*, 171*f*
  - HTLC, 169*f*
  - isolated disulfide compounds, 172*f*
  - isolated sulphur-containing aroma compounds, 171*f*
  - overview, 167
- α-Ylangene, 3*f*

B

- Base peak ion chromatograms, coffee drinker urine, 18*f*
- Biomarker discovery, metabolomics, 3
- Biomarker structures
  - citrus fruit, 14*f*
  - whole-grain rye, 14*f*
  - wine, 14*f*
- Box-Whisker plots, coffee drinker urine, 20*f*

C

- Calibration curve properties, coffee drinker saliva, 22*t*
- Cantaloupe, aroma-impact compounds
  - aroma extract preparation
    - gel permeation chromatography, 43
    - solid phase extraction, 43
  - aroma-impact compounds, 45, 46*t*
    - C9, 48, 50*f*
  - collision energy, 52*t*, 53*t*
  - GC-MS/MS analysis, 44
    - standard compounds, synthesis schemes, 44, 44*f*
  - GC-O/MS analysis, 44
  - overview, 41

Downloaded by 89.163.35.42 on May 29, 2012 | http://pubs.acs.org
Publication Date (Web): May 29, 2012 | doi: 10.1021/bk-2012-1098.ix002

Downloaded by 89.163.35.42 on May 29, 2012 | http://pubs.acs.org
Publication Date (Web): May 29, 2012 | doi: 10.1021/bk-2012-1098.ix002

  - plant materials, 42
  - selected reaction monitoring, 52*t*, 53*t*, 54*t*, 55*f*
  - volatile compound isolation, 45
- Capillary GC-MS
  - overview, 177
  - statistical analysis, 181
  - volatile analysis, 181, 183*f*, 184*f*
- C9 aroma compounds, 48, 50*f*
- Cheese
  - frequency sweep, 195*t*
  - linear regression lines, 197*f*
  - overview, 191
  - power law regression lines, 194*f*
  - rheological values, 196*t*
- Citrus fruit, biomarker structure, 14*f*
- Citrus oils
  - furocoumarin concentration, 85*t*
  - recovery data, furocoumarins, 82*t*
- Coffee consumption, biomarker identification
  - base peak ion chromatograms, 18*f*
  - Box-Whisker plots, 20*f*
  - calibration curve properties, 22*t*
  - coffee specific compound identification, urine, 16
  - coffee specific compound quantification, urine, 17
  - ion visualization, 17*f*
  - LC-MS/MS chromatograms, 21*f*
  - NMP, dietary sources, 23, 24*t*
  - NMP, salivary fluid, 20, 22*t*, 23*f*
  - NMP analysis, 16
  - NMP quantification, saliva, 15
  - NMP quantification, urine, 15
  - overview, 13
  - trigonelline, dietary sources, 23, 24*t*
  - trigonelline, salivary fluid, 20, 22*t*, 23*f*
  - trigonelline analysis, 16
  - trigonelline quantification, saliva, 15
  - trigonelline quantification, urine, 15
  - urinary NMP, 19
  - urinary trigonelline, 19

D

- Deuterium-labeled alkyl pyrazines
  - alkylpyrazines, 60
  - food occurrence, 59
  - formation, 59, 59*f*
  - overview, 57
  - SIDA, 61, 66*t*
    - concentrations, 67*t*, 68
    - $[^2H_5]$-2-ethyl-3,6-dimethylpyrazine synthesis, 61, 62*f*, 65*f*
    - instrumental analysis, 65
    - odor active values, 67*t*, 68
    - quantification, 64*f*, 65
    - stable isotopes addition, 63
    - volatile extract preparation, 63
  - synthesis, 60
- 2D HPLC. *See* two-dimensional high pressure liquid chromatographic (2D HPLC)
- Diastereoisomers
  - capillary gas chromatographic separation, 36*f*
  - odor properties, 38*t*

E

- Enantiomers
  - capillary gas chromatographic separation, 32*f*
  - GC separation, 32
  - GC-elution, 34*f*
  - odor thresholds, 35*f*
- Epoxybergamottin, 78*f*, 85*f*
- EU essential oils hazard classification
  - automated data processing flowchart, 99*f*
  - automatic processing, 98
  - calibration, 93, 96*f*, 98*f*
  - calibration standards preparation, 90
  - component and chemicals, 92*t*
  - data interpretation, 98
  - equipment and settings, 91*t*
  - full scan versus SIM quantitation, 104
  - GC-MS analysis, 90
  - ion ratio tolerances, 104*t*
  - overview, 89
  - qualifier ions, 94*t*
  - quantifier ions, 94*t*
  - recovery, 100
  - reproducibility, 100
  - sample preparation, 91
  - spiked analytes, 101*t*, 105*t*

F

- Fast gas chromatography–surface acoustic wave sensor (FGC-SAW)
  - analysis time versus chromatographic resolution, 182
  - chemicals, 179
  - orange, 179
  - orange juice, 187, 187*f*

Downloaded by 89.163.35.42 on May 29, 2012 | http://pubs.acs.org
Publication Date (Web): May 29, 2012 | doi: 10.1021/bk-2012-1098.ix002

  overview, 177
  peak identifications, 184
  statistical analysis, 181
  strawberry, 179
    cultivar principle component analysis, 185, 186*f*
  volatile analysis, 180, 183*f*, 184*f*
Fenoxycarb, 76*f*
Fermentation volatiles, GC-MS analysis, 6
FGC-SAW. *See* fast gas chromatography–surface acoustic wave sensor (FGC-SAW)
Furocoumarins
  analyte peak area ratios, 77*t*
  analytical standards, 73
  angelicin, 74*f*
  chromatography, 78
  citrus oils
    furocoumarin concentration, 85*t*
    recovery data, 82*t*
  epoxybergamottin, 78*f*, 85*f*
  fenoxycarb, 76*f*
  identification, 76
  isoimperatorin, 85*f*
  LC/MS/MS analyte specific parameters, 75*t*
  lemon oil
    control sample data, 86*f*
    precision data, 83*t*
  overview, 71
  oxypeucedanin, 77*f*
  psoralen, 74*f*
  quantitation, 79
  standard peak area ratios, 77*t*
  standard stock solutions, 74
  TIC chromatograms, 80*f*

H

Haloanisoles
  ECD analysis, 121*t*
  extraction
    alternative cork extraction, 119
    liquid microextractions, 118
    sorptive extractions, 111
  GC detection, 120
  GC-ion trap MS/MS detectors, 121*t*
  HS-SPME optimization, 113*t*
  overview, 109
  SBSE analysis, 117*t*
  SPME analysis, 117*t*

I

Ion visualization, coffee drinker urine, 17*f*
Isoimperatorin, 85*f*
Isolated disulfide compounds, 172*f*
Isolated sulphur-containing aroma compounds, 171*f*

L

LC/MS/MS analyte specific parameters, furocoumarins, 75*t*
LC-MS/MS chromatograms, coffee drinker saliva, 21*f*
Lemon oil
  control sample data, furocoumarins, 86*f*
  precision data, furocoumarins, 83*t*
Liquid microextractions, haloanisoles, 118

M

Marker identification, grapes, 4
4-Mercapto-2-alkanones
  capillary gas chromatography, 30
  chromatographic data, 36
  diastereoisomers
    capillary gas chromatographic separation, 36*f*
    odor properties, 38*t*
  enantiomers
    capillary gas chromatographic separation, 32*f*
    GC separation, 32
    GC-elution, 34*f*
    odor thresholds, 35*f*
  gas chromatography-mass spectrometry, 31
  gas chromatography-olfactometry, 31
  high-performance liquid chromatography, 31
  ^{1}H-NMR anisotropy method, 32
  lipase-catalyzed kinetic resolution, 32
  overview, 27
  sensory data, 36
  sensory properties assessment, 35
  (S)-MαNP-thioesters, HPLC separation, 30, 33*f*
  synthesis, 28
Metabolomics
  biomarker discovery, 3
  fermentation volatiles, 6
  marker identification, 4

- overview, 1
- targeted metabolic profiling, 4
- volatile trace metabolites, 3
- volatile yeast metabolites, 7*f*
- yeast strain development, 6
- α-Ylangene, 3*f*

N

N-methylpyridinium (NMP), 13
- coffee powder, 16
- dietary sources, 23, 24*t*
- quantification, saliva, 15
- quantification, urine, 15
- salivary fluid, 20, 22*t*, 23*f*

NMP. *See* *N*-methylpyridinium (NMP)

O

Orange, FGC-SAW, 179
Orange juice, FGC-SAW, 187, 187*f*
Oxypeucedanin, 77*f*

P

Pentafluorophenyl hydrazine (PFPH), 131
PFPH. *See* pentafluorophenyl hydrazine (PFPH)
Potato chips
- acrolein generation, 133*t*
- deep-frying, 130
- key aroma compound generation, 134
- key aroma compound quantitation, 131

Preparative high-speed countercurrent chromatography and mass spectrometry (prepHSCCC-ESI-/APCI-MS/MS), 145
- base peak chromatogram, 150*f*, 152*f*
- concentrated anacardic acids, 150*f*
- schematic diagram, 148*f*

PrepHSCCC-ESI-/APCI-MS/MS. *See* preparative high-speed countercurrent chromatography and mass spectrometry (prepHSCCC-ESI-/APCI-MS/MS)
Psoralen, 74*f*

S

Shiraz grapes, volatile trace metabolites, 3
SIDA. *See* stable isotope dilution analysis (SIDA), pyrazines
Sorptive extractions, haloanisoles, 111
Stable isotope dilution analysis (SIDA), pyrazines, 57, 58*f*, 61, 66*t*
- concentrations, 67*t*, 68
- [$^2H_5$]-2-ethyl-3,6-dimethylpyrazine synthesis, 61, 62*f*, 65*f*
- instrumental analysis, 65
- odor active values, 67*t*, 68
- quantification, 64*f*, 65
- stable isotopes addition, 63
- volatile extract preparation, 63

Standard peak area ratios, furocoumarins, 77*t*
Standard stock solutions, furocoumarins, 74
Strawberry, FGC-SAW, 179
- cultivar principle component analysis, 185, 186*f*

T

Targeted metabolic profiling, grapes, 4
Taste compound analysis, 2D HPLC
- chemicals, 139
- chromatogram, 141*f*
- data analysis, 140
- HPLC analysis, 139
- overview, 137
- peak distributions, 143*f*
- whole grain bread crust, 140*f*

Trigonelline
- dietary sources, 23, 24*t*
- salivary fluid, 20, 22*t*, 23*f*

Trigonelline analysis, coffee powder, 16
Trigonelline quantification
- saliva, 15
- urine, 15

Two-dimensional high pressure liquid chromatographic (2D HPLC), 137
- *See also* taste compound analysis, 2D HPLC

U

Urinary NMP, coffee drinkers, 19
Urinary trigonelline, coffee drinkers, 19

Downloaded by 89.163.35.42 on May 29, 2012 | http://pubs.acs.org
Publication Date (Web): May 29, 2012 | doi: 10.1021/bk-2012-1098.ix002

V

Volatile trace metabolites, 3
Volatile yeast metabolites, 7*f*

W

Whole-grain rye, biomarker structure, 14*f*
Wine, biomarker structure, 14*f*

Y

Yeast strain development, 6

Downloaded by 89.163.35.42 on May 29, 2012 | http://pubs.acs.org
Publication Date (Web): May 29, 2012 | doi: 10.1021/bk-2012-1098.ix002

In Recent Advances in the Analysis of Food and Flavors; Toth, S., et al.;
ACS Symposium Series; American Chemical Society: Washington, DC, 2012.